Very high energy cosmic gamma rays from radio and x-ray pulsars

Chadwick, Mary Paula

ABSTRACT

This thesis is concerned with the detection of very high energy cosmic gamma-rays from isolated pulsars and X-ray binary sources using the atmospheric Cerenkov technique. A general introduction to gamma ray detection techniques is followed by a description of the properties of atmospheric Cerenkov radiation and a discussion of the principles of the atmospheric Cerenkov technique. The Mark I and Mark II gamma-ray telescopes operated in Dugway , Utah by the University of Durham between 1981 and 1984 are briefly described.

There follows a discussion of the results from observations at many different wavelengths of Cygnus X-3. This object was observed by the Durham group between 1981 and 1983 in Dugway , Utah and also in Durham during Autumn 1985. The detection in the Dugway data of the 4.8 hr X-ray period and the possible detection of a 19.2 day intensity variation are considered.

The discovery of a 12.59 ms pulsar in data taken on Cygnus X-3 in 1983 is described. Evidence is presented which suggests this periodicity is also present at a weaker level in ealier data and also in the data taken in Durham in 1985.

Results from observations of PSR1937+21 , PSR1953+29 and six radio pulsars , are presented.

The design and construction of the Mark III telescope , now operating in Narrabri , N.S.W. , is described in detail.

Preliminary results from observations with the Mark III telescope of three objects , LMC X-4 , the Vela pulsar and Centaurus X-3 , are presented , with particular reference to periodicities

inherent in the sources. An observation of the supernova in the Large Magellanic Cloud is discussed.

A brief discussion of the mechanisms by which V.H.E. gamma-rays may be produced in isolated pulsars and X-ray binary pulsars is given , followed by a description of the future prospects for the Mark III and Mark IV telescopes.

VERY HIGH ENERGY COSMIC GAMMA RAYS FROM RADIO AND X-RAY PULSARS

by

Paula Mary Chadwick, B.Sc., F.R.A.S.

A thesis submitted to the University of Durham in accordance with the regulations for admittance to the degree of Doctor of Philosophy

Department of Physics
University of Durham

September 1987

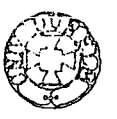

To my parents,

without whom.....

VERY HIGH ENERGY COSMIC γ-RAYS FROM RADIO AND X-RAY PULSARS

Contents

Chapter 1 - An Introduction to Gamma Ray Astronomy

1.1. Introduction 1
1.2. Method of Generation of Cosmic γ-rays 2
1.2.1. Nuclear Processes 2
1.2.2. Annihilation of Particles with Antiparticles 2
1.2.3. The Decay of Elementary Particles 3
1.2.4. Acceleration of Charged Particles 3
1.3. The Absorption of Cosmic γ-rays 5
1.4. The Detection of γ-rays 6
1.4.1. Energies between 0.5 and 3 MeV 7
1.4.2. Energies between 3 MeV and 10 GeV 7
1.4.3. Energies between 100 GeV and 100 TeV 8
1.4.4. Energies > 100 TeV 8

Chapter 2 - The Detection of V.H.E. Gamma Rays using the Atmospheric Cerenkov Technique

2.1. Introduction 10
2.2. The Cerenkov Effect 11
2.3. The Discovery of Cerenkov Radiation from the Night Sky 13
2.4. The Characteristics of γ-Ray Initiated Cerenkov Radiation 14
2.4.1. The Threshold Energy for Emission 14
2.4.2. Lateral Distribution of Light 14
2.4.3. Angular Distribution of Light 15
2.4.4. Absorption and Scattering in the Atmosphere 16
2.5. Experimental Techniques 17
2.6. Astronomical Observations Using the Atmospheric Cerenkov Technique 18
2.7. The University of Durham Facility at Dugway, Utah 20
2.7.1. The Mark I Telescope 20
2.7.2. The Mark II Telescope 22
2.7.3. Information Recorded 22
2.7.4. General Performance 23

Chapter 3 - Data Analysis Techniques for Use in Gamma-Ray Astronomy

3.1. Introduction 24
3.2. Format of Data Files 25
3.3. Count Rate Analysis 27
3.4. Adjustments to the Times of Arrival of γ-rays 28
3.4.1. Clock Uncertainties 28
3.4.2. The Adjustment of Event Times to the Solar System Barycentre 30
3.4.3. Focusing Event Times to the Barycentre of a Binary Orbit 31
3.5. Periodicity Searches 33
3.5.1. Epoch Folding 33
3.5.2. The Rayleigh Test 35
3.5.3. The Modified Hodges-Ajne Test 37
3.5.4. The Z^2 Test 39
3.5.5. The T_n^n Statistic 39
3.6. Searching Over a Range of Periods or for an Unknown Period 40
3.7. The Poincare Correction 42
3.8. Zenith Angle Dependence 43
3.9. Drift Scan Techniques 43
3.9.1. The Relative Likelihood Ratio 44
3.9.2. The Maximum Likelihood Test 45
3.10. Calculation of Fluxes 46
3.11. Calculation of Flux Limits 47

Chapter 4 - Cygnus X-3: Research Background

4.1. Introduction 49
4.2. Observations of Cygnus X-3 49
4.2.1. X-ray Observations 49
4.2.2. Radio Observations 54
4.2.3. Infrared Observations 57
4.2.4. High Energy γ-Ray Observations 58
4.2.5. Ultra High Energy γ-Rays 60
4.2.6. Underground Muons 62
4.2.7. Very High Energy γ-Rays 64

Chapter 5 - Observations of Cygnus X-3 Mode at Dugway, Utah

5.1. Introduction 67
5.2. The Database 67
5.2.1. Drift Scans 67
5.2.2. Tracking Observations 68
5.3. The 4.8 hour Period 69
5.4. Long Term Variability of the 4.8 hr. Maximum 71
5.5. Why Search for a Pulsar? 72
5.5.1. The "cocoon" Model 73
5.5.2. The Target Model 74
5.5.3. The Dynamo Mechanism 75
5.5.4. The Diffusive Shock Mechanism 75
5.5.5. The Absorption of Pulsed Radiation 76
5.6. The Pulsar Search in Dugway Data 77
5.6.1. 12th September 1983 78
5.6.2. Other Data from 1983 80
5.6.3. Twofold Events 81
5.6.4. Tests for the Presence of a Signal in Other Harmonics 82
5.6.5. Instrumental Effects 82
5.7. Support from Earlier and Later Observations of Cygnus X-3 83
5.7.1. Count Rates 83
5.7.2. Unknown Secular Period Derivative 84
5.7.3. Errors in Ephemerides 86
5.8. Observations made in October-November 1985 87
5.9. Observations made in 1982 88
5.10. Observations made in 1981 89
5.11. Periodicity Outside X-ray Maximum 89
5.12. The Secular Period Derivative of the Pulsar 90
5.13. The Orbital Period Derivative 90
5.14. Implications for Models of the Cygnus X-3 System 91
5.15. Other Searches for a 12.59 ms Pulsar in V.H.E. γ-ray Data 92
5.15.1. Whipple Observatory Measurements 92
5.15.2. Haleakala Observations 94
5.15.3. Conclusions 95
5.16. The Durham University Cygnus X-3 Monitor 95

Chapter 6 - Other Observations at Dugway

6.1. Introduction 97
6.2. Radio Pulsars 97
6.3. PSR1937+214 - The 1.5 ms Pulsar 98
6.4. 2CG065+00 101
6.5. Shorter Observations 105
6.6. The Dugway Catalogue of Very High Energy γ-Ray Sources 105
6.6.1. The Crab Pulsar 105
6.6.2. Hercules X-1 107
6.6.3. 4U0115+63 108
6.6.4. The Galactic Plane 109
6.6.5. M31: The Andromeda Galaxy 110
6.7. Conclusions 111

Chapter 7 - The Mark III Telescope at Narrabri, N.S.W.

7.1. Introduction 112
7.2. Choice of Site 113
7.3. The Climate 114
7.4. Mechanical Design 115
7.4.1. The Alt-Azimuth Mount 115
7.4.2. The Telescope Framework 116
7.5. Optical Characteristics 117
7.5.1. Mirror Construction 117
7.5.2. Mirror Quality 118
7.5.3. Alignment of Mirrors 119
7.5.4. Aperture Function 120
7.6. Photomultiplier Tubes 120
7.6.1. The Choice of Tubes and their Deployment 120
7.6.2. Operating Conditions 122
7.6.3. Electronic Alignment 123
7.7. Control and Monitoring Electronics 124
7.7.1. Steering Monitoring and Control 124
7.7.2. Maintenance of Detector Performance (PMTs) 125
7.7.3. Environmental Monitoring 127
7.8. Logging Electronics 128
7.8.1. Amplification and Discrimination 128
7.8.2. Coincidence Units and Register 129
7.8.3. Scalers 129
7.8.4. The Logic Unit 129
7.8.5. The MC68000 Processor 130
7.8.6. Dead Time Events 131
7.8.7. Housekeeping 131
7.9. Timekeeping 132
7.9.1. The Rubidium Oscillator 133
7.9.2. Relative Timing 133
7.9.3. Absolute Timing 135
7.10. Modes of Operation 137
7.10.1. Tracking 137
7.10.2. Drift Scanning 137
7.11. Telescope Performance 138
7.12. Energy Threshold 139

Chapter 8 - Observations and Preliminary Results from the Mark III Telescope

8.1. Introduction 140
8.2. The Observing Programme 140
8.2.1. Pulsars 140
8.2.2. X-ray Binaries 143
8.2.3. "Galactic" Objects 144
8.3. The Database 145
8.4. Routine Data Analysis 145
8.5. The Guard Ring Technique for Improved Telescope Sensitivity 147
8.6. Results of Initial Data Analysis 150
8.6.1. LMC X-4 150
8.6.1.1. Research Background 150
8.6.1.2. Data and Results 151
8.6.1.3. Conclusions and Future Requirements 153
8.6.2. The Vela Pulsar 154
8.6.2.1. Research Background 154
8.6.2.2. Data and Results 157
8.6.3. Centaurus X-3 158
8.6.3.1. Research Background 158
8.6.3.2. Data and Results 160
8.6.3.3. Conclusions and Future Requirements 162
8.6.4. Supernova 1987A 163
8.6.4.1. Research Background 163
8.6.4.2. Data and Results 165
8.6.4.3. Future Observations 167

Chapter 9 - Discussion of Results and Future Work

9.1. Introduction 169
9.2. V.H.E. γ-rays from Isolated Pulsars 169
9.3. V.H.E. γ-rays from Radio Pulsars in Binary Systems 173
9.4. V.H.E. γ-rays from X-ray Binary Pulsars 174
9.4.1. The Energy Source 175
9.4.2. The Relationship between the γ-ray Emission and the X-ray Cycle 177
9.4.3. Bursts of γ-ray Emission 178
9.4.4. Conclusions 179
9.5. Improvements to the Mark III Telescope 180
9.5.1. The Guard Ring Technique 180
9.5.2. Improved Telescope Efficiency 181
9.5.3. The Mark III Telescope as a Survey Instrument 182
9.6. The Mark IV Telescope 183
9.7. Prospects for the University of Durham Telescopes 184
9.8. The Future of V.H.E. γ-ray Astronomy using the Atmospheric Cerenkov Technique 185

References 187

Acknowledgements 207

PREFACE

The University of Durham Mark III Very High Energy gamma-ray telescope was established near Narrabri , N.S.W., Australia during September 1986. The author was involved in the design , construction and commissioning of the telescope from 1984-6 , being responsible for the design , construction and testing of the detectors used on the telescope. The telescope is described in detail in Chapter 7. She was also responsible for the observing programme of the Mark III telescope. She took part in the first period of observing with the telescope in October and November 1986.

Along with her colleagues , she shared in the analysis of the first data from the Mark III telescope. The results of this preliminary analysis on four objects are presented in chapter 8.

In addition , the author was involved in the analysis of the data from the earlier experiment operated by the University of Durham in Dugway , Utah. The results of this analysis are presented in chapters 5 and 6 , together with a summary of the acheivements of the Dugway telescopes.

None of the material contained in this thesis has been submitted previously for admittance to a degree in this or any other university.

CHAPTER 1

AN INTRODUCTION TO GAMMA RAY ASTRONOMY

1.1. Introduction

The γ-ray region of the electromagnetic specrum extends from 10^6 eV (the so-called "soft" γ-rays) to 10^{16} eV (ultra high energy γ-rays). The systematic study of cosmic γ-rays is generally considered to have begun with a paper by Morrison (1958) which provided the stimulus for much experimental work. However, measurements of the flux of cosmic γ-rays in the upper atmosphere were made in the early 1950s using both balloons and rockets (Bergstrahl and Schroeder, 1951; Reiffel and Burgwald, 1954; Johnson et al., 1954), and the first attempt to measure cosmic γ-rays from a specific astronomical object was made in 1954 by J.V. Jelley and T. Gold when they observed the Crab nebula (see section 2.6). Attempts at observing cosmic γ-rays at balloon altitudes failed, largely due to the confusion caused by charged cosmic ray secondaries. The first firm detection of cosmic γ-rays had to wait until the flight of OSO-III in 1967 (Kraushaar et al., 1972). Measurements were made at $E>100$ MeV which indicated that there was a broad peak in emission towards the centre of the galaxy. During the 1970s the SAS 2 and COS-B satellite experiments, both of which carried spark chamber detectors, were particularly successful in mapping the galaxy and studying discrete sources such as the Crab and Vela pulsars. The study of

this region of the electromagnetic spectrum has been extended using ground-based observations around 10^{12} eV and 10^{15} eV. It is the former energy range with which this thesis is concerned.

1.2. Methods of Generation of Cosmic γ Rays

Methods of celestial γ-ray generation can be divided into four broad categories.

1.2.1. Nuclear Processes

The relaxation of a nucleus from a highly excited state to the ground state takes place via a number of energy levels, which gives rise to the production of several possible γ-ray lines. In astrophysical environments, the radioactive nuclei are usually produced by the impact of particles and quanta on the local medium. Such lines are to be found in supernova remnants. One process which has been identified involves ^{22}Ne, which is excited in many ways including neutron capture, radioactive decay, and collisional excitation. The nucleus then decays to the ground state producing γ-rays of energy 1.2746 MeV.

1.2.2. Annihilation of Particles with Antiparticles

When a positron and an electron annihilate, two or more γ-rays are produced. The interaction of two such particles at rest, when only two γ-rays are produced, is of particular interest since the result is a sharp γ-ray line of energy 0.511 MeV (which constitutes

the rest mass of an electron). Nucleons and antinucleons annihilate with the emission of pions, which brings us to:

1.2.3. The Decay of Elementary Particles

The neutral pion, produced either by the annihilation of a nucleon and antinucleon, or by the collision of two protons, decays on a timescale of about 10^{-16}s to produce two γ-rays. This gives a broad band of γ-ray energies and so is classified as continuum emission. This is only one of a number of decay mechanisms leading to the production of γ-rays (although possibly the most important in astrophysical terms). Many elementary particles are unstable and decay; when this decay is electromagnetic it is associated with the emission of one or more γ-rays.

1.2.4. Acceleration of Charged Particles

This is the most important group of γ-ray production mechanisms for astrophysical processes. There are three methods of importance: bremsstrahlung, synchrotron or cyclotron radiation and inverse Compton scattering. These are illustrated in figure 1.1.

Bremsstrahlung is the radiation produced when an electron is accelerated in the electrostatic field of a nucleus or any other charged particle. The radiation energy depends on the amount by which the electron's track is deviated - it is less for small deflections than for large ones. As very few electrons pass sufficiently close to nuclei to undergo a large deflection, most

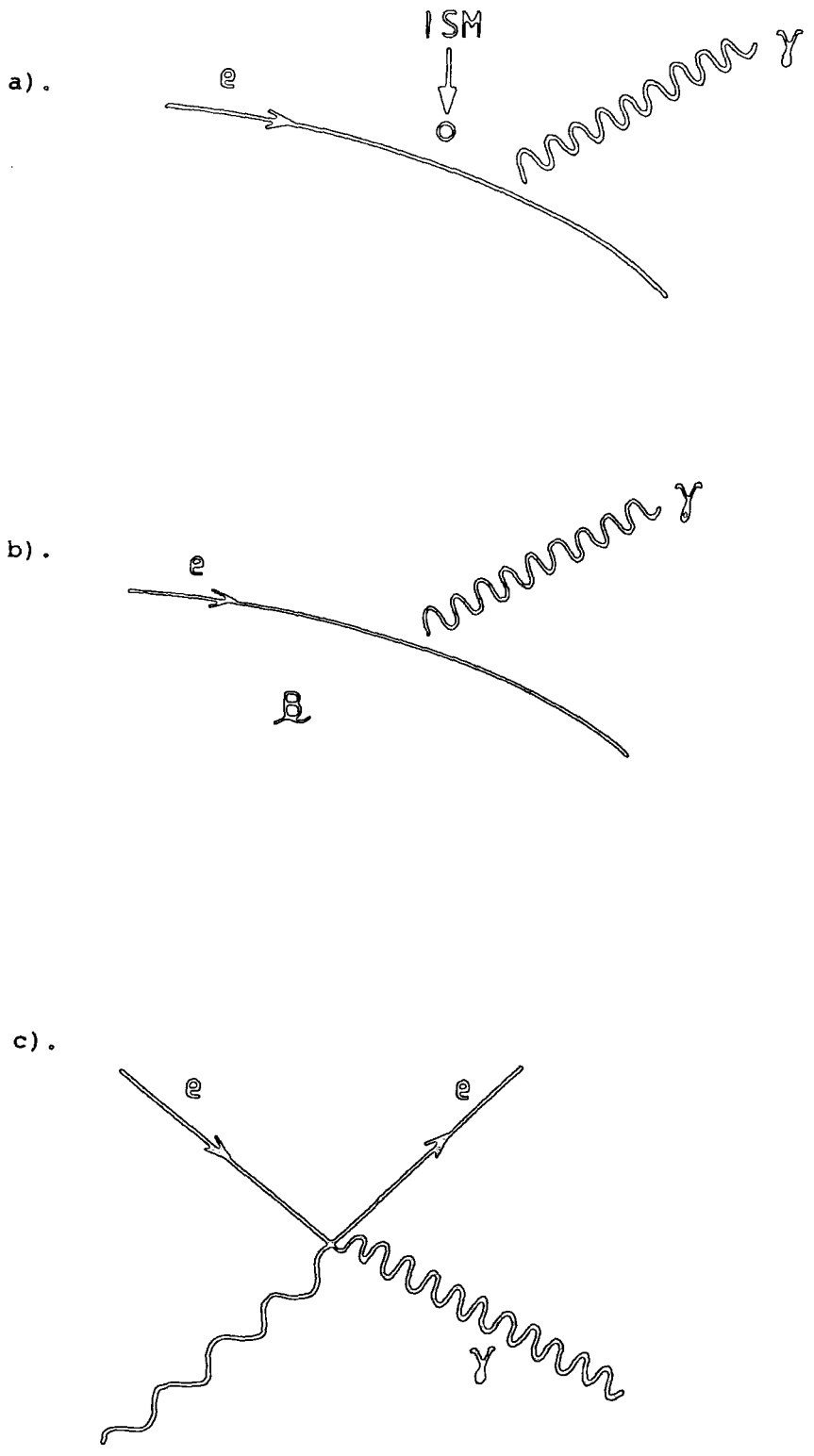

Figure 1.1 Methods of generation of cosmic gamma rays by the acceleration of charged particles: a). bremsstrahlung b). synchrotron radiation c). the inverse Compton effect.

photons produced in this way have energies at the lower end of the γ-ray spectrum. Regions of high matter density (even stellar atmospheres) are sites of production of γ-rays via this mechanism.

Both synchrotron and cyclotron radiation result from the interaction of electrons with a magnetic field. A change of direction of the electron results in a change of velocity vector, and thus radiation is emitted. When the radiation is produced by a non-relativistic electron it is known as cyclotron radiation. Synchrotron radiation is produced by relativistic electrons moving in a magnetic field. Cyclotron lines have been observed in the spectrum of the X-ray binary Hercules X-1 at energies of 53 keV (X-ray) and 106 keV (γ-ray) (Trumper et al., 1978) and possibly in another X-ray binary 4U0115+63 (Wheaton et al., 1979). The observation of such lines in the γ-ray region indicates the presence of a very strong surface magnetic field (about 10^8 T). In general, the importance of synchrotron radiation to γ-ray astronomy is that, when observed in other regions of the electromagnetic spectrum, it suggests the existence of relativstic electrons capable of producing γ-rays by other interactions such as bremsstrahlung or inverse Compton scattering. It may be important in the high magnetic fields in pulsar magnetospheres, though it seems likely that the γ-rays so produced would be absorbed soon after production (Smith, 1987).

The elastic scattering of photons by electrons is known as Compton scattering. The inverse Compton interaction is important

for γ-ray production. When relativistic electrons collide with photons, the photon is scattered to much higher energies (in the more usual Compton interaction the photon loses energy to a particle initially at rest.) The situation most often encountered in astrophysical conditions is the limit in which the energy of the photon in the centre of momentum frame of the collision is much less than the rest mass energy of the electron i.e. $\gamma h\upsilon << mc^2$. In the interstellar medium, the photon involved is usually from the 3K background (in which case a low energy (10 MeV) photon is produced) or an optical photon (which produces γ-rays of typical energy 100 MeV).

1.3. The Absorption of Cosmic γ-Rays

Interactions of γ-rays with matter are not important for photon energies > 100 keV, as the interaction cross section with matter in the galaxy is negligible. The two main processes of importance are:

a) Absorption by low energy photons

b) Absorption in magnetic fields

These are essentially the same process: in case b), the γ-ray is scattered by a "virtual photon" from the magnetic field.

Process a) is the inverse of electron-positron annihilation and occurs whenever the combined photon energy is $\geq 4m^2c^4$ where m is the mass of the electron. The maximum cross-section for this process is 1.7×10^{-25} cm^2 (Greisen, 1971), which occurs at an energy

of about twice the threshold value. Since the cross-section for this process is so small, absorption of γ-rays by starlight is only important over large intergalactic distances. However, absorption by the microwave background is important within the galaxy (Nikishov, 1961) - cascade processes impose a "cut-off" around 10^{14}eV, when the γ-rays are severely attenuated for those sources further than 10kpc from earth. This view was modified by the detection of γ-rays at energies > 10^{15} eV from Cygnus X-3 (Stamm and Samorski, 1983), a source which is almost certainly at least 10 kpc away.

Absorption of γ-rays by pair production in a magnetic field may only occur if the magnetic field is very intense (about 10^{8}T), as discussed by Erber (1966) and Ogelman et al. (1976). The only known site of such strong magnetic fields is near the surface of a neutron star. It is concluded that γ-rays emitted by pulsars are produced some distance away from the surface of the neutron star.

1.4. The Detection of Gamma Rays

Since the γ-ray region of the electromagnetic spectrum covers an equivalent range in wavelength as, say, from shortwave radio to ultraviolet radiation, it is clear that many different techniques will be employed to detect cosmic γ-rays. All systems do, however, rely on measurement of the electrons produced when a γ-ray interacts with matter.

1.4.1. Energies Between 0.5 and 3 MeV

Throughout this energy range, Compton scattering in the detector material is the most important interaction. Since the direction of motion of the electron thus produced is not necessarily correlated with the direction of energy of the γ-ray, telescopes designed to detect photons of this energy usually consist of a detector measuring the energy of the γ-ray placed behind a collimator. The two main types of detector are scintillation counters and solid state detectors.

A scintillation counter consists of a scintillator which is either an inorganic crystalline material (NaI for instance), or a plastic loaded with a scintillating organic compound. In a small detector, a photomultiplier is optically coupled to one face of the scintillator. With larger detector areas, only a small fraction of the scintillator can be covered by the phototube, and so a light guide or diffusing light box must be employed.

Solid state detectors are used when energy resolution is important. Large area detectors are required for γ-ray astronomy, and so Ge or Si types are used. Both must be operated at low temperatures for good energy resolution.

1.4.2. Energies between 3 MeV and 10 GeV

The predominant interaction of γ-rays with matter at these energies is pair production. In this process the direction of the secondary particles is closely aligned to that of the original

γ-ray photon, and they are of sufficient kinetic energy not to undergo undue scattering. Spark chambers may thus be used to detect the secondary particles. Most of the spark chambers used have electrodes in the form of wire grids to locate the spark positions. They were employed very successfully on the SAS 2 and COS-B satellites and will be used again on the NASA Gamma Ray Observatory which is due to be launched from the space shuttle towards the end of the decade.

1.4.3. Energies between 100 GeV and 100 TeV

As energy increases beyond 10 GeV, the primary photon flux becomes so low that spark chambers cannot be made large enough to have any chance of recording a reasonable count rate. At still higher energies, however, another method becomes possible. This is the detection of atmospheric Cerenkov light produced by the cascade of charged particles initiated by a primary high energy γ-ray entering and interacting with the earth's atmosphere. This technique will be discussed in much greater detail in Chapter 2.

1.4.4. Energies > 100 TeV

At ultra high energies it becomes possible to detect at ground level the particles produced in the atmosphere by the primary γ-ray photon. The lateral extent of the air shower, as well as its penetration through the atmosphere, is of importance since a detector at ground level which is some distance from the projected

impact point of the primary may still record a signal, thus increasing the effective detector area. The extensive air showers can be detected with an array of charged particle detectors. Directional information can be obtained by the well-established inter-detector fast timing techniques. This method has been successfully refined in recent years to give arrival directions of sufficient accuracy to allow point source identification and is used by groups working at Haverah Park, Leeds; Kiel, West Germany; Plateau Rosa, Italy; Los Alamos, New Mexico; and Akeno, Japan.

CHAPTER 2

THE DETECTION OF V.H.E. GAMMA RAYS USING THE ATMOSPHERIC CERENKOV TECHNIQUE

2.1. Introduction

The detection of celestial γ-rays of energy 10^{12} eV (V.H.E. γ-rays) using the atmospheric Cerenkov technique relies on the detection of the Cerenkov light produced by the cascade of fast particles generated in the atmosphere as a result of primary high energy γ-rays impinging on the earth's atmosphere. This method is the only one available for studies of γ-rays of this energy and is likely to remain so for physical reasons. The flux of V.H.E. γ-rays is so low (of the order of 10^{-10} cm^{-2} s^{-1}) that in order to detect a reasonable number of photons a satellite-borne detector would be prohibitively large. The advantage of the atmospheric Cerenkov technique is that it is ground-based, and therefore relatively simple and inexpensive compared with satellite-borne detectors. Of extreme importance is the fact that Cerenkov detectors have large effective collecting areas since the collecting area is defined by the size of the pool of light on the ground rather than the dimensions of the detector itself. This pool of light has a typical area of 10^4 m^2.

The major limitation of this technique is that there is no simple way of distinguishing between the γ-ray induced airshowers

and those essentially similar signatures produced by the more abundant cosmic-ray protons. Very High Energy γ-ray Astronomy in its simplest form must therefore depend on the spatial and temporal anisotropy of γ-rays in contrast to the isotropic cosmic ray particles.

2.2. The Cerenkov Effect

When a fast charged particle traverses a dielectric medium at a velocity in excess of the phase velocity of light in that medium, an optical shock wave is produced around the track of the particle in the medium. This is known as Cerenkov radiation. It was noted by Mallet (1926) as the blue light generated by the products of radioactive decay passing through dense dielectrics. Quite independently, it was studied experimentally by Cerenkov (1934, 1937) and was given the first theoretical treatment by Frank and Tamm (1937) based on classical electromagnetic theory. The following is a short account of that theory drawn from reviews by Jelley (1958) and Boley (1964).

Cerenkov radiation is emitted by a charged particle passing through a dielectric medium if:

$$\beta n > 1 \qquad 2.1$$

where $\beta = v/c$ and n is the refractive index of the medium. From this it is clear that radiation may only be emitted in the U.V., visible, I.R., and microwave regions of the electromagnetic spectrum. As the particle passes through the medium, Cerenkov

radiation is emitted by each single element of track. Due to the constructive interference of wavelets of light from each part of the track, the radiation is emitted at an angle Θ with respect to the direction of motion of the particle. This can be seen clearly from a Huygens construction (see figure 2.1). The requirement for coherence is:

$$\cos \theta = 1/\beta n \qquad 2.2$$

This is known as the Cerenkov relation and leads back to the equation 2.1. For $\beta = 1$, the maximum angle of light emission is given by:

$$\cos \theta_{max} = 1/n \qquad 2.3$$

Since the system has axial symmetry, the light wavefront has a conical form in three dimensions whose axis coincides with the particle track and whose semi-apex angle is θ. The light wave front propagates at a velocity c/n.

Frank and Tamm (1937) also derived a relation which gives the rate of production of radiation, W, with path length, l as:

$$dW/dl = \frac{e^2}{c^2} \int_{\beta n>1} (1- (\beta n)^2) \omega d\omega \qquad 2.4$$

where ω is the mid-band frequency and d the bandwidth; e is the charge on an electron. In air it is found that, if n is taken as 1.00029, β =1, and θ_{max}= 1.3°, dW/dl = 30 photons m^{-1} between 350 and 550 nm.

The original classical theory summarised above made no attempt to include the effects of radiation reaction. However, since the

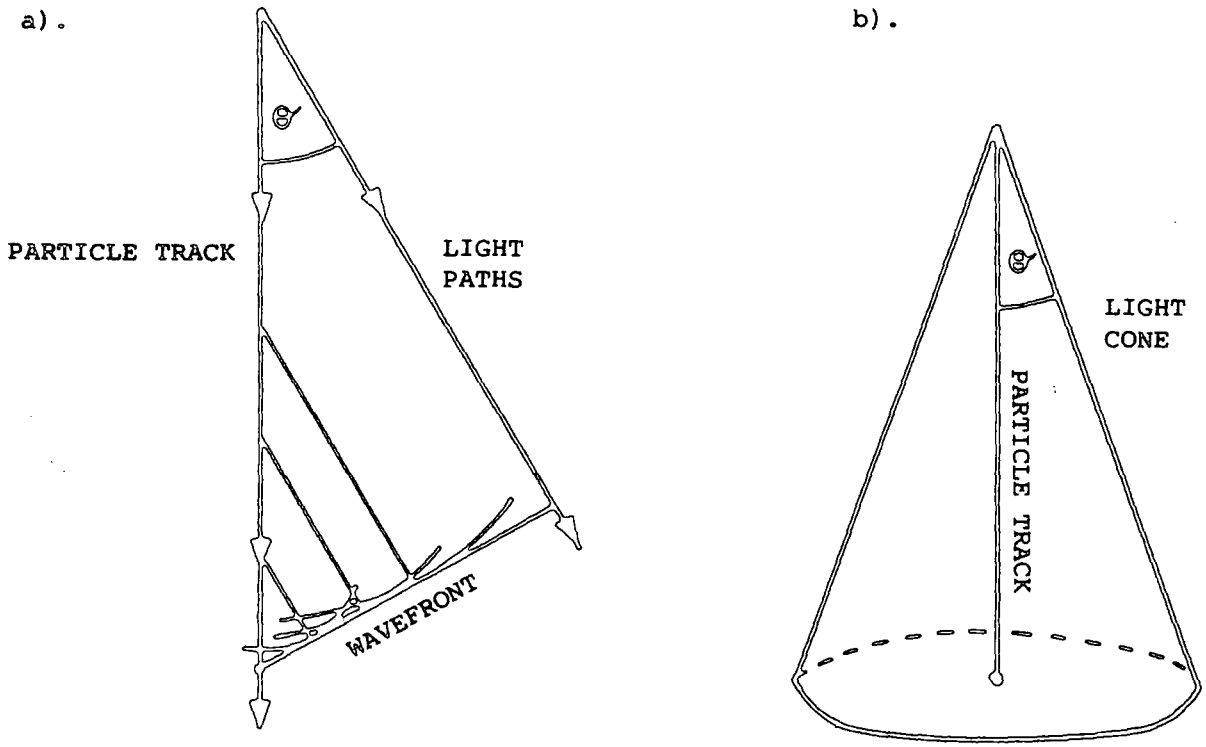

Figure 2.1 a). Huygens construction to illustrate the coherence of Cerenkov radiation.
b). The formation of the Cerenkov cone.

energy carried away is very small when compared with the kinetic energy of the particle concerned these recoil effects are negligible, as demonstrated by Ginsburg (1940) and Cox (1944).

2.3. The Discovery of Cerenkov Radiation from the Night Sky.

Blackett (1948) first suggested that Cerenkov radiation would be produced in the atmosphere by the general flux of cosmic rays. These were calculated to contribute a fraction of about 10^{-4} of the total background light of the sky on a dark night, making it almost impossible to detect. However, it was later realised (Galbraith and Jelley, 1953) that extensive airshowers would produce a strong pulse of Cerenkov light, as in this case many particles move through the atmosphere together (the resultant flash of light being about 10 ns in duration). Galbraith and Jelley made the first measurements of Cerenkov light in the atmosphere. Their apparatus consisted of a 25cm f/0.5 parabolic World War II signalling mirror placed in a dustbin with an EMI phototube at the focus coupled to the fastest amplifier then available (0.032 ns rise-time), a pulse height discriminator and a triggered oscillator. Superimposed on the "noise" due to the background light, single pulses were observed at a rate of about 1 per minute when the apparatus was pointed at the zenith on a clear moonless night. These first experiments were repeated by Nesterova and Chudakov (1955), and then in more detail by other experimenters such as White, Porter, and Long (1961) and Boley et al. (1961).

2.4. The Characteristics of Υ-Ray Initiated Cerenkov Radiation

2.4.1. The Threshold Energy for Emission

The energy E of an electron of mass m and velocity v is given by:

$$E = mc^2 \left(1 - (v/c)^2 \right)^{-0.5} \qquad 2.6$$

From equation 2.1, it can be seen that the minimum energy for emission will occur when $v = c/n$, i.e.:

$$E_{min} = mc^2 \left(1 - 1/n^2 \right)^{-0.5} \qquad 2.7$$

Now, since the refractive index of air varies as a function of pressure and temperature, E_{min} will clearly depend on height above sea level. At sea level, with $n = 1.00029$, electrons have a threshold energy of 21 MeV for emission of Cerenkov radiation. About 85% of shower electrons have energies greater than threshold at sea level and, averaged over the whole shower, about 36% have energies greater than 50 MeV (Richards and Nordheim, 1948).

2.4.2. Lateral Distribution of Light

The size of the light pool produced by an extensive air shower (EAS) initiated by a high energy Υ-ray is defined as the radius (R_o) at which the photon density has fallen to 1/e of its maximum value. It is heavily dependent on the depth of the maximum of the air shower - the nearer the earth's surface this is, the greater the radius of the light pool. R_o is also determined by the Cerenkov angle of emission and the Coulomb and geomagnetic

scattering of the particles in the shower. Since, in general, the r.m.s. scattering angle is much larger than the Cerenkov angle, the angular distribution of the light pool is effectively that of the particles themselves. Detailed computer simulations (Browning and Turver, 1977) taking these effects into account suggest that the maximum radius of the light pool is between 400 and 450 metres, although the radius of the light pool which may be usefully measured is 100-200 m, when the angular acceptance of a typical γ-ray telescope (less than 2^{o}) is taken into account. Simulations by Macrae (Ph.D thesis, 1985) indicate that the typical effective light pool radius of a shower which is produced at a given height in the atmosphere varies between 45m and 110m.

2.4.3. Angular Distribution of Light

As already mentioned, the angular distribution of the light , looking down the shower core from high in the atmosphere, is in general determined by the angular distribution of the particles themselves. It is more important from the point of view of γ-ray astronomy to determine the angular distribution of the light across the image as seen by a detector pointing towards the sky. It is useful for practical reasons, such as the choice of field of view for optimum signal to noise ratio, and also for the optimisation of detectors relying on the measurement of the diameter of the image to improve the telescope's response to γ-rays (Turver and Weekes, 1978).

The general shape of the shower spot arises from the relative geometry of the shower trajectory and the detector axis. A shower whose trajectory coincides with the detector axis gives a circular light spot, but it is elliptical in the off-axis cases. The shapes of the light spots have been predicted by Monte Carlo simulations (Rieke 1969; Browning and Turver 1977; Hillas 1986). As the separation, d, between the detector axis and the shower axis increases, the ellipticity of the shower spot increases and the peak of the light intensity shifts towards the tail of the distribution. The collection area for γ-ray detection is therefore limited both by the displacement of light maximum with d and the detector aperture. For a 1^{o} detector the maximum d is about 50m, giving a collection area of 10^{4} m^{2}.

2.4.4. Absorption and Scattering in the Atmosphere

The atmospheric attenuation of Cerenkov light is primarily due to Rayleigh scattering, aerosol scattering and ozone absorption. As might be expected, the amount of attenuation depends on wavelength and altitude. Rayleigh scattering depends on the molecular number density. Scattering by aerosols (particles of 1-10 μm in diameter) depends both on their sizes and their number density, and is most important near ground level. Ozone absorption is important only at high altitudes and for wavelengths < 290 nm. As the refractive index of air varies very little over the visible region of the spectrum, dispersion is negligible. Refraction and diffraction effects are also small. For a detailed account of the

attenuation processes and their consequences see Protheroe (Ph.D. thesis, 1977).

2.5. Experimental Techniques

A γ-ray telescope using the atmospheric Cerenkov technique requires a flux collector (i.e. a mirror of modest optical quality) with a detector (a photomultiplier tube or image intensifier) at its focus. Since the Cerenkov light pulse produced by a shower has a duration of about 10 ns, the photomultiplier tube (PMT) and its associated electronics must have a fast response in order to achieve a good signal-to-noise ratio. Also, since variations in sky brightness may produce changes in the count rate of a V.H.E. γ-ray telescope (see section 6.6.4.), the maintenance of a constant anode current is desirable. This is usually achieved by shining a light source (a green LED for instance) onto the face of the PMT and using a servo system to vary its brightness such that the total anode current of the tube due to sky brightness and remains constant.

The greatest problem in V.H.E. γ-ray astronomy is that there is not, as yet, any reliable method of clearly distinguishing Cerenkov pulses produced by γ-ray induced showers from those produced by the much more numerous nucleons. Fortunately, the background due to the cosmic ray protons is both spatially and temporally isotropic, whereas it is expected that γ-ray sources will in general be point sources and in many cases may produce periodic γ-rays. In order to reject as many proton-induced showers as possible the angular

acceptance of a γ-ray telescope must be no larger than the angular dimension of the light spot on the sky: too small, and light from γ-ray induced showers will fall outside the field of view of the telescope and be lost; too large, and the number of nucleon induced background pulses detected will rise unnecessarily. Simulations by the Durham Group (Macrae and Turver, 1982, unpublished) suggest the optimum angle is about 1.3^{o} and those made more recently by Hillas and Patterson (1987) confirm this value.

To further improve the signal-to-noise ratio, the use of two or more flux collectors in fast coincidence is essential: the possibility of an accidental coincidence between the detectors is effectively reduced to zero by the use of three collectors in coincidence. This also allows the use of the lowest possible energy threshold. Such a method has been applied on all telescopes operated by the University of Durham.

2.6. Astronomical Observations Using the Atmospheric Cerenkov Technique

The first use of this technique as a tool for astronomical research was by Jelley and Gold in 1954 (Jelley, 1986). A small mirror-phototube combination was taken to the Royal Greenwich Observatory at Herstmonceux and attached to the barrel of a 6" refractor. A search was made for cosmic rays from the Crab nebula, with negative results. A detector was then constructed by Chudakov et al. in the Crimea in 1961 (Chudakov et al., 1962). In 1962 they

performed experiments in which scans were made across the four radio sources Cygnus A, Cas A, the Crab nebula and Virgo A. Results were negative, but proved the efficacy of the method provided detectors could be made more sensitive. In 1964, a group from University College Dublin was established at Glencullen, Eire using equipment constructed by Jelley and Porter (1963). In 1970, this group moved to Malta and in the same year observations commenced at Narrabri, N.S.W. Australia and at the Mount Hopkins Observatory. The latter has since been renamed The F.L. Whipple Observatory. In 1977, a single Cerenkov detector was commissioned at Ootacamund, India. With the exception of those in Ireland and Malta, all these observatories are still functioning. The University of Durham operated an array of four spaced telescopes in Dugway, Utah from 1981 to 1984, when the system was dismantled (see section 2.7).

More recent experiments include an array of four detectors operated by the Crimean Group at high altitude, and a system built by the University of Potchefstroom, South Africa. The University of Durham group has constructed a new telescope (the Mark III) which is now operating near Narrabri, Australia. This thesis will describe the Mark III telescope in detail. Recently, Cerenkov detectors have been completed at Haleakala, Hawaii, Gulmarg and Pachmari in India, and at White Cliffs in New South Wales. At the time of writing, a second new Durham University telescope (the Mark IV) is being built in Durham for proposed deployment in La Palma, Canary Islands.

2.7. The University of Durham Facility at Dugway, Utah

An array of four V.H.E. γ-ray telescopes was established at Dugway Proving Grounds, Utah (40.2°N, 112.82°W, altitude 1450 m a.s.l.) by the University of Durham during the early Summer of 1981. The system comprised four telescopes operated and steered under computer control. The data logging system was comprehensive, and used modern electronics. Long exposures were made of some 7 objects, in particular the Crab pulsar (137 hours), Hercules X-1 (32 hours) and Cygnus X-3 (350 hours). The last observations were made with the system on 29th September 1984.

2.7.1. The Mark I Telescope

The observatory originally comprised an array of four telescopes arranged in an equilateral triangle with one telescope at each apex and one in the centre. Each telescope consisted of three paraxial parabolic searchlight mirrors of 1.5 m diameter mounted on a computer-controlled altazimuth platform which gave a steering accuracy of 0.1°. One 12.5 cm photomultiplier tube (PMT) was placed about 8 cm behind the Cassegrain focus of each mirror, with a circular aperture of diameter 5 cm positioned at the focus in order to define a geometrical field of view of 1.75° FWHM. A cylindrical baffle was placed around each secondary mirror in order to protect the PMT from direct illumination by the night sky. The telescopes were also equipped with a paraxial low light CCTV camera capable of detecting 6th magnitude stars to maintain a check on steering accuracy.

The photomultiplier tubes used were RCA 4522 tubes (available from a previous experiment), which are fast, linear-focussed tubes of diameter 12.5 cm. The photomultipliers were used with a defocussed image in order to illuminate the whole face of the tube. If the PMTs had been placed at the Cassegrain focus, both Cerenkov pulses and any bright stars appearing in the field of view would have been focussed onto the photocathode, resulting in an intensely illuminated region. The use of a slightly unfocussed image avoids problems introduced by the non-uniformity of the quantum efficiency of the photomultiplier tube photocathode.

Since the detection of Cerenkov light-pulses requires a fast response from the PMT, the tubes used at Dugway were operated with a high field per stage requiring a typical EHT of 1800V, and the signal was extracted from the 11^{th} dynode rather than the anode. Typical sky brightness induced currents under such conditions were 5μA. Individual detector rates were set at about 1 kHz at a discrimination level corresponding to an estimated photon threshold of 50-100 photons m^{-2}. Servoed green LEDs were available to stabilise the anode current.

The mirrors used on the Mark I telescopes were army surplus searchlight mirrors. Their optical quality was low and the focal lengths short (60 cm). In an attempt to improve the optical arrangement, the mirrors were operated in the Cassegrain mode, which entails a loss of light as an additional reflecting surface is required.

2.7.2. The Mark II Telescope

During 1983, in an effort to overcome the restrictive optics enforced by the use of surplus searchlight mirrors, one of the detectors was re-mirrored with purpose-built solid aluminium mirrors of 60 cm diameter and focal length 2.2 m. The mirrors were arranged in three hexagons of seven mirrors each with a 2" RCA 8575 PMT at the prime focus of each hexagon ensemble. The geometrical field of view was now reduced to 1.25^{o}, after the experience gained in tracking sources with the Mark I telescopes. Operation of the modified system next to the original detectors showed that the narrowing of the field of view was successful in improving the ratio of detected γ-rays to background cosmic ray events. This was the first instance of such an "in field" improvement in telescope performance. For comparisons of the characteristics of the two telescopes see table 2.1.

2.7.3. Information Recorded

After the detection of a 3-fold coincidence from any one of the four spaced telescopes, the following data were recorded on magnetic tape:

(i) The relative time of occurrence of the light flash, with a resolution of 1μs using an oven-controlled crystal as a timebase (accurate after correction to 1 part in 10^{9}). The clock was regularly synchronised using an off-air signal from radio station WWV at Fort Collins, Colorado. The UT was accurate to about 0.3 ms,

	MARK I	MARKII
DISH AREA	1.77 m^2	2.04 m^2
APERTURE	50 mm	40 mm
FOCAL LENGTH	1.5 m.	1.9 m.
FIELD OF VIEW	1.75^o	1.2^o
REFLECTIVITY	0.35	0.55
COUNT RATE	15 C.P.M.	11 C.P.M.
THRESHOLD	1300 GeV	800 GeV

Table 2.1 Characteristics of the Mark I and II telescopes.

limited by the accuracy of the clock's off-air synchronisation and uncertainties in the propagation of the ground wave radio signal.

(ii) The relative arrival times of signals from other telescopes occurring within a specified gate time. Actual times were accurate to less than 1 ns.

(iii) The charge in the pulse from all 12 PMTs, in the range 0-250 pC, with 0.1 pC per bit resolution.

The atmospheric pressure, temperature, anode currents and individual PMT rates together with the number of coincidences between any two mirrors in each telescope and the accidental 3-fold rate were also recorded every minute.

2.7.4. General Performance

The aggregate counting rate of the system was about 50 min^{-1} near the zenith. Individual telescopes each counted 3-fold coincidences at a rate of about 12-20 min^{-1}. Two telescopes responded at a rate of 10 min^{-1} and three or more telescopes at a rate of 5 min^{-1}. The rate of spurious events recorded due to photomultiplier tube noise was always less than about 1 per hour.

CHAPTER 3

DATA ANALYSIS TECHNIQUES FOR USE IN GAMMA-RAY ASTRONOMY

3.1. Introduction

The data on electromagnetic radiation in the V.H.E. γ-ray region is characterised by the arrival times of single photons, often at a low count rate and in a series of observations each lasting 3-4 hours which may be spread over intervals of a few months. The measurements are also subject to a very high "noise" level from the near identical Cerenkov flashes produced by atmospheric showers initiated by cosmic ray protons. These two problems require that the analysis of V.H.E. γ-ray data be carried out with care, using appropriate statistical techniques.

This chapter provides an overview of the analysis routines applied to data from the Dugway facility and from the Mark III telescope at Bohena Settlement, N.S.W. Prior to any analysis, the data from all experiments are translated into a standard format, first employed in the Dugway Project. This pre-processing is described. The routine methods of data analysis are then discussed: these include the analysis of count rate and timing data taken whilst continually tracking the source (periodicity searches) and the analysis of data taken in the drift scan mode. Finally, the calculation of fluxes and flux limits is described.

3.2. Format of Data Files

Data from both the Dugway and Mark III telescopes are recorded on magnetic tape. The Dugway telescopes used a standard 1600 bpi 9-track tape of 20Mb capacity. In the case of the Mark III telescope the data tapes used are 3M DC600 tape cartridges with a capacity of 68 Mb. Data recording and formatting for the Dugway experiment has already been described in detail (Kirkman, Macrae, Dowthwaite, Ph.D. Theses) and this work will therefore be confined to the description of the preprocessing of data from the Mark III telescope.

The information recorded during one night's observation is:

a) A Run Start File, containing:

(i) Civil and Julian dates of the observation

(ii) Identity of observers

(iii) Comments on, for example, weather and telescope performance

(iv) Mapping of the assignment of data recording channels (servoed photomultiplier gain control system, discriminator threshold for pulse recording, pulse digitisers, HT power supply voltages, photomultiplier anode currents)

(v) A record of the photomultipliers in use

(vi) Weather information (cloud cover, sky clarity, temperature, wind speed and direction)

(vii) Mapping of the allocation of scalers which record the count rate from each set of 3 photomultiplier tubes in coincidence.

b) A Source Start Data File, containing:

(i) Source name and position

(ii) Time of run start

(iii) Observatory position

(iv) Steering (offsets) for the telescope

(v) Comments.

c) A Data File. For each event, the following is recorded:

(i) The time of the event

(ii) The size of the pulse produced by each PMT which responded

(iii) Instantaneous anode currents in the 3 on-source photomultipliers and 5 of the off-source photomultipliers

(iv) Telescope position and drive status

(v) A record of which of the photomultipliers responded.

In addition, every minute the following information is also recorded:

(i) Instantaneous values of all photomultiplier anode currents

(ii) Weather information

(iii) The contents of all scaler channels giving data on the single-fold responses from each PMT during a one second sample period.

These data are recorded in a compact format to economise on the space taken up on tape, so it is necessary first of all to translate the data into an easily read form. Once this has been accomplished (at present using the VAX 11/750 of the Durham Starlink node), the information is translated into ASCII format and split up into "source" files, each of which contains data on a single observation of one

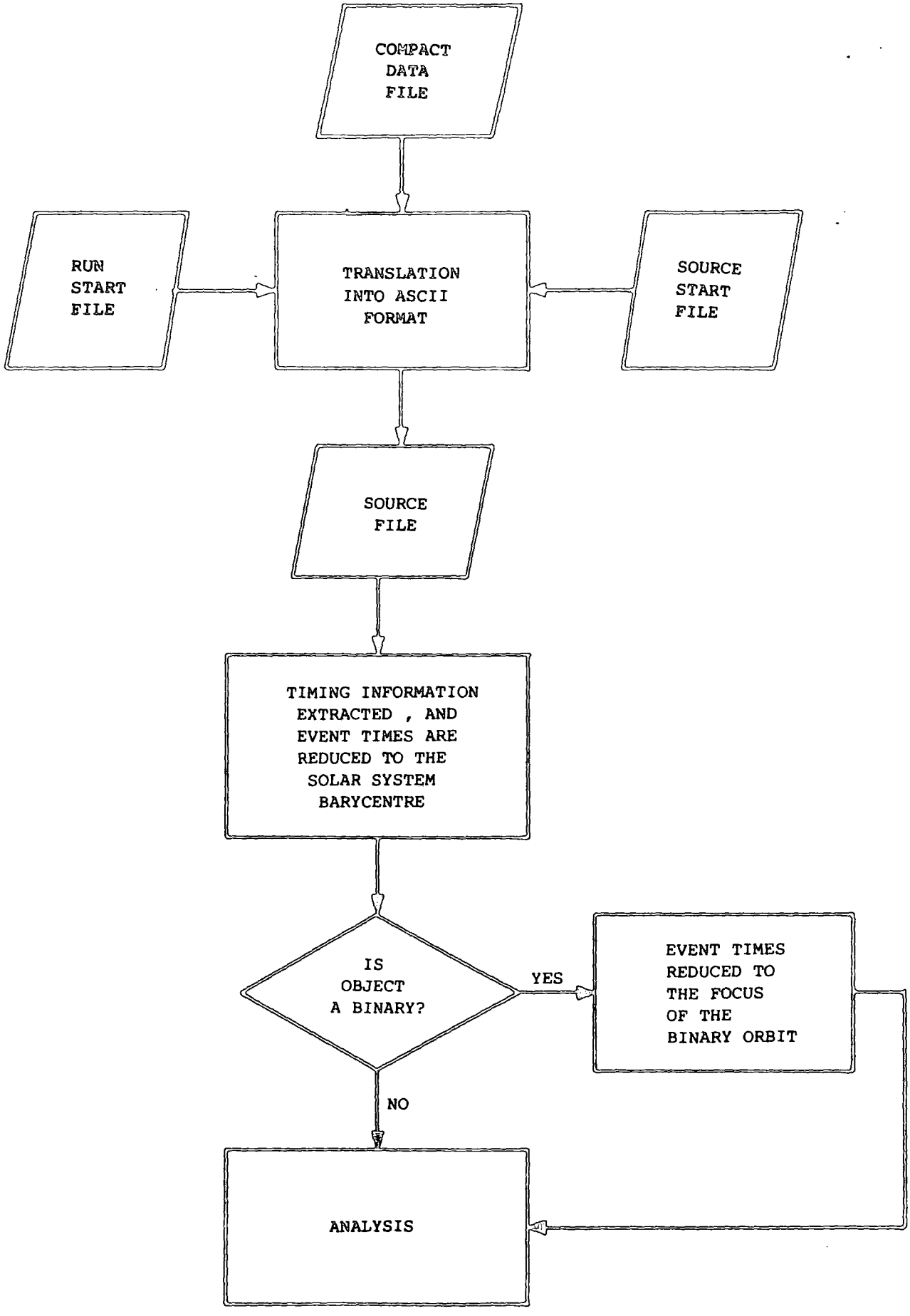

Figure 3.1 Schematic diagram showing the routine processing of data from the Mark III telescope.

object. Since most of the analysis routines employ the arrival times of the Cerenkov pulses, the times of events together with an indication of the channels which responded only are stripped from these files and are stored as 14 decimal digits, of which the last 6 are microseconds. This extraction of timing data also reduces the size of the dataset. The process is represented schematically in figure 3.1.

3.3. Count Rate Analysis

Once the data have been rearranged into the standard format, and the times extracted, the count rates for all off-source and on-source channels are routinely analysed. The count rate analysis of data from the Mark III telescope involves binning the Cerenkov pulses recorded each night into one minute bins. It is then possible to plot the count rate as a function of time for each object observed on each night. The events recorded from the one on axis and three off axis channels, each of which consists of 3 PMTs in coincidence, are plotted separately, and a plot is also produced for all events on all channels. A four-colour printer is employed for this purpose. The reason for this routine count rate analysis of data is two-fold:

a) Quality Control

The data are checked with reference to the relevant observers' log to identify any obvious variations in count rate produced by the experimental conditions: a highly variable count rate due to

cloud intermittently passing over the source, for instance, would be suitable for short-period searches only.

b) Detection of DC Emission from Sources

If the object on which data have been collected is producing bursts of γ-rays, it may be possible to identify the larger bursts simply by inspecting a plot of count rate versus time. The statistical significance of such episodes may then be assessed, and if they are significant they may then be extracted and further analysed by using statistical tests for periodicity for example. Smaller but non-statistical variations must be identified by separate procedures (see section 3.10).

3.4. Adjustments to the Times of Arrival of γ-rays.

If searches for periodicity within γ-ray data are to be made successfully, it is necessary to allow for those effects which may corrupt the periodicity of the pulse arrival times. Clock errors are corrected for, and variations in pulse arrival times due to the motion of the observer are removed by correcting all event times to the Solar System barycentre. If the source observed is in a binary system, an additional correction must be made to take into account the Doppler shift in the pulse arrival times induced by the motion of the γ-ray source around the barycentre of the system.

3.4.1. Clock Uncertainties

There are two corrections which must be made. First, a

correction is made to the relative time of arrival of events. This arises because the crystal oscillator used may not have a constant rate. Secondly, there are uncertainties in the absolute time of the occurrence of an event for which a correction must be made. For further details of timing procedures see section 7.8.

a) Clock drift rate

The first task is to correct the event times for changes in the system clock. Regular measurements of the clock time compared with the radio timing pulses used to synchronise the clock are made to facilitate this. Initial measurements of the Rb clock used in Australia indicate that, over a period of approximately 4 months, the difference between clock time and radio time is very small, the clock having a slip rate with respect to the radio signal of approximately 0.8 ms per month (see section 7.8). The Dugway clock, which featured a high quality crystal, was deliberately set to run slightly fast and had a typical drift rate of 24 ms day^{-1}; considerable corrections were necessary to achieve accuracy of 1 part in 10^9 (see Kirkman, Ph.D. thesis).

b) Radio Signal Propagation Time

A correction must also be made for the delay in the propagation of the radio signal used to synchronise the clock from the transmitter to the observatory. In the case of Lyndhurst to Bohena the delay is approximately 6 ms, an accurate measurement having been made at the Anglo-Australian Observatory which is approximately

100 km from the Mark III site. Observations have not as yet (June 1987) required the use of absolute timing techniques. For observations at Dugway, Kirkman (1985) has demonstrated the validity of a delay of approximately 2.5 ms using the Crab pulsar as a timing reference.

3.4.2. The Adjustment of Event Times to the Solar System Barycentre

There are three stages in this process:

a) Translation of event times to the centre of the Earth

b) Translation of event times to the Solar System barycentre

c) Application of relativistic corrections.

These are described below.

a) Translation to the centre of the Earth

The event times are translated to a point at the centre of the earth to allow for the Doppler effect due to the motion of the observer on the surface of the rotating Earth. This requires precise knowledge of the observatory's geographical co-ordinates. The correction is typically a few milliseconds.

b) Translation to the Solar System barycentre

The second translation is to the Solar System barycentre, which removes the Doppler effect on the pulse arrival times induced by the Earth's orbital motion. The position of the Earth in its orbit at the event time is found using an Earth ephemeris. All Dugway data were corrected using the Massachusets Institute of Technology Earth ephemeris produced by Ash et al. (1967),

since this was used at Jodrell Bank for their measurements of the Crab pulsar. Data from the Mark III telescope are, however, corrected using the Jet Propulsion Laboratory ephemeris. This was necessary because of the changeover by the astronomical community from the MIT ephemeris to the JPL ephemeris. The ephemerides contain the X, Y and Z co-ordinates of the earth for every two hours. A polynomial is fitted to the separate X, Y, and Z co-ordinates to deduce the accurate earth position at the time of arrival of the event, and a timing adjustment is made to the Solar System barycentre for the event in question. The Solar System corrections can be as large as 200 seconds.

c) Relativistic correction

The final correction to be made is to take into account relativistic effects on earth-based clocks orbiting the sun. The correction is of one or two milliseconds' magnitude.

3.4.3. Focusing Event Times to the Barycentre of a Binary Orbit

For X-ray binary objects, which are of considerable interest in γ-ray astronomy, the source is considered to be a pulsar in orbit around a main sequence companion. In observations of such sources, the motion of the pulsar around its companion produces a Doppler shift in the γ-ray arrival times. So, if a successful search for the periodic γ-rays from the pulsar is to be made, the event arrival times must be adjusted to the barycentre of the binary system in which they originated in order to allow for this

effect. The contemporary orbital parameters of the system must be well known to accomplish this. The orbit of a binary system is completely specified by:

a) The binary orbital period P

b) The time t_o of periastron passage

c) The eccentricity e

d) The distance ω between the periastron and the node

e) The product of the semimajor axis a and the sine of the inclination angle along the observer's line of sight, i.

f) The position angle, Ω, of the node.

These parameters are illustrated in figure 3.2. For X-ray binary pulsars, a complete set of parameters is often not available, but it is possible to adjust event times given P, e, and ω from an estimate of the mass function.

The arrival time is calculated from:

$$\phi(t) = \phi_o + W(t-t_o) + \tfrac{1}{2}W(t-t_o)^2 + W(RSP^{-1}-1) \qquad 3.1$$

where

$Q = fg + h\sin E$

$R = g\sin E + h\cos E$

$S = (1 - e\cos E)^{-1}$

$f = \cos E - e$

$g = a\sin i.\sin\omega$

$h = (1-e^2)^{0.5}\, a\sin i.\cos\omega$

P = orbital period

W = longitude of periastron

E = eccentric anomaly

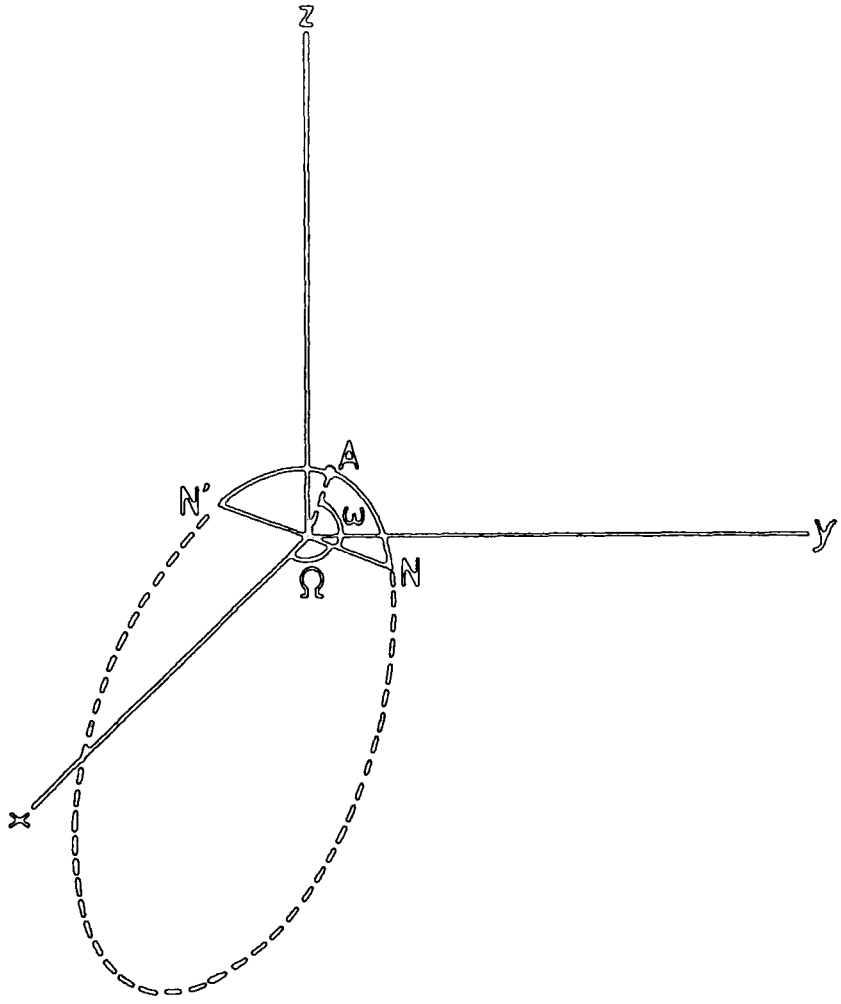

Figure 3.2 The orbital elements of a binary system. The centre of the co-ordinate system is located at the focus of the orbit.

N = node

ω = position angle of the node

Ω = longitude of periastron

A = periastron point

NN' = line of nodes , where the orbital plane intersects the xy plane at inclination i.

The eccentric anomaly E is defined by:

$$\frac{2\phi(t-t_o)}{P} = E - e\sin E \qquad 3.2$$

A detailed discussion of arrival time analysis for pulsars in binary orbits is given by Blandford and Teukolsky (1976). The Durham University group relies on procedures developed by Wallace (Rutherford Appleton Laboratories, private communication).

3.5. Periodicity Searches

Many candidate V.H.E. γ-ray sources are pulsars or X-ray binaries and may show periodicity in the low energy γ-ray, X-ray, optical or radio regions of the electromagnetic spectrum (and in some cases all four). So, V.H.E. γ-ray data recorded during observations of such sources are subjected to searches at the known (or suspected) period. In the case of data taken while tracking an object, the high background of proton induced events means this is a more sensitive method to apply to the data to establish the presence of a γ-ray source than, for example, searching for bursts in the count rate. This is, of course, in the absence of a reliable and proven method for distinguishing between the two types of Cerenkov light flashes. The statistical methods employed in such searches are outlined in the next sections.

3.5.1. Epoch Folding

Due to the often low count rate and high noise level of V.H.E.

γ-ray telescopes, it is not possible to identify periodicity within the data simply by inspecting the count rate over a given period of time. It is necessary to combine the data in some way. One method used is epoch folding. The data is tested at a given period by assigning each event to a phase bin of arbitrary width, then summing the number of events in each bin. The data have been "folded" at the expected period. A V.H.E. γ-ray light curve of that period results.

If it were possible to predict the exact form of a γ-ray light curve, periodicity could be searched for by correlating the observed γ -ray arrival time series with the expected light curve using a maximum likelihood method. However, in most cases only estimates of the expected light curves exist, based on measurements at lower photon energies, so this technique may not be applied. One procedure adopted is to use Poincare's theorem as a null hypothesis: a random time series of sufficient length, unfolded with an arbitrary period, results in a uniform phase distribution. A test for the uniformity of the phase distribution, resulting from experimental data being folded at the trial period, is taken to indicate the absence of that period in the data. Typically, the data is arbitrarily binned to produce a phase distribution and then Pearson's χ^2 test for uniformity applied.

This method has many problems associated with it when applied to V.H.E. γ-ray data. The binning is completely arbitrary: the number of bins into which the data are placed must be chosen and,

where precise phase is unknown, the bin origin must also be chosen. There is a risk that any γ-ray peak in the data will be split between two bins and thus its statistical significance reduced. To avoid this, data may be re-binned many times, and it is difficult to take into account the number of degrees of freedom used in doing so, and hence to calculate the probability of any lack of uniformity being due to chance. Circular statistical methods are now preferred. These are statistical tests designed to deal with cyclic phenomena, and some such tests are described in the following sections.

3.5.2. The Rayleigh Test

This test has been described by Batschelet (1981) and in more detail by Mardia (1972). Its application to γ-ray astronomy was first suggested by Gibson et al. (1982) and it is now widely used in the field as a test statistic. This test requires no prior knowledge of the absolute phase and no arbitrary binning is made. The following is a brief description of its use by the Durham group.

In the Rayleigh test, each event in a dataset is assigned an accurate phase. Binning is not required. Then, a resultant vector, ϕ, is formed from unit vectors at the phases of the events in the time series, normalised to between 0 and 1, and tested for significance. The null hypothesis is that the parent population is uniformly distributed. The statistic $2n\phi^2$ (where n is the number of events in the time series) is essentially distributed as χ^2 with

two degrees of freedom (i.e. a Gaussian distribution). In the case of a trial period T, for each event at a time t_i, we calculate the phase angle θ_i using:

$$\theta_i = 2\pi f t_i \pmod{2\pi} \qquad 3.3$$

where $f = 1/T$. In cases where the period has a known first and second derivative, this becomes:

$$\theta_i = f t_i + \dot{f} t_i^2/2 + \ddot{f} t_i^3/6 \qquad 3.4$$

We then calculate:

$$C = \sum_{i=1}^{n} (\cos\theta_i)/n \qquad 3.5$$

$$S = \sum_{i=1}^{n} (\sin\theta_i)/n \qquad 3.6$$

and

$$R = \sqrt{(C^2 + S^2)} \qquad 3.7$$

The probability of nR^2 is calculated either from the χ^2 distribution for 2 degrees of freedom which is $\exp(-nR^2)$ or (more accurately when n is small) from:

$$\text{Prob.}(nR^2 > K) = \exp(-K)\ (1 + (2K - K^2)/4n - (24K - 132K^2 + 76K^2 - 9K)) \qquad 3.8$$

There are two points to be noted concerning the Rayleigh test.

Firstly, it is designed to test for a unimodal distribution and is not sensitive to bimodal distributions such as would be encountered in a light curve consisting of a pulse and an interpulse. However, in many cases where the light curve is double-peaked, the Rayleigh test is sufficiently sensitive to the power in the first harmonic to show an effect. This is thus a reasonable test to apply in the absence of any a priori knowledge of the form of the light curve. Where the light curve is known to consist of a pulse and an interpulse the problem may be circumvented simply by testing at half the given period. Secondly, the Rayleigh test in essence tests for the correlation between the time series and a sine wave at the period being tested and is therefore relatively insensitive to light curves with narrow peaks, as shown empirically by Leahy et al. (1983).

3.5.3. The Modified Hodges-Ajne Test

The basis of this test was first proposed by Ajne (1968) and is, in fact, a special case of a test devised by Hodges (1955). It consists of assigning phases of some trial period to data, and then binning the data into two equal phase bins (of width 0.5) and moving the bin origin until one of the bins has the smallest possible number of events, m, in it. It is clear then that this test is more sensitive to sinusoidal waveforms than light curves with a narrow pulse (short duty cycle), so a modification is required to increase its sensitivity to such light curves. The modification

to the test applied by the Durham group, originally and independently proposed by Cressie (1977), is to rotate a sector of arbitrary phase length through the data and look for the maximum number in the smaller bin. The null hypothesis is again that the parent population is uniformly distributed.

Its application to V.H.E. γ-ray astronomy is as follows. Each event in a section of data is assigned a phase angle using either equation 3.1 or 3.2. The data are then binned into 10000 phase bins, for ease of calculation. On average, there will only be one event per bin, so this is a reasonable approximation. The sector, chosen previously to correspond to the width of the proposed peak in the light curve, is passed through the data by moving the bin origin. The maximum number of events in the smaller bin is found. The probability of finding this number of events is derived according to Orford (private communication):

$$\text{Prob.}(m^* < t) = = \frac{4t}{\sqrt{2\pi}} \sum_{k=0}^{\infty} \exp(-(2k-1)^2 t^2/2) \qquad 3.9$$

where

$$m^* = (n-2m)/n \qquad 3.10$$

This is a very powerful test if the shape of the expected light curve is known a priori.

3.5.4. The Z_n^2 Test.

The circular statistic applied to low energy γ-ray data from radio pulsars obtained using the COS-B satellite (Buccheri et al., 1983) is known as the Z_n^2 test. It is essentially a Rayleigh test with harmonics introduced (T/2, T/4 etc.). The Z_n^2 statistic is defined by:

$$Z_n^2 = (2/N_i) \sum_{k=1}^{n} \left(\left(\sum_{j,1}^{N_i} \cos k\theta_i \right) + \left(\sum_{j,1}^{N_i} \sin \theta_i \right) \right) \qquad 3.11$$

where n is the chosen number of harmonics. Again, this is distributed as a χ^2 function with 2 degrees of freedom. The value of n chosen by Buccheri et al. was 2 in order to optimise the signal: noise ratio. In the absence of pulsation in the data, the expected value of Z_2^2 is 4. When a periodic signal due to Np_i "pulsed" photons exists, the contribution to Z_n^2 (in terms of the number of standard deviations above the average) is:

$$n_\sigma(\theta) = N^2 p\ (\theta)\ C/N_i(\theta) \qquad 3.12$$

where θ is the angle of acceptance of the telescope direction and the constant C depends on the duty cycle of the pulsation.

3.5.5. The T_n Statistic.

Recently, Protheroe (1985) has proposed a statistic for application to V.H.E. and U.H.E. γ-ray data from objects with suspected narrow light curves. The requirements of the statistic were:

(i) It should be sensitive to the distances between pairs of points on the phase diagram, having a high value if more points are closer together than expected.

(ii) It should be sensitive to the grouping of several points.

(iii) The sensitivity to a very small distance between two points should not be so great that an unusually close pair dominates the statistic.

The test is thus specific and assumes some prior knowledge of the shape of the light curve. The distance between two events on the phasogram x_i and x_j is defined as:

$$\Delta_{ij} = 0.5 - \left| \left(\left| (x_i - x_j) \right| - 0.5 \right) \right| \qquad 3.13$$

It is considered that averaging $1/\Delta$ over adjacent pairs would satisfy (i), and averaging over all pairs would satisfy (ii). Requirement (iii) is satisfied by averaging $(\Delta + 1/n)^{-1}$ over all pairs. The statistic proposed, therefore, is:

$$T_n = 2/n(n-1) \sum_{i=1}^{m-1} \sum_{j=i+1}^{m} (\Delta_{ij} + 1/n)^{-1} \qquad 3.14$$

Its null distribution for various numbers of degrees of freedom is computed using Monte Carlo methods.

3.6. Searching Over a Range of Periods or for an Unknown Period

Many objects observed by the University of Durham group have had

no accurately predicted contemporary period available, either due to uncertainties in the radio or X-ray ephemeris or uncertainties in the translation of event times to a binary system barycentre introduced by errors in the orbital details. It has therefore been necessary to search about the given inaccurate period. This introduces further complexities into the analysis by using more degrees of freedom than the simple case with a well-defined expected period.

When a search over a range of periods is conducted, each independent period within that range must be tested. The separation of independent periods is termed the Fourier interval. In an observation of length T seconds, the phase of the last event relative to the first is given by:

$$\phi = T/P_1 \qquad 3.15$$

where P_1 is the test period. If P_1 is now increased to $P_1 + \Delta P$, the phase slips relative to that defined by P_1. Eventually a point is reached, P_2, where the phase slippage is equal to a whole period, and the coherence is lost. P_2 is therefore the next independent period and $P_2 - P_1$ the Fourier interval.

The number of independent periods to be tested in a period search between P_1 and P_n is given by:

$$N_p = T/P_1 - T/P_n \qquad 3.16$$

The Fourier interval is then:

$$F.I. = P_1^2/T \qquad 3.17$$

It can be seen that for any observation the size of the Fourier interval depends both on the period tested and on the length of the observation.

In a search for periodicity, it is important to note the number of degrees of freedom expended in that search. For example, in a search over 10^3 independent periods, only probabilities of uniformity of phase of $< 10^{-6}$ may be considered as indications of the presence of real periodicity. All probabilities of uniformity quoted in this work have been corrected for the degrees of freedom used in the analysis.

3.7. The Poincare Correction

Tests for periodicity rest on Poincare's theorem, which is that a random time series of sufficient length unfolded with an arbitrary period results in a uniform phase distribution. However, for short observations (of the order of an hour) and long periods (of the order of minutes) this no longer holds. Vela X-1, for example, has an X-ray pulsation period of 283 secs: observations of about 100 minutes therefore cover approximately 20 periods. It is highly improbable that the dataset will be a whole number of periods long, resulting in a remainder of events at the end of the data. When these are plotted on a phasogram, an anomalous non-uniformity is produced. This problem is circumvented by dividing the dataset by the period which is being tested, and truncating the dataset to the largest whole number of periods possible. This procedure has been followed

for all cases in this work where the period is long.

3.8. Zenith Angle Dependence

Over a typical observing period of 100 minutes, the zenith angle of an object with a high culmination, such as Vela X-1, may change by 20°. This would cause a change in count rate of 2-3% every 5 minutes (see section 7.10). In the general case, when a dataset is being tested at a short period of a few seconds or less, this presents no difficulties. If, however, the period tested is of the order of a few minutes (as is the case for Vela X-1) a rapidly rising (or setting) object with a consequent rapidly varying count rate produces spurious periodicity in the data. If the telescope is counting 3% more (or less) Cerenkov flashes at the end of one pulse period than at the beginning, a peak will occur in the light curve produced by plotting a phasogram. It is thus necessary to take a continuously rising or falling count rate into account in the data analysis if the background varies significantly over the interval of one cycle of the period being tested.

3.9. Drift Scan Techniques

The drift scan mode of telescope operation is one whereby the telescope remains static and the γ-ray source is allowed to drift through the field of view. Data are therefore collected both on and off source: during the first and last parts of the scan the object

is outside the field of view. If γ-rays are received from an object in the period during which it is in the field of view, an excess of Cerenkov pulses would be expected in the "on" period compared with a similar period off source. If N_a events occur in the first off period, N_b in the second off period and N_{on} during the time on source, and assuming the three observation times are equal, the number of γ-rays attributed to the source is given by:

$$\hat{S} = N_{on} - (N_a + N_b)/2 \qquad 3.18$$

This also assumes:

a) The flux of γ-rays is constant while the source is in the field of view.

b) The aperture of the telescope is defined by a "top hat" function rather than the complex Gaussian function which actually defines the field of view.

A statistical uncertainty must now be ascribed to $\hat{S}$. In the simplest analysis, the number of counts in the "on" period is statistically compared to the expected number (as derived from the "off" periods) and a probability of γ-ray detection ascribed to the scan.

3.9.1. The Relative Likelihood Ratio

The relative likelihood test has been described in detail by Hearn (1969) and O'Mongain (1973). To determine whether the excess

observed from the direction of the source is indeed due to a γ-ray source or is simply the result of statistical fluctuations, it is necessary to know the number of events which one would expect to observe were no γ-ray sources present. The on source events contain those assumed due to the γ-ray source, $\hat{S}$, and a background contribution, B. The relative likelihood of the fluctuation, $\hat{S}$, being due to a source is given by:

$$\lambda = \frac{P(\hat{S}/N)}{P\ (\hat{S}=0/N)} \qquad 3.19$$

where the P is a conditional probability. Assuming the temporal distribution of counts to be essentially Poissonian, this simplifies to:

$$\lambda = (\hat{S}/B + 1)^{N} \exp(-\hat{S}) \qquad 3.20$$

At a confidence level C, the relative likelihood function

$$\lambda > (1 - C)^{-1} \qquad 3.21$$

is used to define a source "discovery".

This test requires an exact knowledge of the background counting rate, although uncertainties may be approximately allowed for. In the general case of both background and source being unknown, another test statistic (described in the next section) must be used.

3.9.2. The Maximum Likelihood Test

The detailed description of this test was given by Gibson et al. (1982). The maximum likelihood is defined as:

$$\lambda = \frac{\max L(N/S=0)}{\max L(N/S)} \qquad 3.22$$

where L is the likelihood of observing N counts when the source strength S is zero. For a drift scan, where the ratio of off source time to on source time is α, N counts are seen and B counts in total off source, it has been shown (Orford, private communication) that:

$$L = \left[\frac{N+B}{(1+\alpha)N}\right]^N \left[\frac{(N+B)}{(1+\alpha)B}\right]^B \qquad 3.23$$

with

$$S = N - B/\alpha \quad \text{(c.f. eqn. 3.16)} \qquad 3.24$$

The error in S is obtained by relaxing the value of L to S_+ and S_- which have 1σ deviations from S.

3.10. Calculation of Fluxes

In order to convert an overall excess of events seen by a γ-ray telescope to a flux measurement, several pieces of information are required:

(i) The effective field of view of the system. In the case of the Mark I telescope this was $(2.2 \pm 0.2)^\circ$, for the Mark II it was $(1.8 \pm 0.2)^\circ$, and for the Mark III it has been calculated to be $(1.4 \pm 0.2)^\circ$.

(ii) The telescope threshold for cosmic ray nucleons and for γ-ray initiated Cerenkov light flashes. This in turn requires knowledge of the integral cosmic ray spectrum.

(iii) The integral cosmic ray flux at threshold, which can be found from the known cosmic ray spectrum.

In the case of the Mark III telescope, the threshold is calculated to be approximately 250 GeV (see section 7.11). At this energy, the cosmic ray flux is approximately 2×10^{-5} cm^{-2} s^{-1} str^{-1}, assuming the integral cosmic ray spectral index is -1.6 (Craig, Ph.D thesis, 1984). The field of view of the Mark III on-axis channel alone is 5.5×10^{-4} str, so 1% of the cosmic ray flux at 250 GeV is 1.1×10^{-11} cm^{-2} s^{-1}. Consider the X-ray binary LMC X-4. This shows an effect at 3.8% of the cosmic ray background around X-ray maximum, corresponding to a peak flux of 4.2×10^{-11} cm^{-2} s^{-1} (see Chapter 8).

3.11. Calculation of Flux Limits

Some objects observed show no significant count rate excess for the duration of the observations. In these cases, it is possible to calculate the flux which would have given a 3σ detection for the length of observation made and use this as the upper limit to the flux of the object.

Consider a light curve containing N events with a % pulsed flux P%. We know that:

$$P(\text{Rayleigh}) = \exp(-N(P\%/100)^2) \qquad 3.25$$

is true for large N. Now, a 3σ effect corresponds to a Rayleigh probability of 1.348×10^{-3}. Rearranging equation 3.25, the percentage pulsed flux for a 3σ effect is given by:

$$P\%^2 = -10^4/N \ln(1.38 \times 10^{-3}). \qquad 3.26$$

For the Dugway telescopes (assuming a 1000 GeV threshold), the background cosmic ray flux is calculated to be 3.4×10^{-9} cm^{-2} s^{-1}. Consider PSR0950+08. The telescopes recorded 63180 Cerenkov flashes from the direction of this object. Applying equation 3.26, a 3σ effect would require a pulsed flux of 1.19%. This corresponds to a flux of 4.1×10^{-11} cm^{-2} s^{-1}, which is the 3σ flux limit.

In the case of a pulsar with a known short duty cycle, the flux limit is calculated as follows. Consider a 20 bin light curve produced for a pulsar with an assumed 5% duty cycle. We require an excess of ε in one bin to produce a 3σ detection. The requirement is expressed as:

$$\frac{\varepsilon}{\sqrt{N/20}} = 3 \qquad 3.27$$

The percentage of pulsed γ-rays corresponding to a 3σ effect is given approximately by:

$$P\% = 100\varepsilon/N \qquad 3.28$$

Let us use PSR0950+08 as an example again. A 3σ excess in one bin requires an excess of 213.6 events, which corresponds to a γ-ray flux of 0.34% of the background. The 5% pulsed flux limit is therefore 1.15×10^{-11} cm^{-2} s^{-1}.

CHAPTER 4

CYGNUS X-3: RESEARCH BACKGROUND

4.1. Introduction

This chapter is devoted to the results of observations at many different wavelengths of one object: Cygnus X-3. This remarkable object, which is probably a binary system, has aroused great interest as a source of X-rays, radio and infrared outbursts, H.E., V.H.E. and U.H.E. γ-rays, and possibly as the origin of exotic particles ("Cygnets") which manifest themselves as high energy muons.

4.2. Observations of Cygnus X-3

In the following sections, observations of Cygnus X-3 in all regions of the electromagnetic spectrum will be considered. The recent results from underground muon experiments will also be briefly described.

4.2.1. X-ray Observations

Since Cygnus X-3 was discovered as an X-ray source, it is appropriate to begin this review with the X-ray observations which have been made to date. The third X-ray source in the constellation of Cygnus was discovered during the flight of an instrumented Aerobee 150 rocket, flown from the White Sands Missile Range on

October 11th 1966 (Giacconi et al., 1967). It was confirmed as a discrete X-ray source by the Uhuru satellite and designated 4U2030+40 in the fourth Uhuru catalogue (Giacconi et al., 1971 and Leong et al., 1971). Cygnus X-3 remains most comprehensively studied in the X-ray region of the spectrum. It has now been detected at energies from 1 keV to 400 keV. No "soft" X-rays (0.1 to 1 keV) have been detected: these are probably absorbed by interstellar material.

a) 4.8 Hour Period

Long-term observations of Cygnus X-3, initially made with the Uhuru satellite (Parsignault et al., 1972, Leach et al., 1975) and then with the Copernicus (Mason and Sandford, 1979), ANS (Parsignault et al., 1976), SAS 3 (Lamb et al., 1979), Einstein (Elsner et al., 1980), Vela 5B (Priedhorsky and Terrell, 1986), Ariel 5 (Holt et al., 1979), OSO-8 (Dolan et al., 1982) and COS-B (Van der Klis and Bonnet-Bidaud, 1981a) satellites showed X-ray emission from the object to be varying with a period of 4.8 hours, the maximum X-ray emission being at phase 0.625 (where phase zero is the centre of the broad minimum). The first ephemeris for the 4.8 hr variation was published by Parsignault et al. (1976) using measurements from the Uhuru satellite only. Further ephemerides were produced both with and without a period derivative (Elsner et al., 1980 and Mason and Sandford, 1979). The most widely used ephemeris was produced by Van der Klis and Bonnet-Bidaud (1981a), which combined the satellite

observations used in the aforementioned ephemerides with COS-B observations. More recent measurements, taken with the EXOSAT satellite (see below) have prompted calculations which will lead to other ephemerides (Mason, private communication, 1986 and Van der Klis, 1985, quoted as a private communication by Ramanamurthy, 1985).

During the COS-B X-ray measurements, it was noted (Van der Klis and Bonnet-Bidaud, 1981b) that the shape of the light curve changes on short timescales (of the order of a week). These changes affect the light-curve asymmetry and shift the position of the maximum of the 4.8 hr cycle. Broadly speaking, the light curve becomes more symmetric with increasing non-pulsing flux intensity. These authors also confirmed earlier suggestions (Manzo et al., 1978; Lamb et al., 1979; Elsner et al., 1980) that the 4.8 hr period is slowly increasing, and the period derivative was found to be $(1.18 \pm 0.14) \times 10^{-9}$ ss^{-1}, which is included in the ephemeris. The ephemeris due to Parsignault et al. (1976), based on measurements from the Uhuru satellite, only contains an upper limit to the period derivative, due to the short timescale of the measurements. This upper limit is not incompatible with the observed period derivative due to Van der Klis and Bonnet-Bidaud (1981a).

In 1985, a 30.6 hr continuous observation of Cygnus X-3 in the energy range 10-50 keV was made using the EXOSAT satellite (Willingale et al., 1985). They observed the 4.8 hr periodic behaviour, though the position of the X-ray maximum was found to

be consistently 600 s before the maximum predicted by the Van der Klis and Bonnet-Bidaud (1981a) ephemeris. Cygnus X-3 also exhibited flaring activity on timescales of 100 seconds. A series of sharp dips observed immediately after each X-ray minimum suggests that the flaring episodes may be a function of the 4.8 hr phase.

b) 20 day Period

It was proposed by Elsner et al. (1980) that the asymmetry of the 4.8 hr light curve is due to a highly eccentric orbit (e being approximately 0.1-0.6), and the observed lengthening of the 4.8 hr period is due to an apsidal motion period of over 22 years. However, data obtained with the COS-B X-ray instruments (Van der Klis and Bonnet-Bidaud, 1981b) gave an indication of phase modulation of the 4.8 hr peak which may arise from a much shorter apsidal motion period of 20 days, and an orbital eccentricity of 0.03. Observations made by the Vela 5B satellite also showed a 20 day period (Priedhorsky and Terrell, 1986). This would make the eccentricity too small to cause the observed light curve asymmetry and implies that the observed period derivative is indeed the secular period derivative of the binary orbit. If this is the case, such a short apsidal motion period would suggest that the companion star nearly fills its Roche lobe and may be a red dwarf or a helium star with an extended envelope.

c) 17 and 34 Day Periods

In 1975 Holt et al. used the Ariel V All Sky Monitor to detect

a 16.75 day periodicity from Cygnus X-3, which was not confirmed in further observations (Holt et al., 1979). It was later suggested on the basis of COS-B measurements that this was probably the 2nd harmonic of a 34.1 day period (Molteni et al., 1980). Indications of a 34.1 day period were also observed by OSO-8 (Dolan et al., 1982). Analysis of the time dependence of the 4.8 hr period in the COS-B data suggested the presence of a Doppler effect also consistent with an orbital motion of period 34.1 days, with the 4.8 hr periodicity then being interpreted as due to the precession of a fast spinning pulsar (Molteni et al.). This observation of a 34 day period was not, however, confirmed by later more extensive COS-B observations (Bonnet-Bidaud and Van der Klis, 1981). If this modulation is genuine, and since it does not show an eclipse, the angle of inclination is required to be significantly different from 90^{o}. The attenuation would then be due to the atmosphere of the companion star. If the 34 day period is assumed to be the orbital period, and if the X-ray emitter is assumed to be a neutron star of about 1 solar mass, the companion would be 10-20 solar masses, suggesting it is an OB star. However, the results could not exclude the possibility of the 34 day period being due to some sort of disc precession, similar to the 35 day period then suggested in Her X-1, which is now considered to the result of precession (Trumper, 1987). Apsidal motion of the binary orbit was also suggested as a candidate cause for the 34 day period, preserving the 4.8 hr period as an orbital period. It is then difficult to explain the 20 day period

observed by Vela 5B and COS-B. It may be noted that Vela 5B did not detect either a 17 or 34 day period in Cygnus X-3 data.

d) X-ray Spectrum and Flux

Measurements of the X-ray spectrum suggest that at low energies (below about 10 keV) the emission falls off, presumably due to X-ray scattering within the source (Reppin et al., 1979; Serlemitsos et al., 1975). The rest of the spectrum corresponds to thermal plasma emission with a kT of 20 keV, coupled with a power law accounting for the high energy X-rays, the spectral index of which may vary with 4.8 hour phase.

The only X-ray spectral line which has been unambiguously detected is the 6.7 keV iron line (Serlemitsos et al., 1975). No cyclotron lines have been observed.

Uhuru measurements gave a flux density for the object of 9.2×10^{-9} erg cm^{-2} sec^{-1} between 2 and 10 keV (Forman et al., 1978). If Cygnus X-3 is assumed to be emitting X-rays isotropically and is assumed to be 11.6 kpc from the solar system, the X-ray luminosity between 2 and 10 keV is 1.4×10^{38} erg s^{-1}.

4.2.2. Radio Observations

On September 2nd 1972, Gregory et al. recorded a powerful outburst of radio emission from Cygnus X-3 at a frequency of 10.5 GHz. The radio flux during the outburst was 1000 times greater than had been observed 2 days previously. Cygnus X-3 was being monitored at

that time by the Uhuru (Parsignault et al., 1972) and Copernicus satellites (Sandford and Hawkins, 1972), but no corresponding outburst at X-ray wavelengths was observed. Two weeks later, a second outburst occurred, reported by Hjellming et al. at NRAO (1972). Peak flux densities of 22 Jy and 14 Jy respectively were observed for the two events. Particularly noticeable at high frequencies was the fact that the second event consisted of three separate bursts at intervals of several days (Gregory et al., 1972). Measurements of the radio spectrum and linear polarisation between 1.4 and 10.5 GHz indicated that the radiation was not thermal, but was characteristic of synchrotron radiation from an expanding cloud of relativistic electrons. Smaller outbursts were observed during the next three years, on average twice a year, and often occurring in groups of two or three. The radio activity then dropped markedly until, in September 1982, a second series of powerful radio outbursts was observed (Geldzahler et al., 1983). The maximum observed flux density during these episodes of activity was 22 Jy. From measurements of the source size during the outburst, the inferred expansion velocity of the emitting region was 0.35c. One year later, in October 1983, two further outbursts, separated by ten days, were observed by the Very Large Array and the U.K. MERLIN array (Spencer et al., 1986). The maximum flux density occurred in the first burst and was 6 Jy. Measurements of the angular dimension of the emitting region were again consistent with symmetrical relativistic expansion about the object with a velocity of 0.35c. Most recently, flaring

events were observed on February 4th and March 3rd 1985 (Johnston et al., 1986) and on October 6th 1985 (Johnston, private communication).

In addition to these flaring events, Cygnus X-3 is a low-level continuous radio source. Recent observations suggest that this emission consists of small flares which recur with a period of 4.95 hr, a period which is significantly different from that observed in the X-ray, Infrared, and γ-ray regions (Molnar et al., 1984, 1985).

Radio observations of the absorption of the 21 cm Hydrogen line during outbursts may be used to infer the distance between Cygnus X-3 and the Earth. The presence of 21 cm absorption lines at various velocities can be used to give a lower limit to the distance when coupled with a model of galactic rotation. The first estimate was that it was between 8 and 11 kpc from Earth (Lauque et al., 1972). Later calculations, based on observations made during the 1982 October outburst, suggested that the source is further away, a lower limit being 11.5 kpc (Dickey, 1983). A maximum distance could not be determined, and the absorption is consistent with Cygnus X-3 being extragalactic. It is of note that a distance of 12 kpc, coupled with the known V.H.E. and U.H.E. emission, requires a power in the proton beam to produce the γ-rays of 3×10^{39} erg s^{-1} if one assumes that the object emits isotropically (Hillas, 1985). Such a source could easily maintain the galaxy's cosmic ray flux.

4.2.3. Infrared Observations

The absorption and scattering of light in the dust and gas between the Earth and Cygnus X-3 typically reduces the absolute magnitudes of stars in that region by 3 to 10 magnitudes, so the identification of an optical counterpart is difficult with present instrumentation. There is no visual candidate for Cygnus X-3 to a limit of an absolute visual magnitude of 23.9 (Westphal et al., 1972; Gaustad and Margon, 1973; Weekes et al., 1981). However, at infrared wavelengths, the gas and dust are more transparent. Initial observations at 0.85μ showed no starlike object brighter than $17^{m}.5$ (Bahcall and Bahcall, 1974). A group observing at longer wavelengths of 2.2 and 1.6μ discovered a source coincident with the radio position to ± 2 arc s (Becklin et al., 1972). Co-ordinated infrared and X-ray observations by Becklin et al. (1973) using a photometer at the focus of the Hale 200-inch telescope and a proportional counter on the Copernicus satellite, showed the infrared source to be variable with a period of 4.8 hr synchronous with the X-ray source. The shape of the infrared light curve is also similar to that of the X-ray light curve, although the modulation is much less in the infrared. Observations in the I-band show a $17^{m}.0$ object, which also appears to show 4.8 hr modulation (Weekes et al., 1982).

In addition, the source displays flaring activity at infrared wavelengths. On 11 July 1973 a flare of amplitude 8 mJy lasting for about 6 minutes was observed (Becklin et al., 1974). More infrared flares were observed in August 1973 and September 1974 (Becklin et

al., 1974, Mason et al., 1976). During the August flare, X-ray and radio observations were also made. The X-ray observations showed no disturbances, but the radio flux was apparently decaying from a radio flare which was estimated to have occurred 2 hours before the infrared flare. Further simultaneous X-ray and infrared observations were made on September 2nd 1984 using the 3.0 metre telescope on Mauna Kea and EXOSAT (Mason et al., 1985). The infrared light curve shows a series of short (a few minutes' duration), intense flares imposed on the 4.8 hr modulation, which involve up to a two-fold increase in flux. These flares occur throughout the 4.8 hr cycle. There is no clear case of an X-ray flare counterpart, although a possible X-ray flare event was observed in the data just before the largest of the infrared flares. The flare events are interpreted by Mason et al. (1986) as emission from clumps of material being ejected from the system in jets, and may be precursors of radio flares.

4.2.4. High Energy γ-Ray Observations

The first detection of periodic emission from Cygnus X-3 in this range was reported by Gal'per et al. (1975) at energies of 50-200 MeV from a balloon flight made in October 1972. The γ-ray emission showed a 4.8 hr modulation, but the γ-ray maximum was recorded in the 4.8 hr phase interval 0.1-0.2 rather than at the X-ray maximum. Further observations were made during balloon flights in September 1972 and July 1973, producing less statistically

significant results, the final combined excess being 15 counts. The γ-ray flux averaged over the three flights was $(6.4 \pm 2.7) \times 10^{-5}$ photons cm^{-2} s^{-1}, which is very large. Balloon flights in September 1972 and July 1973 made by McKechnie et al. (1976) at energies > 70 MeV yielded an upper limit well below the flux of Gal'per et al. However, the detection was later confirmed by the SAS 2 collaboration (Lamb et al., 1977) for energies > 35 MeV although with a flux a factor of 3 lower than observed by Gal'per et al. The excess observed above the galactic and diffuse radiation appeared to be modulated with the characteristic 4.8 hr period in phase with the X-ray emission. No evidence was found for large diurnal variations or for bursting on a 10 minute timescale (Fichtel et al., preprint, 1987). It has been suggested (Gal'per et al., 1984) that the difference in phase of high energy γ-ray emission of these two observations is related to the 34 day cycle, the suggestion being that γ-ray emission is at phase 0.2 of the 4.8 hr cycle if the 34 day phase is in the range 0.0-0.5 and at 0.6 in the 4.8 hr cycle if the 34 day phase is in the range 0.5-1.0. Then, the γ-ray detector (E > 50 MeV) on board COS-B failed to observe any emission from Cygnus X-3 during prolonged observations (Bennet et al., 1977; Swanenberg et al., 1981; Hermsen, 1983; Hermsen et al., 1987). No resolved source structure was observed at the object's X-ray position, nor was any pulsed emission detected during any of the 5 exposures of the source taken during the period 1975-1980. For some of the observation periods, the X-ray detector was observing Cygnus X-3

simultaneously, and recorded emission from the object. The COS-B 2σ flux limit for the energy range 150-300 MeV was 6.5×10^{-7} photons cm^{-2} s^{-1}, which is significantly lower than the flux of $(4.4 \pm 1.1) \times 10^{-6}$ photons cm^{-2} s^{-1} for energies > 100 MeV reported by Lamb et al. It has been suggested that the total γ-ray excess observed in the Cygnus region by SAS 2 is due to CO emission and may not be uniquely ascribed to Cygnus X-3, since the COS-B satellite also observed an excess in that region (Hermsen et al., 1987). However, later analysis using a revised estimate of the galactic high energy γ-radiation from radio measurements produced no significant differences (Fichtel et al., preprint, 1987). Long-term observations of Cygnus X-3 made by Vela 5B suggest an alternative explanation for the discrepancy, namely that the SAS 2 observations may have been made during an X-ray high state whereas the COS-B observations were made during a relatively quiescent period (Priedhorsky and Terrell, 1986). However, it is difficult to reconcile a difference of nearly two orders of magnitude from Gal'per's measurements to the COS-B flux limit with the observed X-ray variability.

4.2.5. Ultra High Energy γ-Rays

The first detection of Cygnus X-3 at PeV energies was made by Samorski and Stamm (1983) using an extensive air shower experiment at Kiel, Federal Republic of Germany which had an angular resolution of 1°. Their data, taken from 1976-1980, showed a significant excess

from the direction of Cygnus X-3: the probability of the excess being due to a random fluctuation was 10^{-4}. The excess showers were also found to be correlated with the 4.8 hr X-ray period as derived from the ephemeris of Parsignault et al. (1976). The more widely used ephemeris due to Van der Klis and Bonnet-Bidaud (1981a) was not initially applied to these data. If a more recent ephemeris (Van der Klis, 1985, quoted as a private communication by Ramanamurthy, 1985) is used to analyse the data, the U.H.E. γ-ray peak is broadened and shifted from its original phase of 0.35 to 0.1-0.3, and is reduced in significance (Samorski and Stamm, 1985). The integral γ-ray flux from Cygnus X-3 averaged over all phases was calculated to be $(7.4 \pm 3.2) \times 10^{-14}$ photons cm^{-2} s^{-1} for $E > 2 \times 10^{15}$ eV. This result was later confirmed in observations made at Haverah Park over 3 years (Lloyd-Evans et al., 1983). The 4.8 hr maximum was in the phase interval 0.225-0.25. The integral flux above 3×10^{15} eV was $(1.5 \pm 0.3) \times 10^{-14}$ photons cm^{-2} s^{-1}. No evidence was found for any long-term periodicity on the timescales of 10 and 34 days.

Further measurements of Cygnus X-3 in this energy range have been made at Plateau Rosa (Morello et al., 1983), Ootacamund (Tonwar et al., 1985), Baksan (Alexeenko et al., 1985, Alexeenko et al., 1986), Akeno (Kifune et al., 1986) and Gulmarg (Bhat et al., 1986). With the exception of the Gulmarg result, all the fluxes measured in these experiments are in broad agreement with those observed by the Kiel and Haverah Park experiments. The U.H.E. γ-ray flux calculated

from the Gulmarg data is $(1.6 \pm 0.4) \times 10^{-12}$ photons cm^{-2} s^{-1} for $E > 5 \times 10^{14}$. Despite the slightly lower threshold of this experiment when compared with other U.H.E. γ-ray experiments, this flux is much larger than would be expected.

All the above experiments found an excess at phase 0.6 rather than around 0.25 as had been observed at Kiel and in the early Haverah Park data. Later results from Haverah Park show a peak around phase 0.6 (Lambert et al., 1985). However, simultaneous observations made with the Fly's Eye in Utah showed an excess at phase 0.25 (Baltrusaitis et al., 1985). With the exceptions of the Baksan and Akeno data, all these data were analysed using the Van der Klis and Bonnet-Bidaud (1981a) ephemeris. The PeV results obtained from Cygnus X-3 are summarised in table 4.1.

4.2.6. Underground Muons

In May 1985, an excess of muons from the direction of Cygnus X-3 was reported in data from the Soudan-1 underground proton decay detector in Northern Minnesota (Marshak et al., 1985). The single muons showed the 4.8 hr periodicity chararacteristic of emission from Cygnus X-3, and bursts of multiple muons seemed to show an excess from the $30^{\circ} \times 30^{\circ}$ area of sky centred around Cygnus X-3. Evidence of a signal from Cygnus X-3 was also found by the NUSEX nucleon decay detector, the data from which showed a slight excess of muons in a bin $10^{\circ} \times 10^{\circ}$ centred on the object. This excess showed a 4.8 hr period (Battisoni et al., 1985). Soudan-1 recorded

GROUP	APPROX. DATES	PHASE OF EMISSION	FLUX (cm^{-2} s^{-1})	THRESHOLD (TeV)
Nuclear Res. Lab. (Gulmarg)	1976-77	0.6	2.6×10^{-12}	500
Univ. of Utah	1983	0.2	3.2×10^{-13}	500
Univ. of Turin	1982	0.2 0.6	4.2×10^{-12}	30
Inst. of Nuc. Res. (Baksan)	1984	0.6	6×10^{-14}	100
Univ. of Kiel	1976-80	0.2	7.4×10^{-14} 1.1×10^{-14}	2000 10^4
Univ. of Leeds	1979-84	0.2 0.6	1.5×10^{-14}	3000
Univ. of Tokyo	1981-84	0.6	8.8×10^{-14} 1.1×10^{-14}	600 1000

Table 4.1 U.H.E. gamma-ray observations of Cygnus X-3.

a flux of 7×10^{-11} cm^{-2} s^{-1} ($E > 600$ GeV) whereas NUSEX observed a flux of 2.5×10^{-12} cm^{-2} s^{-1} ($E > 5000$ GeV). Results from the Frejus detector and the Homestake Gold Mine detector show no excess in the direction of Cygnus X-3, and no evidence for periodicity (Berger et al., 1986; Cherry et al., 1986). The upper limits for emission are respectively 0.8×10^{-12} cm^{-2} s^{-1} and 4.2×10^{-11} cm^{-2} s^{-1}, both with a muon energy upper limit of 5000 GeV. These upper limits in particular throw some doubt on the flux observed by NUSEX. The Baksan underground scintillator telescope has also failed to detect any muons from the direction of Cygnus X-3 (Chudakov, private communication).

If Cygnus X-3 is indeed giving rise to the observed high energy muons, and if they are 4.8 hr periodic, it is difficult to imagine what the signal-carrying particle may be. It must be neutral, as charged primaries would disperse in the interstellar magnetic field with the consequent loss of phase information. The flux of muons observed is greater than the observed flux of PeV γ-rays, so these are not the carriers. Neutrons would have to be of very high energy (10^6 TeV) in order to traverse the 10 kpc from Cygnus X-3. This would produce an enhancement in the total cosmic ray flux: such an enhancement is not observed. Finally, the zenith angle dependence of the muon signal shows that they are of atmospheric origin and are not produced by neutrinos. One possible solution to this problem is to postulate the existence of new, neutral, long-lived elementary particles which produce the muons. It has been suggested that these

may be balls of quark matter (Barnhill et al., 1985).

4.2.7. Very High Energy γ-Rays

A summary of observations made from 10^{11} to 10^{14} eV is contained in table 4.2.

Cygnus X-3 was first detected in this energy range by a Soviet group working at the Crimean Astrophysical Observatory in 1972, just after the radio outburst (see section 4.2.2). The mean flux was found to be $(1.8 \pm 0.5) \times 10^{-11}$ photons cm^{-2} s^{-1}, for $E > 2 \times 10^{12}$ eV, and the well established 4.8 hr period was identifiable (Vladimirskii et al., Denver, 1973). Initially, two equal γ-ray maxima were observed, one at phase 0.15-0.2 and the other at 0.6-0.8. These data were analysed using a definition of X-ray minimum due to Canizares et al. (1973), which was not used in later measurements either by the Crimean group or by others. Further observations and a new analysis of all four years' data showed the earlier peak to be stronger (Stepanian et al., 1977). Sporadic bursts were observed, specifically in September 1973, August 1974 and October 1980. The later observation was preceded by a radio outburst (Fomin et al., 1981). The 34.1 day period apparent in some X-ray data was also observed (Neshpor et al., 1980). The Crimean detection was followed by a positive result from a group connected with the Crimean group but working at T'ien Shan (Mukanov, 1981). The peak in their γ-ray light curve was in the 4.8 hr phase interval 0.157-0.212 and during this time the flux was found to be 1.6×10^{-10} photons cm^{-2} s^{-1} for an

GROUP	APPROX. DATES	PHASE OF EMISSION	FLUX (cm^{-2} s^{-1})	THRESHOLD (TeV)
Crimean	1972	0.2 0.7	1.6×10^{-11}	2
Astrophysical	1973	0.2 0.7	to 1.6×10^{-10}	
Observatory	1974-79	0.2		
Lebedev Phys. Inst.	1977-78	0.2 0.8	1.6×10^{-10}	5
Whipple	1980	0.6	1.5×10^{-10}	2
Collaboration	1983	0.6	5×10^{-10}	0.8
Univ. of	1981-83	0.6	3×10^{-10}	1
Durham	1985	0.6	3.6×10^{-10}	1
ISU-JPL-UC	1982	0.6	8×10^{-11}	0.5

Table 4.2 V.H.E gamma-ray detections of Cygnus X-3.

energy threshold of 3 x 10^{12} eV.

Confirmation of the results of Vladimirskii et al. and Mukanov et al. came in 1981 from the collaboration between University College, Dublin and the Harvard-Smithsonian Center for Astrophysics working at Mt. Hopkins, Arizona (Danaher et al., 1981). The data were found to be 4.8 hr periodic, with the maximum emission between phase 0.7 and 0.8. This phase was determined using the ephemeris derived from the Crimean Astrophysical Observatory results. If the data are analysed using the Van der Klis and Bonnet-Bidaud ephemeris (1981a), the emission is found to be at phase 0.6-0.7 (Weekes et al., 1981). The few observations at other phases showed no significant excess. The flux corresponding to the peak in the data is approximately 1.5 x 10^{-10} photons cm^{-2} s^{-1} for a threshold of 2 x 10^{12} eV. Two apparent eight-minute transients were also observed in 1981 at phase 0.80 and 0.87 (Weekes, 1982).

Observations made by Lamb et al. (1982) using two 11m solar concentrators of the Jet Propulsion Laboratory's solar energy facility at Edwards Air Force base as a V.H.E. γ-ray telescope showed a positive signal between phases 0.5 and 0.7 of the 4.8 hr cycle corresponding to an average flux of 8 x 10^{-11} photons cm^{-2} s^{-1} for an approximate energy threshold of 500 GeV.

The first results on Cygnus X-3 from the Durham group came from data taken in 1981, early in the life of the Dugway project, when a small excess, significant at the 2σ level, was observed in data recorded in the 4.8 hr phase interval 0.625-0.655 (Gibson et al.,

1982). There was also some indication that the data were periodic with a period of 34.1 days, although no other periods were tested. Observations in 1982 produced further evidence for the 4.8 hr periodicity (Dowthwaite et al., 1983).

Most recently the Durham University group has found evidence for the existence of a 12.59 ms pulsar in the Cygnus X-3 system (Chadwick et al., 1985). The discovery was made in data from the last months of operation of the Dugway telescopes, when an outburst of γ-ray emission of sufficient duration to allow a periodicity search was observed from Cygnus X-3. The observations of Cygnus X-3 made at Dugway will be described in detail in the following chapter.

CHAPTER 5

OBSERVATIONS OF CYGNUS X-3 MADE AT DUGWAY, UTAH

5.1. Introduction

This chapter contains a description of the observations and results from Cygnus X-3 obtained using the University of Durham facility at Dugway, Utah, including the discovery of a 12.6 ms pulsar in the system. The implications for models of Cygnus X-3 are briefly considered. Finally, the prospects for the University of Durham's proposed Cygnus X-3 monitor are described.

5.2. The Database

The Durham University Cygnus X-3 Database comprises more than 350 hours of data taken over 4 years. Observations were made with telescopes operating in both the tracking and drift scan modes.

5.2.1. Drift Scans

The Dugway telescopes made 76 drift scan observations of Cygnus X-3 during 1981 from August to October. Each 36 minute drift scan was divided into three 10-minute intervals as follows:

(i) A 10 minute transit of Cygnus X-3 through the field of view of the telescopes.

(ii) Each side of the transit, 10 minutes of off-source data.

The extra 6 minutes were used in steering the four telescopes between 10 minute observations, and allowing a clear 2 minute region between ON and OFF source scans. In contrast to other V.H.E. γ-ray observations, the drift scans of Cygnus X-3 were all made at predetermined phases in the 4.8 hr X-ray period as found from the Van der Klis and Bonnet-Bidaud ephemeris (1981a). Most ON source observations were made in 10 minute (0.035 in phase) intervals centred at a precise X-ray phase, which were separated by 0.125 steps from phase 0 to 1.0. The drift scans recorded in October 1981 were again separated by intervals of 0.125 in phase but at phases offset by +0.03 from the earlier observations in an attempt to give equal coverage to all phases.

5.2.2. Tracking Observations

The drift scan method is a reliable, but inefficient mode of operation, as only one third of the time available is spent observing the source. Later Dugway obserations were therefore made in the tracking mode in order to investigate the duration of any activity detected in the drift scan data and to search for short outbursts and pulsar activity. Some 50 tracking observations with good skies were made from July to November of 1982 and September and October of 1983. Many of these observations covered a whole 4.8 hr. cycle.

Further to the Dugway observations of Cygnus X-3, some tracking observations were made in Durham on 6 nights in October and November 1985, around the time of a radio flaring episode (Johnston, private

communication). Observations were typically of one hour's duration around the X-ray maximum as predicted by the Van der Klis and Bonnet-Bidaud ephemeris (1981a). A single telescope from the Dugway array, which had been re-mirrored to increase its sensitivity, was used.

5.3. The 4.8 hour Period

The following is a summary of results reported in greater detail by Kirkman (Ph.D. thesis, 1985) and Dowthwaite (Ph.D. thesis, in preparation).

The first Dugway observations of Cygnus X-3 made in 1981 were taken in the drift scan mode of operation. The aggregate ratio ON/OFF for all the data was 1.00 ± 0.01, where ON is defined as the total on-source events in a scan and OFF as the total number of off-source events (divided by two to allow for the double exposure). When the ratio ON/OFF was calculated for each phase separately, it was found to be 1.076 ± 0.031 for the phase centred on 0.625/0.655 (see figure 5.1). This corresponds to evidence at the 2.4σ level for an excess count from Cygnus X-3 at the X-ray maximum. During 1981, one telescope in particular was known to have a lower energy threshold and a higher count rate than the other three. An investigation of the data from this telescope showed that it contributed most of the effect observed at X-ray maximum, and when taken alone showed an excess of 14% corresponding to a 3.35σ effect. This suggests that the energy spectrum of Cygnus X-3 may be steeper than the cosmic ray spectrum, as reported by Vladimirskii et al. (1973).

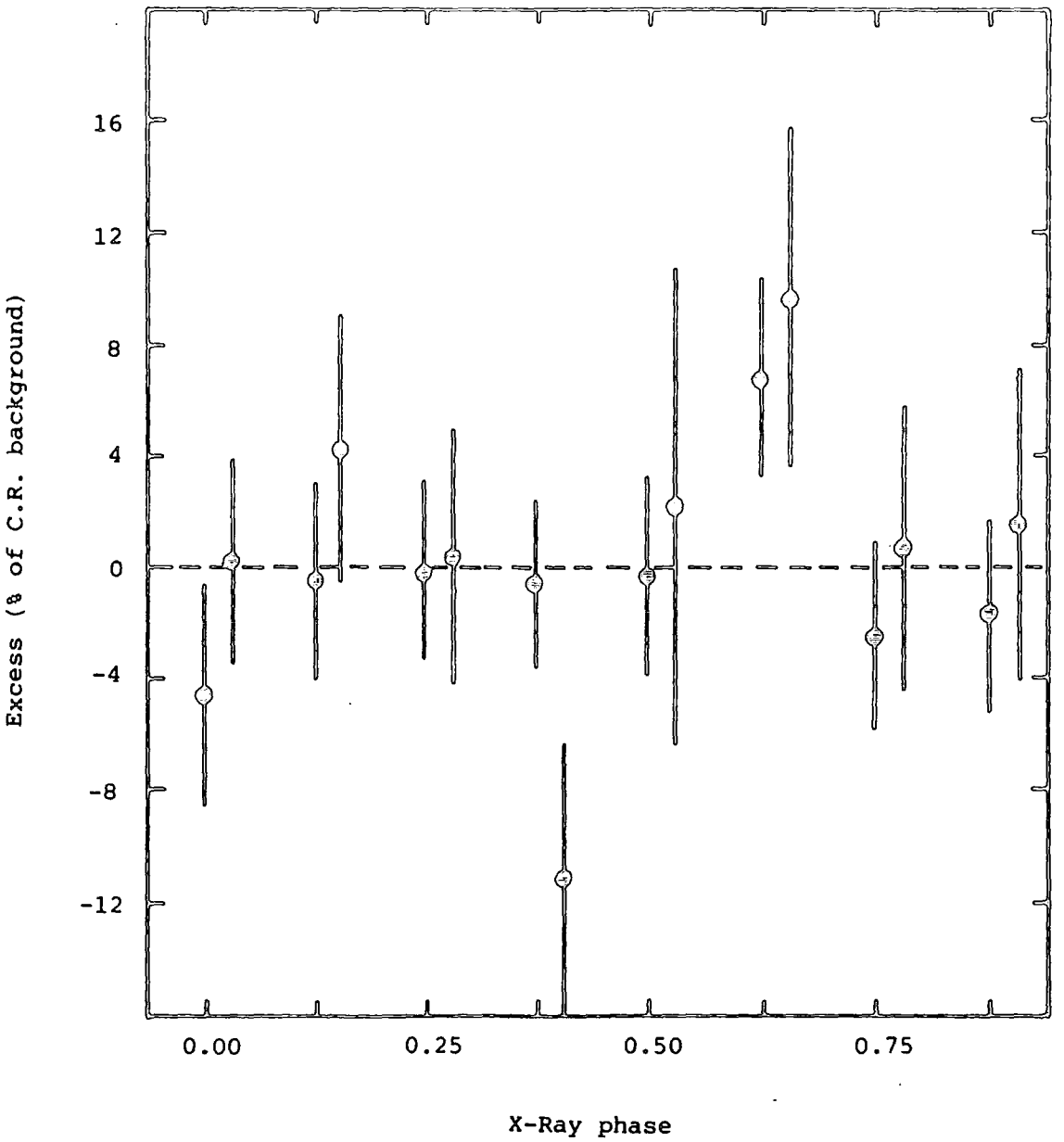

Figure 5.1 The observed excess of counts ON/OFF source for the aggregate response of four telescopes during drift scan measurements in 1981 plotted as a function of the phase of the 4.8 hr X-ray cycle.

Later observations of Cygnus X-3 were made in the tracking mode. To allow the data to be combined (and compared) with the 1981 data, the 10 minute section around each of eight equally spaced phases was used as ON source data, and the 10 minutes before and after as OFF source data. This assumes that the activity occurs in a short (10-15 min.) period as suggested by the 1981 data. A problem with this method is that the background count rate observed is continually changing due to the variation in zenith angle of the object. From the observed variation of rate with zenith angle, it is estimated that from 12 min. before phase 0.625 to 12 min. after phase 0.625 the rate changes by 1.5% at a zenith angle of 10^{o}, 5% at 30^{o} and 9% at 45^{o}. The systematic error in the background assignment due to this effect is less than 0.15% at all zenith angles. The aggregate ON/OFF ratio for these data is again 1.00 $\pm$ 0.01.

By 1982, two of the four Dugway telescopes had low energy thresholds. The results from these two telescopes show evidence for emission at 6.8% of the background count rate at phase 0.625 at the 2.7σ level, as shown in figure 5.2. The significance of the combined 1981 and 1982 low energy threshold detector data at phase 0.625 is at the 4.05σ level and corresponds to a flux of about 3×10^{-10} cm^{-2} s^{-1} at a 1000 GeV threshold.

There is, however, a further background effect to take into account. Drift scan observations of the galactic plane made in 1981 and 1983 showed that the galactic plane in the Cygnus region

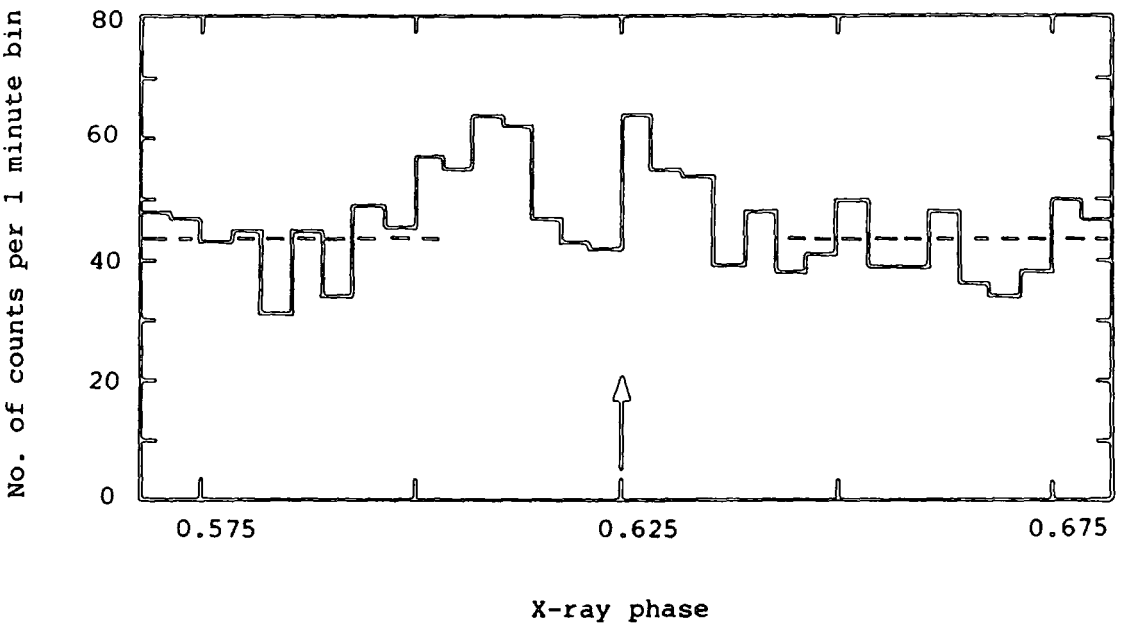

Figure 5.2 The accumulated count rate in one minute intervals for the low energy telescopes during five intervals of tracking Cygnus X-3 during 1982 , each of which showed an overall excess around phase 0.625 of the 4.8 hr X-ray cycle.

is an emitter of V.H.E. γ-rays at a higher flux than was expected, and that Cygnus X-3 is located in a V.H.E. γ-ray "hole" (Dowthwaite et al., 1985). This causes the effective background for point source detection to be different in the region of Cygnus X-3. If allowance is made for this non-uniform background, an excess of 9.4% of the cosmic ray flux is found at phase 0.64 ± 0.03, based on the data taken under good weather conditions (see figure 5.3). The excess is significant at the 4.4σ level assuming that, in the light of X-ray and earlier γ-ray measurements, this was the expected emission phase. There is also a small (3.8%) excess at phase 0.14 ± 0.03, which is significant at the 1.4σ level.

5.4. Long Term Variability of the 4.8 hr Maximum

Some evidence for a possible 34.1 day variation in the strength of the γ-ray peak was found in early data by folding the values of the amplitude of the 4.8 hr peak at phase 0.625 in individual scans modulo 34.1 days (Dowthwaite et al., 1983). However, this was the only long-term period fitted to the data. In a further more general investigation of the long-term variation of the peak strength at X-ray maximum, a sine wave was fitted to the excess observed in all the individual obserations at 0.625 phase (Chadwick et al., 1985). The fit was constrained to have the observed strength averaged over all scans and to have a peak-peak amplitude ranging from zero to twice the average. The results of this search are shown in figure 5.4. Two periods with small r.m.s. deviations from the sine wave

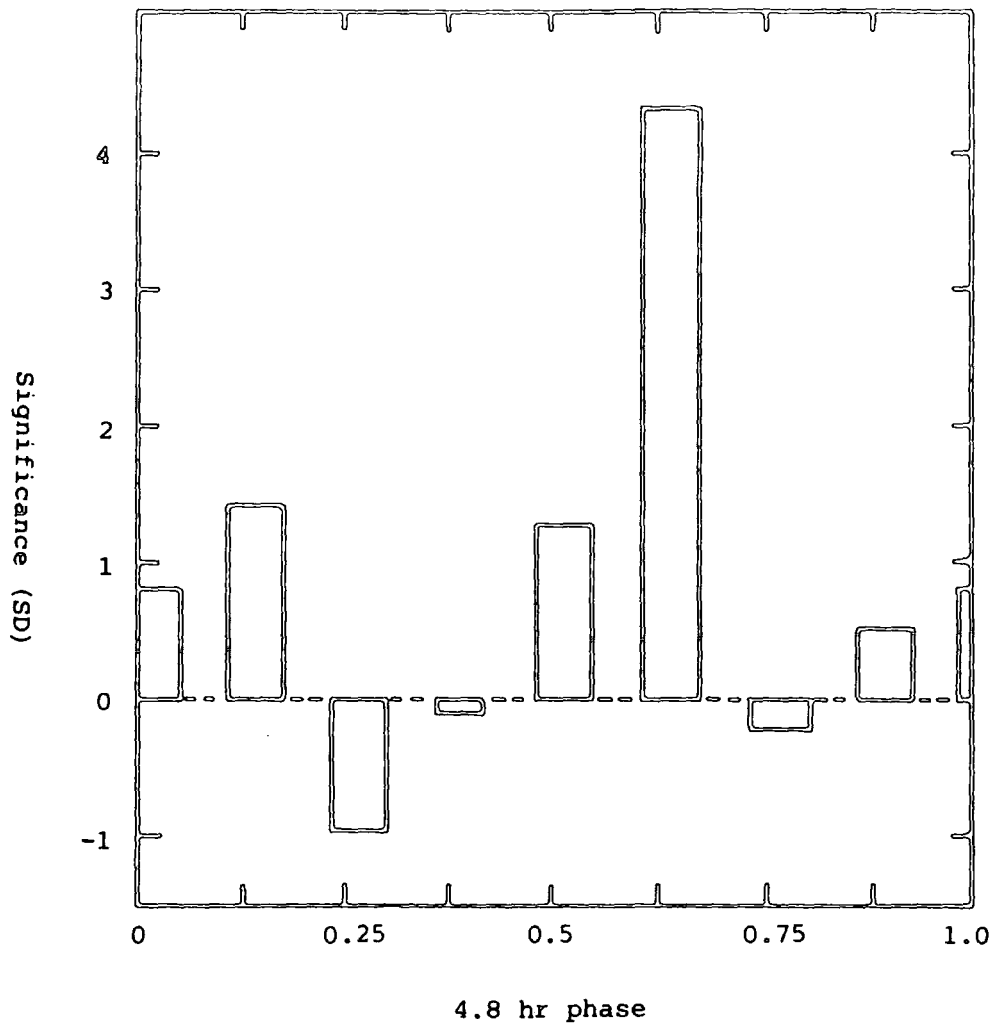

Figure 5.3 The 4.8 hr light curve for Cygnus X-3 at E > 1000 GeV based on all data taken on clear nights in 1981-3. Allowance has been made for the non-uniform background in the Cygnus region.

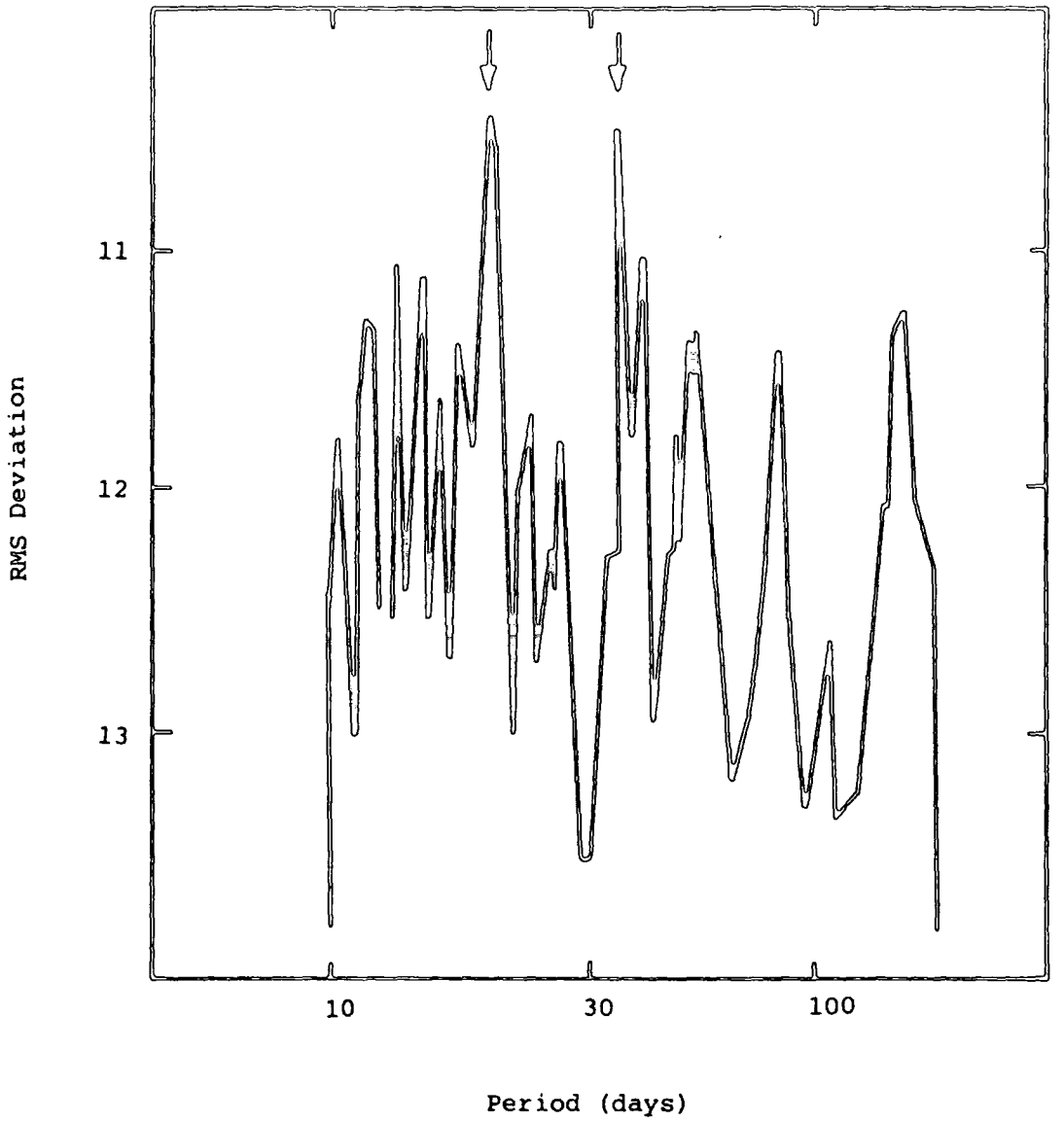

Figure 5.4 The R.M.S. deviations from a sine wave fit to the strength of gamma-ray emission in individual scans of Cygnus X-3 at 0.625 phase at independent periods in the range 8-100 days. This is the original fit without use of accurate times of X-ray maximum.

fit exist: 19.2 ± 0.4 days and 36.8 ± 1.5 days. The magnitudes of the r.m.s. deviations for the two "best fit" periods are very similar.

The work presented here has followed the same method. The observation times of the excesses originally analysed were integer Julian Days. This analysis has used more accurate times of X-ray maximum (± 0.02 days), and one further observation when a large count rate excess was observed (12th September 1983) has been included. The result of the sine wave fitting procedure for the independent periods in the range 5 to 150 days is shown in figure 5.5. Clearly, the best fit period is 19.2 ± 0.4 days. The sine wave fit at this period is an improvement on the fit shown in fig. 5.4. The other two periods with small deviations (37.2 ± 1.7 and 57 ± 4 days) may be interpreted as the first and second harmonics of 19.2 days respectively. The 19.2 day sine wave fit to the data can be seen in figure 5.6. The tentative result of the early 1981 data is not supported, and there is no evidence for any 34 day period in the Dugway data.

5.5. Why Search for a Pulsar?

The presence of V.H.E. and U.H.E. γ-ray emission from Cygnus X-3 is a challenge to theoretical models of the system. To produce the observed photons of 10^{16} eV, particles of at least 10^{17} eV must exist in the emitting region, and it is difficult to accelerate particles to such energies via a stochastic shock acceleration

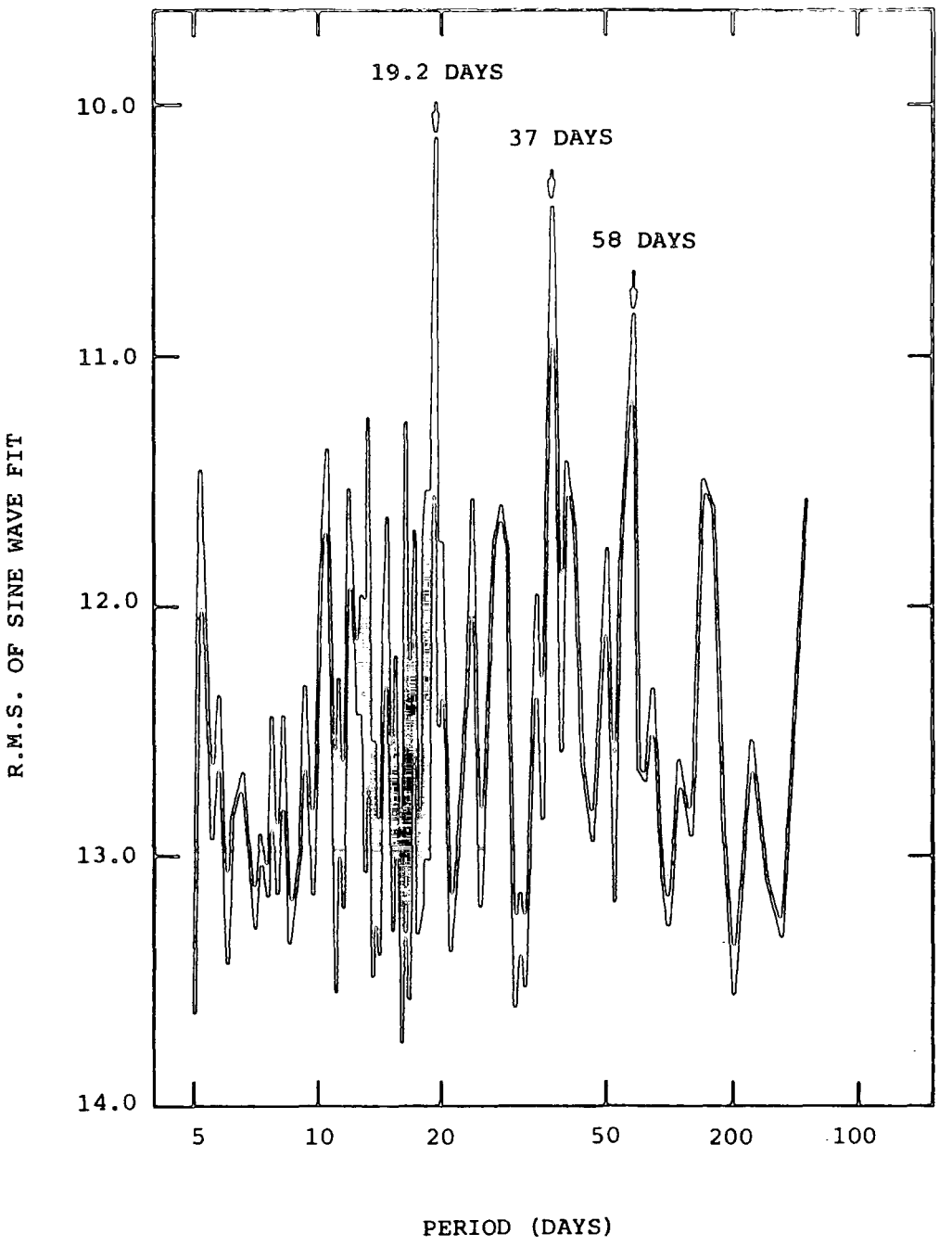

Figure 5.5 The R.M.S. deviations from a sine wave fit to the strength of gamma-ray emission in scans of Cygnus X-3 at 0.625 phase. All independent periods in the range 5 to 100 days were tested. This fit uses more accurate times of X-ray maximum than used in the result shown in figure 5.4.

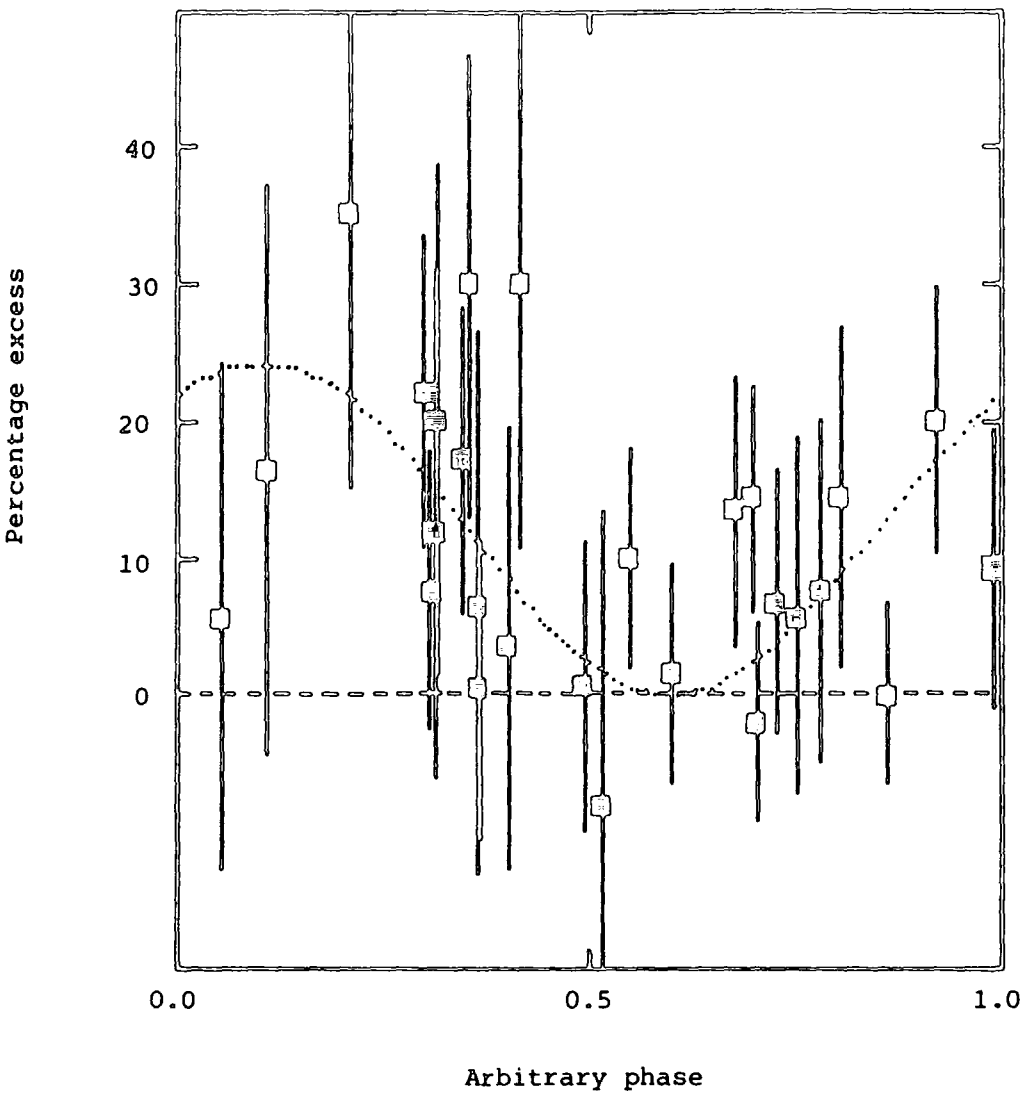

Figure 5.6 The sine wave fit to the count rate excesses in individual drift scans of Cygnus X-3 taken in 1981-3 folded modulo 19.2 days.

mechanism. The U.H.E. γ-ray light curve appears to be very narrow, which is also difficult to achieve if the progenitor particles are accelerated in a strong shock since this requires scattering, whereas a narrow pulse implies a straight trajectory. These two considerations suggest that the U.H.E. particles may be accelerated by some other method. Pulsar acceleration was proposed as a mechanism some time before the first U.H.E. observations of Cygnus X-3 (Basko et al., 1974; Bignami et al., 1977), and is now invoked to explain the γ-ray emission. I propose to describe briefly three of the more recent models of the Cygnus X-3 system, with particular reference to the requirements of any pulsar. These models are:

(i) The cocoon model

(ii) The target model

(iii) The dynamo model

(iv) The diffusive shock mechanism

The reasons why γ-ray measurements may provide the only means of observation of a pulsar in Cygnus X-3 will then be considered.

5.5.1. The "Cocoon" Model

Milgrom and Pines noted (1978) similarities between the spectrum of Cygnus X-3 and the Crab pulsar. The fluxes observed follow a power law, where $1.8 < \alpha < 2.2$, differing markedly from that observed from accreting objects, which usually have a much steeper spectrum at $E > 20$ keV. A pulsar would therefore need to be present in the system. The pulsar is considered to be accreting material from a main sequence

star, and the whole system is surrounded by a gaseous envelope which absorbs and re-emits the X-rays produced by the pulsar, hence producing the observed X-ray spectrum. The envelope consists of matter blown off the surface of the pulsar's companion and is formed at a radius of about 10^{12} cm as a consequence of the combined action of the radiation and charged particles produced by the pulsar, and the gravitational field of the system. This shell as proposed should not cause any attenuation of pulsed γ-ray radiation from the pulsar. If the pulsar radiation and particle pressure is to be sufficiently high to cause substantial mass loss from the companion as a result of X-ray heating, the pulsar would require a rotation period of between 10 and 30 ms.

5.5.2. The Target Model

In an attempt to find a mechanism to produce γ-rays of $E > 10^{16}$ eV, Eichler and Vestrand (1984) have proposed a model in which the atmosphere of the companion provides a target for the relativistic wind from the pulsar, the resulting interaction producing γ-rays. Shock acceleration is capable of accelerating particles to energy 10^{14} eV. An electromagnetic wave (Gunn and Ostriker, 1969) accelerates particles to higher energies close to the pulsar. To produce particles of the required energy, a young pulsar with a large spin-down rate is needed, contrary to the spin-up usually observed in binary systems. The γ-ray light curve would consist of two peaks separated by $\phi = 0.4$ (for which there is some evidence) and the minimum would be due to

the eclipse of the pulsar by the secondary. It may be noted that this model predicts that the pulsar would be a strong source of gravitational waves.

5.5.3. The Dynamo Mechanism

This model (Chanmugam and Brecher, 1985) derives both the X-ray and γ-ray emission from an accretion disk surrounding a neutron star. As the disc rotates differentially around the neutron star, the ambient magnetic field, which is considered to be anchored in the disc, becomes amplified and poloidal. This induces an electric field in the plane of the disc (c.f. a unipolar inductor). The high voltages generated accelerate particles in two jets, which collide with gas nuclei and generate γ-rays. The magnetic field required from the neutron star in this model is about 10^4T. Such a neutron star would be spinning rapidly with a period of the order of 1 ms. It may be, then, that Cygnus X-3 corresponds to an intermediate phase in the formation of an isolated millisecond pulsar.

5.5.4. The Diffusive Shock Mechanism

This model, developed by Kazanas and Ellison (1986) uses accretion of material from a companion star onto a neutron star as the energy source with first order (or diffusive) shock acceleration as the mechanism for the transfer of energy to the ions required for the production of the observed U.H.E. radiation. It is thought that

shocks will form when plasma accretes onto compact objects because the accretion velocities are much higher than the thermal velocities of the accreting matter. The accelerated ions produce neutrons via high energy proton-proton collisions and via the photo-dissociation of U.H.E. nuclei (particularly ^{4}He nuclei). These neutrons would then, by interaction with the companion star, produce the observed narrow U.H.E. γ-ray pulse. The production of neutrons is crucial in this model since it allows the transport of energy from the neutron star without a requirement for a particular magnetic field configuration. It is also less difficult to produce a narrow pulse of γ-rays using neutrons as the progenitor particles: charged particles are easily scattered by the magnetic field. A rapidly rotating pulsar is not explicitly required in this model. However, the magnetic field assumed in calculations (10^{4}T) implies that the neutron star is probably spinning with a period of the order of a few milliseconds.

5.5.5. Absorption of Pulsed Radiation

X-ray and infrared measurements indicate that there is a column density of between 3×10^{22} and 2×10^{23} atoms cm^{-2} of hydrogen between the earth and the emitting region of Cygnus X-3 (Weekes and Geary, 1984; Gursky et al., 1967; Parsignault et al., 1972). The observed absorption of radiation is due to gas both in the inter-stellar medium (Cygnus X-3 lies almost directly along the Cygnus spiral arm) and in the immediate vicinity of the source. Radio

measurements of the HI line indicate that the column density is 1.7×10^{22} atoms cm^{-2} (Chu and Beiging, 1973). The slight difference between these measurements suggests that the radio emission may originate in a different location in the source from the X-ray and infrared emitting region. This high column density of hydrogen represents a severe limitation on searches for short period pulsation from Cygnus X-3 in the radio region due to the effects of frequency dispersion. For instance, the interstellar matter between earth and the Crab pulsar (which is only 2 kpc from the Earth) is such that the regular 33 ms pulsation would be smeared out completely. Its discovery was dependent on the detection of single large pulses and not on the periodicity (Smith, 1979). It may therefore be very difficult to detect a rapidly rotating pulsar in Cygnus X-3 from radio measurements. Since the delay in travel time of an electromagnetic pulse is proportional to ν^{-2}, this is not a problem for pulsed high energy radiation.

5.6. The Pulsar Search in Dugway Data

There are two problems inherent in any search for pulsar periodicity from Cygnus X-3 using V.H.E. γ-ray data.

(i) Orbital motion induces a Doppler shift on the arrival times of the pulses from any pulsar in a binary system. In the case of Cygnus X-3, which is probably in a binary system, the orbital parameters are unknown, so it is impossible to adjust event arrival times to remove this effect (see section 3.4.3). The

data which are analysed must therefore have been taken over a short time to obviate this problem. If one assumes that the 4.8 hr period observed in Cygnus X-3 is orbital in nature, the dataset may be no longer than about 1000 seconds.

(ii) As the pulsar period is obviously unknown, many trial periods must be tested. For an effect to be statistically significant in this case it requires a very low probability of chance occurence. Since, in the case of the Rayleigh test, the probability of chance occurrence of an effect is proportional to e^{-nR^2} (see section 3.5.2) where n is the number of counts and R is the vector length at the main pulse, and from (i) we require a short dataset, it follows that the telescope must have a high count rate. For example, if we require a genuine 10^{-4} effect for 10^4 trials, the Rayleigh probability must be 10^{-8}. If we assume that 20% of the events are periodic, this implies that n is approximately 500. If we are to obtain this over a short duration of perhaps 10 minutes, the count rate must be approximately 1 Hz.

5.6.1. 12th September 1983

In 1983, one of the telescopes of the Dugway facility was re-mirrored and had its aperture reduced in order to increase its sensitivity. This resulted in an average count rate for the four telescopes of about 1 Hz (see section 2.7.2). Observations of

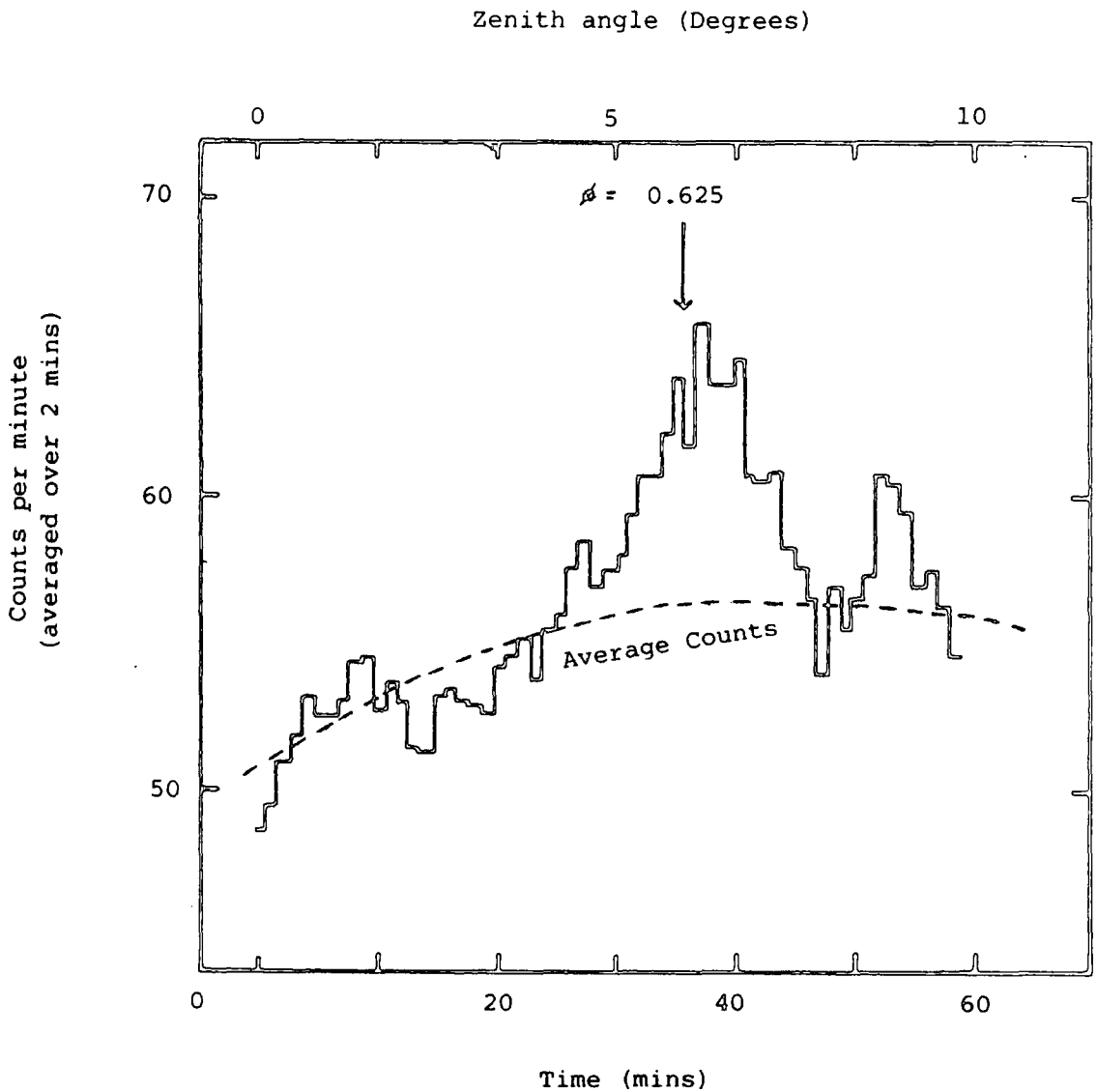

Figure 5.7 The count rate of the Dugway telescopes during the 12th September 1983 observation of Cygnus X-3.

Cygnus X-3 were made with this improved system in August-October of that year, the source being continuously tracked under a wide range of weather conditions. The best weather conditions during that period were encountered on 12th September 1983 when the sky was completely clear for the duration of the observation. The X-ray maximum was predicted (using Van der Klis and Bonnet-Bidaud, 1981a) to occur at 0519 U.T. on that date. At this phase a 20% excess in counts lasting for 7 minutes was observed (see figure 5.7). This single dataset fulfils the criteria i) and ii) above, so a pulsar search within this sample was deemed worthwhile.

The 450 events contained within the 7 minute interval were tested for periodicity over the range 10 ms to 50 sec, using the Rayleigh test. The period with much the smallest probability of chance occurence was 12.5908 ± 0.0003 ms, the uncorrected probability being 4.8×10^{-8} (see figure 5.8). At all other periods the probability distribution was consistent with that which would be expected by chance. When allowance is made for the number of periods tested, the significance of this period is 3.3×10^{-3} or 3σ. The light curve at this period is shown in figure 5.9. This is not in itself of compelling significance, but it is also found that the strength of the periodic component is correlated with the count rate during the 7 minutes of the burst. If the effect is genuine, the onset and decay of the count rate excess should correlate with the fraction of counts which are periodic. This will not be so if the apparent periodicity is the result of a random fluctuation, and any

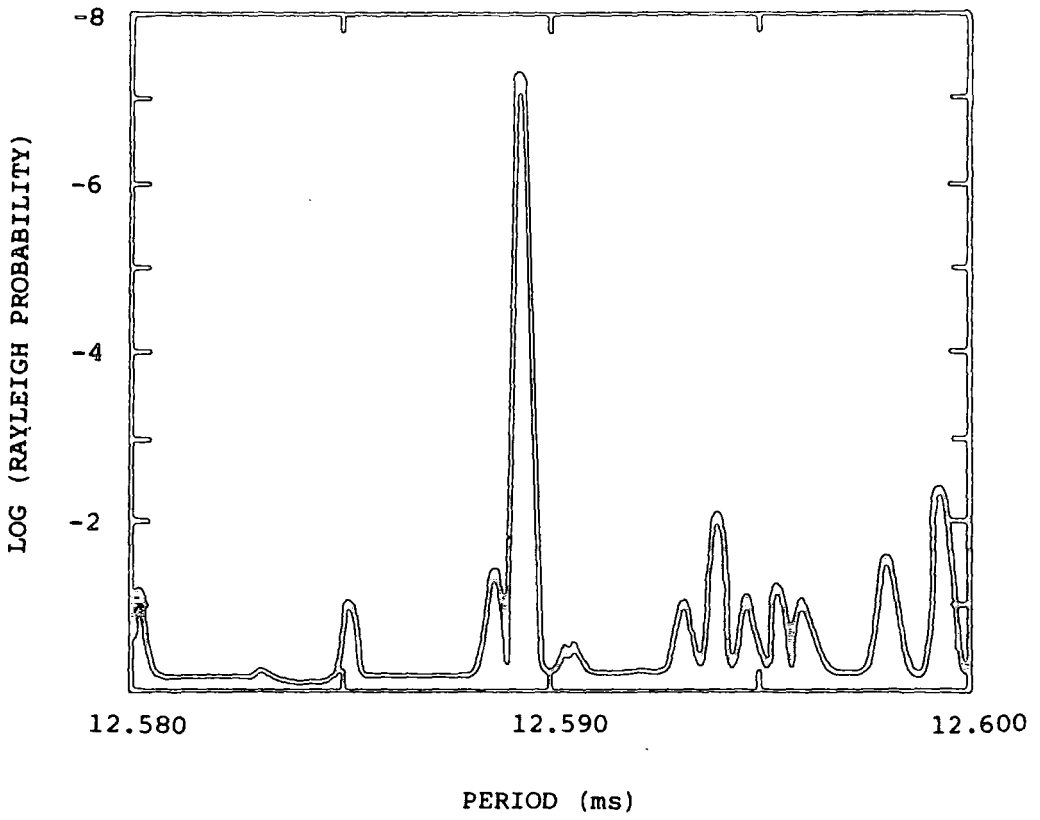

Figure 5.8 The Rayleigh chance probability of periodicity in the 450 events containing the count rate excess on September 12th 1983 as a function of trial period.

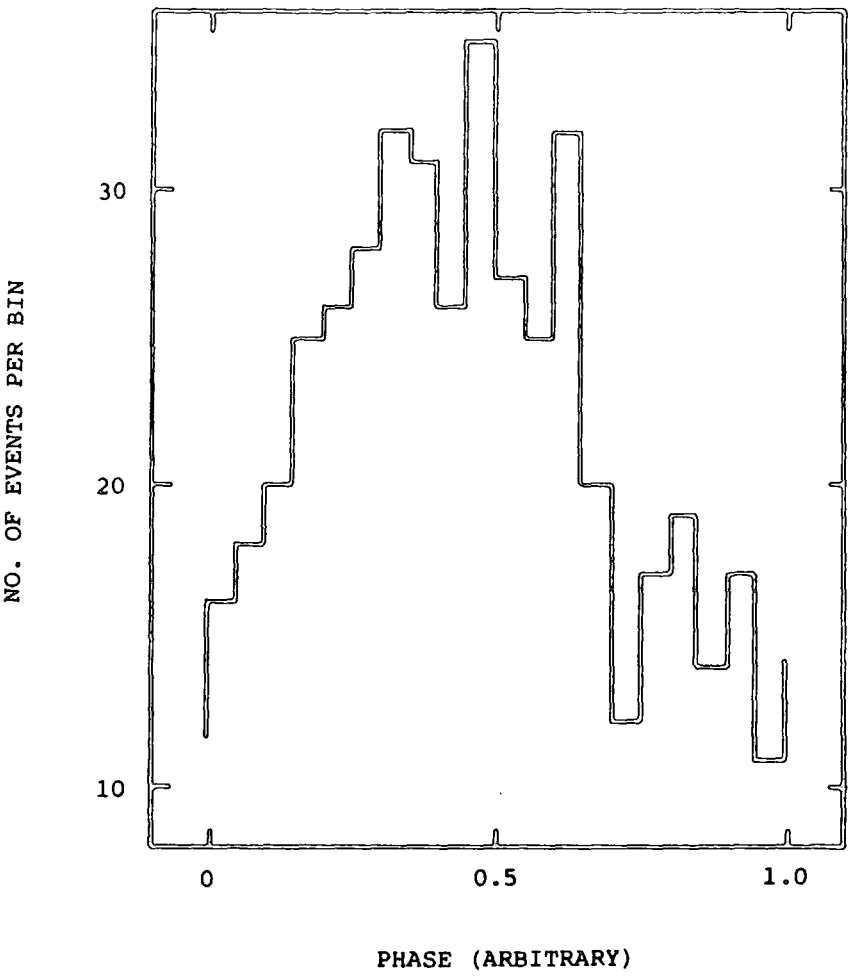

Figure 5.9 The light curve for gamma ray emission from Cygnus X-3 at E > 1000 GeV on 12th September 1983 at a trial period of 12.5908 ms.

correlation will provide independent evidence of periodicity (Eadie et al., 1971). It is found that the strength of the periodic component correlates (at a significance level of 9.5×10^{-4} or 3.1 σ) with the count rate in independent 1 minute datasets within the 7 minute burst interval (see figure 5.7).

5.6.2. Other Data from 1983

During August-October, seven further observations of Cygnus X-3 spanning the time of predicted X-ray maximum were made (see table 5.1). The weather conditions were not sufficiently stable to allow the unambiguous identification of count rate excesses, but it was possible to test the data at the same phase as the excess on September 12th for periodicity at the specified period. As can be seen in figure 5.11, data from one of the seven nights, 2nd October 1983, shows periodicity at 12.5908 ms during precisely the same 7 minute interval in the orbit as the earlier detection. The periodicity has a chance probability of 4×10^{-4}, the lower significance of this result reflects the lower count rate on that night, but this is a genuine probability in the absence of any degrees of freedom.

As mentioned in section 5.4, the data show some evidence for a long-term amplitude modulation of the X-ray maximum of 19.2 ± 0.4 days. There is also the possible 18.7 day phase modulation in amplitude found from observations made with the COS-B X-ray detector, which results in an advance or retardation of $\pm$ 3 min. In the time of

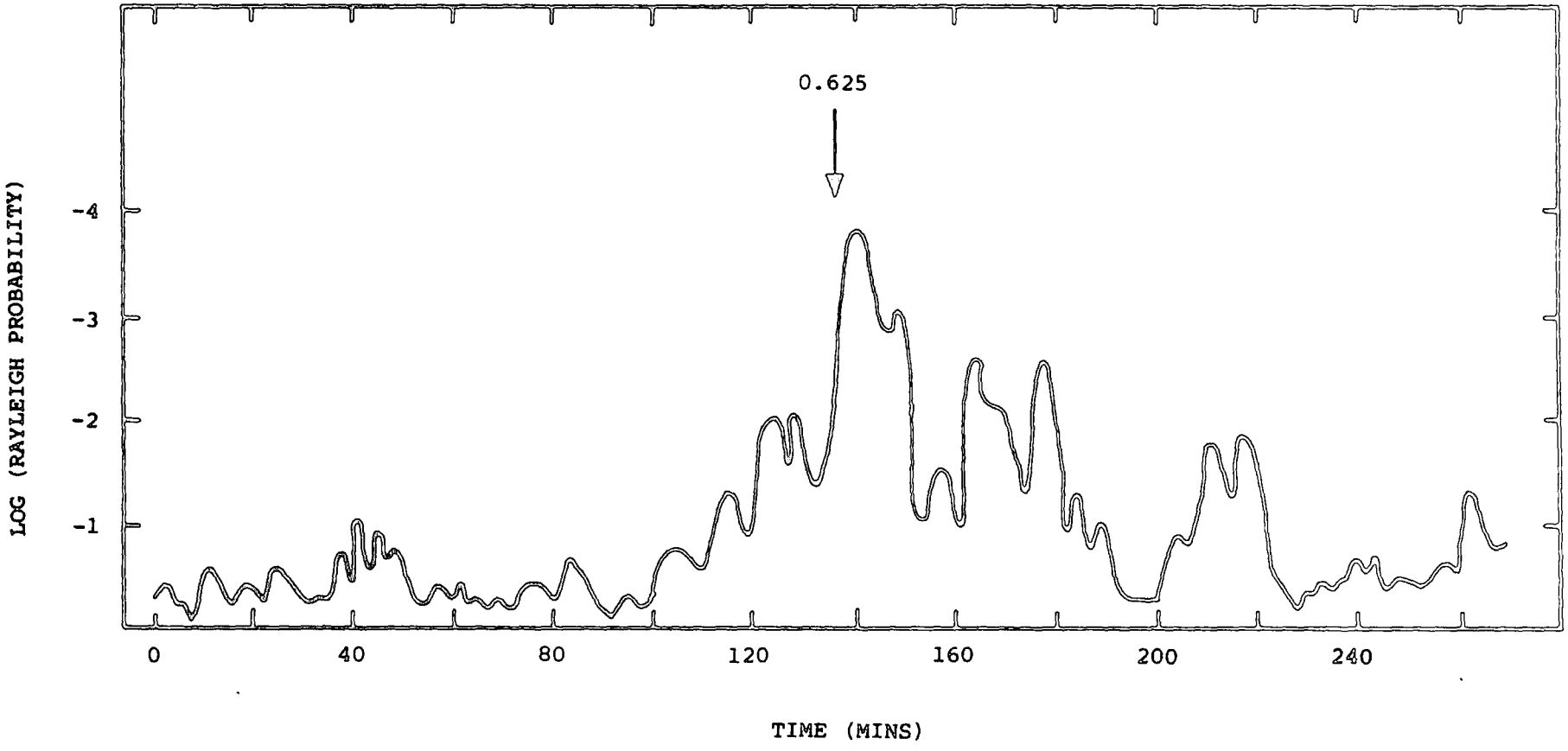

Figure 5.10 The probability of no periodicity in 100 event datasets moved in increments of 10 events throughout the Cygnus X-3 data obtained on 12th September 1983. The trial period is 12.5908 ms. This may be compared with figure 5.7.

DATE	TIME (U.T.)
150483	1045 - 1113
310883	0347 - 0602
010983	0435 - 0614
070983	0321 - 1040
120983	0345 - 1031
290983	0233 - 0548
021083	0226 - 0731
041083	0225 - 0427

Table 5.1 The dates of tracking observations of Cygnus X-3 spanning X-ray maximum made from Dugway.

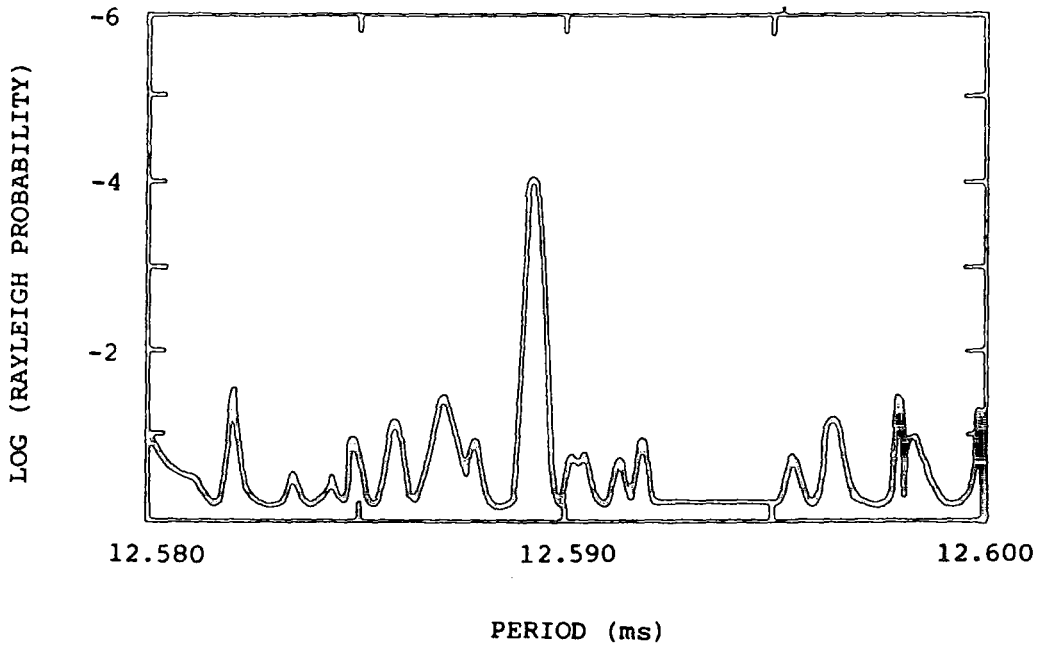

Figure 5.11 The Rayleigh chance probability of periodicity for the events on 2nd October 1983 at precisely the same phase in the 4.8 hr cycle as was investigated on September 12th 1983 as a function of trial period. This may be compared with figure 5.8.

X-ray minimum (Bonnet-Bidaud and Van der Klis, 1981). If our suggested 19.2 day modulation is genuine, and as the September observation of periodicity was near a peak in the 19-day amplitude cycle, the October 2nd observation would be expected to show the most significant periodic excess. The 18.7 day phase modulation would have the effect of producing up to a minute in phase difference between the two observations. Data in a 7 minute interval centred on a time 1 minute after the time of X-ray maximum predicted by the ephemeris does indeed show a periodic content at a smaller chance probability (4×10^{-5}).

If we ignore the significance of any possible 19-day amplitude modulation, and also ignore the improvement in statistical significance produced by moving the 7 min interval searched in accordance with the 18.7 day phase modulation, the final chance probability for the detection of a 12.5908 ms effect on any one of the 7 nights examined becomes 2.8×10^{-3}. This may be combined with the chance probability from the discovery of 12.6 ms on September 12th and with the independent chance probability from the correlation of count rate with periodicity on that night, so that the overall probability of chance occurrence becomes 4×10^{-7}.

5.6.3. Twofold Events

It has been previously demonstrated that events which trigger any two of the four Dugway telescopes ("twofold events") have a narrower acceptance angle than those which trigger one telescope

alone (Dowthwaite et al., 1984; Walmsley, Ph.D. thesis, in preparation). This means that a point source of γ-rays centred in the field of view of the two telescopes will have a proportionally greater effect as more background (proton) events will have been rejected (see section 2.5). The twofold events on the Cygnus X-3 nights in question were tested for periodicity at 12.5908 ms and showed an enhancement in signal by a factor of 1.5. However, since fewer events are available for analysis using this method, the uncertainty in the enhancement is $\pm$ 0.5. It is thus not possible to use two-fold events to improve the signal:noise ratio in this case.

5.6.4. Tests for the Presence of a Signal in Other Harmonics

The possibility that the 12.59 ms period detected in our data is not the fundamental was considered. Whilst longer periods (up to 50 ms) were tested, the test for periodicity was terminated at 10 ms to avoid a possible loss of coherence at short periods (Dowthwaite, Ph.D. thesis, in preparation). Datasets shorter than 7 minutes were tested at the harmonics of 12.59 ms and the distribution of Rayleigh probabilities was found to be consistent with that due to chance.

5.6.5. Instrumental Effects

To check for the origin of the 12.59 ms periodicity in any instrumental effects, data taken on other objects on the nights when

observations were made of Cygnus X-3, and observations made of other objects on adjacent nights were analysed in the same fashion. The Rayleigh test probability distributions were found in all cases to be consistent with those expected by chance. The 12.5908 ms periodicity in the Cygnus X-3 data was detected in all four telescopes, excluding the possibility that local electrical pick-up on any one telescope was responsible for the observed effect. The telescopes were all operated and triggered separately, making electrical pick-up on all four telescopes also unlikely. In addition, the charge recorded in each photomultiplier for every event in the Cygnus X-3 sample was consistent with that expected for Cerenkov light flashes. All values for the anode currents and threshold count rates for the photomultipliers were also recorded and are found to be normal throughout the 7-minute burst interval.

5.7. Support from Earlier and Later Observations of Cygnus X-3

Other Cygnus X-3 data presents three problems if any search for periodicity is to be made, these being the lower count rate of the early Dugway telescopes, the unknown pulsar period derivative and uncertainties in X-ray ephemerides.

5.7.1. Count Rates

In 1981 and 1982 the Dugway telescope array did not have as high a count rate or sensitivity as in 1983. Count rate excesses are therefore less easily identified, and any periodicity present

within this data would not make a significant contribution to the overall chance probability. Although the 1985 data were taken on a single, more sensitive telescope, the overall contribution is still low. Additionally, much of the data from 1981 were taken in the drift scan mode of operation, and are therefore less suitable for periodicity searches than tracking data.

5.7.2. Unknown Secular Period Derivative

If Cygnus X-3 is a binary system (as much of the evidence suggests), then the pulsar would be spinning up due to accretion from the companion. However, a fast pulsar such as that proposed may be expected to spin down rapidly. It is possible to make an order-of-magnitude calculation to determine which effect might be expected to dominate.

If we assume that Cygnus X-3 is an accreting binary, and that the accretion is mediated by a roughly circular disc, the rate of change, $\dot{P}$, of the pulsar period P is related to the X-ray luminosity and to the properties of the neutron star by the following approximate formula after Rappaport and Joss (1983):

$$\frac{\dot{P}}{P} \simeq -3 \times 10^{-5} \left[\frac{\xi \nu_r}{\nu_{ff}}\right]^{\frac{1}{2}} \left[\frac{M_x}{M_o}\right]^{-\frac{10}{7}} \left[\frac{R}{10\text{km}}\right]^{\frac{6}{7}} \left[\frac{R_g}{10\text{km}}\right]^{-2} \left[\frac{\mu}{10^{30}}\right]^{\frac{2}{7}} \left[\frac{L_x}{10^{37}}\right]^{\frac{6}{7}} \left[\frac{P}{1_s}\right] \text{yr}^{-1} \qquad 5.1$$

ξ is the fractional solid angle subtended at the neutron star by the infalling matter at the magnetopause.

v_r / v_{ff} is the ratio of the average radial infall velocity of a particle to its free fall velocity just outside the magnetopause.

M_x is the mass of the neutron star

R is the radius of the neutron star

R_g is the gyroradius of the neutron star

μ is the magnetic dipole moment of the neutron star

L_x is the X-ray luminosity (assuming it to be accretion-driven). Most of these ratios do not differ greatly from unity for the "standard" neutron star, so this formula can be simplified to:

$$\frac{\dot{P}}{P} \simeq -3 \times 10^{-5} f \left[\frac{P}{1s}\right] \left[\frac{L_x}{10^{37}}\right]^{\frac{6}{7}} \quad yr^{-1} \qquad 5.2$$

where f is a dimensionless function of the order of 1. Now, the period postulated for Cygnus is 12.59 ms, and the average X-ray luminosity is 4.4×10^{37} erg s^{-1}. This results in an accretion-induced period derivative of approximately -5×10^{-16} ss^{-1}. This assumes that the sense of the orbital angular momentum in the accreting matter is the same as that of the rotation of the neutron star (accretion in the opposite direction would serve to slow the rotation rate of the pulsar down). If we compare this to the spin-down of a fast pulsar such as the Crab pulsar, which is of the order of 10^{-13} ss^{-1}, it is

clear that this spin-down may be expected to dominate.

5.7.3. Errors in Ephemerides

An important requirement in searching data taken some time before or after 1983 is to predict accurately the short intervals in the 4.8 hr cycle corresponding to the 7 minute intervals of activity in 1983. A limitation in this case is the accuracy and also the choice of the ephemeris. Throughout this work, the "standard" ephemeris is the widely used Van der Klis and Bonnet-Bidaud ephemeris (1981a). In 1985, EXOSAT measurements of Cygnus X-3 indicated that the X-ray maximum occurred 0.035 of an X-ray cycle earlier than predicted by Van der Klis and Bonnet-Bidaud (Molnar, Ph.D. thesis, 1985). If this is indeed so, one might expect that prior to 1983 the activity will occur at later times to those predicted by Van der Klis and Bonnet-Bidaud. Assuming that the γ-ray emission occurs at a fixed X-ray phase and allowing for a simple linear variation with time, any activity in 1982 should be detectable in a 1000 sec. interval 200 sec. later than the time of X-ray maximum predicted by Van der Klis and Bonnet-Bidaud (see fig. 5.12). Note that such an interval also covers the original prediction of X-ray maximum.

A further ephemeris, which seeks to remove this discrepancy is at present being produced by Mason (quoted as a private communication, Watson, 1987) and has in fact been used in the analysis of U.H.E. data from Haverah Park (Watson, 1987).

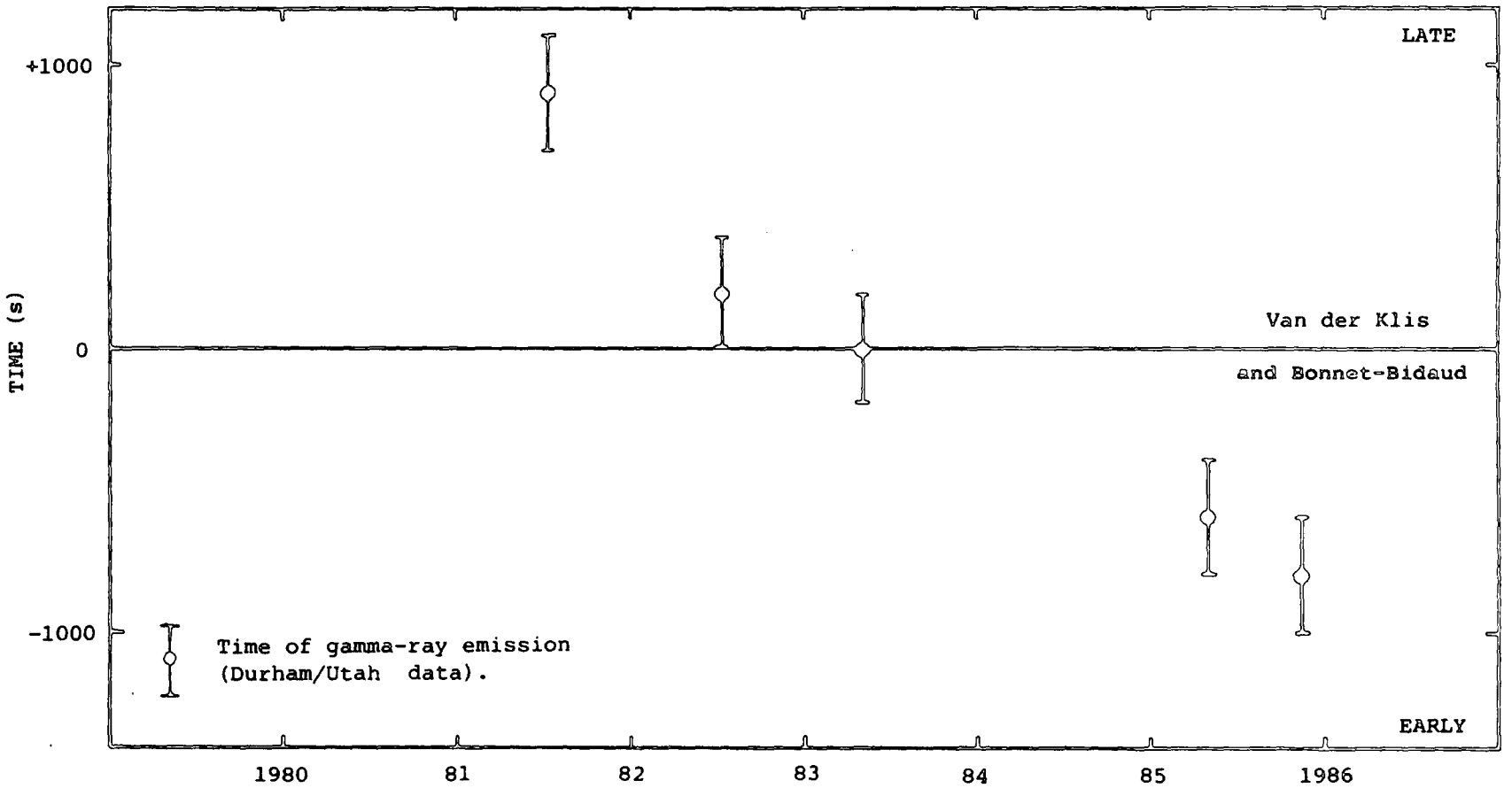

5.12 The times of pulsed gamma-ray emission in 1981-85 compared with the time of X-ray maximum as defined by the Van der Klis and Bonnet-Bidaud (1981a) ephemeris.

5.8. Observations made in October-November 1985

After the dismantling of the Dugway array in late 1984, the telescopes and their associated electronics were transported back to Durham. One of those telescopes (the Mark II) was again remirrored, this time with high-reflectivity long focal length aluminium mirrors of the type later used on the Mark III telescope (see section 7.5.1). Observations of Cygnus X-3 were made with this further improved telescope on six nights in 1985 between 12th October and 11th November, around the maximum of the 4.8 hr cycle. Since EXOSAT measurements suggest the X-ray maximum is earlier than predicted by the Van der Klis and Bonnet-Bidaud ephemeris (Molnar, Ph.D thesis, 1985), 1000 second intervals of data centred on a time 600 seconds before the predicted X-ray maximum were selected for analysis. On the assumption that the Cygnus pulsar is slowing down with a period derivative of possibly 10^{-13} ss^{-1}, the 40 independent periods in the range 12.5908 to 12.5950 ms were tested using the Rayleigh test. The combined chance probabilities for all six nights are shown in figure 5.13. When allowance is made for the number of periods searched the probability of the effect at 12.5928 ± 0.0001 ms arising by chance is approximately 0.01.

The periodicity at 12.5928 ms arises mainly from the observation on October 12th. The probability distribution for October 12th alone is illustrated in figure 5.14. Of the data taken in late 1985, this observation is closest to the radio burst of 6th October 1985 (Johnston, private communication). The constrictions of Durham

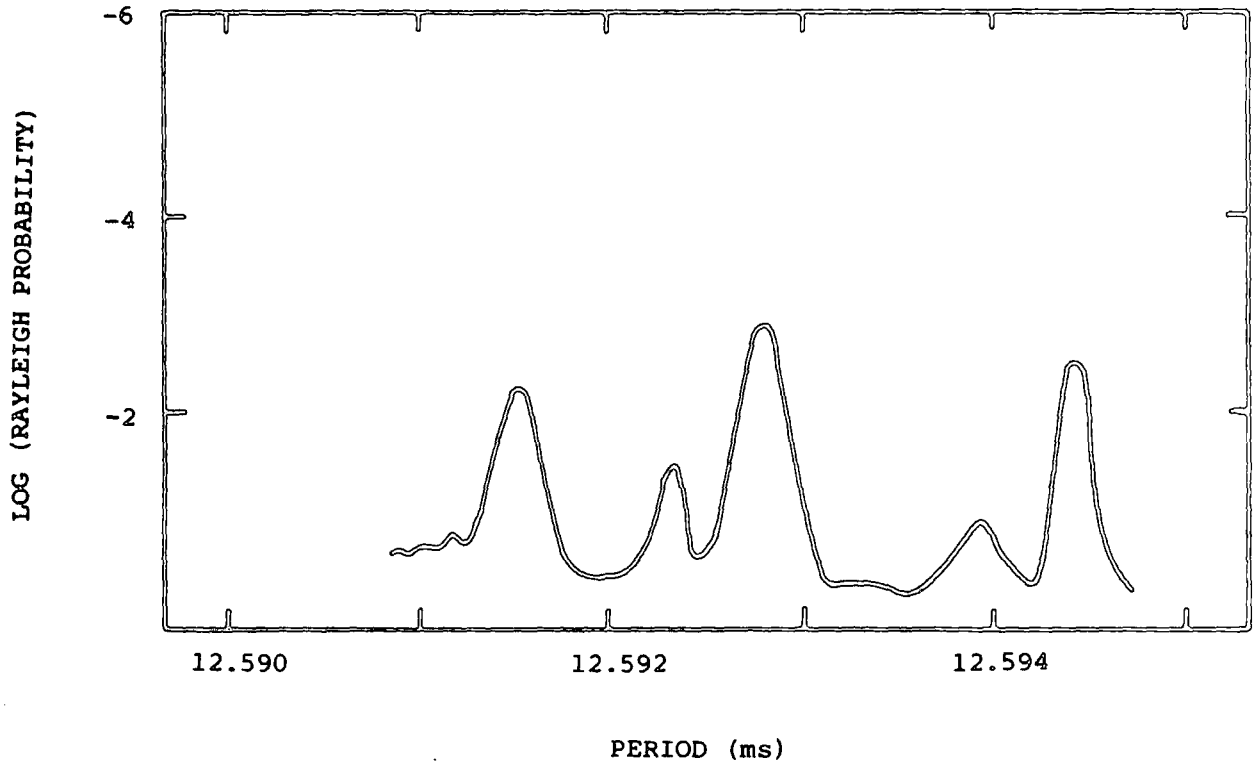

Figure 5.13 The Rayleigh probability of chance occurrence as a function of trial period for all Cygnus X-3 data taken in 1985.

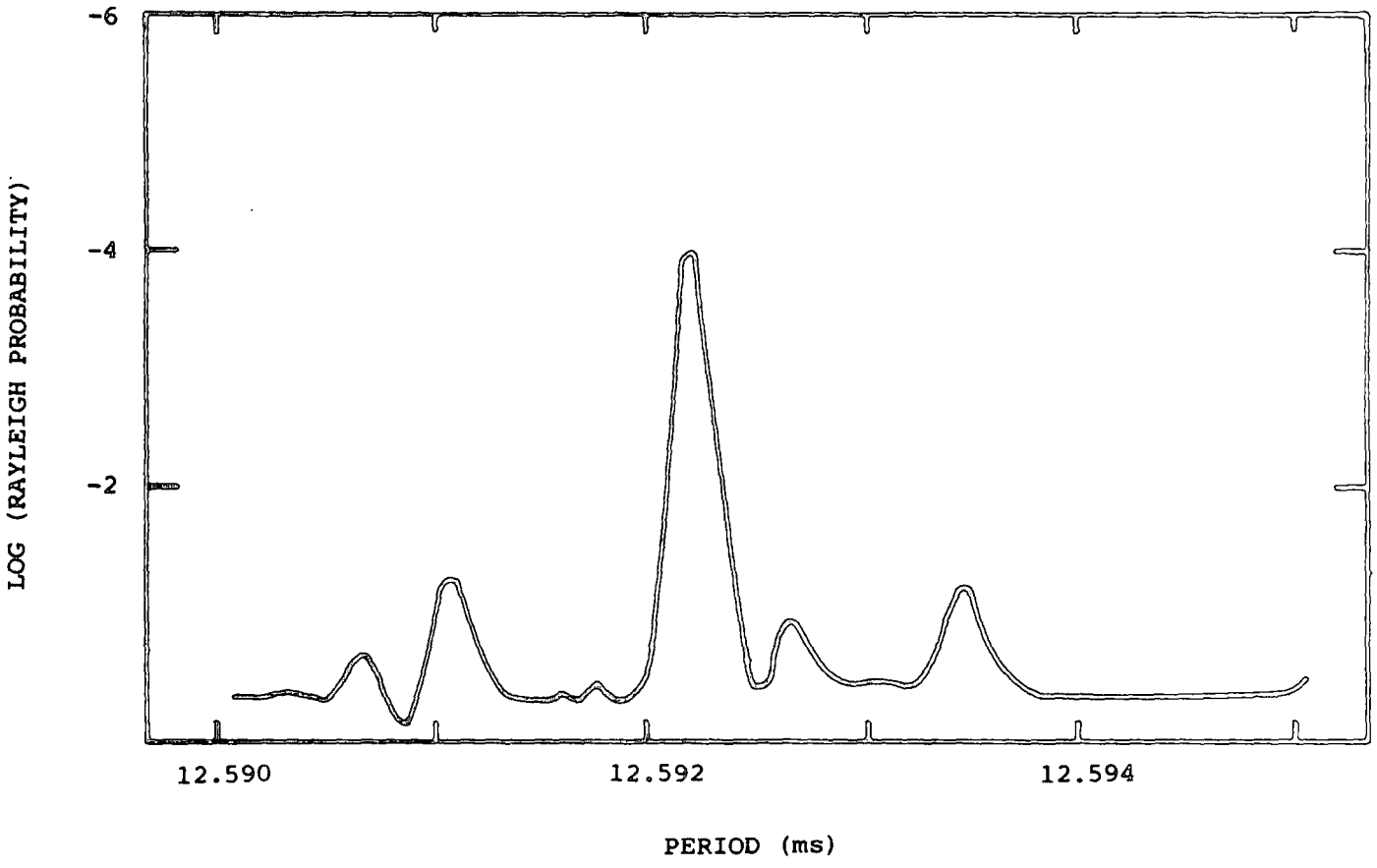

Figure 5.14 The Rayleigh probability of chance occurrence as a function of trial period for the observation of Cygnus X-3 on Oct 12th 1985 (X-ray phase 0.59 +/- 0.06).

weather rendered any observations nearer that date impossible.

5.9. Observations made in 1982

Initial analysis of 1982 data showed some qualitative evidence for activity at 12.5908 ms on two nights only. However, the evidence from the EXOSAT measurements, and from the Durham observations in October 1985 of 12.59 ms periodicity in Cygnus X-3 suggests that the X-ray maximum occurs before the time predicted by the Van der Klis and Bonnet-Bidaud ephemeris, and that the pulsar period is longer than in 1983. It may therefore be expected that prior to 1983 any pulsar activity will occur at times later than the ephemeris prediction, and the pulse period, should it exist, will be shorter than that observed in 1983. Assuming that the γ-ray emission occurs at a fixed X-ray phase, and allowing for only a linear variation with time of both the 4.8 hr cycle and the pulsar period, in 1982 data any pulsar activity should be detectable in a 1000 second interval centred 200 seconds after the predicted time of X-ray maximum, and the pulsar period should be in the range 12.5895 to 12.5905 ms. The result of the analysis of data from all 29 nights in July-November 1982 is shown in figure 5.15. Allowing for the number of periods searched, the smallest corrected chance probability is 0.01 at a period of 12.5900 ± 0.0001 ms.

The 1982 data were also analysed month-by-month, as the assumption of the constancy of period over 5 months, implicit in the earlier analysis, may not be valid. This analysis shows there

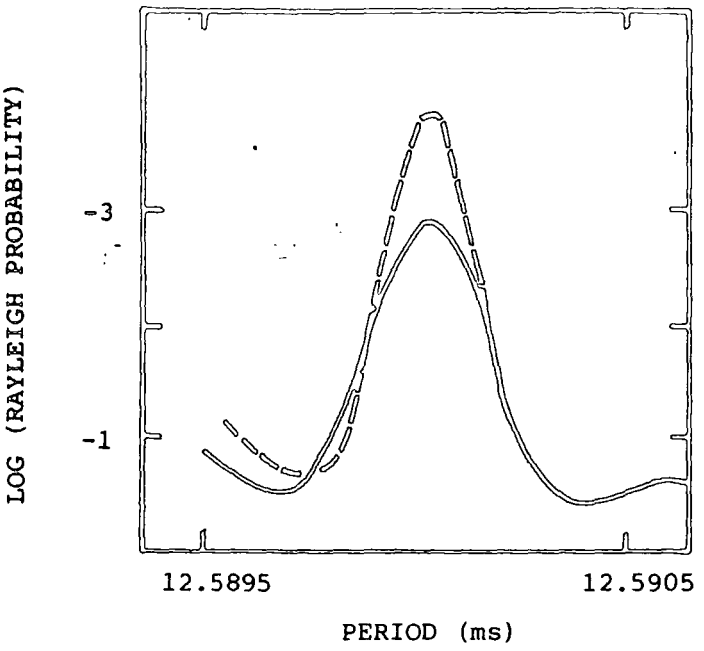

Figure 5.15 The Rayleigh probability of chance occurrence as a function of trial period for Cygnus X-3 data taken in 1982 at X-ray phase 0.635 +/- 0.06 (the solid line indicates all 1982 data , the broken line July only).

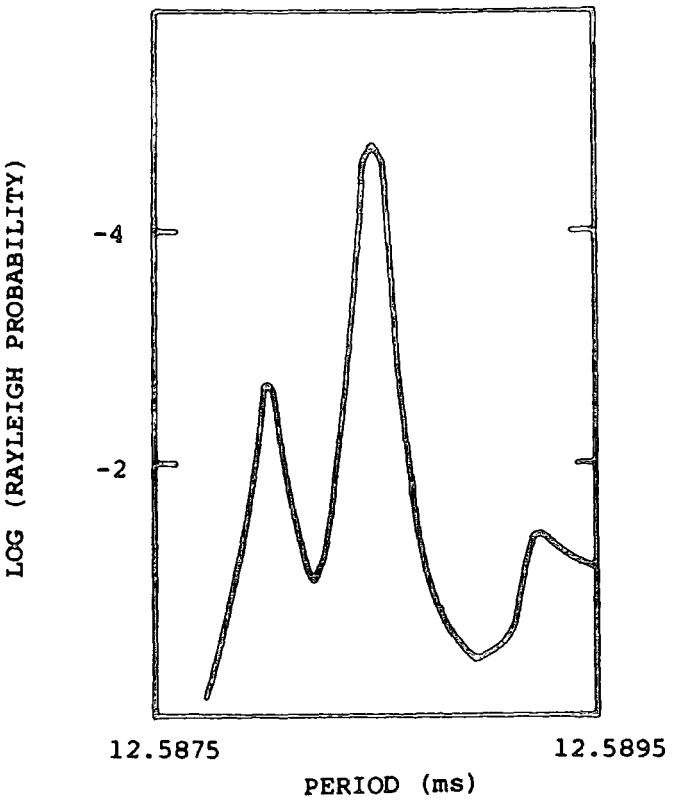

Figure 5.16 The Rayleigh probability of chance occurrence as a function of trial period for all Cygnus X-3 data taken at X-ray phase 0.675 +/- 0.06 in Dugway in 1981.

is a strong effect during the 5 observations made in July 1982 (see figure 5.15).

5.10. Observations made in 1981

As mentioned in section 5.2.1, much of our 1981 data were taken in drift scan mode and are therefore less suitable for periodicity searches. However, observations were made in the tracking mode for 3 nights in October 1981. We have assumed that the activity will be about 1000 seconds after the predicted X-ray maximum. The combined Rayleigh probability for non-uniformity of these data is shown in figure 5.16. The period with the smallest chance probability is 12.5885 ± 0.0003 ms, with a corrected Rayleigh probability of 0.01.

5.11. Periodicity Outside X-ray Maximum

As mentioned in section 5.2.2, some of the tracking observations made in 1982 and 1983 covered a whole 4.8 hr cycle. A window of 7 minutes duration was passed through 3 such datasets (one of which was the 12th September 1983), incrementing the start time by 1 minute steps spanning the complete 4.8 hr X-ray cycle. Each 7 minute long dataset was tested for periodicity at the expected period. No evidence for pulsar activity outside the X-ray maximum was found, though it should be noted that the lack of any orbital parameters for the system makes the Doppler effects on the arrival times of the pulsed γ-rays unknown.

5.12. The Secular Period Derivative of the Pulsar

While the results from 1981, 82, and 85 are not particularly significant (which is as would be expected for the telescope systems operating at those times) they do provide some qualitative evidence for the spin-down of the Cygnus X-3 pulsar. Figure 5.17 shows the variation of period with time. The best linear fit to these tentative results corresponds to a period derivative of $(2.8 \pm 0.5) \times 10^{-14}$ ss^{-1}. This gives a characteristic age for the pulsar of approximately 7000 years.

5.13. The Orbital Period Derivative

If the 4.8 hr period is due to an orbit, datasets suggesting periodicity and lasting 7 minutes should show some evidence of a period derivative due to the orbital motion. The periodicity test has therefore been repeated using a range of period derivatives between -10^{-8} and $+10^{-8}$ ss^{-1}, the results of which are shown in figure 5.18. The combined chance probability for the two datasets showing the 12.59 ms periodicity was found to minimize for a small negative period derivative of $-(1.2 \pm 0.7) \times 10^{-9}$ ss^{-1}. A similar treatment of the two nights showing strong pulsar activity in 1982 resulted in a best period derivative of $-(0.6 \pm 0.4) \times 10^{-9}$ ss^{-1}. These estimates combine to give a period derivative of $-(7.5 \pm 3.5) \times 10^{-10}$ ss^{-1}, significant at the 2σ level. This negative value (if real) places the source of the V.H.E. γ-ray emission in the rear half of the orbit at the time of X-ray maximum, in contrast to the

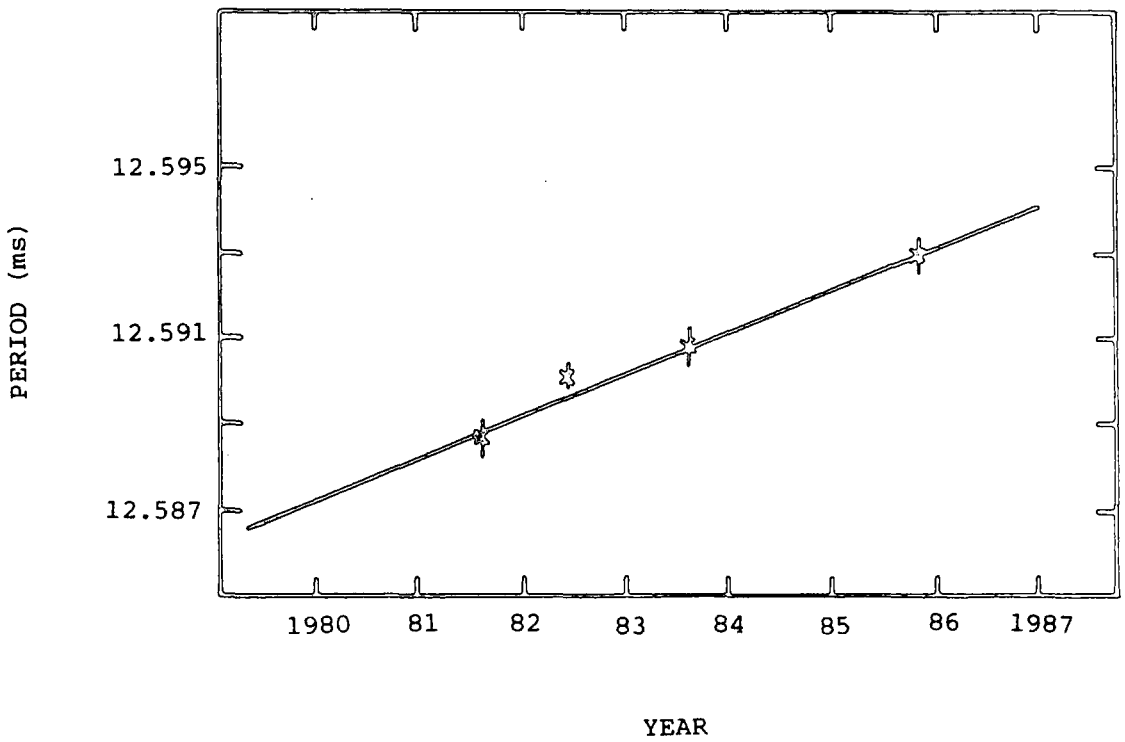

Figure 5.17 The secular variation of the Cygnus X-3 pulsar period.

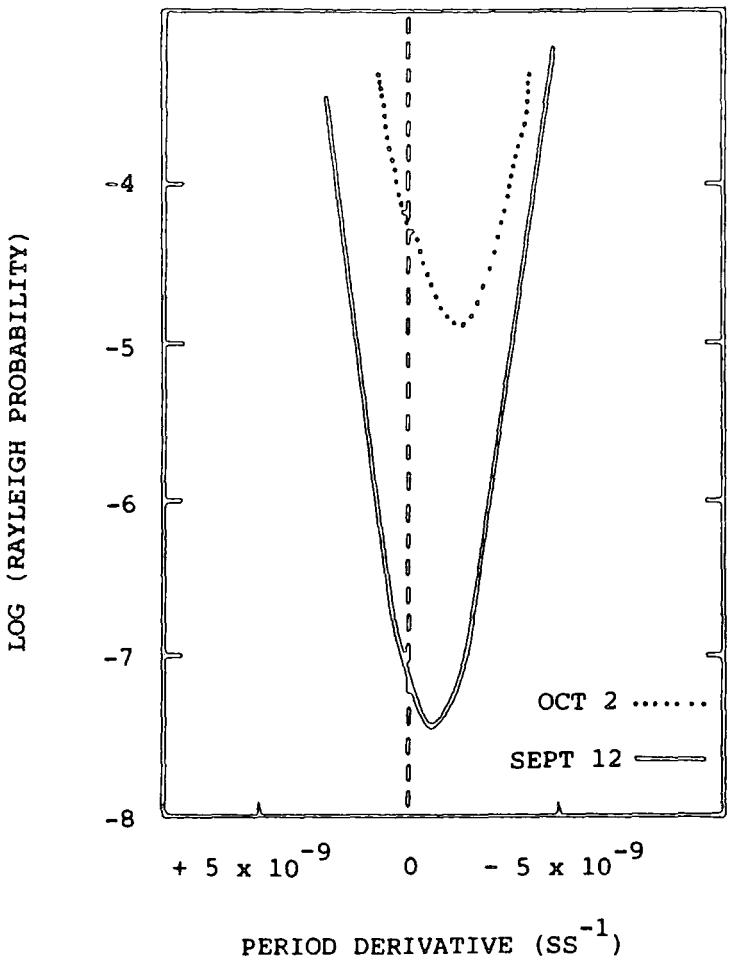

Figure 5.18 The sensitivity of the 12.59 ms effects on September 12th and October 3rd 1983 to different values of orbital period derivative.

expectations of the models described below.

5.14. Implications for Models of the Cygnus X-3 System

While the "Cocoon" model does not explicitly account for the high energy emission from Cygnus X-3, the "Target", "Dynamo" and "Diffusive Shock" mechanisms described in sections 5.5.2, 5.5.3 and 5.5.4. respectively require high-energy ions to interact with the atmosphere of the companion to produce V.H.E. and U.H.E. γ-rays. The light curves of the emission on September 12th (see figure 5.9) and October 2nd 1983 are broad, having the same form as the light curves from other X-ray binaries (see Chapter 9). This is in contrast to the sharp-peaked light curve produced in the case of an isolated pulsar such as the Crab and suggests that accretion plays an important part in the V.H.E. emission.

The orbital period derivative observed is not consistent with the "cocoon" model or with any of the "stellar wind" models. In these models the X-ray emitter is in front of the companion at X-ray maximum. In both cases it is assumed that the X-ray modulations are due to variations in the absorption or scattering, and a significant orbital eccentricity is required. However, the sign of the period derivative is consistent with the "target" model (5.5.2), and places the source of the very high energy ions behind the companion's atmosphere at the time of V.H.E. γ-ray emission. Assuming that the pulsar is almost directly behind the companion at the time of V.H.E. emission and that the orbit is nearly circular, the observed

period derivative corresponds to an orbital velocity of about 80 kms^{-1}, giving a Keplerian mass function of about 0.01 $M_{\odot}$.

5.15. Other Searches for a 12.59 ms Pulsar in V.H.E. γ-ray Data

Two attempts to confirm the results described above have been reported to date, from the Whipple Collaboration (Fegan et al., 1987) and from the group working at Haleakala (Resvanis et al., 1987a).

5.15.1. Whipple Observatory Measurements

The Whipple Observatory Cygnus X-3 database which was subjected to millisecond searches consists of 44 observations made in the tracking mode each of approximately 28 minutes' duration. The data were taken between April 1983 and November 1985, yielding a total of 1205 minutes of data. Each scan was split into six 8 minute segments overlapping each other by 4 minutes to minimise the effects of the unknown orbit (see section 5.6). The datasets thus produced were subjected to three separate analyses:

(i) Testing 31 independent periods between 12.586 and 12.596 ms, with no allowance for a period derivative.

(ii) As (i) above, but with a period derivative of -0.75×10^{-9} ss^{-1}, although a period derivative of this magnitude will have little effect on an 8 minute dataset.

(iii) A control test involving a periodicity search between 14.5459 and 14.5593 ms.

The authors claim that, although a "tail" of low probability periods

was found in the power spectrum, no evidence was found for any significant periodic emission when the number of trials was taken into account. It was noted that during the observation period no count rate excesses were observed, so it was not possible to identify a specific dataset which could be tested for periodicity.

Let us consider further the published data comprising the "tail" of the probability distributions in the Whipple data. The details of the scans contributing to the tail are shown in table 5.2. If the results of analysis (i) on the 1985 data are taken, and the "best" periods plotted against the 4.8 hr phase at which the data were taken, the data points lie on a straight line and indicating a shortening of the period at a rate of $-(2.55 \pm 1.68) \times 10^{-9}$ ss^{-1}, as shown in figure 5.19. These results suggest a value of the period at phase 0.625 which compares favourably with the pulsar period measured in Durham in 1985 which is also shown in figure 5.19. This result also compares well with the value for the average local period derivative of $-(7.5 \pm 3.5) \times 10^{-10}$ ss^{-1} suggested by the 1983 and 1982 Durham data. It is clear that the results of Cawley et al. are in agreement with the 1985 Durham pulsar period. However, the single Whipple observation in 1983 which contributes to the "tail", shows a period of 12.5955 ms at $\phi = 0.625$. Of course, some of the "tail" values will be expected by chance, and will not be representative of any pulsar period. These are interesting results, suggesting that further observations of Cygnus X-3 with the Whipple telescope are urgently required.

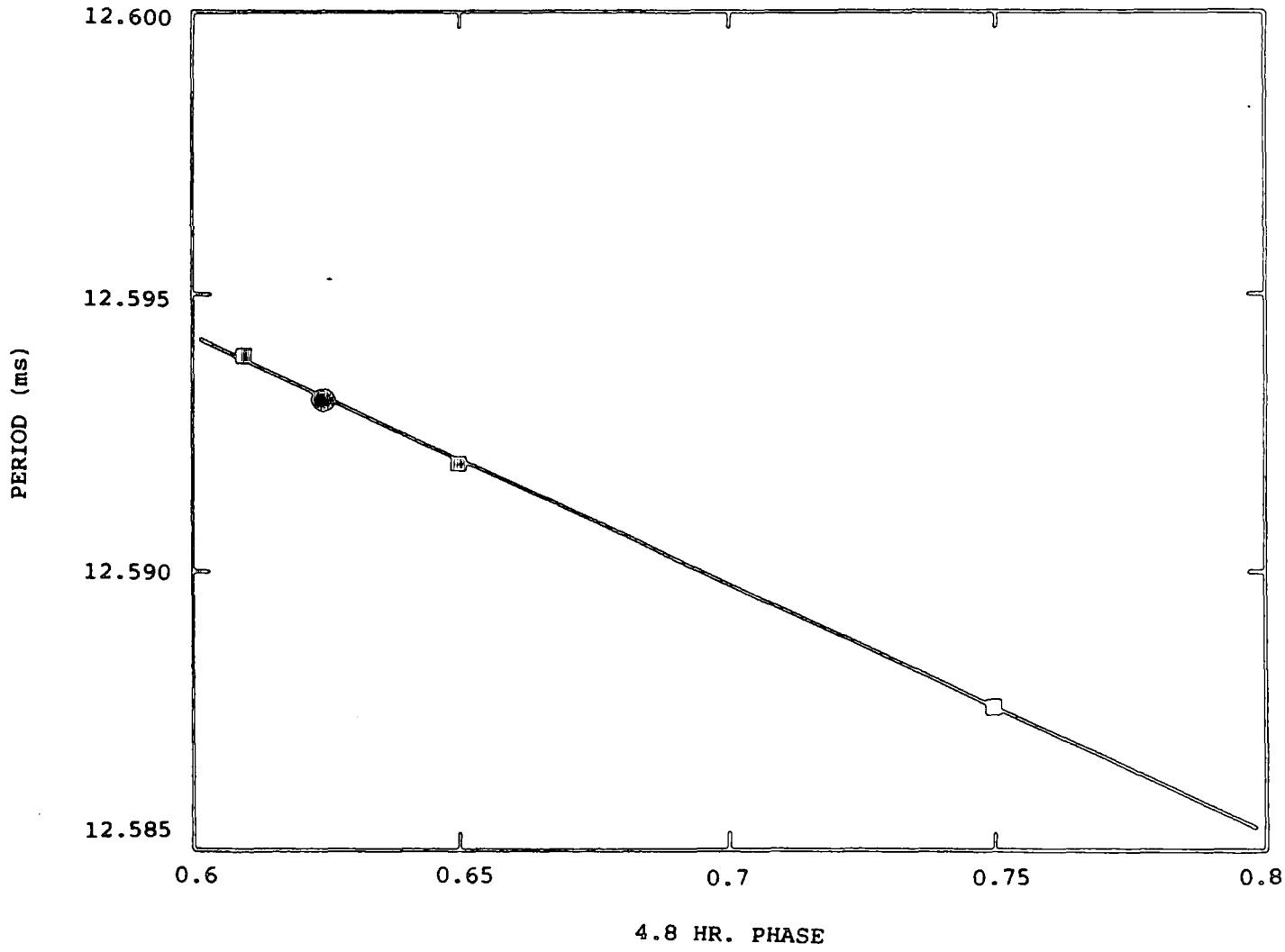

Figure 5.19 The "Best" periods from the Whipple Observatory data taken in 1985 plotted against 4.8 hr phase. The circle indicates the value of pulsar period at phase 0.625 derived from the Durham data also taken in 1985. The best fit orbital period derivative is $-(2.55 \pm 1.68) \times 10^{-9}$ ss^{-1}.

5.15.2. Haleakala Observations

The Haleakala telescope consists of a mirror system with two apertures, each with 18 photomultipliers, which routinely trigger on a coincidence of 7 photomultiplier tubes within 10 ns. In this case less than half the triggers are induced by random coincidences (Resvanis et al., 1987b). The database consists of 113 hours of data taken during the Summer and Autumn of 1985. On October 12th 1985, a 60 second burst of events from the direction of Cygnus X-3 was observed, at phase 0.74 of the 4.8 hour cycle according to the Van der Klis and Bonnet-Bidaud ephemeris (1981a). The coincidence threshold for event selection was then relaxed from 7 phototube triggers to 5 phototubes in 10 ns at which the noise level is much higher. This procedure has been previously applied in this experiment for observations of isolated pulsars (the Crab pulsar for example, Resvanis et al., 1987c), where it was considered that the standard threshold may be unduly restrictive. Here it is applied to a pulsar usually considered to be in a binary system. A period scan over the range of 10 ms to 2.2 sec. was made of the data recorded during the 60 second burst (a surprisingly wide range, bearing in mind the suggestion of 12.59 ms periodicity), and no conclusive evidence for pulsar activity was found when the number of degrees of freedom were taken into account (Resvanis et al., 1987a).

An earlier preliminary analysis of independent data taken on October 12th had shown some evidence for a pulsar signal occurring shortly after the burst. The candidate period was 12.5903 ms with

a Rayleigh probability of 2.8×10^{-5} and an imposed period derivative of -0.8×10^{-10} ss^{-1}, as suggested by the Durham Group. Without this period derivative the peak did not appear, and the effect was not observed when the threshold triggering requirement was relaxed (see the above procedure). There was also no excess count rate observed at this time, so this evidence was considered inconclusive.

A further search was made throughout the 113 hour database. Data taken at phase 0.625 ± 0.058 were searched for periodicity, this time around 12.59 ms only and not the wide range over which the burst data were searched (Szentgyorgi, Ph.D. thesis, 1986). No evidence for pulsar activity was claimed.

5.15.3. Conclusions

None of these results are in direct conflict with those obtained by the Durham Group, and perhaps the Whipple results lend more support to the claim for 12.6 ms periodicity in Cygnus X-3 than the authors suggest. As is so often the case, more observations are required. These are to be made with the Mark IV telescope at present under construction in Durham.

5.16. The Durham University Cygnus X-3 Monitor

The Mark IV telescope, described in Chapter 9, has been designed to be readily portable and may be used for short observing programmes. It is planned to use at least one such short campaign in Summer 1988

to make further observations of Cygnus X-3. If a burst of γ-rays similar to that observed on 12th September 1983 were observed with this much more sensitive telescope, it is predicted that the pulsar would be detected at a Rayleigh probability of approximately 10^{-15}. The Mark IV telescope should thus be able to confirm or deny the earlier measurements during a relatively short observing period.

CHAPTER 6

OTHER OBSERVATIONS AT DUGWAY

6.1. Introduction

During its 5 years of operation, the Dugway array took some 1000 hours of data on 24 objects other than Cygnus X-3. The following is an account of the results from these objects.

6.2. Radio Pulsars

Observations were made at Dugway of 7 radio pulsars listed in table 6.1. These were selected on the hypothesis that the pulsed radiation is emitted by pulsars in proportion to their loss of rotational energy, E, given by:

$$E = I\omega\dot{\omega} \qquad 6.1$$

where I is the pulsar's moment of inertia and ω the angular velocity. The pulsars selected were therefore those with short periods and large period derivatives. A further selection criterion was the distance of the pulsar from the solar system, close pulsars being favoured.

Data from each pulsar were combined and analysed using the epoch folding technique in which the barycentred time of each event was converted to a pulsar phase and the resulting 20 bin light curves examined. Where known, absolute phase was included. Where

PULSAR	PERIOD (ms)
0950+08	253
1929+10	226
2224+65	682
0355+54	156
1508+55	739
1930+22	144
1133+16	1188

Table 6.1 Pulsars which were observed with the Dugway telescopes.

PULSAR	FLUX LIMIT (cm^{-2} s^{-1})
0950+08	1.1×10^{-11}
1929+10	2.8×10^{-11}
2224+65	1.9×10^{-11}
0355+54	2.0×10^{-11}
1508+55	2.1×10^{-11}
1930+22	2.8×10^{-11}
1133+16	2.3×10^{-11}

Table 6.2 Pulsed flux limits for radio pulsars observed at Dugway.

absolute phase was unknown, the ephemeris was considered to apply to phase zero. In most cases where phase information was available, this made little difference to the certainty of the position of the main pulse due to errors in the ephemeris.

No single light curve shows evidence for pulsed emission. In order to determine whether individually undetectable signals combine to give a detectable global signal, the 7 values measured for the χ^2 probability for chance occurrence (g_i) were combined using the relation (Eadie et al., 1971):

$$\alpha_i = -2\ln \prod_i g_i \qquad 6.2$$

which gives $\alpha_i = 11.04$. Since the variable has a χ^2_{14} p.d.f., this value corresponds to a probability for chance occurrence of 66.7%. It is thus concluded that there is no evidence for global emission from this sample of radio pulsars on our data. Table 6.2 shows the derived flux limits (3σ level) for a 1000 GeV threshold, assuming a light curve with a duty cycle of 5%.

6.3. PSR1937+214 - The 1.5ms Pulsar

The extended radio source 4C21.53 had long been suspected to contain a short-period pulsar. After some early unsuccessful fast pulsar searches, a survey was conducted with the 305m antenna at the Arecibo Observatory in September and November of 1982. A compact source with a period of 1.558 ms was found and designated

PSR1937+214 (Backer et al., 1982). The period derivative was later measured and found to be extremely low (approximately 10^{-19} ss^{-1}) (Ashworth et al., 1983). A highly accurate ephemeris based on long-term studies of the object was made available in 1985 (Davis et al.). It was suggested that, despite its differences from the Crab pulsar, the 1.5 ms pulsar may also have a significant part of its electromagnetic emission in the form of V.H.E. γ-rays between approximately 100 and 1000 GeV (Usov, 1983).

The first V.H.E. γ-ray observations of PSR1937+21 (the 1.5ms pulsar) from Dugway were made in 1983, but their usefulness is limited by the size of the dataset (44 hrs) and by the system timing uncertainties applicable in this case. However, in July - September 1984, 85 hours of data were taken on this object using an improved timing system. On the basis of other observations of γ-ray emitters (e.g. the Crab pulsar) it was expected that the weak signal would require that data taken over a considerable amount of time be merged together in order to detect a significant signal. This requires an ephemeris with very small errors, such that the error in the predicted pulsar phase over several months is much less than one pulsar cycle. Initially, radio ephemerides were insufficiently accurate, but in 1985 an ephemeris of unprecedented accuracy was made available with a residual phase uncertainty over two years of 1-2 μs (Davis et al., see table 6.3).

Determination of the time of each event was limited by the accuracy of the oven controlled crystal used in the system clock

R.A. (1950.0)	19h 37m 28.76400 +/- 0.00003 s
Dec. (1950.0)	21h 28m 001.4606 +/- 0.0010 s
Period	0.0015578064488724 +/- 2 s
Period derivative	(1.05110 +/- 0.00008) 10^{-19} ss^{-1}
Epoch (JD)	2445303.2731658

Table 6.3 The ephemeris of PSR1937+21 (Davis et al., 1985)

(see section 3.4.1). The absolute times are estimated to be accurate to 0.3 ms, which is confirmed by measurements of the Crab pulsar (Kirkman, Ph.D. thesis, 1985).

Initial data analysis used the epoch folding technique as applied to the radio pulsars (see section 6.2). The difficulty encountered here was that even the smallest errors in the clock rate or synchronization smear the light curve, making any statement concerning γ-ray emission impossible.

The second approach to this problem was to produce three separate datasets of event times corrected to the Solar System barycentre, each confined to 7 or 8 days' observations during the months of July, August, and September 1984, and to test each for uniformity in phase over a given range of periods. The range of periods was chosen to allow for the possible timing uncertainties in the data. It is estimated that these could cause a true periodicity at a predicted value of 1.55780645 ms to appear in the data at any period between 1.55780643 and 1.55780647 ms. The radio light curve is double-peaked (Ashworth et al., 1983), so it was advisable to allow for significant power in the second harmonic. The search for non-uniformity in phase was therefore made at half the expected period (see section 3.5.2). The result of this procedure shows independent evidence for such non-uniformity at significance levels of 5×10^{-3}, 10^{-3}, and 5×10^{-4} for July, August, and September respectively at a period of $1.55780642 \pm 0.00000003$ ms with the double pulse structure seen at other wavelengths. The result is

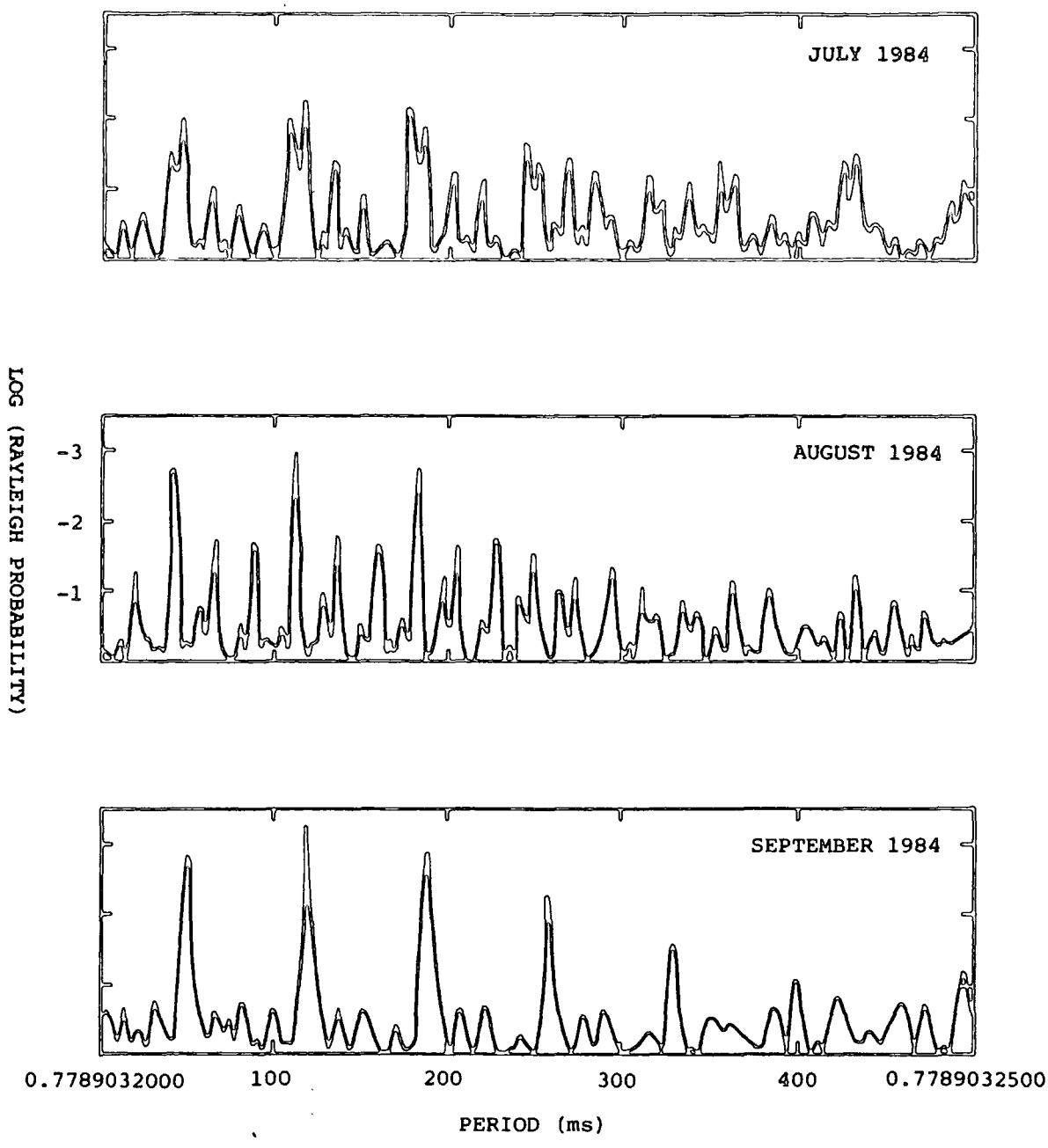

Figure 6.1 The probability of chance origin of periodicity from PSR1937+21 in 3 independent datasets as a function of trial period. The sidebands arise from the 24 hr separation between observations , each of typically 3-4 hours' duration. Additional structure is due to timing uncertainties.

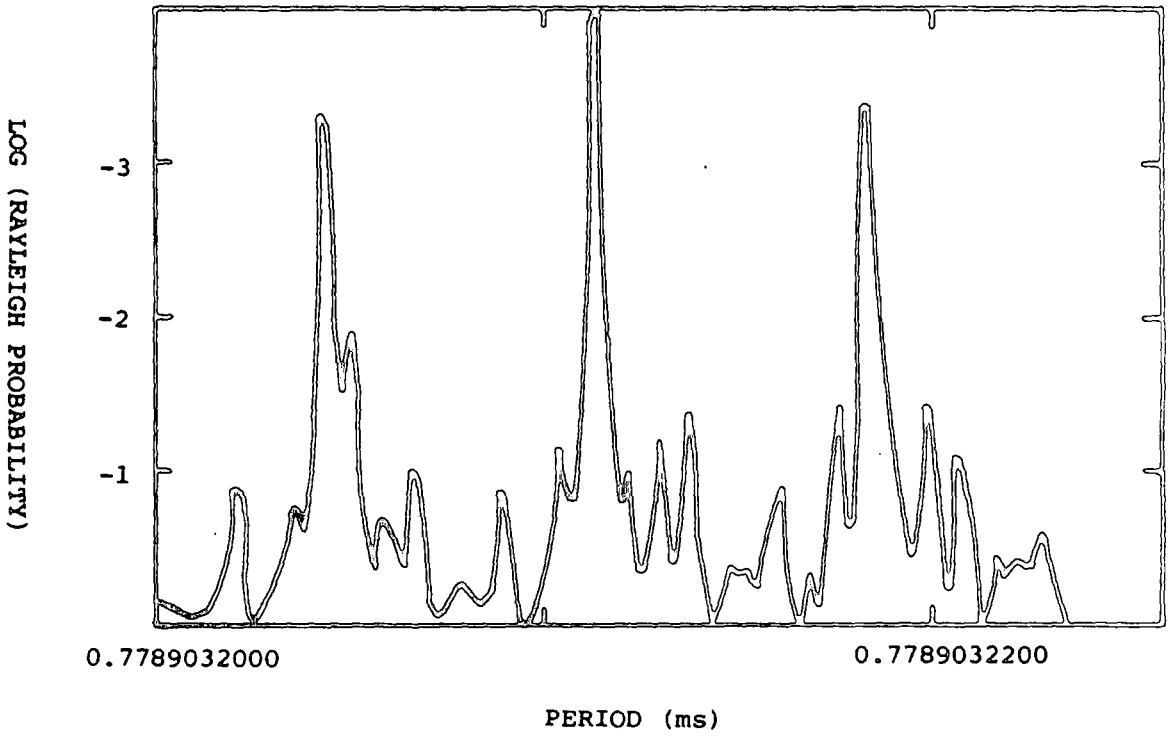

Figure 6.2 The combined Rayleigh probability of chance origin as a function of trial period. The three independent datasets from PSR 1937+21 shown in figure 6.1 have been combined after allowing for the effects of the pulsar period derivative.

shown in figure 6.1. These three were then combined (after allowing for the effects of the small period derivative) as shown in figure 6.2. The combined Rayleigh probability of these non-uniformities arising by chance is 1×10^{-4}. Limitations in the timing accuracy of the system prevent any further investigation of the detail of the emission.

Assuming a distance of 5 kpc to PSR1937+21 (Heiles et al., 1983), the observations suggest a flux above 1000 GeV of $(3 \pm 0.6) \times 10^{35}$ erg s^{-1}. This assumes a spectral index of 3, although even if the spectral index were as large as 6 the flux would only be reduced by a factor of 2. It therefore appears that the flux above 1000 GeV is about 10% of the total energy flux as deduced from the period derivative.

6.4. 2CG065+00

The second COS-B catalogue object 2CG065+00 was discovered in 1977 (Hermsen et al.), but could not be associated with any known object. A systematic search for fast pulsars within the COS-B error boxes was later conducted (Boriakoff et al., 1983) and resulted in the discovery of a 6.1 ms pulsar, PSR1953+29, in the error box of 2CG065+00. The pulsar is in a binary system, initially estimated to have an orbital period of 120 ± 4 days. However, it was not possible to associate the two objects unambiguously in the absence of either a precise position for the γ-ray source or the detection of 6.1 ms periodicity in the γ-rays. A later comparison of the

COS-B results with accurate surveys of the CO and HI distribution within the galaxy suggested that the interaction of cosmic rays with the interstellar gas could account for almost all the observed γ-rays above 300 MeV, including those ascribed to 2CG065+00 (Lebrun et al., 1983). A fuller analysis showed that while the emission above 300 MeV is almost certainly caused by the interstellar gas, the origin of the emission below this energy is unclear as 2CG065+00 is located in a complex region of the Galaxy between the Sagittarius and Perseus spiral arms (Pollock et al., 1985).

Observations of PSR1953+29 were made at Dugway between 4th July and 10th October 1983 and during July 1984. The data were corrected to the Solar System barycentre as described in section 3.4.2, and a homogeneous dataset used comprising only the eight observations of at least 4 hours' duration. This enabled the results of the periodicity search on each night to be meaningfully combined with approximately equal weights. (The uncertainties in the orbital ephemeris and in the system clock cause progressive phase errors and preclude the use of datasets of 24 hours or more.)

Events which triggered any two of the four telescopes ("two-folds") were then selected, as this has been shown to increase the sensitivity of the telescope array (Dowthwaite et al., 1984; Walmsley, Ph.D. thesis, in preparation). This dataset of 14,286 events was obtained during the half of the orbit where the pulsar was approaching the Earth, but spanned approximately three orbits.

Each individual observation of approximately 4 hours or longer was tested for periodicity over the range 6.133162 ms to 6.133170 ms. This takes into account:

(i) Uncertainties in the orbital ephemeris

(ii) The effects of statistical sampling on a true periodicity on sparse data

(iii) Residual uncertainties in the precise rate of the system clock.

The Rayleigh test was applied to each dataset independently and the eight probabilities of chance occurrence of each of a fixed set of trial periods were combined. This combined probability of chance occurrence is shown as a function of trial period in figure 6.3. A $3.5 \pm 0.9\%$ periodic excess is found within the trial range, with a Rayleigh probability of 1.6×10^{-5} at a period of 6.133166 ± 0.000002 ms. The Rayleigh probability is increased to 5.4×10^{-5} when the number of independent periods searched is taken into account.

Further independent evidence of this periodicity was furnished by the responses of the Mark II telescope (see section 2.7.2) which was known to have approximately the same signal:noise ratio as the two-telescope responses. This dataset comprises 17,302 events none of which are contained within the twofold dataset and shows a $3.2 \pm 0.8\%$ pulsed signal at a Rayleigh probability of 4×10^{-5} within the expected position of the radio period allowing for uncertainties in the determination of the binary orbit. The overall probability of the effect occuring by chance is about 4×10^{-8}, or 5.4σ. This is strong evidence to suggest that the γ-ray source

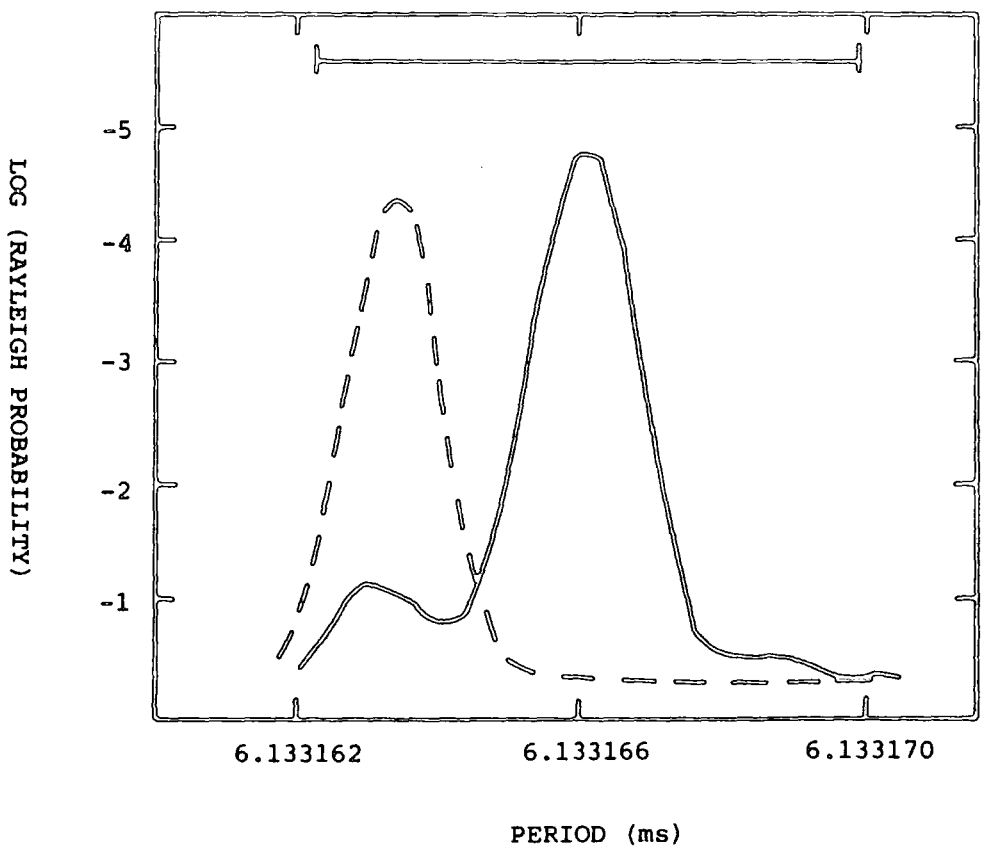

Figure 6.3 The probability of chance occurrence as a function of trial period for data from PSR1953+29. The horizontal bar shows the expected postion of the radio period allowing for uncertainties in the binary orbit parameters. The solid line refers to the two-telescope responses (twofolds) and the broken line to the independent sample from the single (sensitive) telescope responses.

2CG065+00 and the radio pulsar PSR1953+29 are the same object.

The γ-ray signal on the eight nights concerned was further investigated on a night-by-night basis. The average signal:noise for a two-telescope response is 3.5% of the cosmic ray background, although this may vary from below the background level to as much as 8.5%. There is no apparent pattern to this variation, in that the signal averaged over observations taken at a similar phase in the orbit remains at approximately 3.5%, despite the observations being up to a year apart. An established test for the constancy of the signal from night to night was applied (Mardia , 1972) , and the variation of signal strength was found to be consistent with sampling variations from a constant signal strength, although variations from zero to about three times the average signal strength cannot be precluded. However, strong bursts (approximately 30% of the cosmic ray rate) of a few minutes' duration can be excluded.

The time-averaged flux of γ-rays of energy > 2000 GeV (the energy threshold for "twofold" responses) is $(3 \pm 0.8) \times 10^{-11}$ cm^{-2} s^{-1}. Assuming a distance of 3.5 kpc and a spectral slope of 3.0 the derived luminosity is $(3.0 \pm 0.8) \times 10^{35}$ erg s^{-1}.

As it is not possible to maintain phase from night to night for such a fast pulsar in an imprecisely known orbit, an overall light curve for the dataset cannot be derived. The light curve for the twofold events on the night of the single strongest signal has been produced at the radio period (6.133166 ms) and is shown in figure 6.4. It is interesting to note that this is a broad light

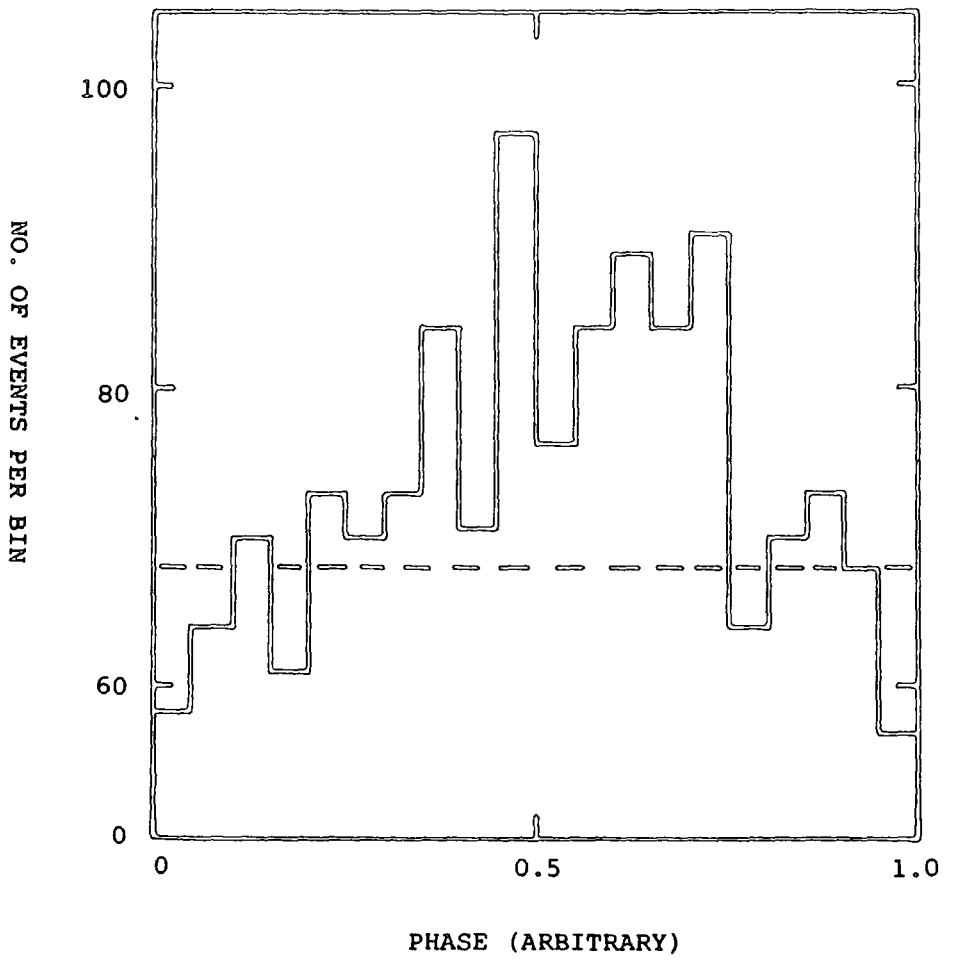

Figure 6.4 The light curve for V.H.E. gamma ray emission at E > 1000 GeV from PSR1953+29 on 6th August 1983.

curve, similar to Hercules X-1 (figure 6.6), 4U0115 + 63 (figure 6.7) and Cygnus X-3 (figure 5.5), again suggesting that accretion plays an important role in the V.H.E. γ-ray emission mechanisms of binary pulsars.

6.5. Shorter Observations

A number of short observations of between 2 and 13 hours' accumulated duration were made of objects of interest including other COS-B γ-ray sources and black hole candidates. No V.H.E. γ-ray flux was detected from these objects, and flux limits are presented in table 6.4. Note that the flux limits are high when compared to the fluxes of objects detected using the Dugway facility, reflecting the short duration of the observations made, and emphasising the need for long exposures if meaningful conclusions are to be drawn from V.H.E. γ-ray data.

6.6. The Dugway Catalogue of Very High Energy γ-ray Sources

The following sections provide a summary of all the V.H.E. γ-ray objects thus far unmentioned which have been detected by this group. The results are further summarised in table 6.5, which provides a comprehensive list of all objects detected by the Durham Group during the life of the Dugway experiment.

6.6.1. PSR0531+21: The Crab Pulsar

The first observation of V.H.E. γ-rays from the Crab Pulsar was

OBJECT	FLUX LIMIT (cm^{-2} s^{-1})
2CG195+04	3×10^{-11}
CYG X-1	5×10^{-10}
SS433	3×10^{-10}
PER X-1	3×10^{-10}
2CG135+01	5×10^{-11}
3C273	5×10^{-10}
NGC4151	3×10^{-10}
CAS-A	6×10^{-10}

Table 6.4 Flux limits for objects of which short observations were made in Dugway.

SOURCE	HOURS DATA	FLUX (x 10^{-12} CM^{-2} S^{-1}) MEAN	PEAK	D (kpc)	LUMINOSITY (ERG S^{-1}) MEAN	PEAK
PSR0531	137	7.9 +/- 1.8	200 +/- 30	2	2.1 10^{34}	1.6 10^{36}
CYG X-3	350	5.0 +/- 1.2	300 +/- 70	11	9.0 10^{35}	5.4 10^{37}
HER X-1	32	30 +/- 15	1200 +/- 300	32	2.0 10^{35}	1.2 10^{37}
4U0115	25	70 +/- 14	-	25	6.0 10^{35}	-
GAL. PLANE	4	3 10^{5} $Ster^{-1}$	-	1-2	10^{39} - 10^{40}	-
M31	5	220 +/- 70	-	670	4.0 10^{40}	-
PSR1953	64	30 +/- 15	-	3.5	3.0 10^{35}	-
PSR1937	132	36 +/- 18	-	5	3.0 10^{35}	-

Table 6.5 The Durham Northern Hemisphere V.H.E. gamma-ray catalogue.

made at the Smithsonian Astrophysical Observatory (Grindlay et al., 1976), and was followed by a number of other observations which gave conflicting results (Porter et al., 1976; Erickson et al., 1976; Gupta et al., 1978).

The Crab pulsar was first observed at Dugway between September and November 1981. Two 15 minute bursts of activity were observed, one on 23rd October and one on 31st October, and were found to be periodic at the same period as the radio ephemeris. The Rayleigh probabilities of the periodicity arising by chance were 10^{-6} and 10^{-4} respectively, after correction for the number of degrees of freedom.

Observations made by the Durham group during 1982 and 1983 showed evidence for persistent, weak periodic emission with the characteristic 33 ms period. The light curve for this emission shows a narrow peak coincident with the radio main pulse (see fig. 6.5). A conservative value for the chance probability of this effect is 10^{-5}. Also, a correlation of the V.H.E. light curve with the COS-B light curve is significant at the 5.6 σ level with a contribution from γ-rays at phases other than the main pulse. The excess constitutes a time-averaged pulsed flux of $(7.9 \pm 1.8) \times 10^{-12}$ cm^{-2} s^{-1}. No evidence was found for any emission from the nebula surrounding the pulsar in a series of drift scans made in 1981, the upper limit being 3.4×10^{-10} cm^{-2} s^{-1}. For a detailed account of Dugway data on the Crab pulsar see Kirkman (Ph.D. thesis, 1985).

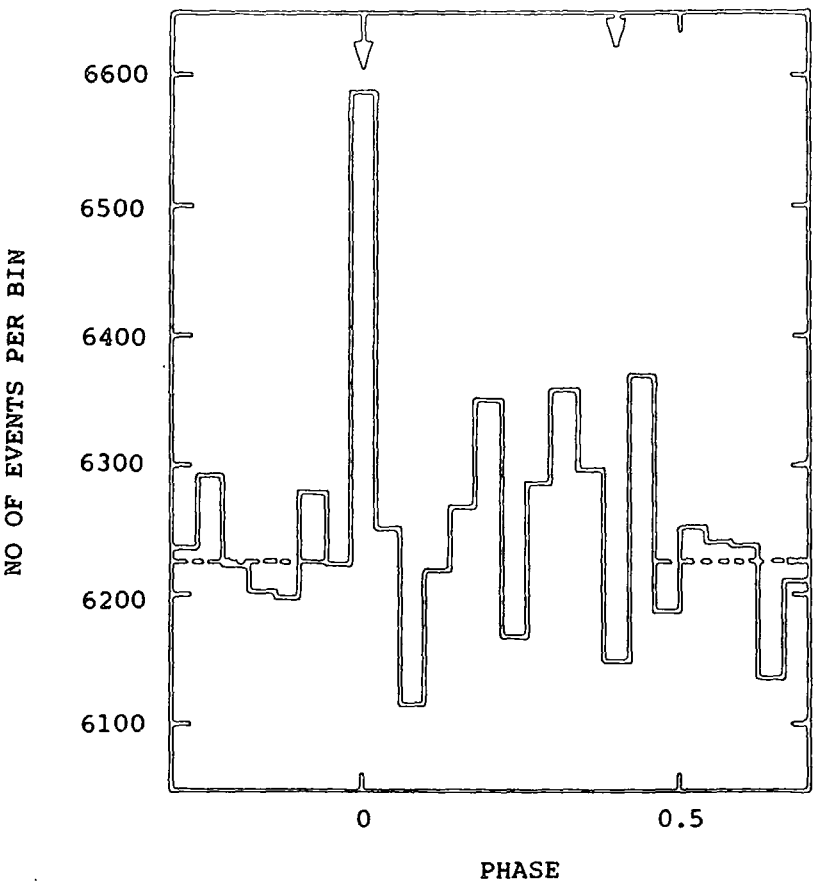

Figure 6.5 The light curve for all events recorded from PSR0531 (the Crab pulsar) in September 1982 - November 1983. The radio main pulse and interpulse are indicated by arrows.

6.6.2. Hercules X-1

Hercules X-1 was discovered as a pulsing, eclipsing binary source by Tananbaum et al., (1972). It is multiply periodic, with a pulsar period of 1.24s, an orbital period of 1.7 days and a 35 day amplitude modulation.

The first detection of V.H.E. γ-rays from this object was made by the Durham group. During a drift scan on 17th April 1983, a 3 minute burst of γ-rays was detected from the object, during which an enhancement of 33 $\pm$ 10% in the gross count rate of the four telescopes occurred. The events during this outburst showed the characteristic 1.24 sec X-ray pulse period, with a chance Rayleigh probability of 4×10^{-4}. The light curve for this emission is shown in figure 6.6. The increase in count rate and periodic content were shown both by those events triggering a single telescope, and independently by those events in which two telescopes were triggered simultaneously. The outburst was detected 35 days before the onset of a 35 day cycle was observed with the TENMA satellite (Nagase et al., 1983), and may therefore be associated with the 35-day "turn-on".

Following the outburst, Hercules X-1 was tracked during the months of July and October 1983. No further burst was seen. The July data showed some evidence for persistent periodic emission at the 2σ level of significance.

Confirmation of these results came from observations made by the Whipple Observatory Collaboration (Gorham et al., 1986). Between

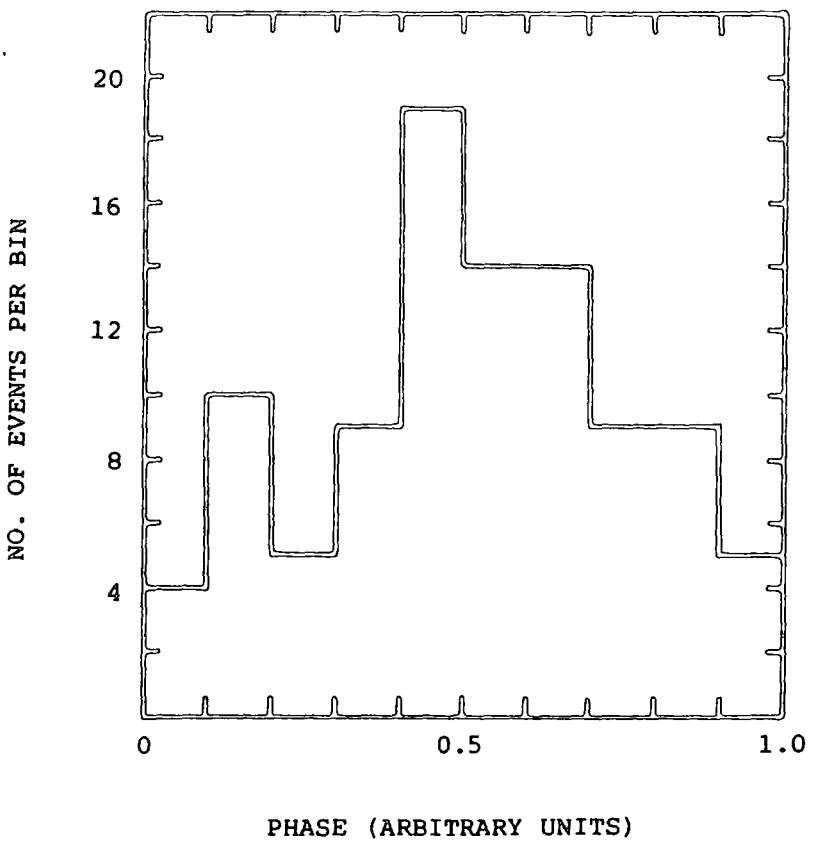

Figure 6.6 The light curve for the V.H.E. gamma rays from Hercules X-1 using the trial period of 1.237 sec. The data are from the 3 minute outburst on 17th April 1983.

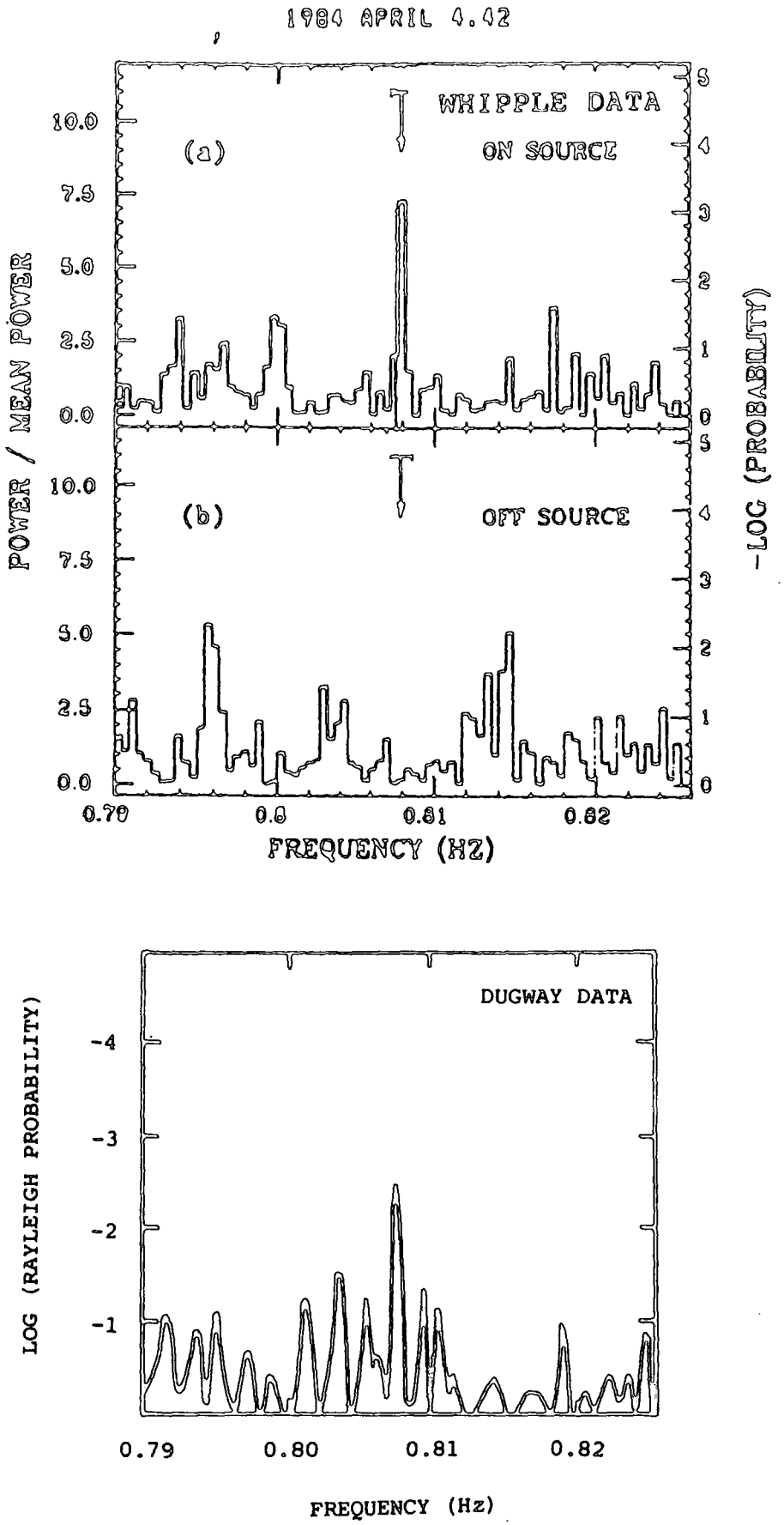

Figure 6.7 The Rayleigh probability of chance origin as a function of trial period for the observation of Hercules X-1 made at Dugway on April 4th 1984. The result from the Whipple telescope data taken on the same day , reproduced from Gorham (1986) is shown above for comparison.

1984 and 1986 eight separate episodes of pulsed emission were observed. On April 4th 1984, observations were made by the Whipple group simultaneously with the University of Durham group. In both observations, evidence for emission of V.H.E. γ-rays showing the same periodicity and significant at the 3σ level was obtained (see fig. 6.7).

6.6.3. 4U0115+63

Following the discovery of V.H.E. γ-ray emission from Hercules X-1, a study was made to identify an X-ray binary with similar values of period, period derivative and luminosity. The sporadic pulsar 4U0115+63 was first observed as an X-ray source in 1976 in data from the Uhuru satellite (Forman et al., 1976). It was subsequently identified as a sporadic 3.6 sec pulsed X-ray emitter, with the collapsed object in a 24.3 d orbit (Rappaport et al., 1978).

Twenty-five hours of observations of 4U0115+63 were made between 21st and 29th September 1984 at Dugway. A search for periodicity over a limited range was necessary because of the previously variable behaviour of the X-ray pulse period and the uncertainties in the orbital ephemeris used (Ricketts et al., 1981). The search range was 3.615 to 3.6147 sec. The Rayleigh test was applied to the combined 25 hours of data, and showed evidence of pulsation with a Rayleigh chance probability of 5×10^{-7} at a period of 3.61457 ± 0.00001 sec. The flux observed was $(7 \pm 1.4) \times 10^{-11}$ cm^{-2} s^{-1} and the light curve for the emission is shown in figure 6.8. With the knowledge that the

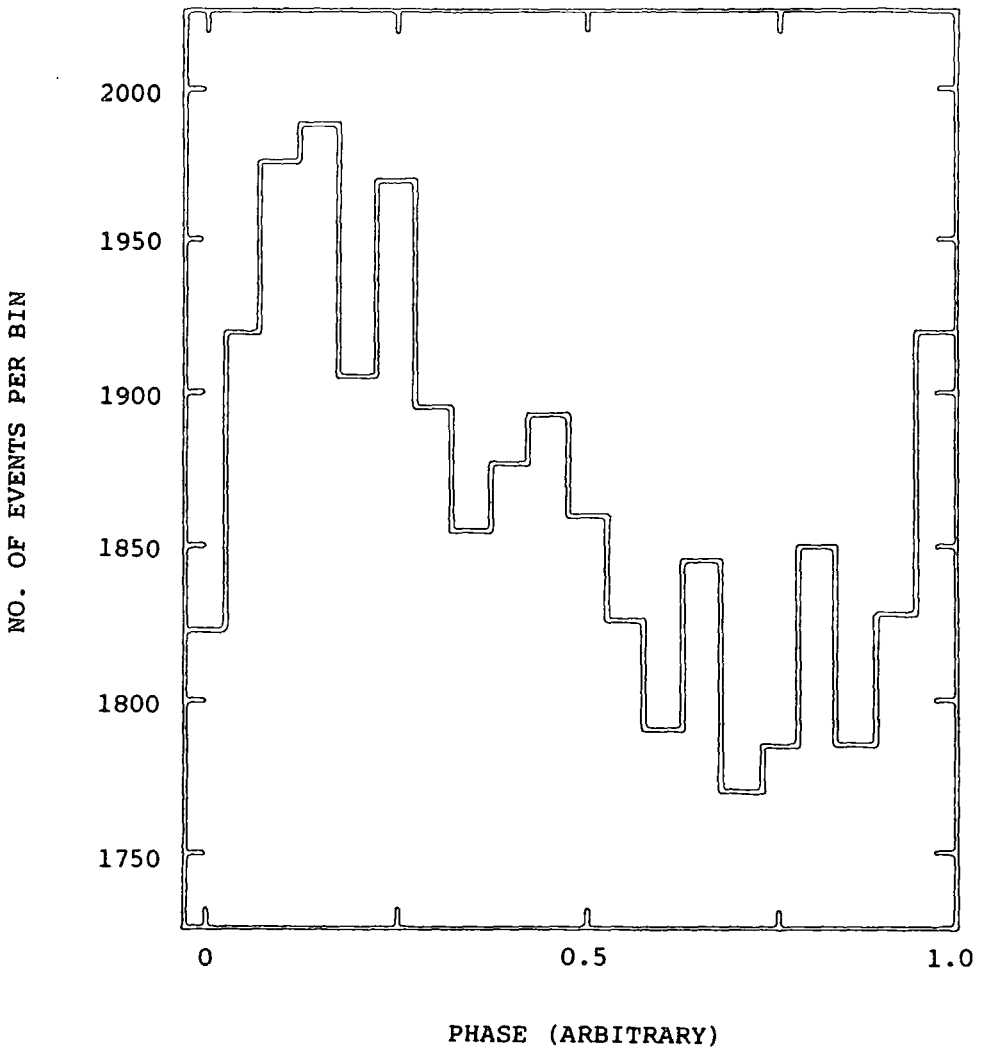

Figure 6.8 The light curve for 1000 GeV gamma ray emission from 4U0115+63 , with a trial period of 3.61457 seconds.

X-ray source is sporadic in nature, the data were also analysed on a night-by-night basis. Particularly strong emission was noted during the observations on one night (26th September), with most of the pulsed emission occurring during a one hour interval. The emission was not found to occur at any particular phase in the orbit (the observations spanned 40% of an orbit).

4U0115+63 was subsequently observed by the V.H.E. γ-ray groups working at Haleakala and the Whipple Observatory (Resvanis et al., 1987; Lamb et al., 1987). The Haleakala group observed 3 bursts of γ-rays from the object in observations made between August and December 1985 which exhibited significant pulsation at the characteristic 3.6 sec. pulsar period. The Whipple Observatory observed 4U0115+63 between September 1985 and January 1986. When these observations were grouped into 9 intervals of 3 days or less, one interval was found to show significant pulsation at 3.6 seconds.

6.6.4. The Galactic Plane

Early experiments to detect γ-rays above 150 GeV from the Galactic plane yielded positive results, with the strength of the emission varying with longitude (Weekes et al., 1979; Fomin et al., 1977). In particular, the flux was found to be in the region of 3×10^{-10} cm^{-2} s^{-1} at energies > 150 GeV between Galactic longitudes 40 and 80 degrees. At these longitudes, a complex variation in intensity is seen across the Galactic plane with peaks at $\pm 5^{o}$ and no emission from the galactic equator. The main problem for

atmospheric Cerenkov telescopes in making drift scan observations of the galactic plane arises from the increase in sky brightness encountered in crossing it. This causes a change in the gain of the photomultiplier tube and hence the threshold of the telescope. These changes could simulate the detection of additional γ-rays as the galactic plane is traversed. The Dugway telescopes circumvented this problem by supplementing the off-plane sky brightness with accurately controlled artificial light, such that the total anode current in each photomultiplier tube remained constant. Such a system also operates on the Mark III telescope, and is described in section 7.6.2. During the 1983 observations of the galactic plane, the anode currents and noise rates of the photomultipliers were constant to better than 2%, except when the bright star γ Cygni passed through the field of view. The central part of the 4h drift scan across the galactic plane illustrated in figure 6.9 (i.e. $\pm 8^{o}$) shows positive correlations at the 3.2 and 2.7σ level with the results of Weekes et al. (1979) and a correlation at the 2.2 and 1.9σ level when compared with the results of Fomin et al. (1977).

6.6.5. M31: The Andromeda Galaxy

Drift scan observations of M31 were made with the Dugway telescopes for 15 hours between September 5th and November 5th 1983. The data from 7 drift scans were combined and the ON and OFF source data compared (section 3.10). Excess counts were found ON source, corresponding to (6.7 $\pm$ 2.2)% of the cosmic ray background and a

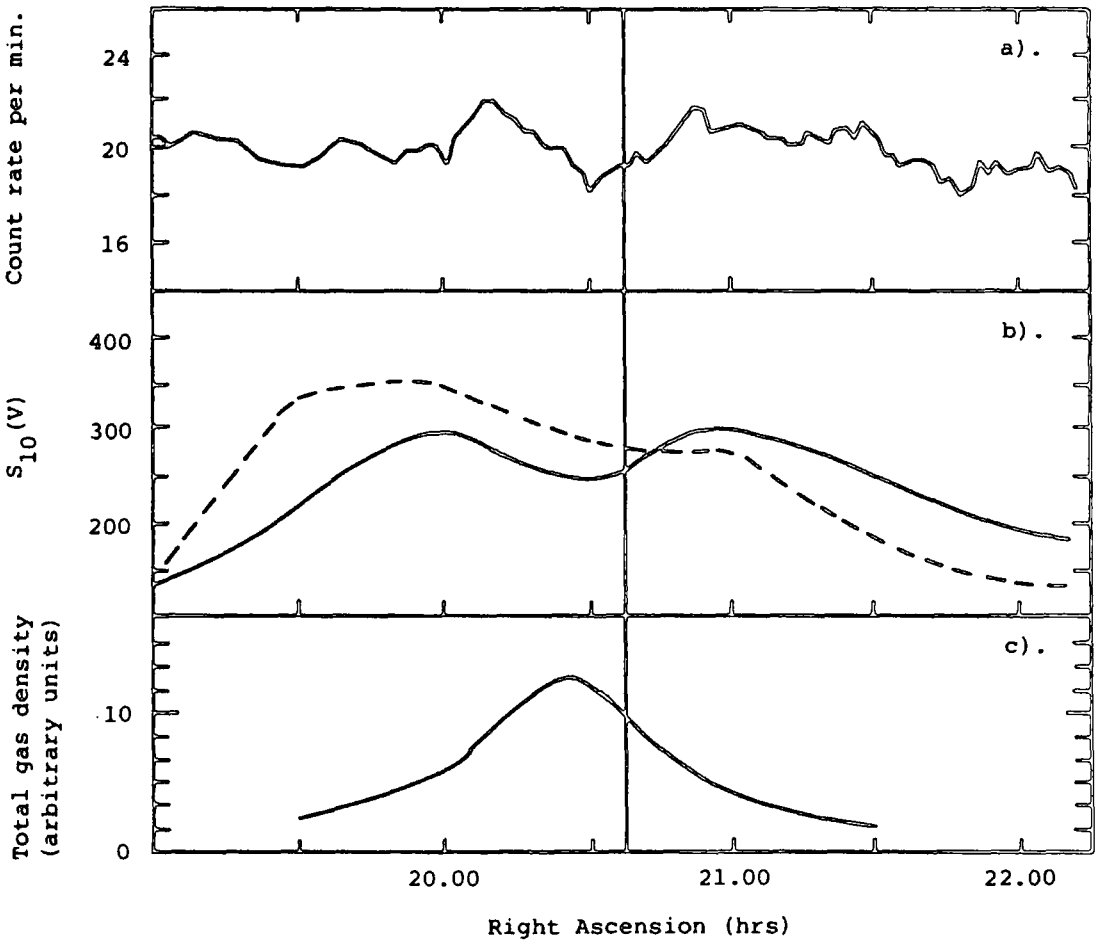

Figure 6.9 a). The count rate per minute of the low energy telescopes (averaged over 20 min) during a 4 hour drift scan across the galactic plane in the Cygnus region. b). The number of 10th magnitude stars within 1.4 kpc per square degree (solid line) and the perceived local brightness during the scan (broken line) c). The total gas density (HI + HII) in the field of view during the drift scan.

γ-ray flux of $(2.2 \pm 0.7) \times 10^{-10}$ cm^{-2} s^{-1} at energies $>$ 1000 GeV. The measured spatial distribution of the excess was consistent with the angular dimension of the emission being approximately 1^{o}. Confirmation of these results is required.

6.7. Conclusions

The University of Durham V.H.E. γ-ray telescopes at Dugway produced many important results, in particular the first detections of V.H.E. γ-rays from Hercules X-1, 4U0115+63, 2CG065+00 (PSR1953) and PSR1937. In addition, there is the exciting result that Cygnus X-3 may contain a 12.6 ms pulsar. Taken as a whole, they suggest that while some isolated pulsars do produce γ-rays (the Crab pulsar, for instance), the objects with the highest γ-ray luminosities are the X-ray binary systems. The new Mark III telescope has been deployed at a site in the Southern Hemisphere, from which the majority of known X-ray binary pulsars may be observed. This also allows other interesting objects from earlier measurements, such as the Vela pulsar, the active galaxy Cen A and the galactic centre to be observed. The design, construction and operation of the Mark III telescope are described in the following chapters, together with preliminary results.

CHAPTER 7

THE MARK III TELESCOPE AT NARRABRI, N.S.W.

7.1. Introduction

The University of Durham Mark III V.H.E. γ-ray telescope was established during September 1986 at Bohena Settlement (149^{o} 49' 1" E, 30^{o} 28' 59" S, altitude 260 m a.s.l.), which is in the Piliga State Forest 20 km South of the town of Narrabri, New South Wales. It comprises a light collector of 34 m^2 deployed as 3 dishes of 11 m^2 mounted on an alt-azimuth mount. Each dish consists of approximately forty 0.6 m diameter spherical mirrors, and has at its focus four 2" diameter photomultiplier tubes, arranged to provide three off-axis data recording channels surrounding one on-axis channel. The telescope is illustrated in plate 1.

The telescope is operated from a transportable control room which houses the control and logging electronics. The data logging system comprises CAMAC analogue and digital electronics in communication with a purpose-built MC 68000 based data logger. Telescope control and performance monitoring is achieved using seven BBC microcomputers operating as a Local Area Network and communicating with the 68000 data logger. An internal view of the control room is shown in plate 2.

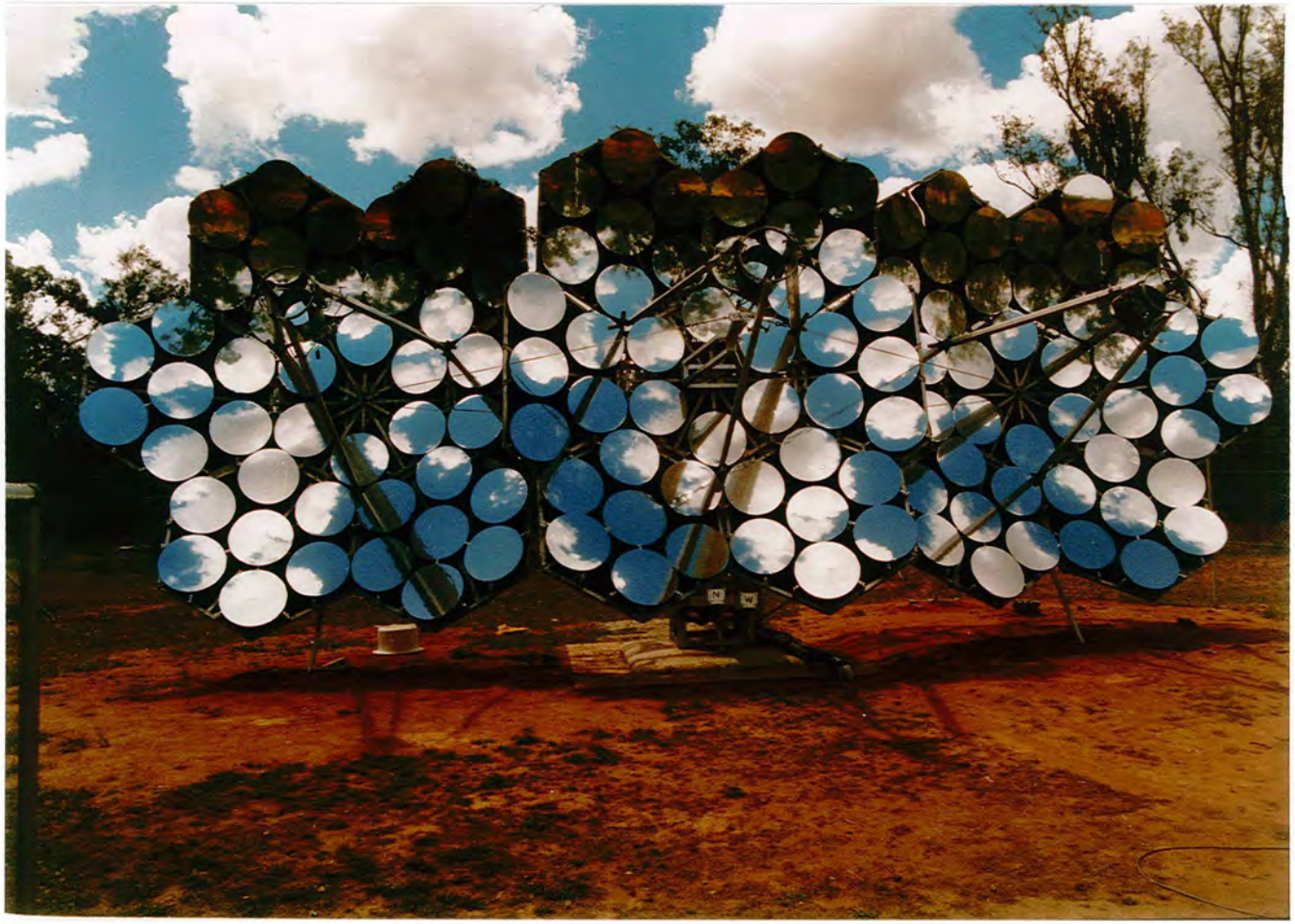

Plate 1 The Mark III telescope.

Plate 2 The Mark III control room.

7.2. Choice of Site

The Narrabri site was chosen for a number of reasons:

(i) It is well placed for the study of large numbers of astronomical objects of particular interest to V.H.E. γ-Ray Astronomy. Earlier observations, using the V.H.E. γ-ray detectors at Ootacamund, India have claimed emission from the Vela pulsar and a γ-ray signal from Centaurus A has also been claimed using data from equipment operated at Narrabri (Bhat et al., 1980; Grindlay et al., 1975). In addition, the majority of X-ray binary systems containing pulsars, which appear to be strong candidates as V.H.E. γ-ray emitters, are to be seen from a Southern Hemisphere observing site. Finally, the galactic centre may be observed from Narrabri.

(ii) The climate has a moderate rainfall and a reasonably high percentage of clear nights. Data from the Anglo Australian Observatory (which is located approximately 100 km from the Mark III telescope) show that on average 49% of the nights during the year are useable.

(iii) Support facilities, such as accommodation and power, were already supplied on the site, which is leased by the Durham Group from the University of Sydney. Additional logistic support is also available from other neighbouring facilities, in particular the University of Sydney Wheat Research Station.

As an historical note, Bohena Settlement was established in 1967 and used until 1978 as the site of SUGAR - the Sydney University Giant Airshower Recorder.

7.3. The Climate

At the time of writing, the Mark III telescope has been operational for only eight months (October 1986 - June 1987), so a detailed summary of the climate as it effects the operation of a γ-ray telescope over the course of a year is not yet available. However, it is possible to make preliminary comments and summarize the features of the annual observing cycle. A summary of the factors relevant to γ-ray astronomy: the changes in maximum and minimum temperature, number of hours' darkness per night and the number of thunderstorms during the year is shown in figures 7.1a - 7.1d. These figures use a combination of measurements taken on site and at the nearby Siding Springs Observatory. The following features of the climate have been noted:

(i) During January and February, the high frequency of convectional storms (and the migration of fruit bats) result in many interruptions of the electrical power supply. The long signal cables used on the telescope make the electronics susceptible to damage from lightning strikes, so in the event of a local thunderstorm precautions must be taken to ensure the isolation and protection of the electronics.

(ii) Immediately after Summer rain, when humidity is high, condensation forms on the telescope mirrors if their temperature drops below the dew point. This reduces reflectivity and hence count rate. The problem occurs during 2-3 nights in a given month during the Southern Summer. During the cooler Winter nights, the immediate formation of

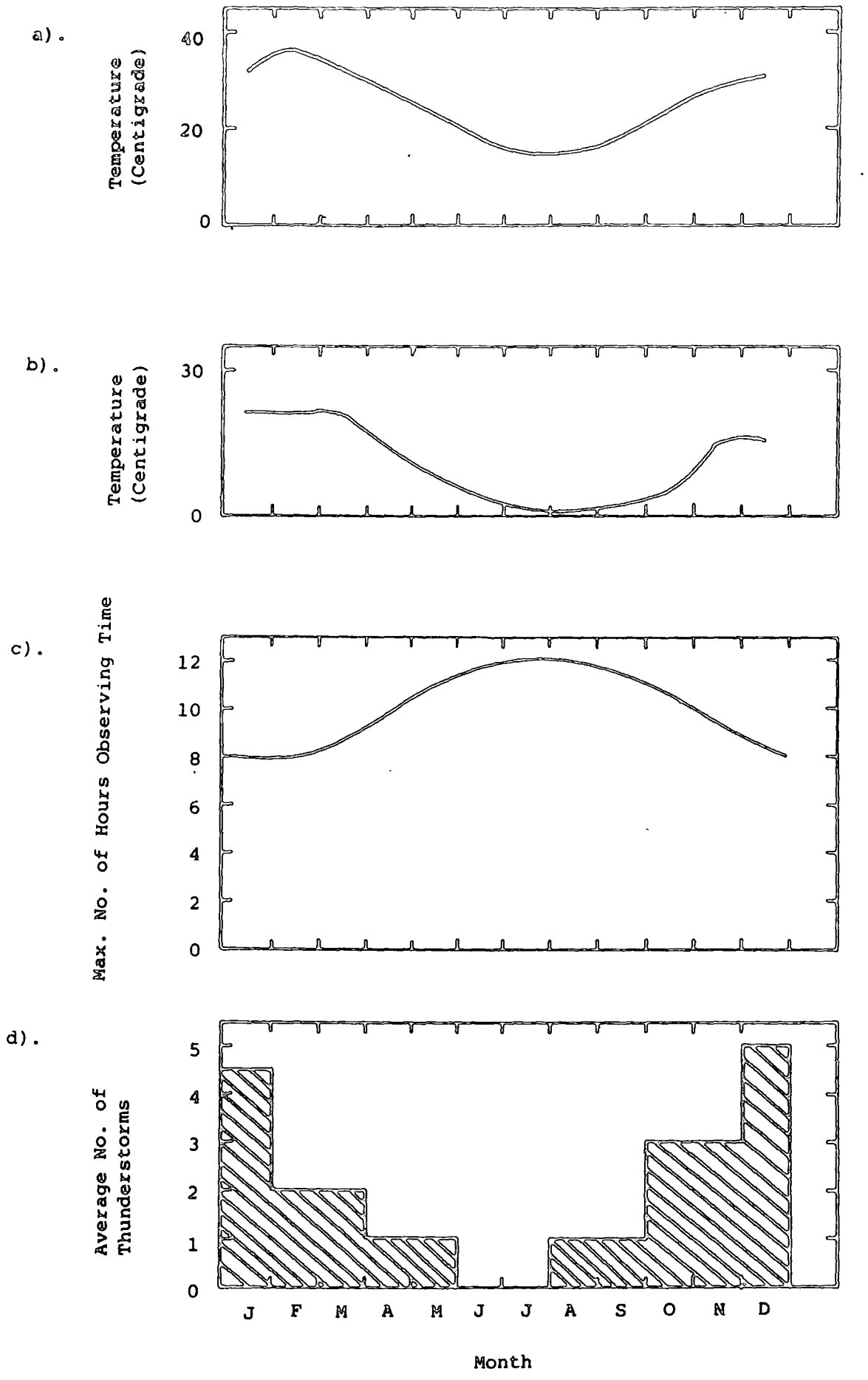

Figure 7.1 Features of the Narrabri climate. Figures 7.1 a). and b). show the average maximum and minimum diurnal temperatures each month respectively. 7.1 c). shows the number of hours observing time available and fig. 7.1 d). shows the frequency of convectional storms.

condensation is a regular problem and can prohibit observations for the rest of the night. After trials with various substances, it was found that a concentrated solution of high-quality detergent applied to the mirrors at the beginning of a night when condensation is expected prevents its formation for at least 12 hours. The performance of the telescope is unaffected by the wetness and the detergent also serves to keep the mirrors clean.

(iii) During the Antipodean Winter, the night-time temperature can fall below freezing point, so that any condensation or water on the mirrors freezes. The icing may be delayed using the detergent solution, and removed using methanol. Following the melting of the ice by the methanol, a clear glaze forms which allows limited further operation.

It is probable that observations will be concentrated between the months of February to November each year.

7.4. Mechanical Design

The Mark III telescope main framework was designed and built by the Department of Physics technical staff during 1984 and 1985.

7.4.1. The Alt-azimuth Mount

An alt-azimuth mount was chosen for the telescope because of its ready availability and low cost, despite the necessity to be driven in two axes rather than one. The mount used is a surplus gun mount. The weight of the telescope is taken on a single central

thrust bearing which allows the azimuthal motion, while motion in zenith angle is taken on two smaller trunnion bearings. The telescope is steered under computer control and driven by two DC electric servomotors and direction sensing is via two absolute digital shaft encoders, giving position resolution of 0.1^{o}. As the target direction is approached, the speed of the telescope is reduced progressively under computer control to avoid unnecessary strain on the motors, gear boxes and structure caused by the rapid deceleration of a high inertia system. In addition to this computer control, the telescope may also be steered manually using a joystick. To protect the bearings and motors from damage by gusts of wind when the telescope is not in use, the telescope is parked with the flux collectors pointing towards the zenith and two clamps, the lower ends of which are securely set in concrete, are attached to each extremity of the telescope.

7.4.2. The Telescope Framework

The telescope consists of three large flux collectors of area 11.4 m^2 (i.e. three sets of approximately 40 mirrors with each set having a common focus). It is built entirely from aluminium, which is light, strong and relatively easy to work with. Each dish is constructed from seven smaller "hexagons", each of which has seven mirrors, the smallest unit in each dish, attached to it. The mirrors may be moved individually on the framework of each "hexagon" for purposes of precise alignment (see section 7.5.3). Where individual

mirrors would have been obscured, either by other mirrors or (in the case of the central mirror on each dish) by the detector package which contains the photomultiplier tubes, gaps were left on the framework (see plate 1).

7.5. Optical Characteristics

A major development incorporated in the Mark III and Mark IV telescopes is the new lightweight, low-cost mirror. The construction and features of these mirrors are described below. The general optical characteristics of the telescope are also described.

7.5.1. Mirror Construction

The design of the Mark III telescope required the production of some 150 mirrors, each of area 0.3 m^2. It was therefore not only necessary to produce mirrors with reasonable optical quality and reflectivity, but they also had to be light, cheap and easy to produce. The starting point was the mirror design successfully employed on the Mark II telescope in Utah. This was for a 60 cm diameter mirror made of solid aluminium which had been machined and polished to give a reflectivity of 55%. The production of these mirrors was time-consuming and they were heavy (12 kg), so clearly they were not suitable for the Mark III telescope. Investigations were made into pressing and spinning thin aluminium sheet, thermo-forming aluminium coated perspex, bonding thin aluminium sheet to a solid former, and pressing thin glass mirrors. Most of these methods

were found to be capable of producing mirrors of suitable optical quality on occasion, but they each had difficulties, including a lack of consistent mirror quality.

The method of manufacture finally adopted is the bonding of a backplate made up of aluminium honeycomb to a high reflectivity anodised aluminium sheet (Alanod) after stretching the latter over a steel former. A similar method was used for the manufacture of the antenna sections for the James Clerk Maxwell telescope. The Alanod sheet is stretched tightly over a 60 cm diameter metal former of the required radius of curvature. A polyamide-based epoxy resin is then used to bond the aluminium sheet to a backing plate which is filled with crushed aluminium honeycomb. The whole assembly is then cured in an oven at 100^{o}C for an hour. A section through a finished mirror can be seen in plate 3. Image quality and reflectivity are consistently good (section 7.5.2), although the focal length was found to vary slightly from batch to batch. Two types of mirrors were produced, one with a design focal length of (240 ± 8) cm and the other with a design focal length of (260 ± 8) cm, for reasons which are explained in section 7.5.2.

7.5.2. Mirror Quality

The aluminium sheet used as the reflecting surface of the mirrors was specified by the manufacturers to be approximately 80% reflective; this was confirmed by measurements made at the Whipple Observatory (Weekes, private communication: see table 7.1). One mirror was left

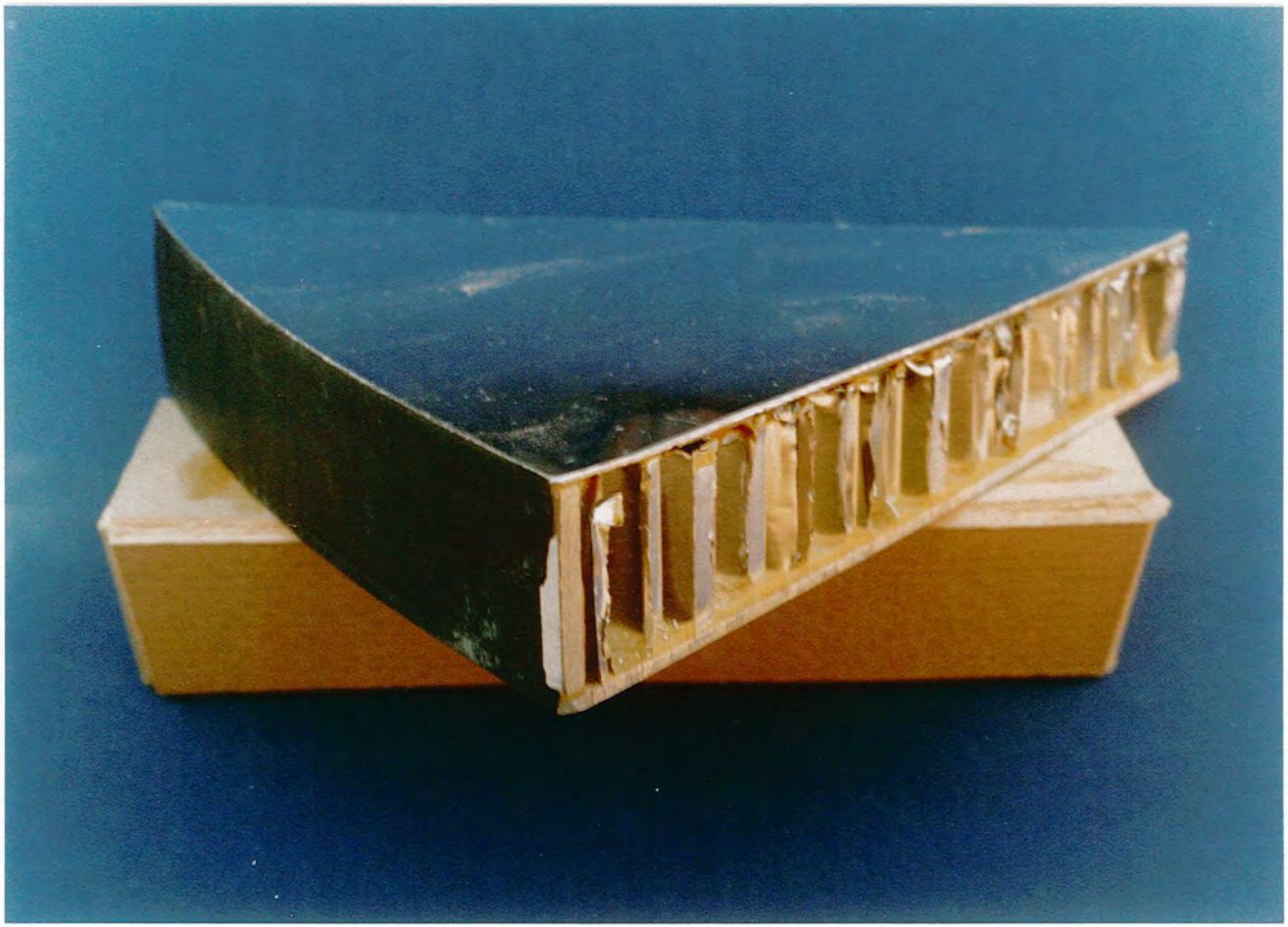

Plate 3 Section through a "Durham mirror".

Wavelength (nm)	Reflectivity
350	75%
450	80%
540	77%
720	75%

Table 7.1 The reflectivity of the Alanod sheet used to construct the mirrors on the Mark III telescope (Weekes , private communication).

outside in Durham for over 12 months and, despite the considerable atmospheric pollution, the mirror surface did not deteriorate appreciably. It is concluded that the mirrors on the Mark III telescope will weather well during its period of operation in a site with less atmospheric pollution.

Image quality for atmospheric Cerenkov work does not have to be particularly high: indeed, this can be a disadvantage (see section 2.7.1). The 240 cm focal length mirrors have a typical stellar image size of less than 1 cm on-axis, rising to about a 5 cm image size 200 cm off-axis. Since most of the mirrors are producing an off-axis image at the focus of the dish, it was decided that the outer mirrors should have a longer focal length than the inner mirrors and be selected to reduce this image size. The result is that a completed dish of 40 mirrors produces a composite image approximately 2 cm in diameter for a point source at infinity.

7.5.3. Alignment of Mirrors

With a large number of mirrors to be aligned, a quick and simple method of alignment was required. The method employed was to measure the angular position of each mirror relative to the optic axis of the telescope using a theodolite located at a distance of about 50m. This information then allowed the telescope to be steered under computer control such that each mirror in turn was pointed at a laser which was located in the same position as the theodolite. In this way, the laser provided an effective distant object on which the mirrors could

be aligned. The image of the laser beam was then moved to the focus of the dish by making small adjustments to the position of the mirror. The overall alignment was checked at night on bright objects such as the Moon and planets. This alignment procedure was found to be accurate and was undertaken both in Durham and Australia, and may be repeated easily should there be doubt about the alignment of the telescope for any reason.

7.5.4. Aperture Function

The geometrical aperture of the telescope as defined by the focal length of the mirrors (240cm) and the sensitive area of the photomultiplier tubes (4.0 cm) is 0.9°. The combination of this with the known angular diameter of a Cerenkov light flash suggests an effective aperture of $(1.4 \pm 0.2)^{\circ}$. Measurements of the aperture function made by scanning across a star and noting the anode currents of the photomultiplier tubes show that the aperture of the telescope is $(1.5 \pm 0.2)^{\circ}$ FWHM, which takes into account a certain amount of optical and electronic smearing of the image.

7.6. Photomultiplier Tubes

This section is concerned with the choice of photomultiplier tubes which act as the light detectors on the telescope. Their arrangement and operation will be described.

7.6.1. The Choice of Tubes and their Deployment

The main requirement for a photomultiplier tube used in

atmospheric Cerenkov studies is that it should have a low noise performance under the unusual conditions of high photocathode illumination induced by sky brightness. In figure 7.2, the noise performances of a number of tubes under typical sky illumination conditions are shown. It is clear that the 5" RCA 4522 tube, used extensively in the Dugway experiment and in others, is far from ideal, having a steep increase in noise with increased illumination. The initial choice of photomultiplier tube for the Mark III was a fast 3" diameter tube (EMI 9821). However, extensive tests showed that the gain was not stable on these particular tubes even after a "warm-up" period. A fast linear-focused 2" diameter tube was chosen instead (RCA 8575). The characteristics of these tubes are well known, since three such tubes were used in the Mark II telescope. The tubes have stable gain and the spectral response of the tubes peaks at approximately 370 nm, making it a good choice for this application, as Cerenkov light peaks in the region 350-550 nm.

Each individual photomultiplier tube is placed in a watertight unit and isolated from the effects of the Earth's magnetic field by a cylindrical mu-metal shield maintained at the cathode potential. The tubes are then placed in cylindrical plastic and perspex holders in three groups of four as shown in figure 7.3, to form the detector elements in the package at the focus of each large dish. The tubes are operated in three-fold coincidence. By this it is meant that, in order to record an event, three paraxial tubes in separate detector packages must trigger within 10ns of each other. For

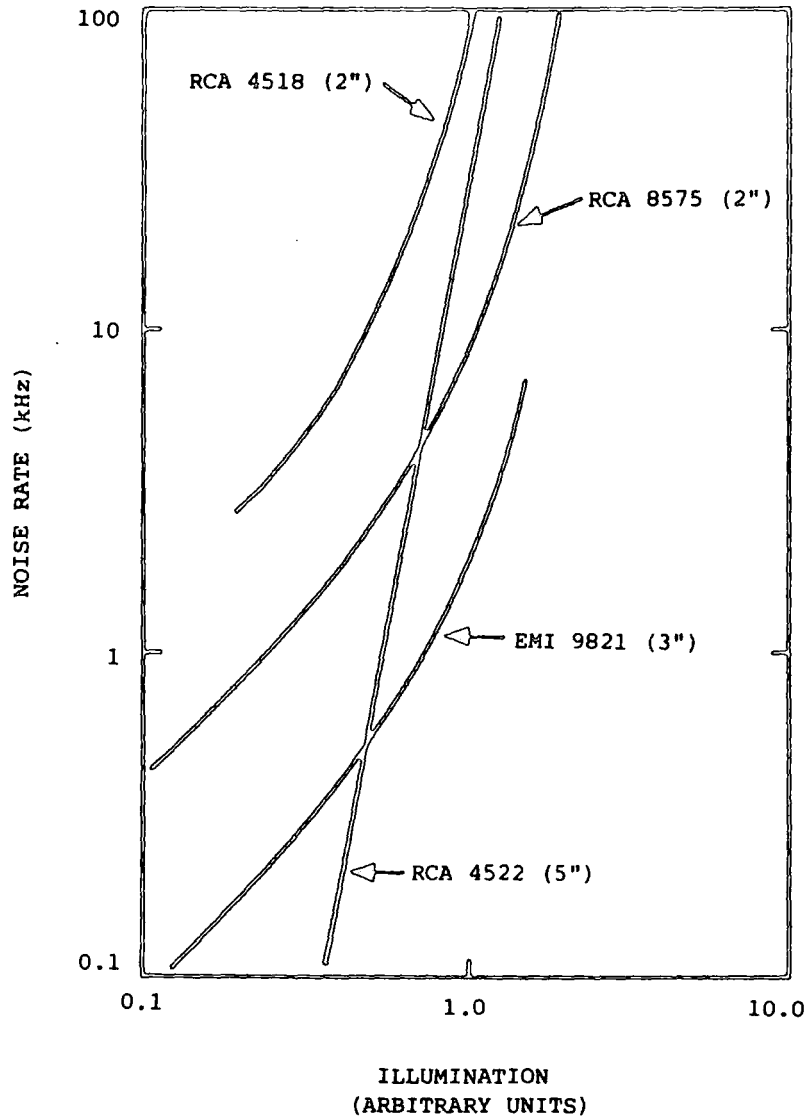

Figure 7.2 The variation of noise count rate (for a discrimination level typical of the experimental conditions in Narrabri) with illumination for a number of fast photomultplier tubes. The RCA 4522 was run at a lower gain than the others.

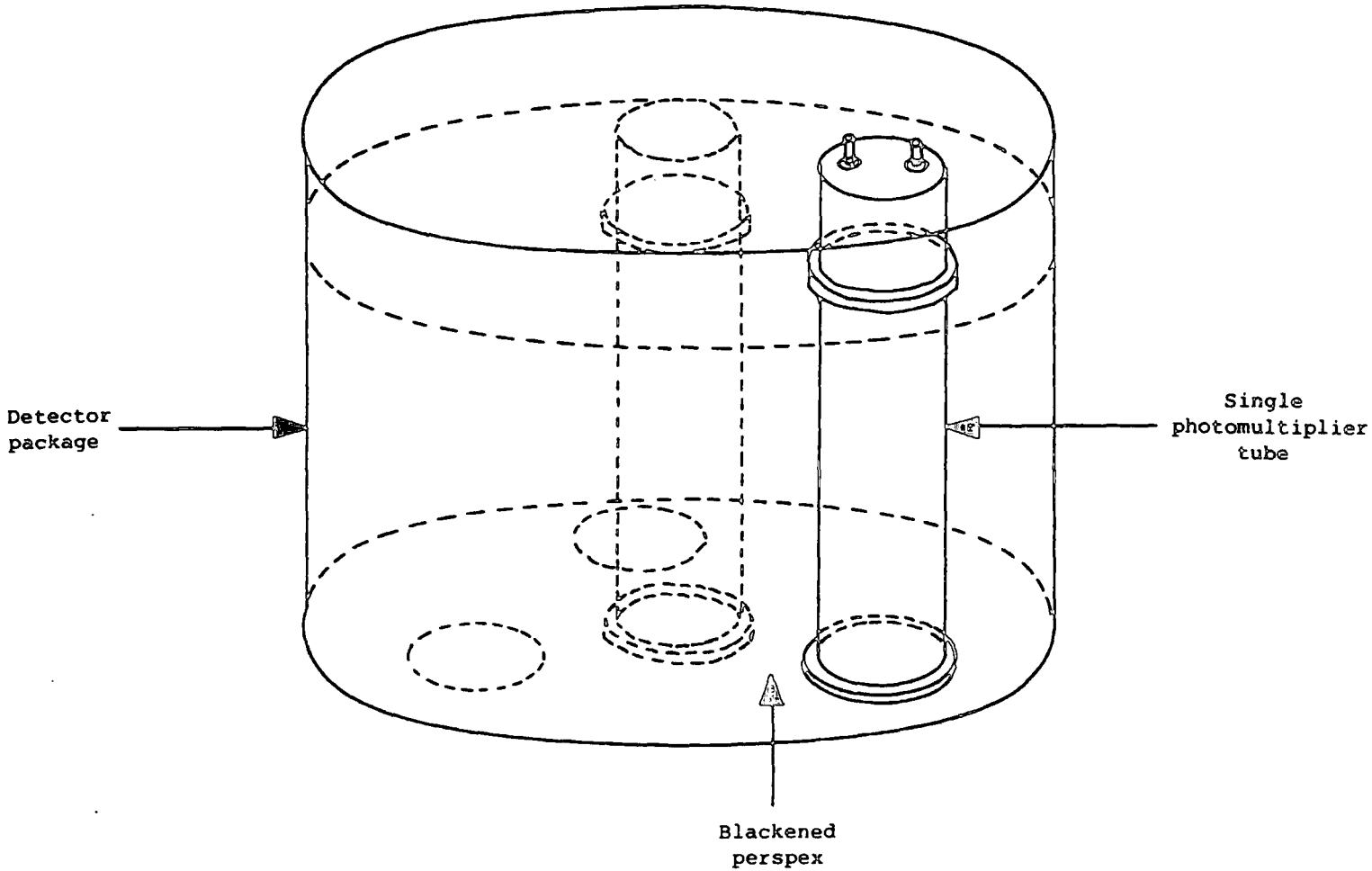

Figure 7.3 A schematic diagram showing the design of the detector packages , one of which is placed at the focus of each 11 m2 dish of the Mark III telescope.

instance, if an event is to be recorded from the central channel, each of the three central tubes (one at the focus of each flux collector) must record the Cerenkov light flash simultaneously. This defines one on-axis channel surrounded by three off-axis channels allowing continuous monitoring of the background cosmic ray rate. The area of sky viewed by each off-axis channel is 1.1^{o} removed from the central on-axis channel. The telescope has been designed such that photomultiplier packages may be easily changed. For example, when operating in drift scan mode there is the option of using single 5" phototubes, thereby increasing the aperture to a larger value suitable for drift scanning.

7.6.2. Operating Conditions

As has been mentioned, an important requirement of a phototube employed in this type of work is that it is capable of a fast response. For this reason, the voltage across each stage must be maintained at a high value. This results in a high gain, and so the overall gain must be reduced to an acceptable level by discarding two amplification stages and taking the signal from the 11th dynode rather than the anode itself. The operating voltage of an RCA 8575 under dark sky conditions is typically 1850V, and the EHT voltage is supplied by a computer-controlled LeCroy model HV4032A EHT unit. Under a clear sky, the operating conditions adopted give an individual PMT rate with a 50mV discrimination threshold of approximately 30 kHz with a typical anode current of 25 μA.

It is known that variations in sky brightness can change the gain of the photomultiplier tubes and complicate the detection of V.H.E. γ-ray sources (section 6.6.4). This is not of great importance when an object has a known periodicity and is being tracked, as the star field remains the same. The data may be searched for periodicity in the arrival times of the γ-ray induced Cerenkov pulses, and small count-rate excesses in the on-source channel need not be searched for. However, where a tracked object is considered to be a D.C. γ-ray source, or when the telescope is being operated in the drift scan mode, it is important to maintain constant anode currents (and hence gain) in all photomultiplier tubes. This is achieved by the use of servo-controlled L.E.D.s set into the perspex face of each individual PMT assembly (section 7.7.2).

7.6.3. Electronic Alignment

If the telescope is to register a coincidence between the signals from the three flux collectors, the signals from all three PMTs constituting a given channel (i.e. one set of three paraxial PMTs) must arrive at the coincidence unit within < 10 ns (see section 7.8.3). Although care was taken in the construction of the telescope to ensure that equal lengths of cable were used for each signal path, small differences are inevitable. Initial alignment was achieved by injecting a pulse into the system using a pulse generator capable of producing very short pulses. The signals from each set of three photomultiplier tubes corresponding to one channel were observed on

an oscilloscope and aligned in time by inserting different delays into each signal path. Final checks were made which allowed for small variations in the travel time of the signals from the PMTs by pointing the telescope at the zenith and optimising the count rate in each of the four channels by the addition of small delays.

7.7. Control and Monitoring Electronics

The control and monitoring of the Mark III telescope is achieved via a Local Area Network of BBC microcomputers. Extensive use is made of the MHz and RS232 ports which are available on all BBC microcomputers. The control and monitoring functions may be split into three main areas:

(i) control and monitoring of the telescope steering

(ii) maintenance of detector performance (PMTs)

(iii) environmental monitoring

A schematic diagram of both the control and logging electronics is shown in figure 7.4.

7.7.1. Steering Monitoring and Control

One BBC microcomputer is dedicated to the control and monitoring of the telescope steering. It can communicate directly with the microcomputer which exercises overall control via its RS232 port. Communication between the telescope shaft encoders, motor drive units and the steering computer is made through an interface unit on the MHz bus.

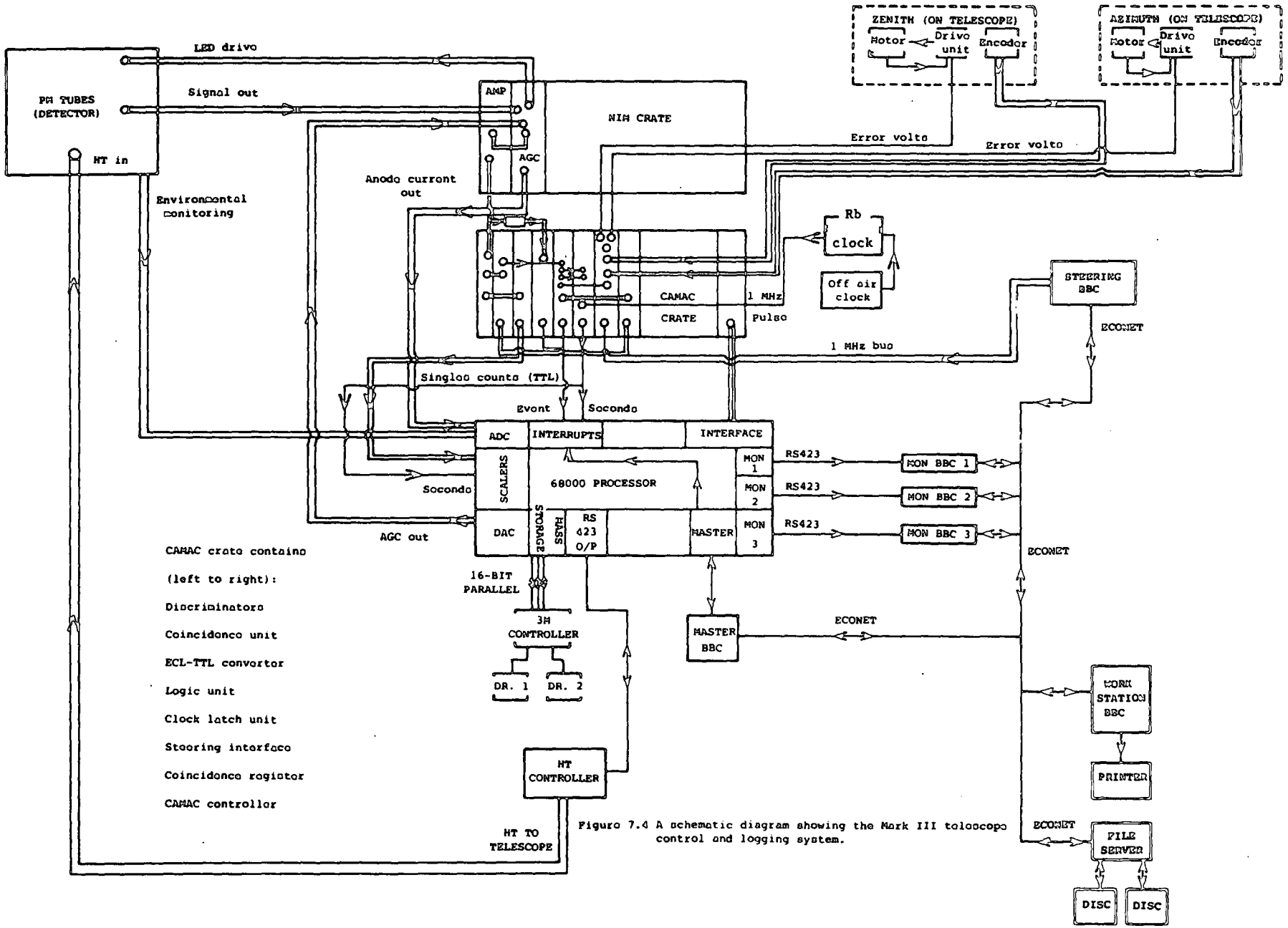

Figure 7.4 A schematic diagram showing the Mark III telescope control and logging system.

At every change of source during a night, the steering program is booted by the control BBC microcomputer. Ten times every second, the position of the telescope in azimuth and zenith is derived from the absolute shaft encoders via the steering interface. The actual position of the telescope is checked against the target position, and if the actual position is more than 1 bit (or 0.1^{o}) away from the target position in either azimuth or zenith, a signal is sent through the steering interface to the relevant motor drive unit(s). Every 6 seconds, the steering control program drops out of this servo loop in order to re-calculate the target source position in alt-azimuth co-ordinates. The target and actual positions are displayed on the steering BBC video monitor once every second. An alarm is incorporated so that the observers are alerted if the telescope stops steering or fails to steer correctly.

Telescope pointing information is extracted from the steering interface via the CAMAC bus by the 68000 data logger for recording on a data tape together with the main datastream (see section 7.9.5).

To enable the observers to check steering accuracy directly, the telescope is also equipped with a paraxial low light CCTV camera. This is capable of detecting 6th magnitude stars.

7.7.2. Maintenance of Detector Performance (PMTs)

The high tension voltage required for the operation of the 12 photomultiplier tubes in the 3 standard detector packages is supplied by a multi-channel LeCroy HV4032A E.H.T. unit, under the direction of

the controlling BBC microcomputer. The target voltage across each tube is read from the 68000 logger, where it is recorded in the housekeeping once every minute (see sections 3.2 and 7.8.7), and displayed on one of the monitor computer screens.

The 12 analogue signals from the photomultiplier tubes are DC-coupled into Automatic Gain Control (AGC) units. Each PMT anode current is sampled, and the PMT signals then pass immediately to an amplifier and thence to the discriminator and logging electronics described in section 7.9. The AGC unit is designed to provide control of the anode currents in the presence of variations in sky brightness by adjusting the brightness of an LED viewed by the PMTs such that the total anode current for each PMT is constant. A reference current is sent to the AGC unit from the 68000 via a Digital to Analogue Converter (DAC); an error signal is generated by comparing the anode currents with the reference value. The resulting output (after amplification) is used to drive the LED on the photomultiplier tube face. The feedback loop is designed to stabilise the difference between the anode current and the reference value. The anode currents are then fed from the AGC to an Analogue to Digital Converter (ADC). They are displayed on a dedicated monitoring BBC microcomputer and are also recorded in the housekeeping dataset. The anode currents are an important indicator of detector behaviour, so this display is watched closely by the observers, and a visual alarm is included to alert them to any abnormally high anode currents.

After processing the signals through the discriminators, ECL to TTL converters and scalers (described in section 7.8), the single fold count rates of each PMT are also monitored and displayed by another BBC microcomputer to provide a further sensitive indication of the behaviour of the detector gain for each PMT.

7.7.3. Environmental Monitoring

During the operation of the telescope, the outside environment is monitored by a weather station placed on an aluminium pole some distance above the control room. It incorporates a windvane, anemometer, shielded thermistor (for air temperature measurement) and wet and dry bulb thermometers (which are used to measure humidity). The information from the windvane, anemometer and thermistor is displayed on the monitor of dedicated microcomputer, together with a schematic of the telescope pointing direction. The wet and dry bulb thermometers have thermistors attached to them, and the voltages produced by these are similarly fed to a microcomputer where they provide a measure of the outside humidity, which is useful for predicting whether condensation will form on the mirrors (see section 7.3). All this information is displayed on the computer video monitors while the telescope is in operation. Weather information is also logged by the 68000 and included in the housekeeping (see section 7.8.7).

7.8. Logging Electronics

The heart of the Mark III data logging system, which was built by the University of Durham Microprocessor centre specially for this project, is an MC 68000 microprocessor. With 12 channels of analogue information to record (with the possibility of an increased number of data channels later: see chapter 9), a CAMAC system has been used as the data processing standard because of its high speed and consequent high channel density. CAMAC units are used to amplify and discriminate the PMT signals and provide the event registering logic. Reference is again made to figure 7.4.

7.8.1. Amplification and Discrimination

The individual PMT signals are input to a LeCroy model 612A amplifier, after they have been through the AGC unit (section 7.7.2). The amplifier provides two outputs, one to a charge-to-time converter (QT unit) via a delay line and the other to a discriminator. The QT unit is a fast analogue to digital converter (LeCroy model 2249A) which digitises the charge from the PMTs occurring within a 30 ns gate time. This information is stored in scalers until required by the 68000 (i.e. until an event is recorded). The discriminators have a variable threshold which may be set by the 68000 data logger via its CAMAC interface. The threshold is 50 mV. Any pulses which exceed this amplitude at the discriminator cause output to be passed to the ECL-TTL converters and thence to the coincidence unit and scalers.

7.8.2. Coincidence Units and Register

Each telescope "channel" consists of 3 photomultiplier tubes operated in coincidence, so there are 4 three-fold coincidence units, each dealing with one channel. Pulses from the separate phototubes within a given channel of three photomultiplier tubes are tested for overlap, within a total gate width of approximately 10 ns. If there is sufficient overlap between the three pulses, an event in that channel is registered and the logic unit is accessed. As more than one channel of three phototubes may detect a given Cerenkov light pulse, events from each coincidence unit are also passed to a coincidence register. This stores information about which channels have fired.

7.8.3. Scalers

The number of individual phototube responses which exceed the discrimination threshold (i.e. the noise rate) are recorded by the scalers. A 1 sec time reference is provided by the CAMAC clock unit which is set from the Rubidium oscillator (see section 7.10) and the number of counts per tube are then read and recorded by the 68000 data logger to give the single-fold count rates in Hz. The PMT noise is also displayed by a BBC microcomputer and is subject to alarm monitoring.

7.8.4. The Logic Unit

The first function of the logic unit is to ascertain whether an event has occurred during the system "dead time" i.e. while the

system is handling a previous event. The system dead time has been measured to be approximately 0.5 ms (Dipper, private communication). The procedure for handling such dead time events is described in section 7.8.6. When an ordinary event has taken place the logic unit latches the steering and the CAMAC clock latch unit (which gives the time of the event) and accesses the coincidence register. It also (most importantly) interrupts the 68000 processor.

7.8.5. The MC 68000 Processor

The manner in which the MC 68000 deals with an event is programmable, and is controlled by a program loaded from the Local Area Network fileserver at the beginning of a night's observing.

When the logic unit interrupts the 68000, the 68000 is latched until the data logging routine has been completed. The 68000 then reads the information in the following order:

(i) The digitised charge from the QTs

(ii) The anode currents in the three "on-source" phototubes (see section 7.6.1).

(iii) The event time

(iv) The position and drive status of the telescope

(v) The fire pattern of the channels from the coincidence register.

Finally, the 68000 resets the CAMAC logic unit, thus allowing further events to be processed.

This information is then formatted by the 68000 and stored in RAM until such time as the tape drive is available, as defined by

the tape controller. All the events with their corresponding details are then recorded on tape via a 16-bit parallel interface. See section 3.2. for a complete list of the information thus recorded.

7.8.6. Dead Time Events

While the system is processing an event, there is a so-called "dead time" during which the logic unit is latched. If an event arrives during this period, its time is read and is stored in a buffer. When the 68000 has completed its handling of an event, it reads this buffer and the times of these dead time events (no other information is stored) are formatted and stored in the 68000 RAM for recording to tape. Up to 15 dead time events may be stored in the CAMAC buffer, a capacity which is rarely required. Dead-time events do not have their fire patterns recorded and are thus not used in normal data analysis.

7.8.7. Housekeeping

Once every minute, the 68000 logger interrogates the various monitoring systems described in section 7.7. for information concerning system performance and environmental conditions. This information is similarly stored and written to tape by the 68000, and is tagged as a "housekeeping block". For details of the contents of a standard housekeeping block, see section 3.2. As is the case with the specification of a recorded event, the items recorded in the house-

keeping and the interval at which they are recorded may be changed at any time under program control.

7.9. Timekeeping

Experience in previous experiments has shown it is imperative that a good timing standard be available. The Dugway experiment used an oven-controlled crystal which was regularly reset using an off-air timing signal. This system was more than adequate for most purposes, and only observations of very short period objects such as the 1.5 ms pulsar raised difficulties (see section 6.3). In the light of this experience, a highly accurate Rubidium oscillator was chosen as the timing standard. Its specification and operation are described in section 7.9.1.

There are two types of uncertainty which arise in any timing system:

(i) Uncertainties leading to an error in the relative time of arrival of events. This arises, for example because the frequency standard does not have a strictly constant rate. These uncertainties are shown to be small for the Rb oscillator.

(ii) Uncertainties in the absolute time of occurrence of an event. A clock based on the Rb oscillator may be initialised by taking the system to a standards laboratory or by using an off-air timing standard.

These are considered in detail in sections 7.9.2. and 7.9.3.

7.9.1. The Rubidium Oscillator

The timing standard used by the Mark III telescope is an Efratom model FRK-L Rubidium atomic resonance-controlled oscillator, which provides an extremely stable 10 MHz sinusoidal signal of 0.5 V r.m.s. The oscillator is placed inside a unit, in which the sine wave produced by the oscillator is passed through a Schmidt trigger to produce a 10 MHz TTL signal. This is then divided by 10 to produce a 1 MHz gated output, used as the standard by the clock unit (see figure 7.4).

The Rb oscillator is known to be sensitive to magnetic fields which may shift the resonant frequency. The clock unit is housed within the control room, which has a high ambient magnetic field, calculated to be approximately 5 Gauss (McComb, private communication). To avoid this problem, the clock unit is placed in a small mu-metal box in addition to the internal shielding provided by the manufacturer. Long interruptions to the power supply also pose a potential problem, requiring that the oscillator be allowed to re-stabilise after power is restored. For this reason, the oscillator is provided with a long-term (10 day) external battery back-up in addition to its own internal battery support which lasts for 4 hours. This system also allows transportation of the oscillator to a standards laboratory.

7.9.2. Relative Timing

There are two main sources of relative timing uncertainty. Firstly, there is an error in the initial setting of the oscillation

frequency which is performed in the factory. The clock frequency is set to an accuracy of ± 5 parts in 10^{11}, which induces a maximum slip in the clock rate of ± 0.12 ms each month. There is also a slow drift in the oscillator frequency, specified by the manufacturers to be less than or equal to 4 parts in 10^{11} per month. This is effectively a second derivative change in the clock's timing and runs at approximately ± 0.1 ms/month^2. The total clock drift therefore follows a quadratic function.

In order to check the oscillator stability, thrice daily measurements are made of clock time with respect to the VNG time signal used in synchronising the clock (see section 7.9.3). The clock was last synchronised in late January 1987, and the measurements of the clock drift since then are shown in figure 7.5. Note that:

(i) The clock was initially set slightly slow with respect to VNG (this is corrected for in the data analysis).

(ii) There is inevitable jitter on the measurements of UTC derived off-air due to differences in ionospheric conditions from day to day which cause the signal to be very slightly early or late. This makes the quadratic form of the clock rate drift indistinguishable from a straight line over this timescale.

From Fig. 7.5., it is clear that the clock drift rate is approximately 0.8 ± 0.02 ms/month for January to June 1987. From a linear approximation to the manufacturer's specifications, we would expect the drift rate to be slightly less than this, at about

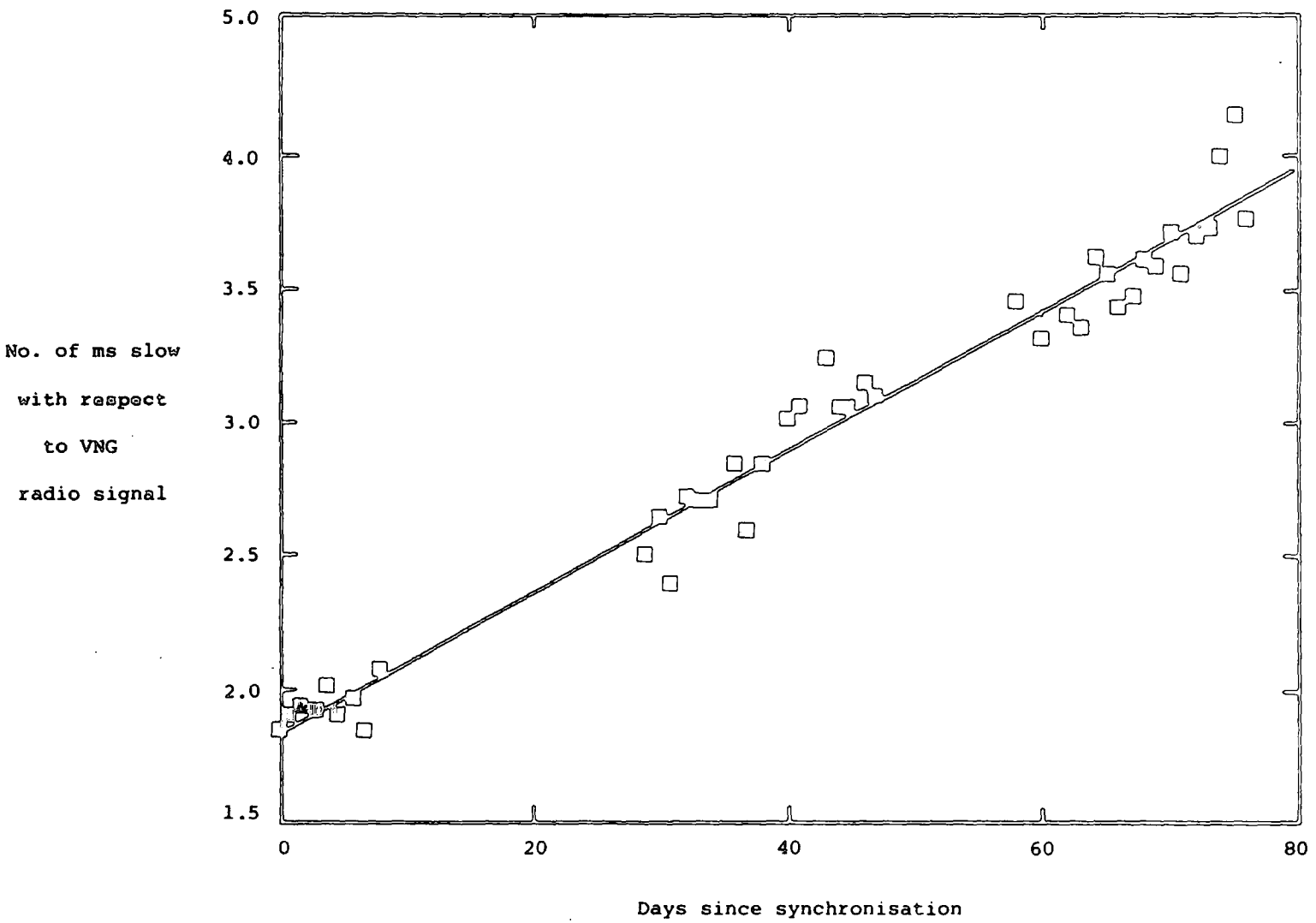

Figure 7.5 The Rb crystal oscillator drift rate. The best fit straight line gives a drift rate of (0.02665 +/- 0.00074) ms d^{-1}.

0.5 ms/month. A further factor which may be affecting clock performance is seasonal temperature variation. The Rb oscillator specifications are such that a temperature variation between $-25^{o}C$ and $65^{o}C$ will produce a change in the crystal rate of up to 3×10^{-10}, or a slip rate of up to about 0.8 ms/month. While the Rb oscillator used in the experiment does not suffer such a large temperature cycle, it probably experiences temperatures of up to $40^{o}C$ for short periods during Summer. This may affect its performance to some extent.

Present measurements of the slip rate of the Rb clock oscillator are more than adequate for the relative pulse arrival times of even the fastest pulsators.

7.9.3. Absolute Timing

In general, it is adequate that the absolute time of the observation of a Cerenkov flash be known to within a few milliseconds. An accurate knowledge of the absolute time is of importance only when an absolute emphemeris is available for the object under investigation - the Vela pulsar, for instance. Absolute timing requires that the oscillator be synchronised with a timing standard, generally Universal Co-ordinated Time (UTC). This may be achieved in one of two ways: the clock unit may be transported to the Australian National Measurements Laboratory in Sydney and synchronised using an atomic standard or it may be synchronised using a suitable radio signal. The latter method is at present used, though the former may be put into practice

at a later date.

The Universal Co-ordinated Time (UTC) signal with which the Rb clock is synchronised is provided by the VNG radio station located at Lyndhurst, Victoria (38^{o} 3' S, 145^{o} 16' E). The VNG signal consists of 54 digitally encoded one-second markers, followed by 5 short tones (consisting of 5 cycles of 1 kHz) between the 55th and 58th seconds, a "silent" 59th second and a long 1 kHz tone on the minute. After its arrival at Narrabri, the time signal is subjected to filtering and re-forming. The clock synchronisation procedure is to initialise the clock (i.e. set the oscillator to zero) after the 58th second tick, and allow the gated 1 MHz output signal to commence on the leading edge of the one-minute tone.

The timing signal is emitted by VNG Lyndhurst at the correct time, but does not re-synchronise the clock until it has traversed the distance to the site (approximately 1000 km). A positive adjustment to the clock re-synchronisation time is therefore necessary, corresponding to the propogation delay at that time. Except when the site is close to the transmitter, the radio signal does not take a direct path but is reflected from the ionosphere. Since the height at which this reflection occurs depends on the atmospheric conditions at the time of the reset which are largely unknown, the correction to be applied cannot be calculated accurately. However, the delay from Lyndhurst to the Anglo-Australian Observatory has been measured by the Australian Mapping Service using a portable standard clock and is found to be 6ms. The delay from Lyndhurst to

Narrabri will be the same to within the uncertainties caused by the variation in height of the ionosphere (± 0.05 ms), and so a 6 ms correction is applied to the data.

7.10. Modes of Operation

The Mark III telescope has three modes of operation: the familiar drift scan and tracking modes, and a further "chopping" mode. These are described below.

7.10.1. Tracking

The operation of tracking is simple and requires little explanation. The object of interest is kept within a specified channel, usually the central channel. (Other channels may be used as the "on-source" channel to preclude any instrumental effects from the data.) It should be noted that in this mode of operation there is an inevitable rotation of the field of view such that the "off-source" channels observe slowly changing areas of sky.

7.10.2. Drift Scanning

If the telescope has all four channels operating then the object being observed will in general pass through one off-axis channel as well as passing through the on-axis channel. As mentioned earlier, 5" photomultiplier tubes may also be used to provide a large single field of view. The development of the chopping technique (section 7.10.3. below) makes extensive use of this technique unlikely.

7.10.3. Chopping

This method of observing was not possible with the Mark I and II telescopes because of their lack of simultaneous off-source observations. Chopping involves tracking an object in the on-axis channel and one off-axis channel alternately at the same zenith angle, with the time spent with the object in each channel (the chopping period) defined by the observer. This is usually between 2 and 5 minutes. Care must be taken in the choice of chopping period such that it is not close to the pulsar (or indeed orbital) period of the object which is observed, to avoid confusion with any periodicity caused by the object itself. This technique allows data to be analysed for both count rate excesses and periodicity in the same way as tracking data, but with the additional security of excluding instrumental effects which may arise when employing one channel only. At the time of writing, investigation into methods of analysing data produced in this way is proceeding.

7.11. Telescope Performance

The most reliable indicator of telescope performance is the coincidence count rate. Before construction, it was predicted that the Mark III telescope would have a count rate of 75 c.p.m. per channel at the zenith (Orford, private communication). On the 28th October 1986, a very clear night during the first data acquisition period, tests were made on the count rate versus zenith angle. The result is shown in figure 7.6. and shows a count rate of 64 ± 4 c.p.m.

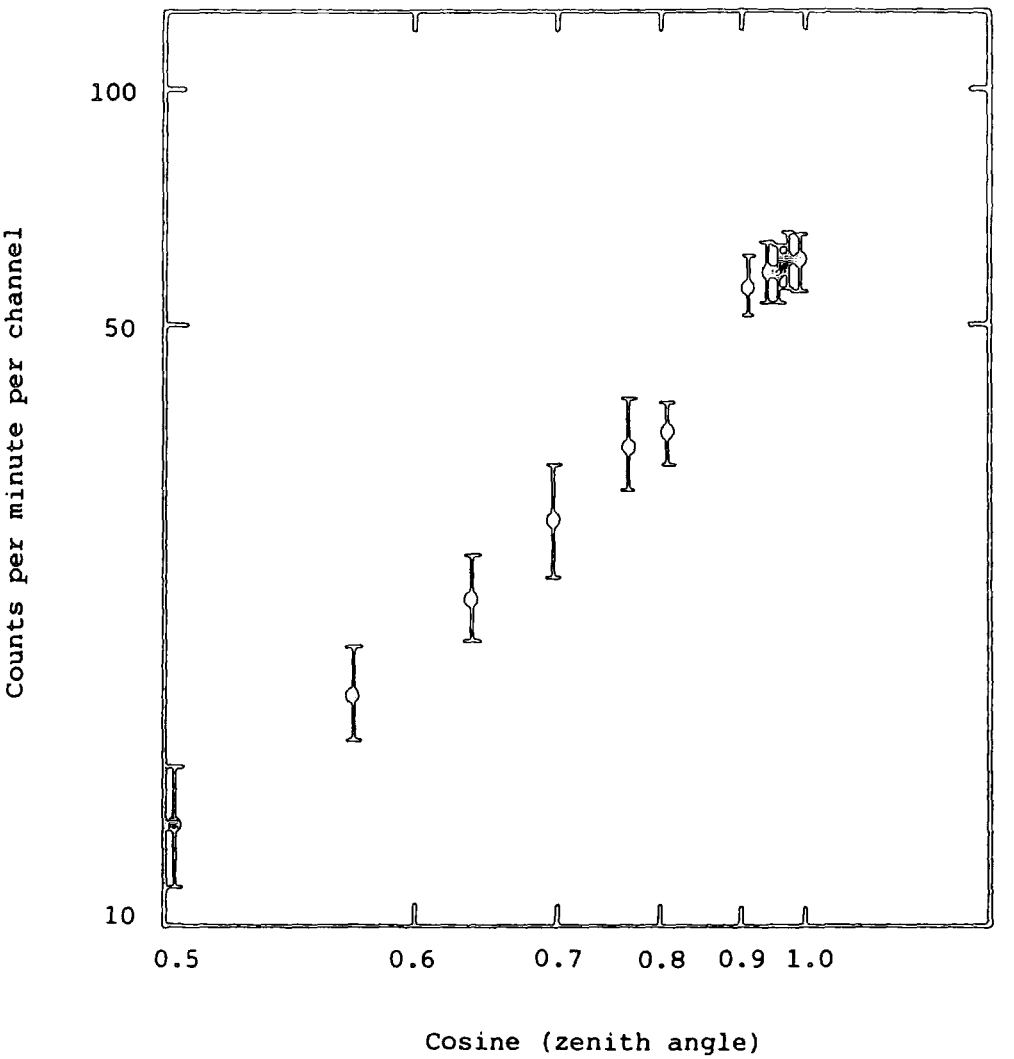

7.6 Count rate versus zenith angle for the Mark III telescope in Narrabri.

5^{o} from the zenith, with no source in the field of view. The count rate versus zenith angle follows a function of the form:

$$C.R. \propto \cos^{2.35 \pm 0.54}\theta$$

where θ is the zenith angle. This is in approximate agreement with results from Dugway. This test was made before alignment had been completed, after which the count rate was indeed approximately 75 c.p.m. Recently, during the Australian Winter nights, the count rate has risen to 100 c.p.m., perhaps due to operation of the telescope at high PMT gain.

7.12. Energy Threshold

It is possible to estimate the energy threshold of a γ-ray telescope by noting the count rate when there is no source in the field of view (i.e. when the telescope is counting the cosmic ray background). By considering the estimated effective collecting area, the flux observed may be found. This allows an estimation of the energy threshold using the well-known integrated cosmic ray spectrum. The most difficult parameter to calculate is the effective detector area, which is a function of the detector's aperture and the area of the Cerenkov light pool. Since the size of the light pool varies with shower development and zenith angle (see section 2.4), any estimate of the effective detector area will be approximate. The effective area for the Mark III telescope is estimated as $(1 \pm 0.5) \times 10^{4}$ m^{2}, giving an energy threshold of 250 ± 100 GeV.

CHAPTER 8

OBSERVATIONS AND PRELIMINARY RESULTS FROM THE MARK III TELESCOPE

8.1. Introduction

The Mark III Southern Hemisphere telescope has now (May 1987) been operational for just over eight months. This chapter describes the observing programme, data base and a preliminary analysis of some of the results to April 1987. A novel method of improving the sensitivity of the telescope is also discussed.

8.2. The Observing Programme

Southern Hemisphere skies present a much wider variety of potential V.H.E. γ-ray sources than Northern Hemisphere skies as the Southern Hemisphere faces the Galactic Centre. Furthermore, the majority of known X-ray binary pulsars are visible from the Southern Hemisphere, as are the two closest galaxies to our own, the Large and Small Magellanic Clouds. It has therefore been necessary to make a selective observing plan for the first year of operation of the Mark III, basing the choice of objects on those types which proved to be γ-ray emitters in the Northern Hemisphere, viz. fast pulsars close to the Solar System and short period X-ray binaries. This must be done in an effort to identify V.H.E. γ-ray sources which may be more closely studied in later years. Catalogues of interesting objects which have been searched for potential V.H.E. γ-ray emitters are the

low energy γ-ray catalogues (the second COS-B γ-ray catalogue and SAS 2 and 3 catalogues), X-ray catalogues (the fourth Uhuru catalogue and the Einstein catalogue), and pulsar surveys (e.g. the Molongolo survey). In addition, recent literature is also scrutinised, especially those papers containing results from satellites which have been in operation recently, such as EXOSAT, from which near contemporary timing data is available. The list of candidate V.H.E. γ-ray sources derived from the literature is given in sections 8.2.1. to 8.2.3. below.

Each observing team who are responsible for the operation of the telescope in a given month have an agreed and detailed observing programme comprising objects which are to be observed and the times during the night when observations should ideally be made. Except under unusual circumstances, observations are not scheduled when the object is at a zenith angle of $> 50^{o}$, as the count rate is then reduced to about 40 counts per minute. In general there are two types of object to be observed: those which have well-known periods and those which have ill-defined periods or no known periodicity. In the latter case, any detection in the first instance must be on the basis of a count rate excess from the source, so observations of objects of this nature are confined to nights when atmospheric conditions are stable. Potential sources with known periodicity do not require such stable conditions and may be observed on nights when the weather is not perfect (for instance when there is variable sky clarity). Most interesting objects are in the galactic plane, which

means that such objects are best observed for only 8 months of the year, from November to June. In terms of the number of potential sources visible, the best months are April and May when the galactic centre culminates at the zenith around midnight. During August to November, attention moves to objects outside the Galactic Plane including those in the Magellanic Clouds.

8.2.1. Pulsars

The criteria for selecting possible V.H.E. emitting pulsars are described in section 6.2. The pulsars should have short periods, large period derivatives and small distances from Earth. A further criterion, given the successful observations of V.H.E. γ-rays from the Crab pulsar, is that they should have a supernova remnant (or suspected remnant) associated with them. A complete list of pulsars which are considered to be candidate V.H.E. γ-ray emitters is given in table 8.1. The following short comments on selected candidate sources may convey the reasoning behind this list.

The most obvious Southern Hemisphere candidate is the Vela Pulsar which has an 89 ms period with a well-measured period derivative and second derivative. In addition it was observed to emit a pulsed γ-ray flux at energies > 500 GeV by the Indian V.H.E. γ-ray group at Ootacamund (Bhat et al., 1980 and 1987). The results of the analysis of data from the Vela pulsar recorded by the Mark III telescope are given in section 8.6.2. Despite its distance from Earth (50 kpc), the X-ray pulsar in the Large Magellanic Cloud is

PULSAR	PERIOD (ms)	DISTANCE (KPC)
1510-59	150	4.2
1055-52	197	0.92
1822-09	769	0.56
0540-693	50	55
0740-28	167	1.5
1642-03	388	1.3
1706-16	653	?
1742-30	368	?
1747-46	742	0.66
0833-45	89	0.5
1830-08	85	?
1823-13	101	?
1802-23	112	?

Table 8.1 Candidate gamma ray pulsars in the Southern Hemisphere.

also a possible V.H.E. γ-ray emitter. This produces both X-ray and optical emission and measurements show it to have a period of 50 ms and suggest it is surrounded by an optical synchrotron nebula (Seward et al., 1984; Middleditch and Pennypacker, 1985). Another strong candidate is PSR 1510-59, detected by the Einstein satellite (Seward et al., 1982). It has a pulse period of 0.15 seconds and the period derivative is very large (1.49×10^{-12} ss^{-1}). It is reasonably close to the Solar System, being 4.2 kpc distant. These characteristics, coupled with the fact that there are indications that the pulsar is surrounded by a small, bright nebula suggest that the object may be similar to the Crab pulsar.

8.2.2. X-ray Binaries

Following the discovery of periodic V.H.E. γ-rays from the archetypal X-ray binary Hercules X-1 (and subsequently from the similar X-ray binary 4U0115+63) by the Durham Group, X-ray binary pulsators have been considered to be strong candidate V.H.E. γ-ray emitters. Experience with objects such as Cygnus X-3 (which appears to show pulsar activity around the maximum of the 4.8 hr X-ray cycle) and Hercules X-1 (which produced a burst of 1.24 second periodic γ-rays just before a 35-day X-ray "turn-on") suggests that any V.H.E. γ-ray emission will be related to the X-ray cycle in some way, emission probably occurring around X-ray maximum if Cygnus X-3 is in any way typical. In the absence of prolonged, recent observations from X-ray satellite experiments, in most cases the pulse periods and orbital

ephemerides of these X-ray binaries are uncertain. This has lead to an observing strategy whereby objects are initially observed during approximately one month, and the data searched for periodicity. If a wide search range has been required, this may result in a candidate period for V.H.E. γ-ray emission of low statistical significance. Further observations are then made to confirm or deny the presence of γ-ray emission at the candidate period without a requirement for the use of a large number of degrees of freedom.

There is a large number of binary X-ray sources visible from the Southern Hemisphere. Prime candidates are LMC X-4 and Centaurus X-3, which will be described in detail in sections 8.6.1. and 8.6.3. respectively. Other obvious possible V.H.E. γ-ray sources are Vela X-1 and SMC X-1. In addition, 4U1626-67 is a highly compact binary observed by the Uhuru satellite with a 7.7 second pulse period and a 2485 second orbital period (Giacconi et al., 1974; Rappaport et al., 1977; Middleditch et al., 1981). The recently discovered 5ms radio pulsar in a binary system, PSR 1855+09 is also included in the observing programme (Segelstein et al., 1986). A complete list of Binary V.H.E. γ-ray candidates visible from the Southern Hemisphere is given in table 8.2.

8.2.3. "Galactic" Objects

Other possible V.H.E. γ-ray emitters include the "galactic" sources. It is proposed to scan the Galactic Centre in the same way

BINARY	PULSE PERIOD (S)	ORBIT (DAYS)
SCO X-1	?	0.7
4U1728-24	120/240	LONG
GX17+2	1913	6.4
CIR X-1	?	16.6
LMC X-4	13.5	1.4
CEN X-3	4.8	2.08
4U1223-62	696.0	41.4
4U1145-619	290	187.5
4U1624-49	?	0.88
A0538-66	0.07	16.66
E1145-6141	298	5.65
4U1822-37	?	0.23
2S1553-542	9.26	30.6
OAO1653-40	38.2	7.8?
SMC X-1	0.71	3.89
VELA X-1	282.0	8.95
4U1626-67	7.68	0.03
4U1700-37	?	67.4
2S1417-624	17.64	>15
OAO1653-40	38.2	7?
4U1538-52	529	3.73
GX304-1	272	?
GX339-4	1 ms?	?
4U1755-33	?	0.18

Table 8.2 Southern Hemisphere X-ray binary sources.

as the Galactic Plane was scanned at Dugway. The position of the observing site is such that at the correct time of year it will be sufficient simply to park the telescope pointing towards the zenith and allow the galactic plane to pass through the fields of view of the telescope. Another clear target for observations is Centaurus A, our closest active galaxy. It was found to emit V.H.E. γ-rays by Grindlay et al., (1975), and an excess of cosmic rays was observed from its direction between 1978 and 1981 (Clay et al., 1984).

8.3. The Database

After four observing periods each of one month's duration, the Mark III telescope has taken 246 hours of data on 11 objects. The largest amount of data (40 hours) has been taken on the Vela pulsar. Table 8.3. shows the number of hours' data taken so far (complete at early April 1987) on each object. Details are given in this chapter of the results from a preliminary analysis of the data from some of these objects.

8.4. Routine Data Analysis

The routine analysis for periodicity in data from the Mark III telescope involves the stages outlined below, which are described in greater detail in chapter 3.

(a) Since the data are logged in a compact format to economise on tape, the data are first of all translated into ASCII format

OBJECT	NO. OF HOURS DATA
VELA X-1	25.5
SMC X-1	28
LMC X-4	24.5
PSR0540-693	26
VELA PULSAR	40
CEN X-3	26
PSR1055	23
SN1987A	4
PSR1510	23
CEN A	19
SCO X-1	6
TOTAL	246

Table 8.3 The Durham Mark III Telescope database to early April 1987.

and then split into files which each contain a single night's observation on a given object.

(b) Event times are then stripped off these files and are adjusted to the Solar System barycentre to remove the variations in pulse arrival time caused by the motion of the observer, and the values of the digitised charges from each PMT for each event are reduced to a single byte. This provides files of the minimum length for useful future work.

(c) If the candidate γ-ray source is in a binary system, the event times are reduced to the focus of the binary orbit.

(d) Events which produce a substantial signal in off-source as well as on-source channels are rejected. This process is described in detail in section 8.5.

(e) The enhanced on-source data are tested for periodicity. If the expected period is well known (for example in the case of the Vela pulsar) that period only is tested and epoch folding is used. Otherwise a period search is initiated. The statistical test generally used is the Rayleigh test, this being the most reasonable test to apply in the absence of any information concerning the shape of the light curve.

(f) Off-source data are also tested as in (e) above to ensure that any periodicity observed in the on-source channel is not attributable to an instrumental effect.

(g) In the light of the results of the above, any further tests required are applied to the data.

8.5. The Guard Ring Technique for Improved Telescope Sensitivity

The off-axis detectors on the Mark III telescope not only provide simultaneous off-source control data, but can also give additional information about the on-axis signal. On a crude level, if the centre (on-source) channel and one off-source channel respond to the same light pool, the most likely position for the centroid of the Cerenkov flash is at an angle halfway between the fields of view of these two detectors. This direction is at the edge of the target field of view and hence such events may be regarded as most probably nucleon-induced and may be routinely rejected (step (d) in section 8.4. above).

In addition, as mentioned in section 7.8.1., the signals from each phototube are routinely digitised and recorded for each event whether or not a given tube actually registered a pulse above the hardware threshold and fulfilled the coincidence condition. This additional information enables the rejection of further events which, while they did not indicate an above threshold (hardware) response on any of the off-axis channels, do nevertheless show a number of photons which is a substantial fraction of the on-axis response. These are also considered to be indicative of an event towards the periphery of the target aperture and may be rejected. A fractional measure of the on-axis response has been used rather than a constant threshold so that large, bright Cerenkov flashes which arrive directly on-axis (and may therefore be considered to be γ-ray induced) but which also produce a signal in the off-axis channels are not rejected.

Empirical tests show that the best criterion to date for the rejection of an event is that the off-axis response exceeds 60%-70% of the on-axis signal (see table 8.4).

The testing of any potentially signal-enhancing technique requires a strong signal in the initial data. The first data with which this technique could be investigated were from observations of Centaurus X-3 taken in January and February of 1987. The effect of the rejection of events which produce signals in the off-axis detectors on the initial dataset (26 hours of observations) will therefore be used to illustrate the increase in sensitivity afforded. Details will be found in table 8.5. The initial effect which was the basis for the claim of periodicity in the data was found in the total sample of events in which at least the central channel responded. This is analogous to the data yielded by a telescope comprising a single on-axis channel alone, such as the Dugway telescopes. The apparent periodic signal yielded by this dataset containing 38663 Cerenkov flashes was 1.4% of the cosmic ray background, or a total of 541 ± 37 γ-ray candidates. The further rejection of events by use of the hardware threshold produced a dataset containing those events in which the central channel alone responded. Here, the periodic effect had a strength of 2.3% of the cosmic ray background in a dataset containing 24013 events (552 ± 39 γ-ray candidates). When the sensitivity improvement was made involving the rejection of further events which did not fulfil the hardware condition but where the off-axis response in any one channel was 60% or more of the on-

REJECTION CRITERION (% OF ON-AXIS SIGNAL)	PERCENTAGE SIGNAL
NO ENHANCEMENT	1.4
40	2.4
50	2.6
60	2.8
70	2.3
80	2.2

Table 8.4 The variation in the signal strength of Cen X-3 as a percentage of the cosmic-ray background with the criterion applied to reject events towards the periphery of the target aperture. In this case , the greatest signal enhancement is produced if the events with an off-axis response exceeding 60% of the on-axis response are rejected.

DATA ANALYSED	NO. OF EVENTS	NO. REJECTED	% EFFECT	NO. OF GAMMA RAYS
(i) On-axis	38663	N/A	1.4	541 +/- 37
(ii) On-axis alone	24013	14650 of (i)	2.3	552 +/- 39
(iii) On-axis enhanced	20027	3990 of (ii)	2.8	501 +/- 35

Table 8.5 The results of the application of sensitivity enhancing techniques to data from Cen X-3.

axis signal, the periodic content was increased to 2.8% of the cosmic ray background in a dataset containing 20027 events (501 ± 35 γ-ray candidates). This final enhancement gives a 100% improvement on the original γ-ray signal. Note that while the number of total events falls as these cuts are applied to the data, the number of periodic γ-ray candidates within the sample remains substantially constant, indicating that mainly nucleon-induced events are indeed being rejected. The increase in the percentage effect more than compensates for the decrease in number of events in the sample being tested so the application of this technique results in a decrease in the Rayleigh probability of chance occurrence (which is approximated by e^{-nR^2} (see section 3.5.2.)). In the above case, the Rayleigh probability of the effect arising by chance (without correction for the number of degrees of freedom used) falls from 4×10^{-4} for light flashes in which at least the on-axis detector responded, to 2.5×10^{-7} after the signal enhancing techniques had been applied.

This technique has also been applied to the LMC X-4 result described in section 8.6.1. The γ-ray signal was 2.5% of the cosmic ray background before any enhancement and increased to 3.8% afterwards, an improvement of 65% in signal strength. Further details may be found in table 8.6. It is noted that the improvement gained in the signal strength from this object is not as great as for Centaurus X-3. The observations of Centaurus X-3, on which this technique has been developed, were made while the object was near

DATA ANALYSED	NO. OF EVENTS	NO. REJECTED	% EFFECT	NO. OF GAMMA RAYS
(i) On-axis	13527	N/A	2.5	338 +/- 18
(ii) On-axis alone	8577	4950 of (i)	3.2	274 +/- 16
(iii) On-axis enhanced	8619	4908 of (i)	3.8	327 +/- 18

Table 8.6 The results of the application of sensitivity enhancing techniques to data from LMC X-4.

the zenith whereas LMC X-4 is always low in the sky from Narrabri (the zenith angle being approximately 40^{o} at best). It may be, then, that a further refinement of this technique is required to take into account the variations in the size of the Cerenkov light pool caused by observations being made at differing zenith angles.

The advantage of this method is its simplicity: there is no attempt to identify and separate the γ-ray induced Cerenkov flashes from those induced by nucleons by any method other than their spatial features. The result is a valuable increase in γ-ray signal of between 65 and 100%, a factor which appears to be dependent on the zenith angle of the object at the time of observation.

8.6. Results of Initial Data analysis

8.6.1. LMC X-4

8.6.1.1. Research Background

The fourth X-ray source in the Large Magellanic cloud was discovered by Giacconi et. al., (1972) using data from the Uhuru satellite. The optical counterpart was identified as a 14th magnitude OB star by Sanduleak and Philip (1977), photometric and spectroscopic observations of which indicated the binary nature of the source, the period being 1.408 days (Chevalier and Ilovaisky, 1977). Occasional X-ray flaring episodes have been observed from this source, and a pronounced 30.5 day periodic modulation in the hard X-ray flux has

also been observed, similar to that of Her X-1 (Epstein et al., 1977; White, 1978; Skinner et al., 1980 and Lang et al., 1981). LMC X-4 was considered a good candidate for an X-ray pulsar due to its massive companion and hard X-ray spectrum (Jones, 1977; Rappaport et al., 1977). After some early attempts to observe a pulsation period from the object, pulsations with a 13.5 second period were observed in SAS 3 data taken in February 1976 and May 1977 (Kelley et al., 1983). These results enabled an orbital determination to be made. Later observations made in November 1983 with the EXOSAT satellite confirmed the pulse period and enabled a more precise orbital determination (Pietsch et al., 1985).

To the writer's knowledge, there have been no V.H.E. gamma-ray observations made of this source with the exception of those made by the Durham Group. However, U.H.E. γ-ray data taken with the Buckland park array show the characteristic 1.4 day orbital period at the 3.2σ level, corresponding to a flux of $(4.6 \pm 1.7) \times 10^{-11}$ m^{-2} s^{-1} for γ-rays $> 10^{15}$ eV (Protheroe and Clay, 1985).

8.6.1.2. Data and Results

The Durham LMC X-4 database comprises 25 hours of data taken on eleven nights in early November 1986, and January/February 1987. Unfortunately the 1986 data contain no off-source information because a LeCroy EHT unit failure required the use of back-up high tension supplies, which at that time were only available for the three on-axis PMTs (see section 7.6.2.). This adds the additional

complication that no sensitivity enhancing techniques can be applied to these data. In the case of the 1987 data, some 38000 events were recorded in the on-axis channel over the 11 nights. Of these 11 datasets, 4 were taken at or near the maximum of the 1.4 day X-ray cycle and 7 were taken near the minimum, as defined by the orbital period and epoch given in Kelley et al., (1983). (Errors on the predicted orbital phases are calculated to be ± 14%.)

Fits to the EXOSAT and SAS 3 periods enables an estimate of the pulse period to be made, which would be 13.491 ± 0.003 sec in January 1987 (Pietsch et al., 1985; Kelley et al., 1983). Similarly, from these X-ray results the period derivative may be estimated as -1.1×10^{-10} ss^{-1}. All γ-ray event times were reduced to the Solar System barycentre and to the focus of the binary orbit using the parameters listed in table 8.7. The technique described in section 8.5 was then applied where possible (i.e. to the 1987 data) and two datasets created. These incorporated data taken in 1987 on 3 nights around X-ray maximum and 4 nights around X-ray minimum. The two datasets were then analysed separately using the Rayleigh test in the period range 13.488 to 13.494 seconds, corresponding to 24 independent test periods, to take into account the uncertainty in the predicted period. The period derivative of -1.1×10^{-10} ss^{-1} associated with the X-ray results was also assumed to apply to the γ-ray data; no variation in this value was allowed.

The result of the application of the Rayleigh test to the data

asin(i)	30 +/- 5 lt.sec.
Orbital period	1.40832 +/- 0.00005 days
Epoch (JD)	2442829.994 +/- 0.019
f(M)	15 +/- 8 $M_{\odot}$
Periastron angle	90°

Table 8.7 The orbital parameters of LMC X-4

(Kelley et al., 1983)

taken around X-ray maximum is shown in figure 8.1. The data show clear evidence for periodicity at 13.49116 ± 0.0003 seconds with a Rayleigh probability of 8.5×10^{-5} after correction for the number of degrees of freedom used, and a strength of 3.8% of the cosmic ray background. The data also show a complicated pattern of side-bands which are induced by the 13.49116 second period beating with 3 and 4 days, the elapsed times between the 3 observations, and their harmonics. The light curve for a period of 13.49116 seconds is shown in figure 8.2. The light curve is broad, and may be compared with the light curves from other X-ray binaries (see Chapter 9.). As a control, the same dataset was also tested at periods around 14.5 seconds and shows no activity (figure 8.3). Off-axis data was analysed at the expected period and again no periodicity was found (figure 8.4). There is no evidence to suggest that the periodic effect is other than attributable to the source.

Precisely the same analysis was applied to the "off-maximum" data, the result of which is shown in figure 8.5. The probability distribution is consistent with that expected by chance, indicating that the emission is confined to near X-ray maximum ($\phi \simeq 0.5$-0.7).

8.6.1.3. Conclusions and Future Requirements

In conclusion, the 1987 V.H.E. γ-ray data from LMC X-4 show evidence for periodicity in the region of the X-ray maximum in the 2.1 day orbit with a period of 13.49116 ± 0.0003 sec., which

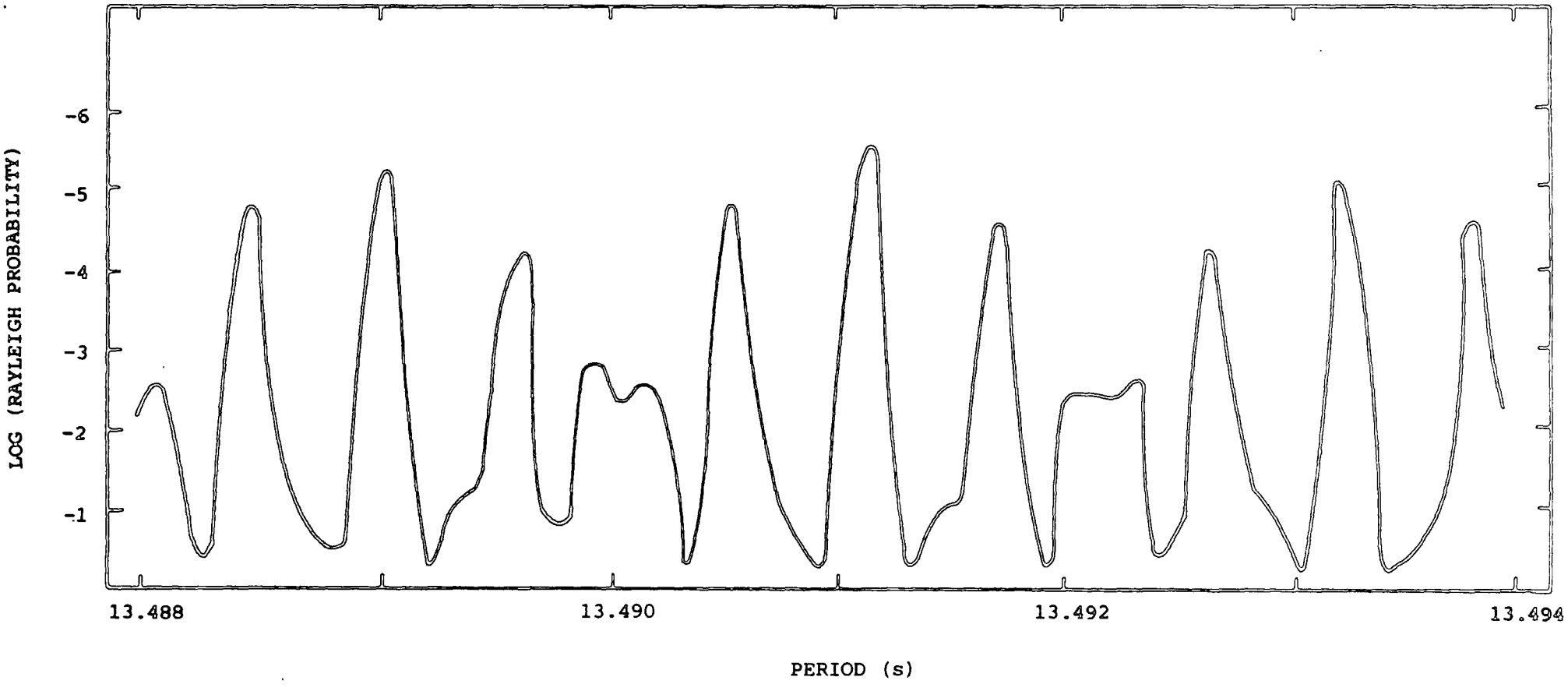

Figure 8.1 The Rayleigh probability of chance occurrence plotted against trial period for data from LMC X-4 taken around X-ray maximum (phase 0.5-0.7).

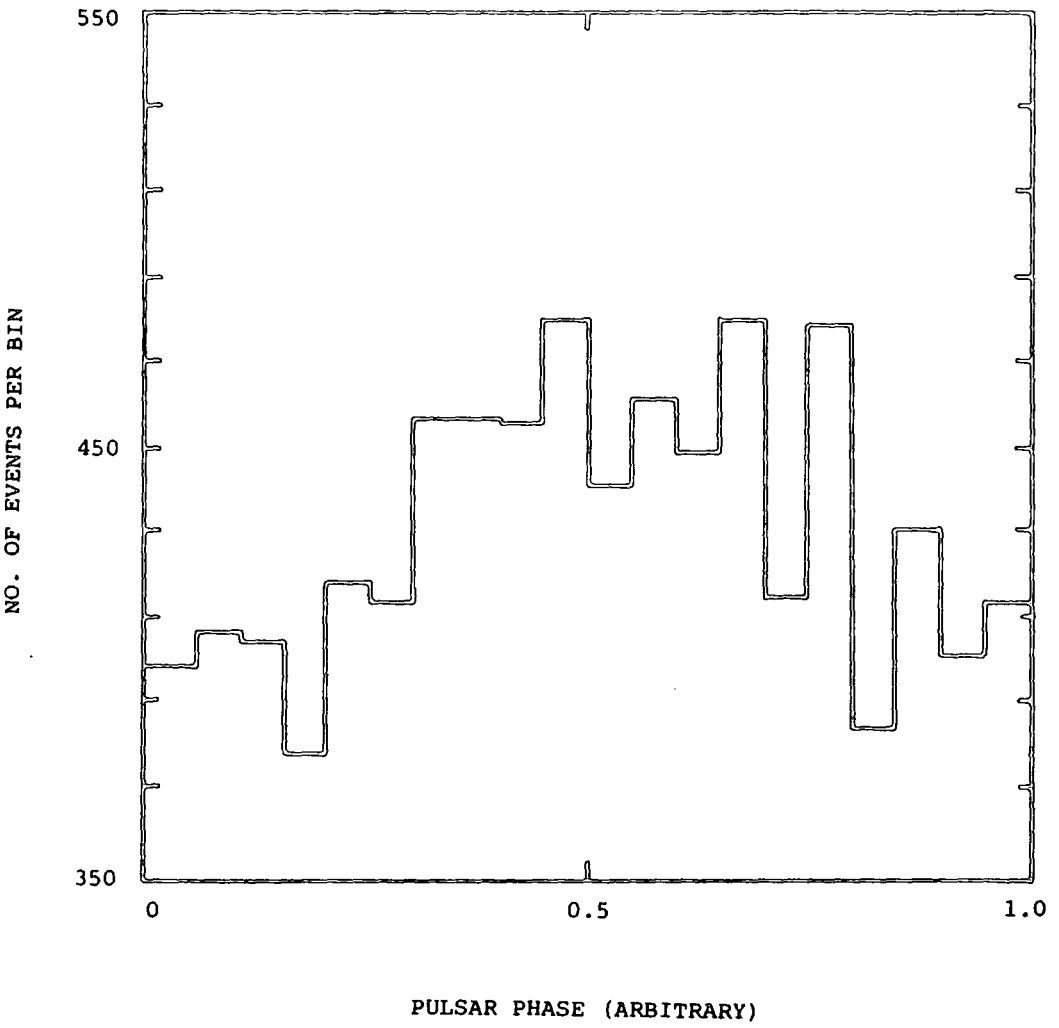

Figure 8.2 The light curve for V.H.E. gamma ray emission at E > 250 GeV from LMC X-4 at trial period of 13.49116 seconds.

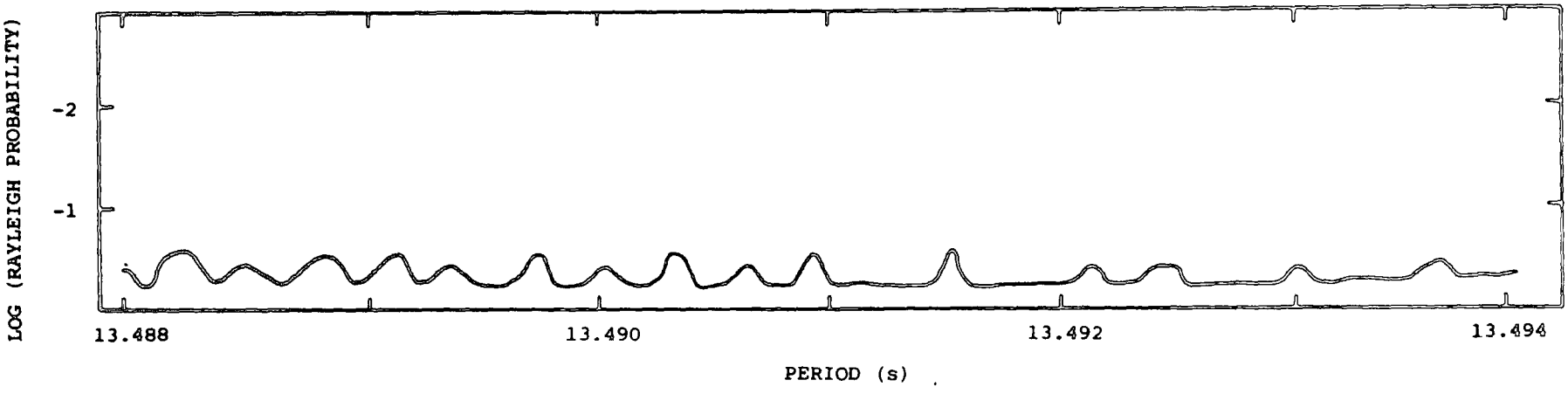

Figure 8.4 The Rayleigh probability of chance occurrence plotted against trial period for off-source data taken simultaneously with the LMC X-4 data shown in figure 8.1.

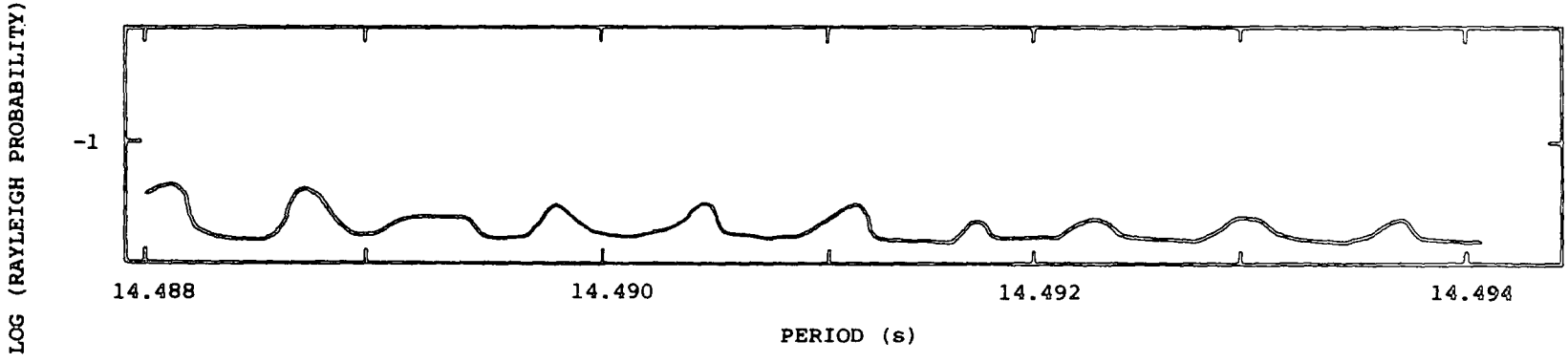

Figure 8.3 A "control" test of the data shown in figure 8.1. The Rayleigh probability of chance occurrence is shown for trial periods around 14.5 s.

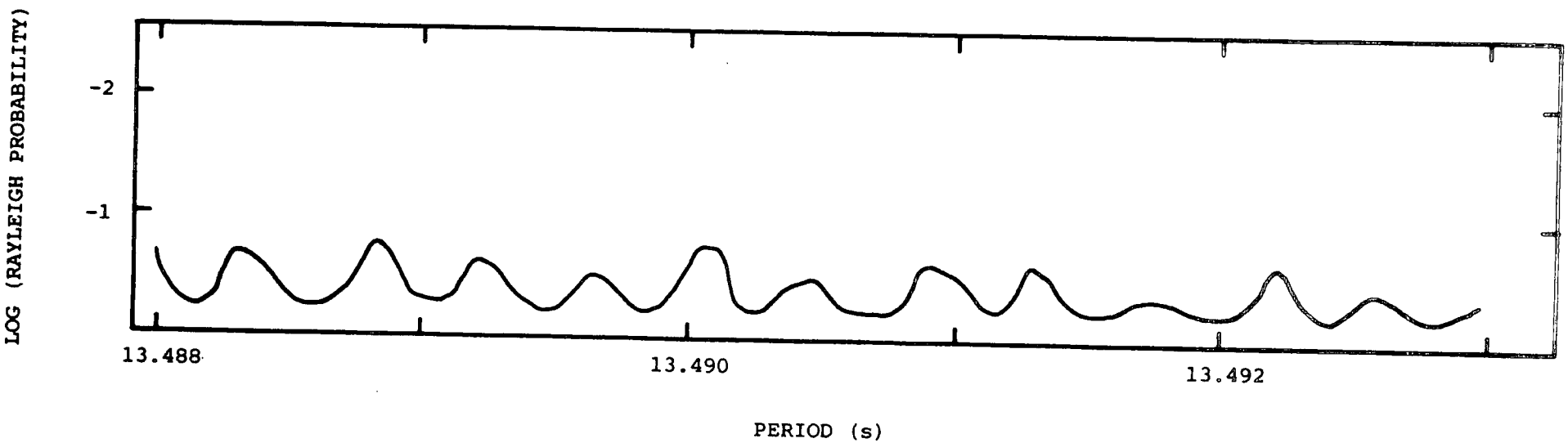

Figure 8.5 The Rayleigh probability of chance occurrence plotted against trial period for LMC X-4 data taken near the minimum of the X-ray cycle (phase 0).

compares very favourably with the predicted period of 13.491 ± 0.003 s derived from the earlier X-ray measurements. The Rayleigh probability of the effect arising by chance is 8.5×10^{-5} (this does not take into account those nights near the minimum of the X-ray cycle which do not show periodicity). The peak flux (i.e. the flux observed in the data taken around X-ray maximum only) is estimated to be $(2.0 \pm 0.8) \times 10^{-10}$ cm^{-2} s^{-1} at E > 250 GeV. When averaged over observations at all phases in the 1.4 day cycle, this gives a time-averaged flux of $(7 \pm 3) \times 10^{-11}$ cm^{-2} s^{-1}. These fluxes correspond to a peak V.H.E. luminosity of $(2.1 \pm 0.8) \times 10^{37}$ erg s^{-1} and an average luminosity of $(7 \pm 3) \times 10^{36}$ erg s^{-1}. This is an exciting result obtained early in the life of the Narrabri experiment, but further confirmatory measurements are needed which will not be available until August 1987, when the source is again visible from Narrabri.

8.6.2. The Vela Pulsar

8.6.2.1. Research Background

The Vela pulsar was discovered in 1968 during the course of a Southern pulsar search made at the Molongolo Radio Observatory (Large et al., 1968). It has a short period (89 ms) and a large period derivative (10^{-13} ss^{-1}). Coupled with its association with a supernova remnant, these suggest that the Vela pulsar is a young pulsar, with an age of approximately 10^4 years. Uhuru observations

revealed an X-ray source near the position of the pulsar which was designated 4U0833-45, but the timing resolution of the satellite was insufficient to allow the detection of any 89 ms periodicity (Kellogg et al., 1973). Later observations led to detections of low significance or to upper limits which were inconsistent with the earlier detections, and X-ray pulsations from the Vela pulsar remain to be conclusively proved (Harnden and Gorenstein, 1973; Ricker et al., 1973; Moore et al., 1974; Pravdo et al., 1976; Zimmerman, 1979). Observations in the γ-ray range were more successful, the first detections of pulsations being made by the SAS 2 satellite at energies > 35 MeV (Thompson et al., 1974). Verifications of these observations by COS-B extended the measurements to 3 GeV and showed the Vela pulsar to be the brightest γ-ray source in the sky (Bennett et al., 1977). Optical pulsations were later observed, suggesting the object is similar to the Crab pulsar (Wallace et al., 1977; Peterson et al., 1978). The radio emission shows a single peak, similar to that observed from other pulsars. The light curves at optical and γ-ray energies, however, have two peaks which are delayed with respect to the radio pulse. To date, two groups have made V.H.E. γ-ray observations of the Vela pulsar. These are described below.

The first attempt to observe V.H.E. γ-rays from the Vela pulsar was made by Grindlay et al., (1975). Early data, taken in 1972, were analysed at the radio period and added together in phase. The resulting light curve shows a peak approximately 4σ above the mean

of all data and about 3 ms early with respect to the radio phase. However, the significance of the effect is only 3σ as its probability must be multiplied by 30 to take into account the number of phase bins in which the peak could occur. The corresponding flux at $E > 3 \times 10^{11}$ eV is $(1.0 \pm 0.33) \times 10^{-11}$ cm^{-2} s^{-1}, which the authors consider to be an upper limit. Data taken a year later showed a similar effect (although this time at the radio phase), and the upper limit derived at $E > 5 \times 10^{12}$ eV is $(7 \pm 3) \times 10^{-13}$ cm^{-2} s^{-1}.

Measurements of the Vela pulsar were made from 1978 to 1985 by the Tata Institute group working at Ootacamund in India at energies between approximately 4.7 and 11.8 TeV (Bhat et al., 1980; Gupta et al., 1982; Bhat et al., 1986, 1987). All the data obtained were analysed at the radio period and, while there is some evidence of time variability (no signal was observed in 1979-80), the resulting phasograms which have absolute phase information show a weak double pulse structure with phases separated by 0.45 of a period, with the first pulse coinciding with the expected position of the optical first pulse. The statistical significiance of this signal improves when lower energy showers only are chosen. If this cut is applied to a subset of the total data from all years, which are subsequently combined, the resultant phasogram shows two peaks at the 4σ and 1.5σ level. Allowing for certain degrees of freedom, the probability that these peaks are due to statistical fluctuations is 8.0×10^{-4}. From the excess events observed at the various

different energy thresholds employed, the integral photon flux received from the source was calculated and is shown in figure 8.7. The estimate of the slope of the integral spectrum at V.H.E. γ-ray energies is $-(1.8 \pm 0.2)$.

8.6.2.2. Data and Results

The Mark III telescope has now taken 40 hours of data on the Vela pulsar, yielding about 60,000 events in the on-axis channel. The observations were made during late January and early February of 1987. The weather conditions were good for the majority of that time, and all four detector channels of the telescope were fully operational providing generous off-source monitoring and full sensitivity enhancement capability.

The analysis followed the usual process. The event arrival times were reduced to the Solar System barycentre, and the sensitivity enhancement procedure described in section 8.5 was applied to the data. Each night was then analysed separately at the local radio period deduced from the radio ephemeris shown in table 8.8 which was supplied by C. Flanagan of the National Institute for Telecommunications Research, Johannesburg (Flanagan, private communication, 1987). The individual light curves were then combined to produce the light curve shown in figure 8.6. It is clear from this that there is no evidence for γ-ray emission from the Vela pulsar at the period defined by the radio ephemeris. The 3σ upper limit to the flux is 6×10^{-11} cm^{-2} s^{-1} at E > 250 GeV. This result is compared to other

R.A. (1950.0)	128.4138
Dec. (1950.0)	-45.00286
PERIOD (s)	0.089278366196
PERIOD DERIVATIVE (ss^{-1})	$0.1244575 \times 10^{-12}$
SECOND DERIVATIVE (ss^{-2})	0.315×10^{-23}
EPOCH (MJD)	46820.00000038449

Table 8.8 The radio ephemeris of the Vela pulsar used for the analysis described in section 8.6.2.2 (Flanagan , private communication).

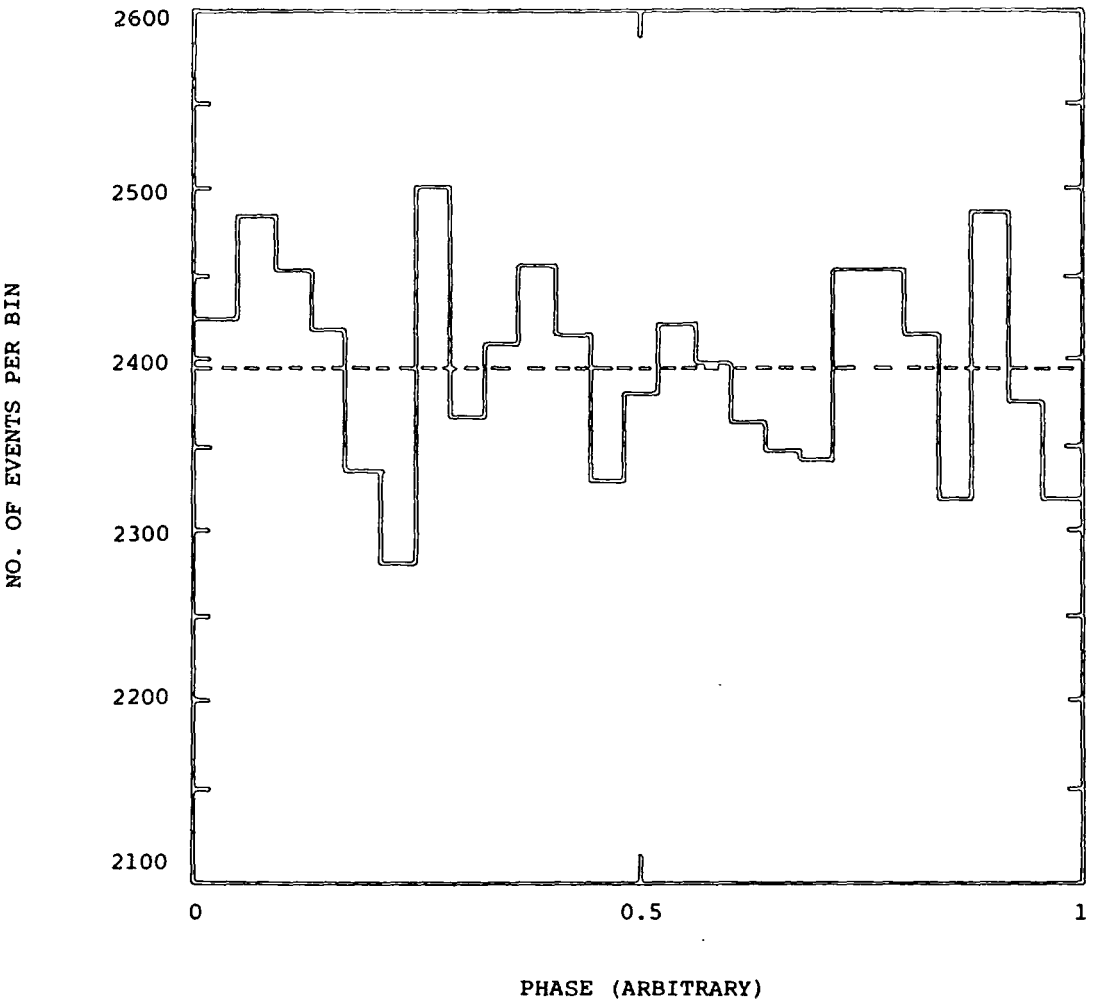

Figure 8.6 The V.H.E. gamma ray (E > 250 GeV) light curve of the Vela pulsar at the trial period defined by the radio ephemeris.

V.H.E. γ-ray measurements and upper limits in figure 8.7. It is not consistent with the integral spectrum as extrapolated from the results of Bhat et al., or the COS-B extrapolated spectrum, but is consistent with the upper limit established by Grindlay et al., a measurement which was made at energies much closer to the threshold of the Mark III telescope.

8.6.3. Centaurus X-3

8.6.3.1. Research Background

On May 18th 1967, a rocket payload which was mainly designed to observe Sco X-1 identified two X-ray sources in the constellation of Centaurus, Cen X-2 and Cen X-3 (Chodil et al., 1967). Pulsations with a period of 4.8 seconds were later detected from Cen X-3 in observations made with the Uhuru satellite (Giacconi et al., 1971). Shortly afterwards, the eclipsing binary nature of the source became clear, the orbital period being 2.1 days (Schreier et al., 1972). The early identification of the companion star with an O-type giant and determination of the orbital parameters (including the mass of the neutron star) made this system the prototype massive X-ray binary (Krzeminki, 1974; Avni and Bahcall, 1974; Bahcall and Bahcall, 1974). The source also appears to alternate between high and low states over a timescale of months, with occasional emission during eclipse (Schreier et al., 1976; Schreier et al., 1972).

The average decrease of the pulsar period was discovered in the

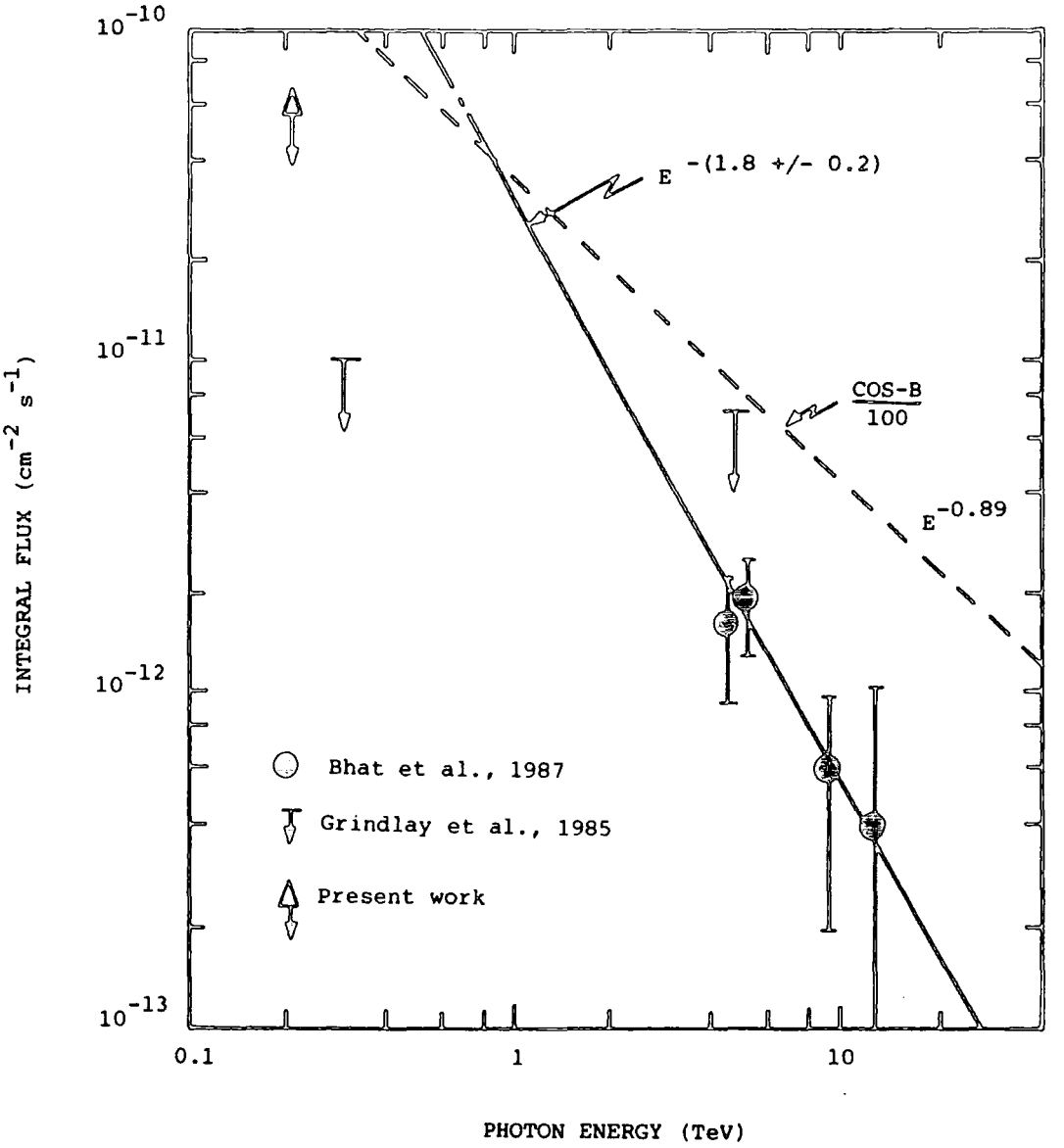

Figure 8.7 The V.H.E. gamma-ray energy spectrum of the Vela Pulsar (after Bhat et al., 1987).

analysis of 2 years of data collected by the Uhuru satellite, a base line which was extended by a measurement made with Ariel V (Gursky and Schreier, 1975; Tuohy, 1976). In general, the pulsation period decreases with a fractional change of the order of -3×10^{-4} yr^{-1}. However, the pulse period derivative is not constant, as is clearly shown in figure 8.8. In August-September 1972, a continuous transition of the pulse period from speedup to slowdown was observed, in addition to smaller variations on short timescales (Fabbiano and Schreier, 1977). In 1976, observations made with the COS-B satellite revealed a spin-up episode (Van der Klis et al., 1980). Later observations made with HEAO 1 showed an average fractional pulse period derivative of -7.6×10^{-5} yr^{-1}, a factor of 4 to 7 less than previously observed (Howe et al., 1983). Correlated observations of pulse period and X-ray intensity included the detection of a high-intensity state during which the pulse period was (on average) increasing, followed by the detection of a transition between spin-down and spin-up episodes coinciding with a rapid decrease in X-ray intensity. It may be noted in passing that a similar behaviour, i.e. small variations in pulse period over short timescales, is observed in Hercules X-1.

The orbital period of Cen X-3 also shows variation. The early Uhuru observations indicated that the binary period of the system was decreasing at a mean fractional rate of $-(8 \pm 4) \times 10^{-6}$ yr^{-1} (Schreier et al., 1973). There was also evidence for a short term increase in the orbital period in 1972 at a fractional rate of

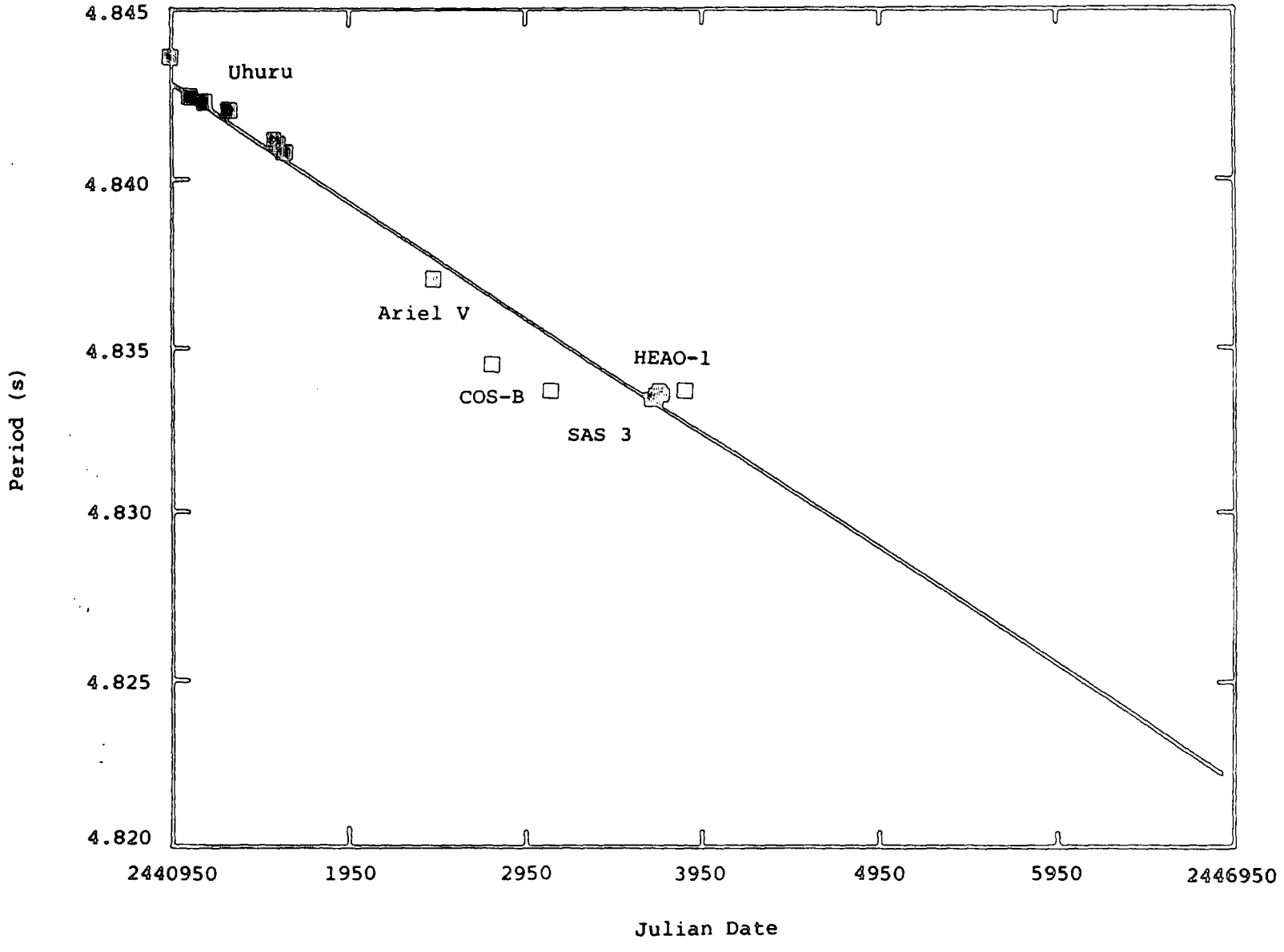

Figure 8.8 The variation in X-ray pulse period of Centaurus X-3.

5×10^{-4} yr^{-1} (Fabbiano and Schreier, 1977). SAS 3 observations showed the orbital period to be decreasing with an average period derivative of -1.8×10^{-6} yr^{-1} (Kelley et al., 1983). There were, however, significant fluctuations about a smooth, linear decrease.

8.6.3.2. Data and Results

Initial observations of Cen X-3 were made with the Mark III telescope in January and February of 1987. This totals 26 hours of data taken in generally good weather conditions. Of these data, approximately half were taken at or near X-ray maximum (i.e. phase 0.5-0.75, c.f. Cygnus X-3) as defined by the orbital ephemeris of Kelley et al. (1983). Errors on the predicted orbital phases are estimated to be ± 4%.

The known variability of the pulse period coupled with the lack of any recent measurements makes the prediction of a precise pulse period for the duration of the observations made by the Mark III telescope difficult. However, a period of approximately 4.823 ± 0.004 sec would be expected in January 1987 on the basis of a least squares' fit to the X-ray measurements available, though this estimate should be treated with some caution.

The data have been formatted and the event times reduced to the Solar System barycentre in the usual way. In addition, they have been reduced to the focus of the binary orbit using the orbital ephemeris given in table 8.9.

Initially, the data from January and February were split into

asin(i)	39.636 +/- 0.003 lt. sec.
Orbital period	2.087097 +/- 0.000008 days
Epoch (JD)	2443870.38910 +/- 0.00002
Periastron angle	90^{o}
Orb. period deriv.	$-(1.8 +/- 0.1)\ yr^{-1}$

Table 8.9 The orbital parameters of Cen X-3 (Kelley et al., 1983).

two datasets, one near X-ray maximum and the other near eclipse, and combined without use of phase information in order to test them for periodicity using the Rayleigh test at periods between 4.8 to 4.84 seconds. This wide range takes into account any possible variations in the pulse period between 1978 and 1987. This procedure revealed evidence for periodicity at 4.815 ± 0.002 sec with a Rayleigh probability of 8.6×10^{-2} in the on-source data taken around X-ray maximum (after correcting for the number of degrees of freedom used in searching between 4.8 and 4.84 seconds). While not of overwhelming statistical significance, this was sufficiently encouraging to initiate further analysis at the candidate period. The same selection of data (i.e. on-axis data from the nights around X-ray maximum only) was thus merged in phase, and analysed over a much shorter range of periods. One problem encountered here was the value of pulse period derivative to be applied to the data. While the general trend of the X-ray results is to show a period derivative of approximately -4×10^{-11} ss^{-1}, individual X-ray observations show significantly different period derivatives, varying between $+2.4 \times 10^{-10}$ ss^{-1} and -3.6×10^{-10} ss^{-1} (Howe et al., 1983). It was decided to search the data over a range of independent period derivatives between -3.0×10^{-11} ss^{-1} and -3.0×10^{-10} ss^{-1} at periods between 4.8150 and 4.8151 seconds. This, of course, assumes the pulsar is spinning up during the observation. The periodic effects on each night require the relatively large period derivative of $-(2.92 \pm 0.03) \times 10^{-10}$ ss^{-1}. The probability distribution at this value of the period derivative is shown in figure 8.9. There is evidence for

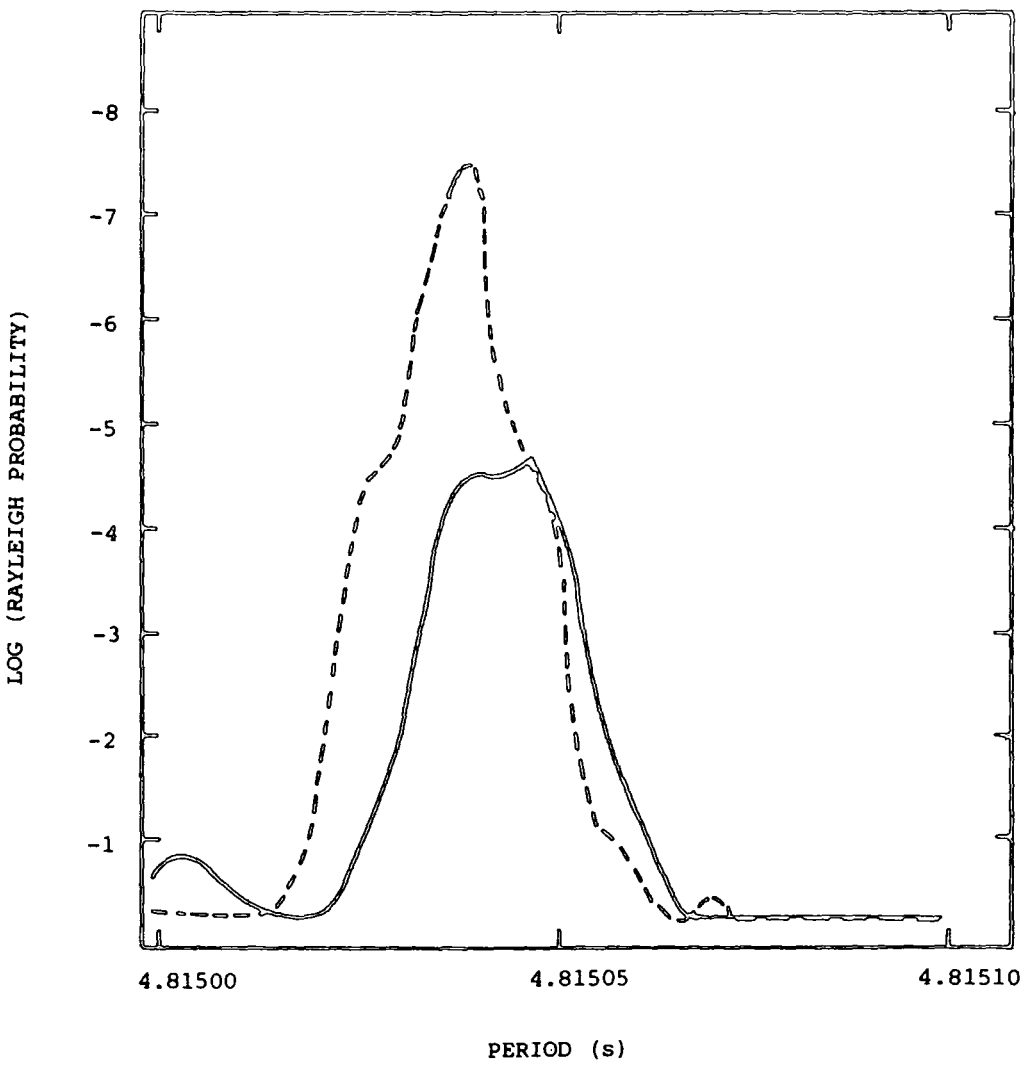

Figure 8.9 The Rayleigh probability of chance occurrence plotted against trial period for data from Centaurus X-3 taken around X-ray maximum (phase 0.5-0.7). The dotted line shows the improvement afforded by use of the guard ring signal enhancement technique.

periodic content in the data at a period of 4.815035 ± 0.000007 seconds. The true significance of this effect is difficult to assess: taking into account the degrees of freedom used in searching both in period and period derivative, the Rayleigh probability of this effect occurring by chance is approximately 10^{-3}. The light curve at this period is shown in figure 8.10. As has been mentioned in section 8.5, the use of the guard ring technique, which was under development at the time of this analysis, results in a significant decrease in the Rayleigh probability of chance occurrence of this effect, and although to be conservative this improvement has been ignored, the resulting probability distribution is shown in figure 8.9. The off-axis data, and the data which were taken near X-ray minimum were analysed in the same way and do not show any similar periodic content as can be seen in figures 8.11 and 8.12.

8.6.3.3. Conclusions and Future Requirements

In conclusion, there is evidence at a Rayleigh probability of approximately 10^{-3} for periodicity at a period of 4.815035 ± 0.000007 seconds. The period derivative is $-(2.92 \pm 0.03) \times 10^{-10}$ ss^{-1}. This effect has a signal strength of 2.3% of the cosmic ray background, which corresponds to a flux around the maximum of the X-ray cycle (i.e. ϕ = 0.5-0.7) of $(1.5 \pm 0.6) \times 10^{-10}$ cm^{-2} s^{-1} at E > 250 GeV. When averaged over the whole orbit this becomes $(6.8 \pm 2.7) \times 10^{-11}$ cm^2 s^{-1}, corresponding to a time-averaged γ-ray luminosity of approximately 7×10^{36} ergs s^{-1}. The candidate period is rather

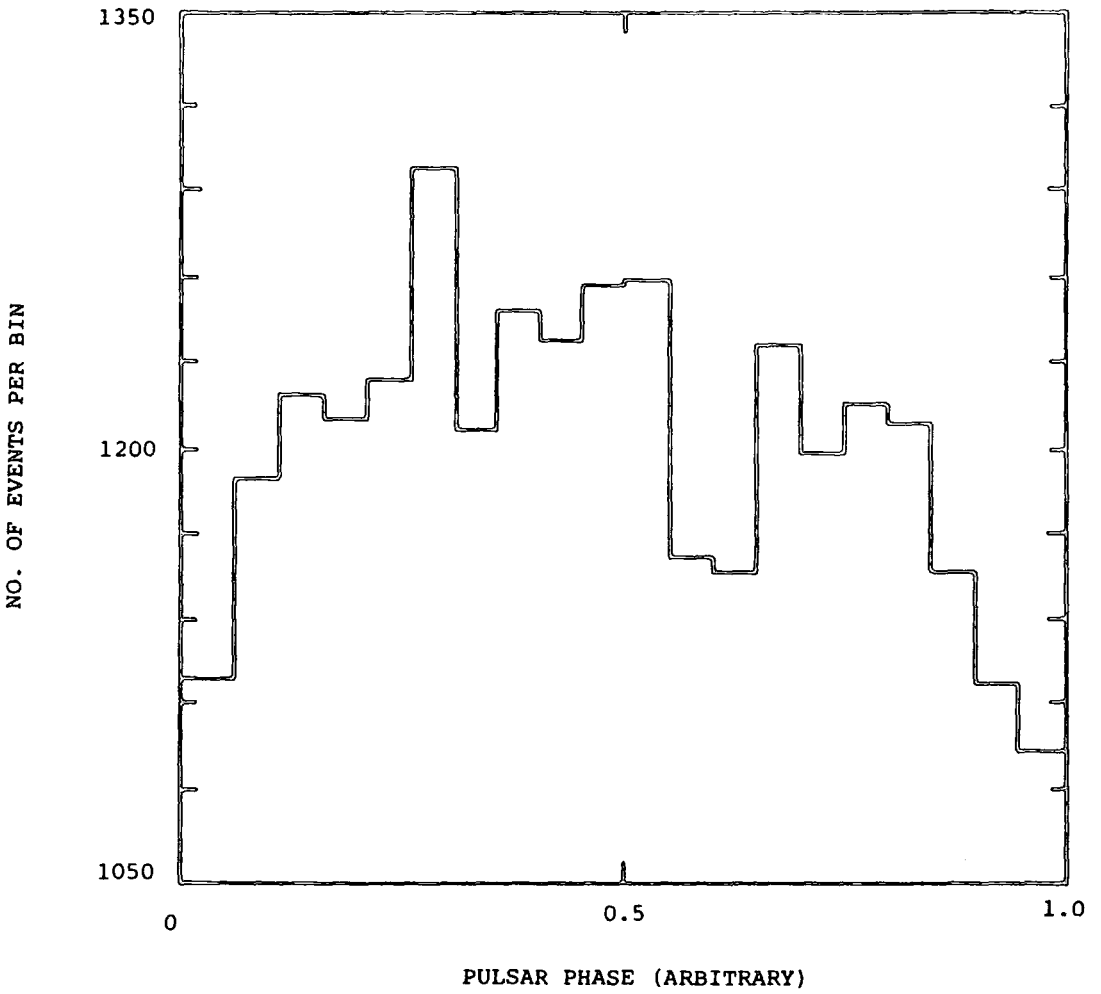

Figure 8.10 The light curve for V.H.E. gamma ray emission from Cen X-3 at a trial period of 4.815035 s. The guard ring sensitivity enhancement technique has not been applied.

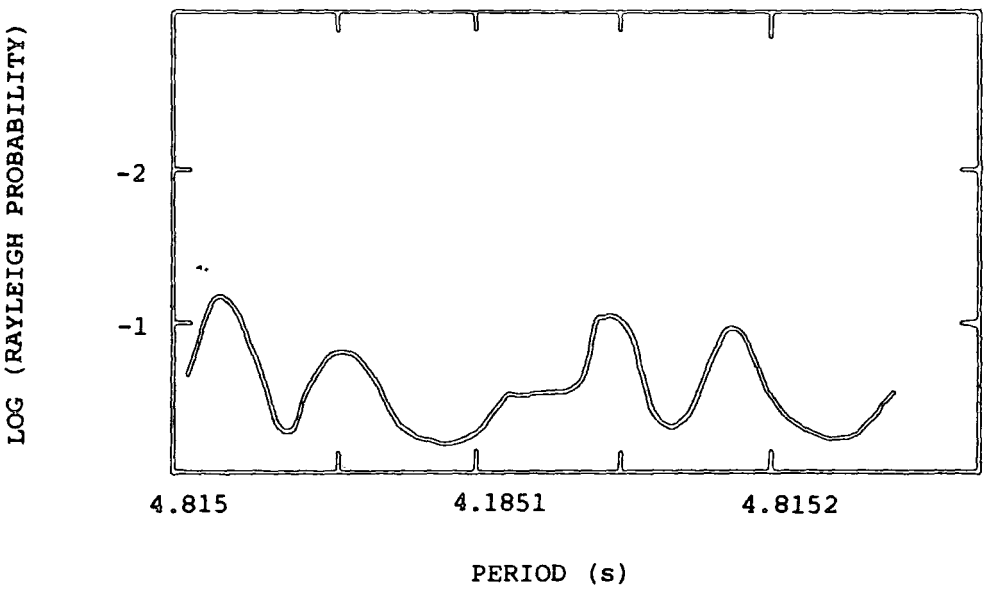

Figure 8.11 The Rayleigh probability of chance occurrence plotted against trial period for off-axis data taken simultaneously with the data shown in Figure 8.9.

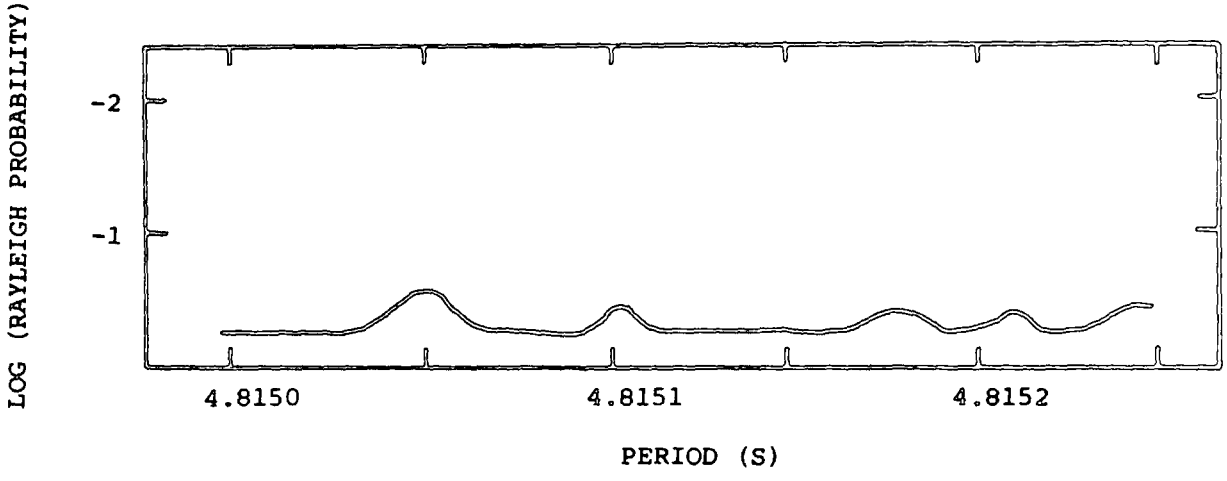

Figure 8.12 The Rayleigh probability of chance occurrence plotted against trial period for Centaurus X-3 data taken near the minimum of the X-ray cycle (phase 0).

shorter than would be expected from the more recent X-ray measurements, but in view of the past fluctuations of the Centaurus X-3 pulsar period and period derivative and the lack of any X-ray measurements in the last 8 years, this may not be surprising.

This source presents some difficulties in analysis due to the uncertainty in the contemporary X-ray period. However, use of the candidate γ-ray period will enable a more accurate prediction of the period to be made for the future data, provided the object is well-behaved. This is required to confirm or deny the above result.

8.6.4. Supernova 1987A

8.6.4.1. Research Background

On 24th February 1987, the exciting discovery was made of a supernova only 50 kpc distant in the Large Magellanic Cloud (Madare and Kunkel, 1987). The object was initially identified in a plate taken at the Las Campanas Observatory in Chile, and was also visible to the naked eye. It was apparent from the study of photographic plates taken on preceding nights that the supernova was first observable on the 23rd February. In addition, two bursts of neutrinos from the direction of the supernova were observed on the 23rd February (Hirata et al., 1987). Soon after its discovery, the search for the progenitor star of the supernova was undertaken. The positional coincidence between a blue supergiant, Sanduleak 69 202, and the supernova gave rise to the suggestion that this was the

progenitor star (McNaught, 1987). Further investigation of photographic plates showed 3 stars to be present within 3 arcs of the supernova position (West et al., 1987). However, spatial and spectroscopic information from data taken with the IUE satellite demonstrate that Sk 69 202 can no longer be detected, and that the other two stars in close proximity are still present (Gilmozzi et al., 1987). This is the closest supernova to the Earth to be observed in modern times and it has understandably been the focus of a large number of observations in all regions of the electromagnetic spectrum.

The calculation of the expected photon flux from the supernova requires a knowledge of the energy spectrum of the progenitor protons and electrons and of the environment in which they propagate after acceleration, especially the form and magnitude of the magnetic field. The acceleration of particles to sufficiently high energy to produce V.H.E. and U.H.E. γ-rays is unlikely to occur in the supernova shock wave itself as a significant fraction of the expanding shell is not converted into relativistic particles until after the shock front slows down, a few thousand years after the initial explosion (Legage and Cesarsky, 1983). Any V.H.E. and U.H.E. γ-rays detected early in the life of the supernova remnant are therefore likely to be the result of the acceleration of particles by a young pulsar. Calculations based on a pulsar wind model suggest that the supernova will produce observable signals in the V.H.E. and U.H.E. γ-ray regions if the spin period of the resulting pulsar is < 10 ms

(Gaisser et al., 1987). The variation in luminosity of the supernova with time suggests that an embedded pulsar may already exist (Shigeyama et al., 1987). However, observations of V.H.E. γ-rays produced close to the pulsar may be difficult, as they will be absorbed by the radiation in the supernova ejecta. This effect should decrease as the column density of the supernova remnant falls, a few years after the supernova explosion (at which time the new radio pulsar should also be detectable).

An alternative model for the supernova has been suggested in which the progenitor star was in fact a close binary companion of Sk 69 202. A significant fraction of massive stars are found in binary systems (Fabian et al., 1987). This model predicts that Sk 69 202 will reappear within the next year or so as the photosphere of the supernova remnant shrinks. If the binary system remains bound, the supergiant will be found in an eccentric orbit and the system will evolve into a massive X-ray binary similar to 4U1223-62 or 1E1145.1-6141. At present, the best opportunity for observing any pulsar left by the explosion is considered to be as a rotation-powered Crab-like X-ray pulsar similar to PSR0540-693, as radiation at longer wavelengths be absorbed within the supernova remnant.

8.6.4.2. Data and Results

On the 23rd February from 10:00 U.T. to 12:30 U.T. observations were being made with the Mark III telescope of a pulsar in the Large Magellanic Cloud, PSR0540-693. As can be seen from figure 8.13, the

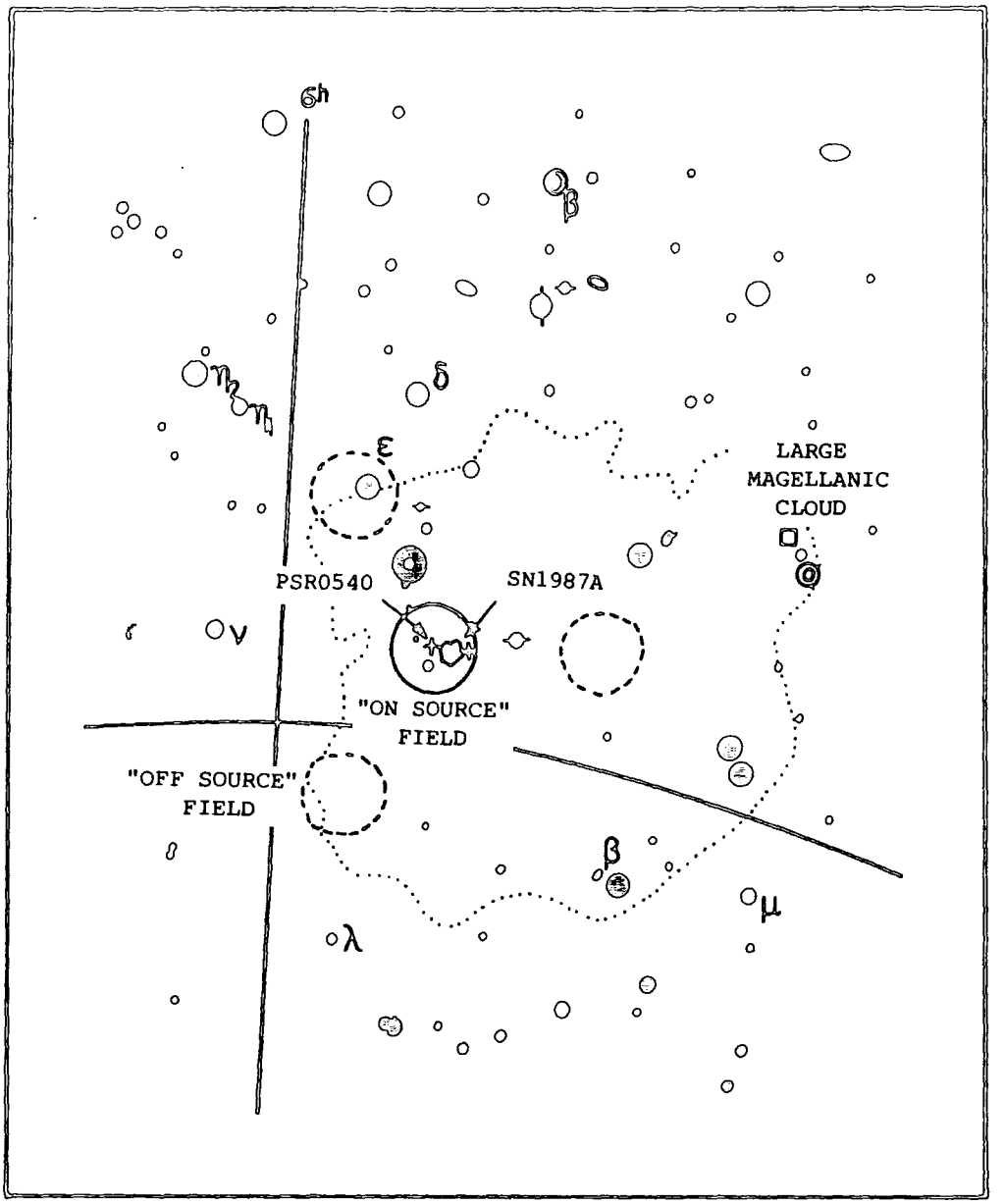

Figure 8.13 Star map to show the position of the Mark III telescope's "on-source" field of view with respect to SN1987A while tracking observations are being made of PSR 0540-693.

supernova was just within the "on-source" field of view of the telescope while the pulsar was being tracked. Neutrino observations suggest that the supernova occurred sometime between 03:00 U.T. and 07:35 U.T. on the 23rd February. Observations of the same region were made on three subsequent nights, and also prior to the 23rd, so by an extraordinary example of serendipity at work in astronomy, V.H.E. γ-ray data from both before and after the supernova explosion are available for comparison. It should be noted, however, that the weather during this period was not ideal, there being intermittent cloud for much of the time.

Since it is very difficult to search for an unknown pulsar period in V.H.E. γ-ray data (see section 5.6), and it is in any case unlikely that a pulsar would be detectable so soon after a supernova, it is necessary to search the data for a D.C. γ-ray flux. The strategy adopted has been to compare the ratio of ON source to OFF source counts for data taken before and after the supernova. Bearing in mind that there are three OFF source channels and one ON source channel, it is found that the ratio ON/OFF before the supernova is 0.311 ± 0.005 and after the explosion 0.29 ± 0.015. It is therefore concluded that there is no evidence for V.H.E. γ-ray emission from SN1987A in this data, corresponding to a 3σ flux limit of approximately 1×10^{-10} cm^{-2} s^{-1} for the 2 days after the detection of the supernova.

A single long observation of the supernova remnant was also made on 22nd March 1987 in good weather conditions. This was the last

opportunity for observations of the object before October, when it is again visible from Narrabri. These data were taken in the "chopping" mode (see section 7.10.3), with data being taken for 5 minutes at a time with the supernova in the central channel followed by 5 minutes with it centred in one of the off-axis channels. The simplest way to search for a V.H.E. signal from the supernova remnant is to test the data from each channel separately for a 5 minute periodicity caused by any excess counts from the supernova remnant moving between the central channel and one of the off-axis channels. No such periodicity was observed and it is therefore concluded that there is no evidence for V.H.E. γ-ray activity at $E > 250$ GeV in these data. The flux limit derived from this observation is 2.5×10^{-10} cm^{-2} s^{-1} approximately 27 days after the supernova.

8.6.4.3. Future Observations

The observations described thus far have been made largely as a result of good fortune and have not in general been specific attempts to observe V.H.E. γ-rays from the supernova remnant. The latitude of Narrabri is such that SN1987A reaches its greatest distance above the horizon (a zenith angle of 40°) during the months of November to January. The low count rate of the telescope (40-45 c.p.m.) at this zenith angle requires that extensive observations be made in order to detect a signal from the object. For example, 9 hours' observation of the supernova at its minimum zenith angle would result in

approximately 22000 on-axis events. A V.H.E. γ-ray signal of 3% of the cosmic ray background would give a maximum likelihood test probability of 0.16 in a dataset of comparable size. A similar dataset taken near the zenith would yield 40500 events and, if the ON-source channel also contained a γ-ray signal of 3% of the cosmic ray background give a maximum likelihood probability of chance occurrence of 3.4×10^{-2}. This emphasises the importance of a carefully planned observing programme to ensure that objects are observed as close to the zenith as possible. It is intended to undertake an extensive program of observations during October-January 1987/8, about 300 days after the explosion. The target is to take approximately 100 hours of data giving approximately 200,000 events and a 3σ flux limit of 1.6×10^{-11} cm^{-2} s^{-1}.

CHAPTER 9

DISCUSSION OF RESULTS AND FUTURE WORK

9.1. Introduction

This chapter contains a broad overview of the present understanding of V.H.E. γ-ray emission from isolated pulsars and X-ray binary systems. It is followed by a description of improvements which are being made to the Mark III telescope and an outline of the Mark IV telescope which is now nearing completion. The chapter concludes with a discussion of the future possibilities for both telescopes and of the field of V.H.E. γ-ray astronomy as a whole.

9.2. V.H.E. γ-rays from Isolated Pulsars

At present, the only isolated pulsar from which V.H.E. γ-rays have been observed by more than one research group is the Crab pulsar. The data obtained at Dugway show particularly good evidence for the emission of V.H.E. γ-rays from the Crab pulsar, with the γ-ray emission occurring at the same phase as the radio pulse and with precisely the same period (see section 6.6.1). The 1.5 ms pulsar, PSR1937+21 and the pulsar candidate PSR1802-23 (period 112 ms) both appear to emit V.H.E. γ-ray radiation, but these results have yet to be confirmed (Chadwick et al., 1987; Raubenheimer et al., 1986). There are conflicting results from observations of the Vela pulsar (see section 8.6.2). Early reports of the detection of

V.H.E. γ-rays from PSR0950+08 and PSR1133+16 were not confirmed (Gupta et al., 1978; Bhat et al., 1980; O'Mongain et al., 1968; Charman et al., 1968; Chadwick et al., 1985a).

The processes by which γ-rays may be generated in the pulsar magnetosphere include curvature radiation, synchrotron radiation and Compton scattering (see section 1.2.4). These mechanisms require the presence of energetic particles, electrons being probable candidates for the progenitors of V.H.E. γ-rays. The identification of the site of electron acceleration (and hence γ-ray generation) is difficult: it must be close enough to the pulsar for acceleration to occur in the high magnetic field, but not so close that the γ-rays cannot escape due to pair production. It is therefore considered that particle acceleration and subsequent γ-ray production occurs in the outer gaps (Holloway, 1973; Cheng et al., 1976; Arons, 1981). These are the regions between the open and closed magnetic field lines associated with the pulsar. Such regions are sufficiently far away from the neutron star surface to enable some of the γ-rays to escape. The voltage drop developed across such outer gaps is proportional to $\Omega^2 B$, where Ω is the angular frequency of the pulsar rotation and B the magnetic field strength. From this standpoint, it is not surprising that all the pulsars from which V.H.E. γ-ray emission has been claimed have periods < 100 ms. On the basis of this criterion alone, PSR1510-59 and PSR0540-693 would be expected to emit pulsed V.H.E. γ-rays (Orford, 1987). Observations of both these objects are being made at present by the Durham group. There

is, however, one caveat which must be added to this generalisation: fast pulsars are expected to emit γ-rays and so more attention has been devoted to them than to the pulsars which rotate less rapidly. It may be that the generation of high energy radiation is not related to the angular velocity of the pulsar, and long period pulsars may also emit V.H.E. γ-rays. While the Durham group did indeed make some observations of longer period radio pulsars, the pressing requirement for making observations of objects such as the Crab pulsar and Cygnus X-3, and the necessary long length of those observations, meant that the derived flux limits for the radio pulsars are considerably above the measured persistent flux of the Crab pulsar. As new, more sensitive telescopes such as the Mark III and IV telescopes become fully operational, it will become less time-consuming to make meaningful observations of pulsars showing a wide range of periods, and it may be possible to establish how rapidly pulsars must rotate in order to emit γ-rays. This is an important parameter in attempts to constrain theoretical models of V.H.E. γ-ray generation in isolated pulsars.

Data from the Crab pulsar taken at Dugway showed some evidence for persistent, low-level emission although given the relatively low sensitivity of the telescopes when much of the data was taken, the possibility that this low-level emission may occur in multiple small bursts cannot be excluded. The 1.5 ms pulsar, PSR1937+21, also seems to show persistent emission, although the low strength of this emission also made any more detailed investigation of its

nature difficult. It may be that pulsars show bursting activity in addition to a weak but persistent emission, or that bursts are the only form of emission of V.H.E. γ-rays from pulsars. Observations made with the Dugway telescopes showed two outbursts from the Crab pulsar in 1981 and the Tata Institute observed a similar burst lasting 10-15 minutes in 1985 (Gibson et al., 1982; Vishwanath, 1987). Two bursts of activity from the Crab pulsar showing periods consistent with the radio ephemeris were observed in early 1986 by the group working at the Haleakala Observatory (Resvanis et al., 1987c). Possible time-variability of the γ-ray emission from the Vela pulsar, a phenomenon which has been suggested before (Gupta et al., 1982), may explain the present conflicting results. The claim for the detection of V.H.E. γ-rays from PSR1802-23 also involves transient emission: six episodes of activity of between 10 and 50 minutes duration were observed over a period of one month (Raubenheimer et al., 1986). This variability is not seen at longer wavelengths and implies that there may be some differences in the emission mechanisms at high energies. This may also be deduced from the energy spectra of the Crab and Vela pulsars. Despite some confusion in the case of the Vela pulsar, it is not clear that the energy spectrum in the V.H.E. γ-ray region is not a continuation of the spectrum at lower energies. A possible mechanism for the production of transient V.H.E. emission could be a small instability in the pair production occurring in the outer gap. V.H.E. γ-ray production is very sensitive to the magnitude

of the local magnetic field, and the absorption of γ-rays is sensitive to small variations in the flow of low-energy secondary photons. The energy spectrum may be very steep above 1 TeV, with an inverse Compton cut-off at approximately 6 TeV. Small variations in this cut off energy could thus produce large variations in flux above about 1 TeV, without having any effect on the lower energy γ-rays or X-rays.

Finally, it should be mentioned that because of the inevitably low signal:noise ratio of V.H.E. γ-ray observations to date, it is vital that accurate pulsar ephemerides from observations at radio wavelengths are readily available wherever possible. This is especially important in the case of the Vela pulsar which is known to show "glitches" at a rate of one glitch every 2 or 3 years.

9.3. V.H.E. γ-rays from Radio Pulsars in Binary Systems

At present, V.H.E. γ-rays have been detected from only one radio pulsar located in a binary system, this being PSR1953+29 (see section 6.4). The detection of V.H.E. γ-rays with the 6ms period characteristic of the pulsar suggests that PSR1953+29 may be the disputed COS-B source 2CG065+00. With statistics of one, it is not possible to make generalisations concerning this class of object except to note that the light curve is broad, like those of the X-ray binary pulsars rather than those of the isolated pulsars (see figure 6.4). A similar object, PSR1855+09 has recently been discovered as a result of a survey designed to detect fast pulsars carried out at

Green Bank and Arecibo, and a search for V.H.E. γ-rays from this object is being made with the Mark III telescope (Segelstein et al., 1986; Stokes et al., 1986).

9.4. V.H.E. γ-rays from X-ray Binary Pulsars

With the discovery of V.H.E. γ-rays from the Hercules X-1 system and the subsequent detection of V.H.E. γ-rays from the similar object 4U0115+63, X-ray binaries now constitute the single most important class of V.H.E. γ-ray source. Table 9.1 shows the fluxes, luminosities etc., of all X-ray binaries from which V.H.E. γ-ray emission has so far been claimed. (Cygnus X-3 has been included in this list as the evidence suggests that it is probably an X-ray binary pulsar, albeit with a very rapid pulse period). The following points concerning V.H.E. γ-ray emission from X-ray binary systems should be noted:

a) The γ-ray luminosity is a substantial fraction of the Eddington luminosity, and exceeds the X-ray luminosity for short periods. This implies a similarly high cosmic-ray luminosity.

b) The V.H.E. γ-ray emission is pulsed at the neutron star rotation period.

c) The V.H.E. light curves are broad. Figure 9.1. shows the light curves of all claimed V.H.E. γ-ray emitting binaries.

d) The V.H.E. γ-ray emission seems to be related in some way to the X-ray cycle.

OBJECT	DIST. (Kpc)	ORBIT(d)	PULSE PERIOD (s)	PEAK FLUX (10^{-10} cm^{-2} s^{-1})	PEAK LUMINOSITY (10^{36} erg s^{-1})	AVE. FLUX (10^{-11} cm^{-2} s^{-1})	AVE. LUMINOSITY (10^{35} erg s^{-1})	THRESHOLD ENERGY (GeV)
Her X-1	5	1.7	1.24	12	4.5	3	2	1000
Cyg X-3	11	0.2	0.012	3.0	5.56	1.9	3.5	1000
4U0115+63	5	24	3.6	-	-	7	2.7	1000
LMC X-4	50	1.4	13.5	2.0	20	6.8	70.4	250
Cen X-3	8	2.09	4.8	1.5	0.37	7.5	1.8	250
Vela X-1	1.9	8.96	283	-	-	2	0.24	1000

Table 9.1 Characteristics of V.H.E. gamma-ray emitting X-ray binaries.

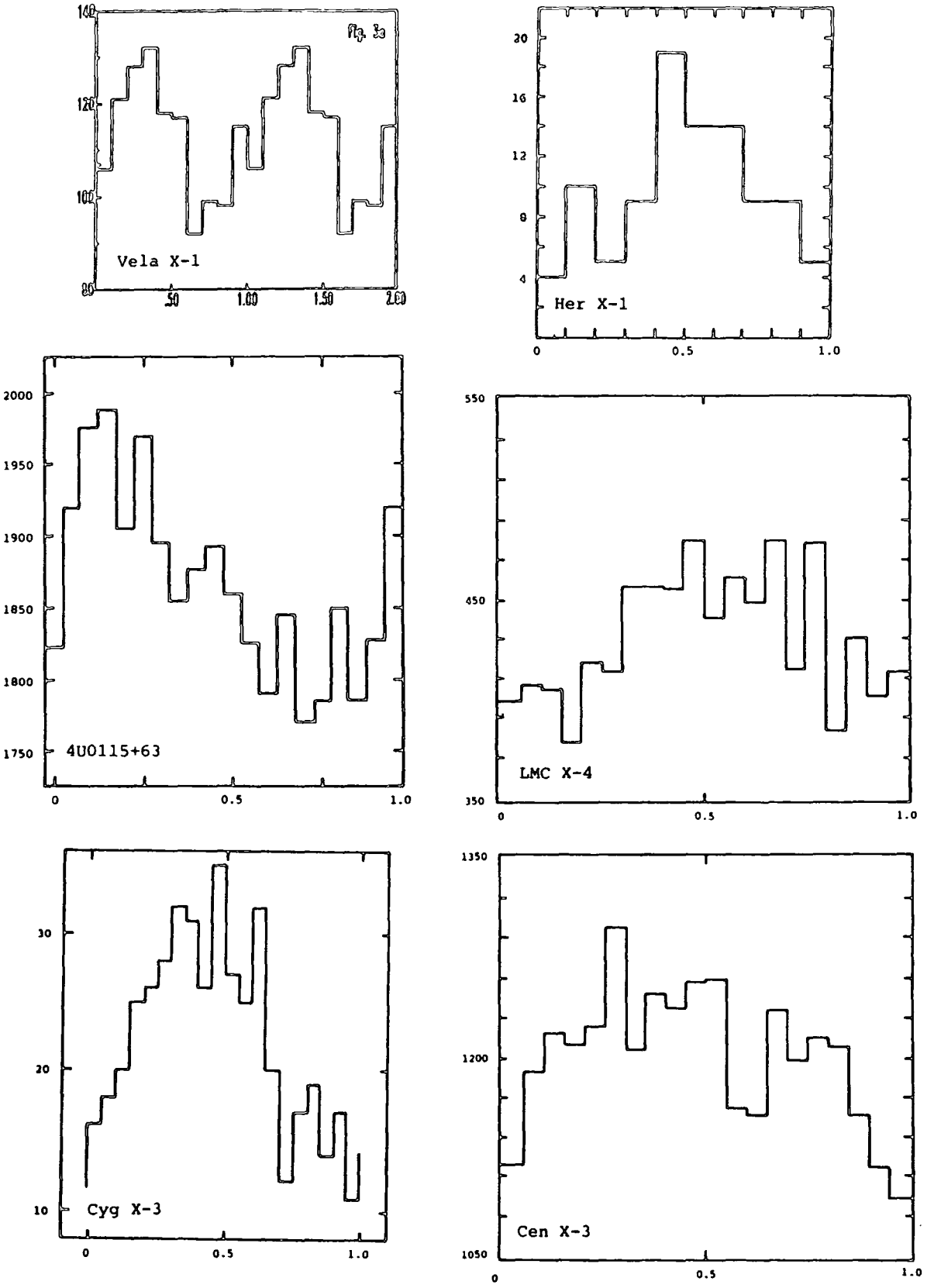

Figure 9.1 The V.H.E. gamma-ray light curves of the six known V.H.E. gamma-ray emitting X-ray binary systems.

e) γ-ray emission may be seen when the neutron star is eclipsed by its companion (Gorham et al., 1986; Raubenheimer et al., 1986).

f) Bursts of pulsed V.H.E. γ-ray activity have been observed from most X-ray binaries from which V.H.E. emission has been claimed.

9.4.1. The Energy Source

The prominence of interacting neutron stars as V.H.E. γ-ray emitters suggests that their energy may be derived from the accretion process in some way. Accretion onto a neutron star is thought to produce a strong shock in which particle acceleration may take place via a mechanism similar to a first order Fermi mechanism. These particles are the progenitors of the observed γ-rays. The maximum energy reached by particles thus accelerated is limited by the energy loss due to synchrotron radiation, and unless the magnetic field strength at the acceleration site is $< 10^{12}$ gauss, this is not sufficient to produce the observed V.H.E. emission (let alone the U.H.E. γ-rays) (Eichler and Vestrand, 1985; Kazanas and Ellison, 1986). Observations of cyclotron lines from Her X-1 and 4U0115+63 imply that these at least have magnetic field strengths $> 10^{12}$ gauss (Trumper et al., 1978; Wheaton et al., 1979). A different mechanism may therefore be required to explain the production of V.H.E. γ-rays in X-ray binaries. The dynamo mechanism, originally proposed for Cygnus X-3 (see section 5.5.3), suggests a different acceleration mechanism whereby the accretion disc

essentially acts as a unipolar inductor. (However, this requires a low magnetic field strength, and may have difficulty explaining the emission observed from Hercules X-1 and 4U0115+63).

The γ-rays themselves (once produced) also suffer absorption in strong magnetic fields due to pair production, so this has lead to the suggestion that the γ-rays are generated by high energy particles (usually protons) which are incident on a target of some sort. This may be the atmosphere of the companion, an accretion wake caused by the interaction of the stellar wind from the companion and the neutron star or knots of matter within an accretion disc (see figure 9.2).

Direct pulsar acceleration mechanisms, similar to those described in section 9.2, have also been proposed for the production of V.H.E. γ-rays. The evidence presented in Chapter 6 suggests that the proposed pulsar in Cygnus X-3 at least may not be accreting matter. Indeed, the jets from Cygnus X-3 which are observed at infra-red wavelengths may be understood in terms of the ejection of matter by a rapidly spinning pulsar (Hillas, 1987). However, these models cannot fit the observed luminosity of binaries with longer pulse periods, such as the Vela X-1 system which has a pulsar period of approximately 5 minutes. They also do not explain why all the observed light curves are broad rather than sharp, as appears to be the case for isolated pulsars.

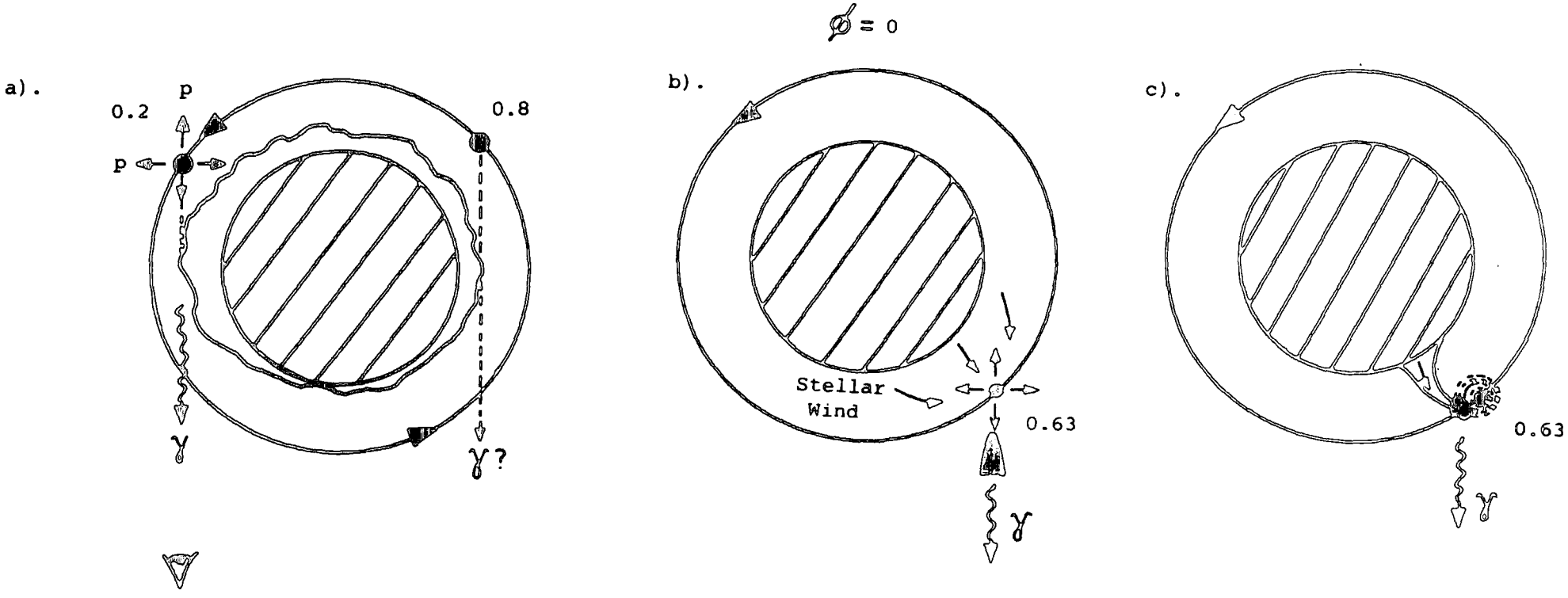

Figure 9.2 Possible gas targets which may appear in the path of isotropically produced protons from the neutron star at given orbital phases. a). The atmosphere of the companion. b). An accretion wake , formed from the stellar wind of the companion. b). Structure attached to the accretion disc (after Hillas , 1987).

9.4.2. The Relationship Between the γ-ray Emission and the X-ray Cycle

The emission of V.H.E. γ-rays appears to be related in some way to the X-ray behaviour of the source. Observations by the Durham group suggest that γ-rays may be emitted around phase 0.5-0.7 by at least three sources: Cygnus X-3, LMC X-4 and Centaurus X-3, where X-ray minimum is defined to be at $\phi = 0$. Others, such as Hercules X-1 are observed to emit γ-rays almost exclusively during the "high" state of the 35-day cycle and may show some preference for emission between phase 0.6-0.8 of the 1.7 day orbital period (Gorham et al., 1987). 4U0115+63 (only observed by the Durham group at phases covering one quarter of an orbit) and Vela X-1 do not seem to show any pronounced orbital modulation (North et al., 1987), but the sporadic nature of the former and the small number of observations of the latter make any comment concerning the phase of emission difficult. If the indications from present observations that γ-ray emission occurs at particular orbital phases are correct, this may be because gas targets (possibly within the accretion disc) are available when the pulsar is at particular places in the orbit.

In addition two sources, Hercules X-1 and Vela X-1, appear to produce γ-rays just after the neutron star has entered eclipse (Gorham et al., 1986; North et al., 1987). This, if correct, may suggest that the γ-ray emission is not associated with the neutron star but with the companion: possibly a "hot spot" is produced in the companion's atmosphere which lags behind the neutron star. It

may be that the directions from which V.H.E. γ-rays are observed may be considerably affected by the presence of a magnetic field (Protheroe and Stanev, 1987). If the protons are indeed being deflected by a strong magnetic field, yet a narrow pulsed beam of γ-rays is seen, the proton beam should be approximately mono-energetic, ruling out a statistical acceleration process (Hillas, 1987).

9.4.3. Bursts of γ-ray Emission

With the exception of the two most recent additions to the list of V.H.E. γ-ray emitting X-ray binaries, LMC X-4 and Centaurus X-3 (where a search for bursting activity has not yet been made) all such sources seem to show bursts of V.H.E. γ-ray emission on short timescales (between 5 and 20 minutes) in addition perhaps to persistent emission. Again, the bursts seem to occur preferentially during periods of X-ray activity. These bursts of V.H.E. γ-ray emission may pinpoint concentrations of gaseous material acting as targets for the production of γ-rays (figure 9.2). Alternatively, they may be connected with spin-down episodes, which are observed in some X-ray binaries such as Centaurus X-3 and Vela X-1. Another mechanism has been proposed by Cohen and Mustafa (1987). They suggest that there is a vacuum near the magnetic poles. Here, charged particles provided by the neutron star surface may be accelerated to extremely relativistic energies by the large component of the electric field along the open magnetic field lines. Pulsed

emission would be observed from the poles if the magnetic moment is not aligned with the rotation axis; bursts of γ-ray emission may be detected by a distant observer if the neutron star is freely precessing. In this case the bursts of V.H.E. γ-rays observed from a given source are expected to be of approximately the same duration. This model can adequately reproduce the observed emission from all the claimed V.H.E. and U.H.E. emitting X-ray binary systems with the exception of LMC X-4 and Vela X-1.

9.4.4. Conclusions

Even a brief consideration of the methods by which X-ray binary pulsars may emit V.H.E. γ-rays underlines the requirement for more observations before an attempt to differentiate between at least some of the suggested models may be made. Further observations are required of the well-established V.H.E. γ-ray binary sources: claimed detections of V.H.E. γ-ray emission during eclipse in particular require further, possibly simultaneous, measurements. There is a need for observations to be made which sample complete orbits as far as possible in order to localise the γ-ray source. Contemporary X-ray ephemerides are important in all cases for the identification of periodicity in γ-ray data; frequently these are unavailable. A greater number of V.H.E. γ-ray binaries must be observed so that meaningful generalisations may be made: for instance, are all X-ray binary pulsars V.H.E. γ-ray emitters, or are only the rapidly rotating pulsars capable of producing high

energy radiation? The observing programme of the Mark III telescope for the next 2-3 years includes scheduled observations of a large number of X-ray binary systems.

Despite the theoretical problems associated with V.H.E. γ-ray emission from accreting binaries, observations of V.H.E. radiation from X-ray binaries now seem well established. It may be that the source of the high-energy cosmic rays within our galaxy has at last been found.

9.5. Improvements to the Mark III Telescope

9.5.1. The Guard Ring Technique

The Guard ring technique for signal enhancement has already proved itself to be extremely valuable, resulting in improvements to the signal:noise (γ-ray to proton) ratio of up to 100% (see section 8.5). The original detector package contained four photomultiplier tubes, three off-axis tubes arranged evenly around one on-axis tube (see section 7.6.1). There are thus considerable gaps between the off-axis PMTs, and information about the light distribution of some of the Cerenkov light spots is lost. Figure 9.3 (a) shows it is possible for a given Cerenkov light spot, which has its centroid in a direction between the on-axis and off-axis channels, to register in the on-axis channel alone. Such events are not rejected by the signal enhancement technique. To obviate this problem, a further three 2" diameter off-axis PMTs have been added

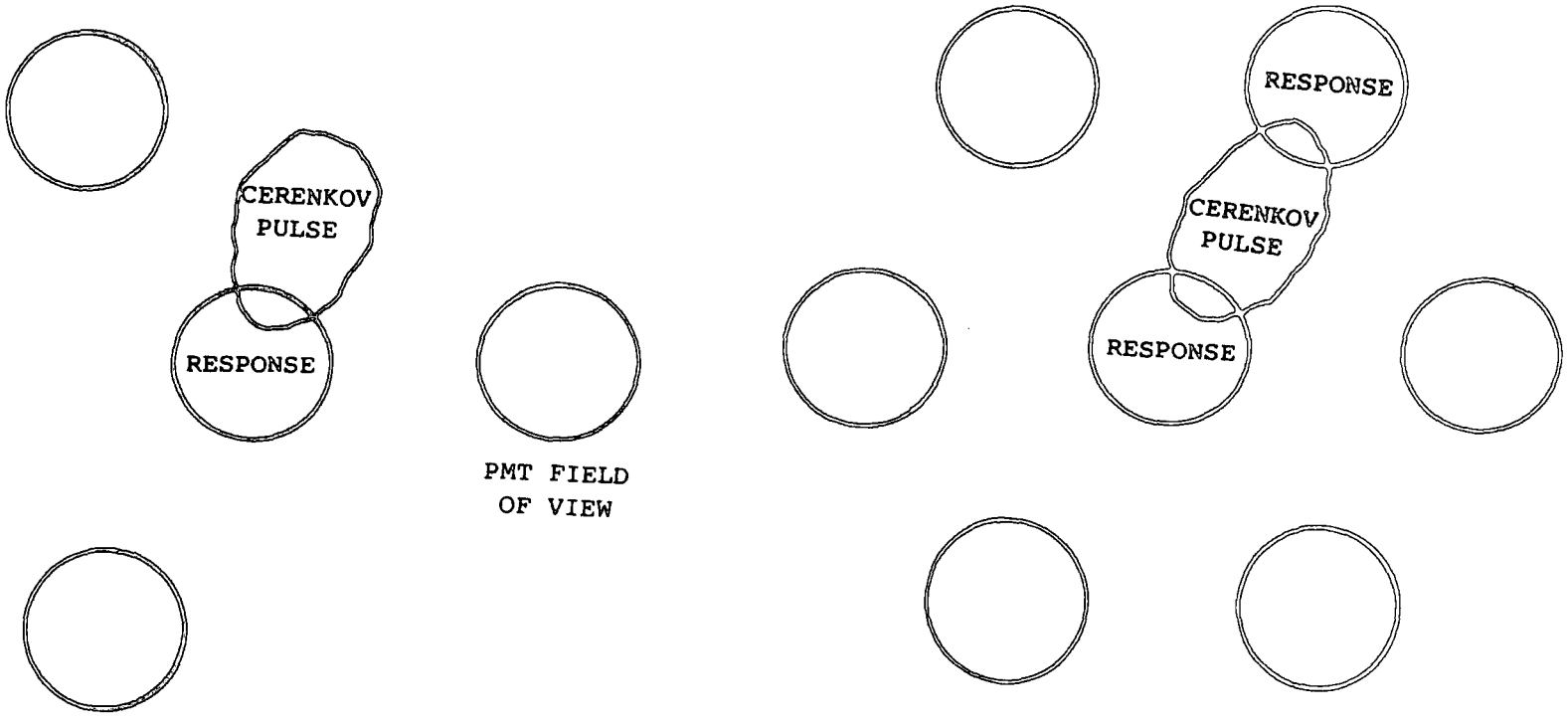

Figure 9.3 Schematic diagram showing the improvement in the guard ring technique of signal enhancement afforded by the use of extra PMTs.

to each detector package, resulting in six off-axis channels completely surrounding one on-axis channel (see figure 9.3 (b)). The design of the telescope monitoring and data logging system is such that the additional data from these PMTs may be accommodated easily. The extra PMTs will enable the rejection of further proton-induced events and an even greater enhancement of any V.H.E. γ-ray signal. Tests on the initial data obtained in July 1987 with these extra off-axis channels in use indicate that the application of the guard ring technique including the new photomultiplier tubes will introduce an additional signal enhancement.

As mentioned in section 8.5, there are indications that the magnitude of the improvement obtained by use of the guard ring technique is dependent on the zenith angle of the object being observed. One possible reason is that the size of the Cerenkov light spot is sensitive to zenith angle. Further investigation of this effect is required together with greater use of the information obtained from the photomultiplier tubes, with a view to a further improvement in the efficiency of this technique.

9.5.2. Improved Telescope Efficiency

Present techniques of mirror manufacture developed by the Durham Group make it possible to construct 100 cm diameter mirrors of better optical quality than those at present used on the Mark III telescope. Deploying 19 of these mirrors on each dish of the Mark III telescope would considerably reduce the amount of "dead

area" due to gaps between mirrors on the existing instrument and could effectively double the telescope's light collecting capability. The count rate would rise to approximately 125 counts min^{-1} per channel and the energy threshold would decrease to 170 ± 80 GeV. The exposure times then required to detect any given object at a specified confidence level would be approximately halved, and the gap between the energy thresholds of ground-based atmospheric Cerenkov detectors and satellite-borne experiments further reduced.

A further possibility is the investigation of the effect of a reduction in geometric aperture of the photomultiplier tube-mirror combination on the efficiency of the telescope. The geometric aperture is at present 0.9^{o} leading to an effective aperture of approximately 1.5^{o} (allowing for the size of the Cerenkov light spot). This aperture has been arrived at in the light of experience with the Dugway telescopes. A further reduction of the telescope's geometric aperture may enable the rejection of more proton-induced Cerenkov pulses and thus increase the signal:noise ratio. Tests will be made in the near future using masks which will be fitted onto the PMT faces to decide if the aperture may be further reduced; if this reduces the number of γ-ray induced Cerenkov flashes recorded as well as those produced by protons, the optimum value for the telescope aperture has been reached.

9.5.3. The Mark III Telescope as a Survey instrument

The Mark III telescope was originally designed in 1983 as a

survey instrument, and this capability has been retained. The addition of extra electronics to allow each channel of recently added PMTs to operate as effectively separate coincidence channels will allow the Mark III telescope to be turned into a survey instrument. This telescope would be capable of sampling an area of sky of approximately 10 square degrees. The count rate of the telescope operated in this way would rise to about 700 c.p.m., but this high data rate would be easily accommodated by the MC 68000 data logger. One problem encountered in using the telescope in this way is that the area of sky sampled in the off-axis tubes would be continually changing due to the rotation of the sky with respect to the PMTs. It may therefore be necessary to incorporate rotation of the detector packages in some way such that the same sections of sky are always viewed by the off-axis channels.

9.6. The Mark IV Telescope

The need for further observations of Cygnus X-3, and indeed for observations of other objects visible in the Northern Hemisphere, has prompted the design of a portable telescope, which will be used initially as a Cygnus X-3 monitor. The telescope is at present nearing completion in Durham and it is planned that it will be deployed in La Palma during Summer 1988 to continue observations of Cygnus X-3. The characteristics of the telescope are summarised in table 9.2.

The Mark IV telescope differs from the Mark III telescope only

DISH AREA	5.1 m^2
APERTURE	40 mm
FOCAL LENGTH	2.54 m
FIELD OF VIEW	0.9^o
REFLECTIVITY	0.8
COUNT RATE (PREDICTED)	44 C.P.M.
THRESHOLD (PREDICTED)	300 GeV

Table 9.2 Characteristics of the Mark IV telescope.

in having smaller (5 m^2) flux collectors and simplified recording electronics. The 19 mirrors deployed on each of the 3 paraxial dishes are of the same type as those used on the Mark III telescope. It will have provision for maintaining constant background light by use of servo-controlled LEDs and simultaneous background (off-axis) measurements in adjacent areas of sky. There will be six off-axis channels arranged around the central on-axis channel in the same way as the improved Mark III telescope described above, thus allowing for full use of the guard ring signal enhancement technique. The telescope will be mounted on an altazimuth mount based on the Mark II telescope mount and will be steered in the same way as the Mark II, utilising DC electric motors and absolute digital shaft encoders. The telescope will have a slightly higher threshold than the Mark III telescope, this being approximately 300 GeV. If a burst of pulsed V.H.E. γ-rays from Cygnus X-3 similar to that detected on September 12th 1983 were to be observed with the Mark IV telescope, it is expected that the 12 ms pulsation would be detected with a Rayleigh probability of 1.6×10^{-15} of chance origin.

9.7. Prospects for the University of Durham Telescopes

The Mark III telescope has, even at this early stage, proved to be a sensitive instrument which is capable of detecting V.H.E. γ-ray sources within a relatively short space of time. It will thus be possible to make meaningful observations of a large number of objects in the Southern Hemisphere in 2-3 years, admitting the

possibility of defining for example how rapidly radio pulsars and X-ray binary pulsars must rotate in order to emit V.H.E. γ-rays. An unprecedented opportunity to observe the possible formation of a pulsar is afforded by the supernova SN1987A, and comprehensive observations are scheduled (see section 8.6.4.3.). The expansion of the telescope into a survey instrument would allow the first V.H.E. γ-ray survey of the Southern skies and would consequently follow the 2-3 year observing programme currently planned.

The Mark IV telescope is ideally suited for short observing campaigns of specific objects, and would be complementary to a large survey instrument such as the modified Mark III telescope. In addition to its use as a Cygnus X-3 monitor, it may be moved easily to observe objects undergoing prolonged X-ray or γ-ray outbursts or even to observe new supernovae. The design is such that it is lightweight and relatively easy to assemble. It may be desirable to construct further such telescopes and operate them together as a high-sensitivity facility, to be established as a Northern Hemisphere γ-ray Observatory.

9.8. The Future of V.H.E. γ-ray Astronomy using the Atmospheric Cerenkov Technique

The field of V.H.E. γ-ray astronomy is rapidly expanding. In addition to the 9 facilities at present in operation, 5 more telescopes are either in the design or construction stage. During the first years, only a few γ-ray sources were reported, with

signals only just above the background of cosmic rays. Now, with results being presented for a much greater number of sources and at a greatly increased level of significance in most cases, V.H.E. γ-ray astronomy is becoming a well-established field. This is aided by the steadily falling energy thresholds of telescopes at present being built. It may be possible in the next 10 years or so to bridge the gap with the upper energy limit of proposed satellite projects such as EGRET. The use of methods such as the guard ring technique will lead to greater signal strengths. With improved statistics, it is becoming possible to test theories which attempt to explain the production processes for V.H.E. γ-rays and hence to pinpoint the origin of high energy cosmic rays within the galaxy.

REFERENCES

Ajne, B. Biometrika, 55, 343 (1968).

Alexeenko, V.V., Chudakov, A.E., Khaerdinov, N.S., Lidvansky, A.S., Navarra, G., Ozrokov, S.S., Sklyarov, V.V. and Tizengauzen, V.A. Proceedings of the 19th ICRC (La Jolla), 1, 91.

Arons, J. IAU Symposium 74: Origin of Cosmic Rays, 1981. p.175.

Ash, M.E., Shapiro, I.I. and Smith, W.B. Astr. J. 72, 338 (1964).

Ashworth, M., Lyne, A.G. and Smith, F.G. Nature, 301, 313 (1983).

Avni, Y. and Bahcall, J. Astrophys. J. (Lett.), 192, L139 (1974).

Backer, D.C., Kulkarni, S.R., Heiles, C., Davis, M.M. and Goss, W.M. Nature, 300, 615 (1982).

Bahcall, J.N. and Bahcall, N.A. Nature, 247, 446 (1974).

Baity, W.A., Ulmer, M.P., Wheaton, W.A. and Peterson, L.E. Astrophys. J., 187, 341 (1974).

Baltrusaitis, R.M., Cassiday, G.L., Cooper, R., Dawson, B.R., Elbert, J.W., Fick, B.E., Gerhardy, P.R., Green, K.D., Liebing, D.F., Lingle, C.P., Loh, E.C., Sokolsky, P., Sommers, P., and Steck, D. Astrophys. J. (Lett.), 293, L69 (1985).

Barnhill, M.V., Gaisser, T.K., Stanev, T. and Halzen, F., Nature, 317, 409 (1985).

Basko, M.M., Sunyaev, R.A. and Titarchuck, I.G. Astron. Astrophys., 31, 249 (1974).

Batschelet, E. Circular Statistics in Biology, Academic Press, London, 1981.

Battistoni, G., Bellotti, E., Bloise, C., Bologna, G., Campana, P., Castaglioni, C., Castellina, A., Chiarella, V., Ciocio, A., Cundy, D., D'Ettore-Piazzoli, B., Fiorini, E., Galeotti, P., Larocci, E., Ligouri, C., Mannocchi, G., Murtas, G., Negri, P., Nicoletti, G., Picchi, P., Price, M., Pullia, A., Ragazzi, S., Rollier, M., Saavedra, O., Satta, L., Sarri, P., Vernetto, S., and Zanotti, L. Phys. Lett., 155B, 465 (1985).

Becklin, E.E., Hawkins, F.J., Mason, K.O., Matthews, K., Neugebauer, G., Packman, D., Sanford, P.W., Schupler, B., Stark, A. and Wynn-Williams, C.G., Astrophys. J., 192, L119 (1974).

Becklin, E.E., Kristian, J., Neugebauer, G., and Wynn-Williams, C.G. Nature (Phys. Sci.), 239, 130 (1972).

Bennett, K., Burger, J.J., Gorisse, M., Mayer-Hasselwander, H.A., Paul, J.A., Pfefferman, E., Shukla, P.G., Stiglitz, R., Swanenburg, B.N., Taylor, B.G., Wills, R.D. Astron. Astrophys., 61, 279 (1977).

Berger, Ch., et al. (The FREJUS Collaboration), Phys. Lett. B., 174, 1, 118 (1986).

Bergstrahl, T. and Schroeder, C. Phys. Rev., 81, 461, (1952).

Bhat, P.N., Gupta, S.K., Ramana Murthy, P.V., Sreekantan, B.V., Tonwar, S.C. and Viswanath, P.R., Astron. Astrophys., 81, L3 (1980).

Bhat, P.N., Gupta, S.K., Ramana Murthy, P.V., Sreekantan, B.V., Tonwar, S.C. and Vishwanath, P.R., in Proceedings of the NATO Advanced Research Workshop on Very High Energy γ-Ray Astronomy, Turver, K.E. (Ed.), Reidel, 1987, p.143.

Bhat, C.L., Sapru, M.L. and Razdan, H., Astrophys. J., 306, 587 (1986).

Bignami, G.E., Maraschi, L., and Treves, A., Astron. Astrophys. 55, 155 (1977).

Blackett, P.M.S., Emission Spectra of the Night Sky and Aurora, Rep. of the Gaissot Comm. of the Roy. Soc., p.34 (1948).

Blandford, R., and Toukolsky, S.A. Astrophys. J., 205, 580 (1976).

Boley, F.I., Rev. Mod. Phys., 36, 792 (1964).

Boley, F.I., Baun, J.H., Palsedge, J.A. and Percue, J.H., Phys. Rev., 124, 1205 (1961).

Bonnet-Bidaud, J.M. and Van der Klis, M., Astron. Astrophys., 101, 299 (1981).

Boriakoff, V., Buccheri, R., Fauci, F., Nature, 304, 417 (1983).

Braes, L.L.E., Miley, G.K., Shane, W.W., Baars, J.W.M., and Goss, W.M. Nature (Phys. Sci.), 242, 66 (1973).

Browning, R., and Turver, K.E. Nuovo Cimento, 38A, 223 (1977).

Canizares, C.R., McClintock, J.E., Clark, G.W., Lewin, W.H.G., Schnopper, H.W. and Sprott, G.F., Nature (Phys. Sci.)., 241, 28 (1973).

Cawley, M.F., Fegan, D.J., Gibbs, K., Gorham, P.W., Lamb, R.C., Liebing, D.F., Porter, N.A., Stenger, V.J., Turver, K.E. and Weekes, T.C., Astrophys. J., 296, 185 (1985).

Cerenkov, P.A., Dokl. Akad. Nauk., 2, 451 (1934).

Cerenkov, P.A., Phys. Rev., 52, 378 (1937).

Chadwick, P.M., Dipper, N.A., Dowthwaite, J.C., Gibson, A.I., Harrison, A.B., Kirkman, I.W., Lotts, A.P., Macrae, J.H., McComb, T.J.L., Orford, K.J., Turver, K.E., and Walmsley, M., Nature, 318, 642 (1985).

Chadwick, P.M., Dipper, N.A., Kirkman, I.W., McComb, T.J.L., Orford, K.J., Turver, K.E. and Turver, S.E. in Proceedings of the NATO Advanced Research Workshop on Very High Energy γ-Ray Astronomy, Turver, K.E. (Ed.), Reidel, 1987, p.159.

Chadwick, P.M., Dowthwaite, J.C., Kirkman, I.W., McComb, T.J.L., Orford, K.J. and Turver, K.E., Proceedings of the 19th ICRC (La Jolla), 1, 79 (1985).

Chadwick, P.M., Dowthwaite, J.C., Kirkman, I.W., McComb, T.J.L., Orford, K.J. and Turver, K.E., Proceedings of the 19th ICRC (La Jolla), 1, 155 (1985).

Chanmugam, G., and Brecher, K., Nature, 313, 767 (1985).

Charman, W.N., Jelley, J.V., Orman, P.R., Drever, R.W.P., and McBreen, B., Nature, 220, 565 (1968).

Cheng, A., Ruderman, M., and Sutherland, P., Astrophys. J., 212, 808 (1976).

Cherry, M.L., Corbato, S., Kieda, D., Lande, K. and Lee, C.K., Preprint, 1986.

Chevalier, C. and Ilovaisky, S.A., Astron. Astrophys., 59, L9 (1977).

Chudakov, A.E., Zatsepin, V.I., Nesterova, N.M., and Dadykin, V.L., J. Phys. Soc. Japan, Sup. A-III, 106 (1962).

/ Chudakov et al 1987

Chodil, G., Mark, H., Rodrigues, R., Seward, F., Swift, C.D., Hiltner, W.A., Wallerstein, G., and Mannery, E.J., Phys. Rev. Lett., 19, 681 (1967).

Chu, K.W. and Beiging, J.H., Astrophys. J. (Lett.), 179, 22 (1973).

Clay, R.W., Gerhardy, P.R. and Liebing, D.F., Aust. J. Phys., 37, 91 (1984).

Cohen, J.M. and Mustafa, E., Astrophys. J. (in press), 1987.

Cox, R.T., Phys. Rev., 66, 106 (1944).

Craig, M.A.B., The Lateral Distribution of Cerenkov Light in Large Cosmic Ray Showers as a Measure of Longitudinal Development, Ph.D. Thesis, Durham, 1984.

Cressie, N., J. Appl. Prob., 14, 272 (1977).

Danaher, S., Fegan, D.J., Porter, N.A. and Weekes, T.C. Nature, 289, 568 (1981).

Davis, M.M., Taylor, J.H., Weisberg, J.M. and Backer, D.C., Nature, 315, 547 (1985).

Dickey, J.M., Astrophys. J., 273, L71 (1983).

Dolan, J.F., Crannell, C.J., Dennis, B.R., Frost, K.J., and Orwig, L.E., Astrophys. Lett., 22, 147 (1982).

Dowthwaite, J.C., Very Energetic Gamma-Rays from Binary X-ray Sources and other Astronomical Objects, Ph.D. Thesis, University of Durham, 1987.

Dowthwaite, J.C., Gibson, A.I., Harrison, A.B., Kirkman, I.W., Lotts, A.P., Macrae, J.H., Orford, K.J., Turver, K.E., and Walmsley, M., Astron. Astrophys., 126, 1 (1983).

Dowthwaite, J.C., Harrison, A.B., Kirkman, I.W., Macrae, J.H., Orford, K.J., Turver, K.E. and Walmsley, M., Astron. Astrophys., 142, 55 (1985).

Dowthwaite, J.C., Harrison, A.B., Kirkman, I.W., Macrae, H.J., McComb, T.J.L., Orford, K.J., Turver, K.E., and Walmsley, M. Astrophys. J., 286, L35 (1984).

Eadie, W.T., Drijard, D., James, F.E., Roos, M., and Sadoulet, B., Statistical Methods in Experimental Physics, North-Holland Publishing Co., 1971.

Eichler, D., and Vestrand, W.T., Nature, 307, 613 (1984).

Eichler, D., and Vestrand, W.T., Nature, 318, 345 (1985).

Elsner, R.F., Ghosh, P., Darbro, W., Weisskopf, M.C., Sutherland, P.G. and Grindlay, J.E., Astrophys. J., 239, 335 (1980).

Epstein, A., Devaille, J., Helmken, H., Murray, S., Schnopper, H.W., Doxsey, R. and Primini, F., Astrophys. J., 216, 103 (1977).

Erber, T. Rev. Mod. Phys., 38, 626 (1966).

Erickson, R.A., Fickle, R.K. and Lamb, R.C., Astrophys. J., 210, 539 (1976).

Fabian, A.C., Rees, M.J., Van den Heuvel, E.P.J., and Van Paradijs, J., Nature, 328, 323 (1987).

Fabbiano, G., and Schreier, E. Astrophys. J., 214, 235 (1977).

Fegan, D.J., Cawley, M.F., Gibbs, K., Gorham, P.W., Lamb, R.C., Porter, N.A., Reynolds, P.T., Stenger, V.J., and Weekes, T.C. in Proceedings of the NATO Advanced Research Workshop on Very High Energy γ-Ray Astronomy, Turver, K.E. (Ed.)., 1987, p.111.

Fichtel, C.E., Thompson, D.J. and Lamb, R.C., Laboratory for High Energy Astrophysics preprint no. 87-004 (1987).

Fomin, V.P., Neshpor, Yu. I., Stepanian, A.A., Zyskin, Yu. L. and Vladimirskii, B.M., Proceedings of the 17th ICRC (Paris), 1, 28 (1981).

Fomin, V.P., Vladimirskii, B.M., and Stepanian, A.A., Proceedings of the 15th ICRC (Plovdiv), 1, 12 (1977).

Forman, W., Jones, C., Cominsky, L., Julien, P., Murray, S., Peters, G., Tananbaum, H., and Giacconi, R., Astrophys. J. (Supp.), 38, 357 (1978).

Forman, W., Jones, C., and Tananbaum, H., Astrophys. J. (Lett), 206, L29 (1976).

Frank, I.M. and Tamm, Ig. Dokl. Akad, Nauk. 14, 109 (1937).

Gaisser, T.K., and Stanev, T. Phys. Rev. Lett., 58, 1695 (1987).

Galbraith, W. and Jelley, J.V. Nature, 171, 349 (1953).

Gal'per, A.M., Kirillov-Ugryumov, V.G., Kurochkin, A.V., Leikov, N.G., Luchkov, B.I., and Yurkin, Yu. T., Proceedings of the 14th ICRC, Munich, 1, 95 (1975).

Gal'per, A.M. and Luchkov, B.I., Pis'ma Astron. Zh. 10, 358 (1984); Sov. Astron. Lett., 10, 150 (1984).

Gaustad, J.I., and Margon, B. Mon. Not. R. astr. Soc., 161, 15P (1973).

Geldzahler, B.J., Johnston, K.J., Spencer, J.H., Klepczynski, W.J., Josties, F.J., Angerhofer, P.E., Florkowski, D.R., McCarthy, D.D., Matsakis, D.N., and Hjellming, R.M., Astrophys. J., 273, 65 (1983).

Giacconi, R., Gorenstein, P., Gursky, H., and Waters, J.R., Astrophys. J., 148, L119 (1967).

Giacconi, R., Gursky, H., Kellogg, E., Schreier, E. and Tananbaum, H., Astrophys. J., 167, L67 (1971).

Giacconi, R., Murray, S., Gursky, H., Kellogg, E., Schreier, E., Matilsky, T., Koch, D. and Tananbaum, H., Astrophys. J. (Supp.), 27, 37 (1984).

Giacconi, R., Murray, S., Gursky, H., Kellogg, E., Schreier, E., and Tananbaum, H., Astrophys. J., 178, 281 (1972).

Gibson, A.I., Harrison, A.B., Kirkman, I.W., Lotts, A.P., Macrae, J.H., Orford, K.J., Turver, K.E. and Walmsley, M. Nature, 296, 833 (1982).

Gilmozzi, R., Cassatella, A., J. Clavel, Fransson, C., Gonzalez, R., Gry, C., Panagia, N., Talavera, A. and Wamsteker, W., Nature, 328, 318 (1987).

Ginsburg, V.L. J. Phys. (USSR), 2, 441 (1940).

Gorham, P.W., Cawley, M.F., Fegan, D.J., Gibbs, K.G., Lamb, R.C., Porter, N.A., Stenger, V.J. and Weekes, T.C., in Proceedings of the NATO Advanced Research Workshop on Very High Energy γ-ray Astronomy, Turver, K.E. (Ed.), Reidel, 1987.

Gorham, P.W., Cawley, M.F., Fegan, D.J., Gibbs, K.G., Lamb, R.C., Liebing, D.F., Porter, N.A., Stenger, V.J. and Weekes, T.C., Astrophys. J. (Lett.), 308, L11 (1986).

Gould, R.J. Astrophys. J., 274, L23 (1983).

Gregory, P.C., Nature (Phys. Sci), 239, 439 (1972).

Gregory, P.C., Kronberg, P.P., Seaquist, E.R., Hughes, V.A., Woodsworth, A., Viner, M.R., Retallack, D., Hjellming, R.M. and Balick, B., Nature (Phys. Sci.), 239, 114 (1972).

Greisen, K. The Physics of Cosmic X-ray, γ-ray and Particle Sources, Gordon and Breach, 1971.

Grindlay, J.E., Helmken, H.F., Hambury Brown, R., Davis, J. and Allen, L.R., Astrophys. J. (Lett.), 197, L9 (1975).

Grindlay, J.E., Helmken, H.F., Hanbury Brown, R., Davis, J. and Allen, L.R., Astrophys. J., 201, 82 (1975).

Grindlay, J.E., Helmken, H.F. and Weekes, T.C., Astrophys. J., 209, 592 (1976).

Gunn, J.E. and Ostriker, J.P., Phys. Rev. Lett., 22, 728 (1969).

Gupta, S.K., Ramana Murthy, P.V., Sreekantan, B.V. and Tonwar, S.C., Astrophys. J., 221, 268 (1978).

Gupta, S.K., Ramana Murthy, P.V., Sreekantan, B.V., Tonwar, S.C., and Vishwanath, P.R., in Proceedings of the International Workshop on Very High Energy γ-Ray Astronomy, Ramana Murthy, P.V. and Weekes, T.C. (Eds), 1982, p.282.

Gursky, H., Gorenstein, P., and Giacconi, R., Astrophys. J., 150, 75 (1967).

Gursky, H., and Schreier, E., in Neutron Stars, Black Holes and Binary X-ray Sources. Gursky, H., and Ruffini, R. (Eds.), Reidel, 1975, p.175.

Harnden, F.R. and Gorenstein, P. Nature, 241, 107 (1973).

Hearn, D., Nucl. Instr. and Meth., 70, 200 (1969).

Heiles, C., Kulkarni, S.R., Stevens, M.A., Backer, D.C., Davis, M.M. and Goss, W.M., Astrophys. J., 273, L75 (1983).

Helmken, H.F. and Weekes, T.C., Astrophys. J., 228, 531 (1979).

Hermsen, W., Space Sci. Rev., 36, 61 (1983).

Hermsen, W., Bennet, K., Bloemen, J.B.G.M., Buccheri, R., Jansen, F.A., Mastichiadis, A., Mayer-Hasselwander, H.A., Ozel, M.E., Pollock, A.M.T. and Strong, A.W., Astron. Astrophys., 175, 141 (1987).

Hermsen, W., Swanenberg, B.N., Bignami, G.F., Boella, G., Buccheri, R., Scarsi, L., Kanbach, G., Mayer-Hasselwander, H.A., Masnou, J.L., Paul, J.A., Bennet, K., Higdon, J.L., Lichti, G.G., Taylor, B.G., and Wills, R.D., Nature, 269, 494 (1977).

Hillas, A.M. Nature, 312, 50 (1984).

Hillas, A.M., Proceedings of the 19th ICRC, La Jolla, 3, 445, (1985).

Hillas, A.M., in Proceedings of the NATO Advanced Research Workshop on Very High Energy γ-Ray Astronomy, Turver, K.E. (Ed.), Reidel (1987) p.289.

Hillas, A.M. and Patterson, J.R. in Proceedings of the NATO Advanced Research Workshop on V.H.E. γ-ray Astronomy, Turver, K.E. (Ed.), Reidel (1987), p.249.

Hirata et. al. (The Kamiokande-II Collaboration) Phys. Rev. Lett., 58, 1490 (1987).

Hjellming, R.M. and Balick, B., Nature (Phys. Sci.), 239, 135 (1972).

Hodges, J.L., Ann. Math. Statist., 26, 523 (1955).

Holloway, N., Nature, 246, 6 (1973).

Holt, S.S., Boldt, E.A., Serlemitsos, P.J., Kaluzienski, L.J., Pravdo, S.H., Peacock, A., Elvis, M., Watson, M.G. and Pounds, K.A., Nature, 260, 592 (1976).

Holt, S.S., Kaluzienski, L.J., Boldt, E.A. and Serlemitsos, P.J. Astrophys. J., 233, 344 (1979).

Howe, S.K., Primini, F.A., Bautz, M.W., Lang, F.L., Levine, A.M. and Lewin, W.H.G., Astrophys. J., 272, 678 (1983).

Jelley, J.V., in Progress in Elementary Particle and Cosmic Ray Physics, Wilson, J.G. and Wouthuyen, S.A. (Eds.), North-Holland Publishing Co., 1967, pp.40-159.

Jelley, J.V., in Proceedings of the NATO Advanced Research Workshop on V.H.E. γ-ray Astronomy, Turver, K.E. (Ed), Reidel (1987), p.27.

Jelley, J.V. and Porter, N.A., Quarterly J. of the R. astr. Soc., 4, 275 (1963).

Johnson, Davies and Siry in Rocket Exploration of the Upper Atmosphere London, 1954, Seaton, M. and Boyd, R. (eds.), p.306.

Johnston, K.J., Spencer, J.H., Simon, R.S., Waltman, E.B., Pooley, G.G., Spencer, R.E., Swinney, R.W., Angerhofer, P.E., Florkowski, D.R., Josties, F.J., McCarthy, D.D., Matsakio, D.N., Reese, D.E., and Hjellming, R.M., Astrophys. J., 309, 707 (1986).

Jones, C., Astrophys. J., 214, 856 (1977).

Kazanas, D., and Ellison, D.C. Nature, 319, 380 (1986).

Kelley, R.L., Jernigan, J.G., Levine, A., Petro, L.D., and Rappaport, S., Astrophys. J., 264, 568 (1983).

Kelley, R.L., Rappaport, S., Clark, G.W. and Petro, L.D., Astrophys. J., 268, 790 (1983).

Kellogg, E., Tananbaum, H., Harnden, F.R., Gursky, H., Giacooni, R. and Grindlay, J. Astrophys. J., 183, 935 (1973).

Kifune, T., Nishijima, K., Hara, T., Hatano, Y., Hayashida, N., Honda, M., Kamata, K., Matsubara, Y., Mori, M., Nagano, M., Tanahashi, G. and Teshima, M. Astrophys. J., 301, 230 (1986).

Kirkman, I.W., Ph.D. Thesis, Univ. of Durham, 1985.

Kraushaar, W.L., Clark, G.W., Garmire, G.P., Borken, R., Higbie, P., Leong, V., and Thorsos, T. Astrophys. J., 177, 341 (1972).

Krzeminski, W. Astrophys. J. (Lett.), 192, L135 (1974).

Lamb, R.C., Cawley, M.F., Fegan, D.J., Gibbs, K.G., Gregory, A.G., Gorham, P.W., Lewis, D.A., Porter, N.A., Stenger, V.J. and Weekes, T.C. in Proceedings of the NATO Advanced Research Workshop in V.H.E. γ-Ray Astronomy, Turver, K.E., (Ed.), Reidel, 1987, pp.139-142.

Lamb, R.C., Dower, R.G., Fickle, R.K., Astrophys. J. (Lett.), 229, L19 (1979).

Lamb, R.C., Fichtel, C.E., Hartman, R.C., Kniffen, D.A. and Thompson, D.J., Astrophys. J., 212, L63 (1977).

Lamb, R.C., Godfrey, C.P., Wheaton, W.A. and Turner, T., Nature, 296, 543 (1982).

Lambert, A., Lloyd-Evans, J., Perrett, J.C., Reid, R.J.O., Watson, A.A. and West, A.A. Proceedings of the 19th ICRC (La Jolla), 1, 171 (1985).

Lang, F.L., Levine, A.M., Bautz, M., Hauskins, S., Howe, S., Primini, F.A., Lewin, W.H.G., Baity, W.A., Knight, F.K., Rothschild, R.E. and Petterson, J.A., Astrophys. J., 246, L21 (1981).

Large, M.I., Vaughan, A.E. and Mills, B.Y., Nature, 220, 340 (1968).

Lauquê, R., Lequeux, J., and Nguyen-Quang-Rieu, Nature (Phys. Sci.), 239, 119 (1972).

Leahy, D.A., Elaner, R.F. and Weisskopf, M.C. Astrophys, J., 272, 256 (1983).

Leach, R.W., Murray, S.S., Schreier, E.J., Tananbaum, H.D., Ulmer, M.P. and Parsignault, D.R. Astrophys. J., 199, 184 (1975).

Lebrun, F., Bennett, K., Bignami, G.F., Bloemen, J.B.G.H., Buccheri, R., Caraveo, P.A., Gottwald, M., Hermsen, W., Kanbach, G., Mayer-Hasselwander, H.A., Montmerle, T., Paul, J.A., Sacco, B., Strong, A.W. and Wills, R.D. Astrophys. J., 274, 231 (1983).

Legage, P.O. and Cesarsky, C.J., Astron. Astrophys., 125, 249 (1983).

Leong, C., Kellogg, E., Gursky, H., Tananbaum, H., and Giacconi, R. Astrophys. J., 170, L67 (1971).

Lloyd-Evans, J., Coy, R.N., Lambert, A., Lapikens, J., Patel, M., Reid, R.J.O. and Watson, A.A., Nature, 305, 784 (1983).

Macrae, J.H.K., The Detection of Very High Energy Cosmic γ-Rays using the Atmospheric Cerenkov Technique, Ph.D. Thesis, Durham, 1985.

Madare, B., and Kunkel, W., IAU Circular No. 4316 (1987).

Mallet, L., C.R. Acad. Sci (Paris), 183, 274 (1926).

Manzo, G., Molteni, D., and Robba, N.R., Astron. Astrophys., 70, 317 (1978).

Mardia et al 1971.

Mardia, K.V., Statistics of Directional Data, Academic Press (1972).

Marshak, M.L., Bartlet, J., Courant, H., Heller, K., Joyce, T., Peterson, E.A., Ruddick, K., Shupe, M., Ayres, D.S., Dawson, J., Fields, T., May, E.N., Price, L.E. and Sivaprasad, K., Phys. Rev. Lett., 54, 2079 (1985).

Masnou, J.L., Bennet, K., Bignami, G.F., Buccheri, R., Caraveo, P., D'Amico, N., Hermsen, W., Kanbach, G., Lichti, G.G., Mayer-Hasselwander, H.A., Paul, J.A., Swanenburg, B.N. and Wills, R.D. Proceedings of the 12th ESLAB Symposium, Frascati, ESA SP-124. (1984).

Mason, K.O., Becklin, E.E., Blankenship, L., Brown, R.L., Elias, J., Hjellming, R.M., Matthews, K., Murdin, P.G., Neugebauer, G., Sanford, P.W. and Willner, S.P., Astrophys. J., 207, 78 (1976).

Mason, K.O., Cordova, F.A. and White, N.E., Astrophys. J., 309, 700 (1986).

Mason, K.O. and Sandford, P.W. Mon. Not. R. astr. Soc., 189, 9P (1979).

McKechnie, S.P., Mount, K.E. and Ramsden, D., Astrophys. J. (Lett.), 207, L151 (1976).

McNaught, R.H. IAU Circular No. 4316 (1987).

McNaught, R.H. and Morel, M., IAU Circular No. 4317 (1987).

Meegan, C.A., Fishman, G.J. and Haymes, R.C. Astrophys. J., 234, L123 (1979).

Middleditch, J., Mason, K.O., Nelson, J.E. and White, N.E., Astrophys. J., 244, 1001 (1981).

Middleditch, J., and Pennypacker, C., Nature, 313, 659 (1985).

Milgrom, M., and Pines, D., Astrophys. J., 220, 272 (1978).

Molnar, L.A., Multiwavelength Studies of Cygnus X-3, Ph.D. Thesis, Harvard University, 1985.

Molnar, L.A., Reid, M.J. and Grindlay, J.E., Nature, 310, 662 (1984).

Molteni, D., Rapisards, M., Robba, N.R. and Scarsi, L., Astron. Astrophys. 87, 88 (1980).

Moore, W.E., Agrawal, P.C. and Garmire, G., Astrophys. J. 189, L117 (1974).

Morello, C., Navarra, G. and Vernetto, S., Proceedings of the 18th ICRC (Bangalore), 1, 127 (1983).

Morrison, P. Nuovo Cimento, 7, 858 (1958).

Mukanov, J.B., Nesterova, N.M., Stepanian, A.A. and Fomin, V.P., Proceedings of the 17th ICRC (Paris), 1, 143 (1981).

Nagase, F., Sato, N., Makishima, K., Kawai, N. and Mitani, K. ISAS Res. Note 234, Institute of Space and Astronautical Science, Tokyo, 1983; Summer Workshop in AStronomy and Astophysics, Santa Cruz (1983).

Neshpor, Yu.I., Stepanian, A.A., Fomin, V.P., Gerasimov, S.A., Vladimirskii, B.M. and Ziskin, Yu.L., Astrophys. Space Sci., 61, 349 (1979).

Neshpor, Yu.I. and Zyskin, Yu.L., Sov. Astron. Lett., 12, 189 (1986).

Neshpor, Yu.I., Zyskin, Yu.L., Vladimirskii, B.M., Gerasimov, S.A., Stepanian, A.A. and Fomin, V.P., Izv. Krym. Astrofiz. Obs., 61, 61 (1980); Bull. Crimean Astrophys. Obs., 61, 51 (1981).

Nesterova, N.M. and Chudakov, A.E., Zh. Eksp. Teor. Fiz., 28, 384 (1955).

Nikishov, A.I., Zh.Eksp. Teor. Fiz., 41, 549 (1961) (Soviet Physics - JETP, 14, 393).

North, A.R., Raubenheimer, B.C., DeJager, O.C., van Tonder and van Urk, G., Nature, 326, 567 (1987).

Ogelman, H., Ayasli, S., and Haciliyar, A., Proc. of γ-ray Symposium, Goddard Space Flight Center, 118 (1976).

O'Mongain, E., Nature, 241, 376 (1973).

O'Mongain, E.P., Porter, N.A., White, J., Fegan, D.J., Jennings, D.M. and Lawless, B.G., Nature, 219, 1348 (1968).

Orford, K.J., in Proceedings of the NATO Advanced Research Workshop on V.H.E. γ-Ray Astronomy, Turver, K.E. (Ed.), Reidel, 1987, p.63.

Parsignault, D.R., Schreier, E., Grindlay, J., and Gursky, H., Astrophys. J., 209, L73 (1976).

Parsignault, D.R., Grindlay, J., Gursky, H., and Tucker, W. Astrophys. J., 218, 232 (1977).

Parsignault, D.R., Gursky, H., Kellogg, E.M., Matilsky, T., Murray, S., Schreier, E., Tananbaum, H., Giacconi, R. and Brinkman, A.C. Nature (Phys. Sci)., 239, 123 (1972).

Peterson, B.A., Murdin, P., Wallace, P., Manchester, R.N., Penny, A.J., Jorden, A., Hartley, K.F., and King, D., Nature, 276, 475 (1978).

Pietsch, W., Pakull, M., Voges, W. and Staubert, R., Space Sci. Rev., 40, 371 (1985).

Pollock, A.M.T., Bennet, K., Bignami, G.F., Bloemen, J.B.G.M., Buccheri, R., Caraveo, P., Hermsen, W., Kanbach, G., Lebrun, F., Mayer-Hasselwander, H.A., and Strong, A.W., Astron. Astrophys., 146, 352 (1985).

Porter, N.A., Delaney, T., Helmken, H.F. and Weekes, T.C. Nuovo Cimento, 32B, 515 (1976).

Pravdo, S.H., Becker, R.H., Boldt, E.A., Holt, S.S., Rothschild, R.E., Serlemitsos, P.J. and Swank, J.H., Astrophys. J. (Lett.), 208, L67 (1976).

Protheroe, R.J. Computer Simulations of Large Cosmic Ray Showers using Recent Models of Hadronic Collisions, Ph.D. Thesis, Durham, 1977.

Protheroe, R.J., Astron. Exp., 1, 137 (1985).

Protheroe, R.J., and Clay, R.W., Nature, 315, 205 (1985).

Protheroe, R.J. and Stanev, T., Nature, 328, 136 (1987).

Ramana Murthy, P.V., in Techniques in Ultra High Energy Gamma Ray Astronomy, Protheroe, R.J. and Stephens, S.A. (Eds.), Dept. of Physics, Univ. of Adelaide (1985), p.78.

Rappaport, S., Bradt, H., Doxsey, R., Levine, A., and Spada, G. Nature, 251, 471 (1974).

Rappaport, S., Clark, G.W., Cominsky, L., Joso, P.C., and Li, F. Astrophys. J. (Lett.), 224, 1 (1978).

Rappaport, S.A. and Joss, P.C. in Accretion-Driven Stellar X-ray Sources, Lewin, W.H.G. and Van den Heuvel, E.P.J. (Eds.), Cambridge University Press, 1983, p.1.

Rappaport, S., Markert, T., Li, F.K., Clark, G.W., Jernigan, J.G. and McClintock, J.E., Astrophys. J. (Lett), 217, L29 (1977).

Raubenheimer, B.C., North, A.R., DeJager, O.C., Van Urk, G., and Van Tonder, A.J., Astrophys. J. (Lett.), 307, L43 (1986).

Reiffel, L. and Burgwald, G.M. Phys. Rev., 95, 1294 (1954).

Reppin, C., Pietsch, W., Trumper, J. and Voges, W., Astrophys. J., 234, 329 (1979).

Resvanis, L., Learned, J., Stenger, V., Weeks, D., Gaidos, J., Loeffler, F., Olson, J., Palfrey, T., Sembroski, G., Wilson, C., Camerini, U., Finley, J., Fry, W., Jaworski, M., Jennings, J., Kenter, A., Koepsel, R., Lomperski, M., Loveless, R., March, R., Matthews, J., Morse, R., Reader, D., Sandler, P., Slane, P. and Szentgyorgi, A. in Proceedings of the NATO Advanced Research Workshop in V.H.E. γ-ray Astronomy, Turver, K.E. (Ed.), Reidel, 1987, pp.135-138.

Resvanis, L., Learned, J., Stenger, V., Weeks, D., Gaidos, J., Loeffler, F., Olson, J., Palfrey, T., Sembroski, G., Wilson, C., Camerini, U., Finley, J., Fry, W., Jaworski, M., Jennings, J., Kenter, A., Koepsel, R., Lomperski, M., Loveless, R., March, R., Matthews, J., Morse, R., Reeder, D., Sandler, P., Slane, P. and Szentgyorgi, A., in Proceedings of the NATO Advanced Research Workshop on Very High Energy γ-ray Astronomy, Turver, K.E. (Ed.), 1987a, p.131.

Resvanis, L., Learned, J., Stenger, V., Weeks, D., Gaidos, J., Loeffler, F., Olson, J., Palfrey, T., Sembroski, G., Wilson, C., Camerini, U., Finley, J., Fry, W., Jaworski, M., Jennings, J., Kenter, A., Koepsel, R., Lomperski, M., Loveless, R., March, R., Matthews, J., Morse, R., Reeder, D., Sandler, P., Slane, P. and Szentgyorgi, A., in Proceedings of the NATO Advanced Research Workshop on Very High Energy γ-ray Astronomy, Turver, K.E. (Ed.), Reidel, 1987c, p.155.

Resvanis, L., Tzamarais, S., Voulgaris, G., Learned, J., Stenger, V., Weeks, D., Gaidos, J., Loeffler, F., Olson, J., Palfrey, T., Sembroski, G., Wilson, C., Camerini, U., Finley, J., Frankowski, M., Fry, W., Jaworski, M., Jennings, J., Kenter, A., Koepsel, R., Lomperski, M., Loveless, R., March, R., Matthews, J., Morse, R., Reeder, D., Sandler, P., Slane, P., and Szentgyorgi, A., in Proceedings of the NATO Advanced Research Workshop on Very High Energy γ-Ray Astronomy, Turver, K.E. (Ed.), Reidel, 1987b, p.225.

Richards, J.A. and Nordheim, L.W., Phys. Rev., 75, 444 (1949).

Ricker, G.R., Gerassimenko, M., McClintock, J.E., Rackman, S.G. and Lewin, W.H.G., Astrophys. J., 186, L111(1973).

Ricketts, M.J., Paul, R., Page, C.G., and Pounds, K.A., Space Sci. Rev., 30, 399 (1981).

Rieke, G. Proceedings of the 11th ICRC, Budapest (1969); Acta. Phys. Acad. Sci. Hung., 29, Suppl. 3, 601 (1970).

Samorski, M., and Stamm, W., Astrophys. J., 268, L17 (1983).

Sandford, P.W. and Hawkins, F.H. Nature (Phys. Sci.), 239, 135 (1972).

Sanduleak, N. and Philip, A.G.D., IAU Circular No. 3023 (1977).

Schreier, E., Giacconi, R., Gursky, H., Kellogg, E.M., Levinson, R., and Tananbaum, H., IAU Circular No. 2524 (1973).

Schreier, E., Levinson, R., Gursky, H., Kellogg, E.M., Tananbaum, H., and Giacconi, R., Astrophys. J. (Lett.), 172, L79 (1972).

Schreier, E., Swartz, K. and Giacconi, R., Astrophys. J., 204, 539 (1976).

Segelstein, D.J., Rawley, L.A., Stinebring, D.R., Fruchter, A.S. and Taylor, J.H., Nature, 322, 714 (1986).

Serlemitsos, P.J., Boldt, E.A., Holt, S.S., Rothschild, R.E., and Saba, J.L.R., Astrophys. J. (Lett.), 201, L9 (1975).

Seward, F.D., Harnden, F.R., and Helfland, D.J., Astrophys. J. (Lett.), 287, L19 (1984).

Shigeyama, T., Nomoto, K., Hashimoto, M. and Sugimoto, D., Nature, 328, 320 (1987).

Skinner, G.K., Shulman, S., Share, G., Evans, W.D., McNutt, D., Meekins, J., Smathers, H., Wood, K., Yentis, D., Byram, E.T., Chubb, T.A. and Friedman, H., Astrophys. J., 240, 619 (1980).

Smith, F.G., Pulsars, Cambridge University Press, 1979 (2nd Ed.)

Smith, F.G. in Proceedings of the NATO Advanced Research Workshop on Very High Energy γ-Ray Astronomy, Turver, K.E. (Ed)., Reidel (1987), p.1.

Spencer, R.E., Swinney, R.W., Johnston, K.J. and Hjellming, R.M. Astrophys. J., 309, 694 (1986).

Stepanian, A.A., Vladimirskii, B.M., Neshpor, Yu.I., and Fomin, V.P. Proceedings of the 15th ICRC (Plovdiv), 1, 135 (1977).

Stokes, G.H., Segelstein, D.J., Taylor, J.H. and Dewey, R.J., Astrophys. J., 311, 694 (1986).

Swanenburg, B.N., Bennett, K., Bignami, G.F., Buccheri, R., Caraveo, P., Hermsen, W., Kanbach, G., Lichti, G.G., Masnou, J.L., Mayer-Hasselwander, H.A., Paul, J.A., Sacco, B., Scarsi, L., Wills, R.D., Astrophys. J. (Lett.), 243, L69 (1981).

Szentgyorgi, A., A Search for Very High Energy Gamma Ray Emission from Cygnus X-3, Ph.D. Thesis, University of Wisconsin-Madison, 1986.

Tananbaum, H., Gursky, H., Kellogg, E.M., Levinson, R., Schreier, E., and Giacconi, R., Astrophys. J. (Lett.), 174, 143 (1972).

Thompson, D.J., Fichtel, C.E., Kniffen, D.A., and Ögelman, H.B., Astrophys. J., 200, L79 (1975).

Tonwar, S.C., Gopalkrishnan, N.V. and Sreekantan, B.V., Proceedings of the 19th ICRC (La Jolla) 1, 242 (1985).

Trumper, J., in Proceedings of the NATO Advanced Research Workshop on V.H.E. γ-ray Astronomy, Turver, K.E. (Ed.), Reidel (1987), p.7.

Trümper, J., Pietsch, W., Reppin, C., Voges, W., Staubert, R. and Kendizorra, E. Astrophys. J., 219, 105 (1978).

Tuohy, I.R. Mon. Not. R. astr. Soc., 174, 45P (1976).

Tuohy, I.R. and Cruise, A.M., Mon. Not. R. astr. Soc., 171, 33P (1975).

Turver, K.E. and Weekes, T.C., Nuovo Cimento, 45, 99 (1978).

Usov, V.V., Nature, 305, 409 (1983).

Van der Klis, M. and Bonnet - Bidaud, J.M., Astron. Astrophys., 95, L5 (1981a).

Van der Klis, M. and Bonnet-Bidaud, J.M., Space Sci. Rev., 30, 419 (1981b).

Van der Klis, M., Bonnet-Bidaud, J.M. and Robba, N.R., Astron. Astrophys., 88, 8 (1980).

Van der Klis, M., and Jansen, F., Adv. Space Res., 5, 109 (1985).

Vestrand, W.T. and Eichler, D., Astrophys. J., 261, 251 (1982).

Vladimirskii, B.M., Gal'per, A.M., Kirillov-Ugryumov, V.G., Kurochkin, A.V., Luchkov, B.I., Neshpor, Yu.I., Stepanian, A.A., Fomin, V.P. and Yurkin, Yu.T., Sov. Astron. Lett., 1, 57 (1975).

Vladimirskii, B.M., Stepanian, A.A. and Fomin, V.P., Proceedings of the 13th ICRC (Denver), 1, 456 (1973).

Wallace, P.T., Peterson, B.A., Murdin, P.G., Danziger, I.J., Manchester, R.N., Lyne, A.G., Goss, W.M., Smith, F.G., Disney, M.J., Hartley, D.F., Jones, D.H.P., Wellgate, G.W., Nature, 266, 692 (1977).

Watson, A.A., in Proceedings of the NATO Advanced Research Workshop on Very High Energy γ-Ray Astronomy, Turver, K.E. (Ed)., Reidel, 1987, p.53.

Weekes, T.C., Astron. Astrophys., 121, 232 (1982).

Weekes, T.C., Danaher, S., Fegan, D.J. and Porter, W.A. Astron. Astrophys., 104, L4-L6 (1981).

Weekes, T.C., Helmken, H.F. and Grindlay, J.E., Proceedings of the 16th ICRC (Kyoto), 1, 133 (1979).

Weekes, T.C., Murphy, P.P., Schild, R., Gursky, H., Geary, J. and Stephenson, T., Pub. Astr. Soc. Pacific, 93, 474 (1984).

West, R.M., Lauberts, A., Jorgensen, H., and Schuster, H.E., Astron. Astrophys. (in press) (1987).

Westphal, J.A., Kirstian, J., Huchra, J.P., Shectman, S.A. and Brucato, R.J., Nature (Phys. Sci.), 239, 134 (1972).

Wheaton, W.A., Doty, J.P., Primini, F.A., Cooke, B.A., Dobson, C.A., Goldman, A., Hecht, M., Hoffman, J.A., Howe, S.K., Scheepmaker, A., Tsiang, E.Y., Lewin, W.H.G., Matteson, J.L., Gruber, D.E., Baity, W.A., Rothschild, R., Knight, F.K., Nolan, P. and Peterson, L.E. Nature, 28, 240 (1979).

White, N.E., Nature, 271, 38 (1978).

White, J., Porter, N.A. and Long, C.D. J. Atmos, Terrestrial Phys., 20, 40 (1961).

Zimmermann, H.U., Astron. Astrophys. 88, 309 (1980).

Addenda

Oversampling

A period search which covers only the minimal number of periods would use the spacing of trial period given by equation 3.16. However , in practice the resultant probability distribution is somewhat smoother if the spacing is closer than this. This technique of testing a larger number of periods than calculated from equation 3.16 is known as oversampling. In the case of all the analysis described in this work from both the Dugway and Narrabri telescopes , three trial periods per fourier interval have been tested.

The use of oversampling requires that the resultant probability of uniformity be adjusted to take into account the further degrees of freedom expended. The periods tested within a given Fourier interval are not entirely independent of each other , and it is found that , in the case of the Rayleigh test , the number of degrees of freedom used in obtaining a given probability of no periodicity should be multiplied by a factor of 2.8 in addition to the number of degrees of freedom calculated from equation 3.16 (Orford , private communication). This factor is constant regardless of the number of trial periods per Fourier interval which have been tested.

LMC X-4

Comparison of the Durham result with that of Protheroe and Clay (1985) suggests that LMC X-4 has a rather flat inegral energy spectrum between 10^{11} and 10^{16} eV , the spectral index being approximately -0.72. At 1000 Gev , the average luminosity of LMC X-4 would therefore be approximately three times the average value for the luminosity of Cygnus X-3 measured by the Durham group. This makes LMC X-4 the most luminous object known in both very high energy and ultra high energy gamma-rays.

ACKNOWLEDGEMENTS

I wish to acknowledge Prof. A.W. Wolfendale for the provision of facilities in the Dept. of Physics and the Science and Engineering Research Council for the provision of a grant. I am indebted to my supervisor, Dr. K.E. Turver for his help, enthusiasm and good advice.

It is a pleasure to acknowledge the company and advice of my colleagues, Dr. J.C. Dowthwaite, Dr. N.A. Dipper, Dr. I.W. Kirkman, Mr. E.W. Lincoln, Dr. T.J.L. McComb, Dr. K.J. Orford, Mr. S.M. Rayner, Mr. V.G. Mannings and Mr. G. Williams. I would also like to thank Mr. P. Cottle, Mrs. S.E. Hilton and Mr. K. Tindale for their technical expertise.

I would like to thank Prof. C. Robson for his kind loan of a typewriter and Mrs. M. Newton for her careful typing of this thesis.

Last but by no means least, my thanks to Phil Mackie, for running around after Greek golfballs and keeping me and the VAX 11/750 company.

- AMDG -